

Synthesis of carbohydrate based tools to explore the biosynthesis of and develop detection methods for prymnesin toxins

Edward Steven Hems

This thesis is submitted in fulfilment of the requirements of the degree
of Doctor of Philosophy at the University of East Anglia

Department of Biological Chemistry

John Innes Centre

Norwich

August 2017

© This copy of the thesis has been supplied on condition that anyone who consults it is understood to recognise that its copyright rests with the author and that no quotation from the thesis, or information derived therefrom, may be published with the author's prior, written consent.

I declare that the work contained in this thesis, submitted by me for the degree of Doctor of Philosophy, is to the best of my knowledge my own original work, except where due reference is made.

Date

21/08/2017

Signed

Edward Steven Hems

Abstract

Prymnesium parvum is a harmful microalga which produces glycosylated ichthyotoxic metabolites called prymnesins. This thesis describes the synthesis of chemical tools to explore the biosynthesis and detection of prymnesins.

Sugar-nucleotides proposed to be involved in the glycosylation of prymnesins were synthesised. UDP- α -D-galactofuranose was biosynthesised from chemosynthetic Gal β -1-P using galactose-1-phosphate uridylyltransferase. GDP- α -D-arabinopyranose and GDP- β -L-xylopyranose were proposed to be involved in the biogenesis of L-xylofuranose, and were stereoselectively synthesised by direct displacement of an acylated glycosyl bromide with GDP. Multiple reaction monitoring transitions for the NDP-sugars were recorded using porous graphitic carbon column based LC-MS, as standards for profiling algal cell extracts.

Prymnesins share a conserved terminal bis-alkyne, which may prove a useful biomarker. Bis-alkyne standards were synthesised by Cadiot-Chodkiewicz coupling, and used to show that there was no appreciable difference in reactivity between terminal alkynes and bis-alkynes under CuAAC conditions. CuAAC based toxin detection shows potential; coupling of authentic prymnesins with 3-azido-7-hydroxycoumarin gave fluorescent species which were separable by TLC and visible under UV-light. Raman detection was also explored, but was dismissed due to fluorescent quenching by algal pigments.

Sugar-glycerol compounds inspired by prymnesin's glycosylated backbone were chemically synthesised. Neighbouring group participation was utilised to synthesise 1,2-*trans* glycosides. SnCl₂ promoted glycosylation with furanosyl fluorides gave 1,2-*cis* furanosides with moderate stereocontrol, whilst TMSOTf promoted glycosylation with pyranosyl imidates gave 1,2-*cis* pyranosides with excellent stereocontrol. 1,2-*trans* Sugar-glycerol fragments gave NMR signals closer to prymnesin literature values than 1,2-*cis* fragments.

Two fragments of prymnesin-1 glycosylated with α -L-arabinopyranose and α -D-ribofuranose were chemically synthesised. Possible CuAAC and carbodiimide conjugation of the fragments to a carrier protein for anti-prymnesin-1 antibody production was considered. Because the stereochemistry of the prymnesin backbones at this region is undefined, both the 2R- and 2S- glycerol isomers were synthesised. The separated isomers were distinguished by comparing NOESY NMR with computational models.

Acknowledgements

First I must thank my supervisor Rob Field for his help, guidance, and patience over the past four years. His generosity with his time has been incredible, and he always has a helpful answer to my questions, no matter when I ask them. Rob has worked tirelessly to ensure we always have what is needed in the lab, and he has always kept me going in the right direction, often without me realising it! I will always remember sitting down to a sea-food lunch in a small harbour in Taiwan with him! Thank you, Rob.

Martin and Sergey have a lot to answer for, having persuaded me 10 years ago as a naïve sixth form summer student that my time at university would be much better spent perusing chemistry than computer science. For this I am incredibly grateful! During my time here, Martin has helped me conquer my fear of enzymes, and Sergey has helped my with NMR and the synthesis of furanosides.

I started my PhD project 4 years ago at the same time as Ben Wagstaff. Ben also works with *Prymnesium* and has been a dependable colleague and friend from the day I met him. There has been some overlap in our projects, and as will be seen, I have chemically synthesised some compounds to try and answer biological questions raised in his project.

I must thank all our external collaborators. Antoinette, Nick and Yuki at The Norfolk Record Office for their support with my DTP project. Duncan Graham and Steve Asiala at the University of Strathclyde leant their lab, spectrometers, and time to the Raman studies. Jenny Pratscher from the UEA has worked closely with both Ben and me on the '*Prymnesium* project', and her ability to set up an *ad hoc* lab in a muddy boat yard is remarkable! Steve Lane at the Environment Agency, Andy Hindes of Fish Track Ltd and John Currie of the Pike Anglers Club have been incredibly supportive, both in facilitating field trials and sampling, and ensuring positive local media coverage of our project.

Thanks to everyone in Rob Field's group. Mike, Brydie and Becky have been a pleasure to share and office with. My fellow chemists, Irina, Simone, Jordan and Ana have been amazing for bouncing ideas off, and we always enjoy sharing our work. Gerhard helped with mass-spec based toxin detection. Giulia, Sue and Lilly have also ensured an amazing four years.

Finally I must thank my family for their unwavering support. Mum, Dad, jet-pilot Mike and Danielle – I couldn't have dreamt of doing this without you.

List of Abbreviations

$[\alpha]_D$	specific rotation at 589 nm, 20 °C
°C	degree Celsius
Å	Ångstrom
4ÅMS	4 Ångstrom pore size molecular sieves
Ac	(C=O)CH ₃
Ac ₂ O	acetic anhydride
AcOH	acetic acid
AgOTf	silver triflate
aq	aqueous
Ar	aromatic
Araf	arabinofuranose
Arap	arabinopyranose
ATP	adenosine triphosphate
AuNP	gold nanoparticle
Bn	benzyl (C ₆ H ₅ CH ₂)
bp	boiling point
BSA	bovine serum albumin
BzCl	benzoyl chloride
<i>c</i>	concentration
CDCl ₃	d-chloroform
CHCl ₃	chloroform
COSY	homonuclear correlation spectroscopy
CuAAC	Cu(I)-catalysed azido-alkyne cycloaddition
<i>d</i>	doublet
DAST	diethylaminosulfur trifluoride
DBU	1,8-diazabicyclo[5.4.0]undec-7-ene
DCE	1,2-dichloroethane
DCM	dichloromethane
dd	doublet of doublets
DMAP	4-dimethylaminopyridine
DMF	<i>N,N</i> -dimethylformamide

DMSO	dimethyl sulfoxide
2D-NMR	two-dimensional nuclear magnetic resonance spectroscopy
Et ₂ O	diethyl ether
Et ₃ N	triethylamine
EtOAc	ethyl acetate
EtOH	ethanol
FCC	flash column chromatography
FTIR	Fourier transform infrared spectroscopy
g	grams
× g	times gravity
Gal	galactose
Gal _f	galactofuranose
Gal _p	galactopyranose
GalPUT	galactose-1-phosphate uridylyltransferase
GalU	glucose-1-phosphate uridylyltransferase
GC-MS	gas chromatography–mass spectrometry
GDP	guanosine diphosphate
Glc	D-glucose
GT	glucosyltransferase
HEPES	4-(2-hydroxyethyl)-1-piperazineethanesulfonic acid
Hex	n-hexane from petroleum distillate
HMBC	heteronuclear multiple bond correlation
HPLC	high performance liquid chromatography
HRMS	high resolution mass spectrometry
HSQC	heteronuclear single quantum coherence
HSQCed	edited heteronuclear single quantum coherence
Hz	Hertz
IgM	immunoglobulin M
IPP	inorganic pyrophosphatase
IR	infrared
<i>J</i>	coupling constant
K	Kelvin
kV	kilovolt
HPTLC	high performance thin layer chromatography

L	litre
LC	liquid chromatography
LC-MS	liquid chromatography–mass spectrometry
LDA	lithium diisopropylamide
LRMS	low resolution mass spectrometry
m	multiplet
M	molarity
mol	moles
m/z	mass to charge ratio
MALDI-TOF	matrix-assisted laser desorption ionization time of flight
Man	D-mannose
mCBPA	<i>meta</i> -chloroperoxybenzoic acid
MeOH	methanol
MeCN	acetonitrile
MHz	megahertz
min	minutes
MRM	multiple reaction monitoring
MQ	Milli-Q®
ms	milliseconds
MU	mass units
NaAsc	sodium ascorbate
NAD(P)H	nicotinamide adenine dinucleotide phosphate
NaOMe	sodium methoxide
NDP	nucleotide diphosphate
NIN	ninhydrin

R-NIN-PAA



note: R will be defined as necessary.

NMR	nuclear magnetic resonance
nOe	nuclear Overhauser effect
NOESY	nuclear Overhauser effect spectroscopy
NTP	Nucleotide triphosphate

PAA	phenylacetaldehyde
PbTx	brevetoxin
PCR	polymerase chain reaction
Pd/C	palladium (10%) on dried carbon
pH	$-\log_{10}c$, where c is the hydrogen ion concentration in mol/L
Ph	phenyl (C ₆ H ₅)
Pi	Inorganic phosphate
pK _a	acid dissociation constant
PPi	pyrophosphate
ppm	parts per million
n-PrOH	1-propanol
PRM-1	prymnesin-1
PRM-2	prymnesin-2
PRM-B1	prymnesin-B1
PRM-B2	prymnesin-B2
Pyr	pyridine
qPCR	quantitative polymerase chain reaction
R	generic group. Note: may be defined in the text.
R _f	retention factor
Ribf	ribofuranose
SAX	strong anion exchange
SPC	solid phase cytometry
t	triplet
t _R	retention time
T-7-HC	1,2,3-triazol-7-hydroxycoumarin
TBAF	tetrabutylammonium fluoride
TES	triethylsilyl
TFA	trifluoroacetic acid
THF	tetrahydrofuran
THP	tetrahydropyran
TLC	thin layer chromatography
TMS	trimethylsilyl
TMSOTf	trimethylsilyl trifluoromethanesulfonate
tol	toluene

UDP	uridine diphosphate
UEA	University of East Anglia
UTP	uridine triphosphate
UV	ultraviolet
UV-vis	ultraviolet–visible spectroscopy
Xylf	xylofuranose
Xylp	xylopyranose
δ	chemical shift
λ_a	absorption at give wavelength

General Experimental Conditions

Reagents and anhydrous solvents were supplied by Sigma Aldrich, and were used without further purification. Analytical grade solvents were supplied by Fischer Scientific. Protected sugars which were not synthesised the lab were supplied by Carbosynth. Glassware was oven-dried and purged with nitrogen immediately before use, and reactions requiring inert atmosphere were run under N₂.

Reactions were monitored by thin-layer chromatography (TLC) on aluminium-backed, pre-coated silica gel plates (Silica Gel 60 F254, E. Merk) with the indicated eluents, and the TLC plates were visualised under UV light (λ 254 nm) and charring by dipping in ethanol-sulfuric acid (95:5, v/v) followed by heating. Semi-preparative TLC was run on Analtech preparative uniplates (silica gel 1000 micron, 20 × 20 cm) and flash column chromatography (FCC) was performed on a Biotage Horizon Isolera One using pre-packed SNAP ULTRA 25 μ m silica gel cartridges.

NMR spectra were recorded using a Bruker Ultrashield Plus 400 spectrometer at 298 K and analysed using TopSpin 3.5pl5 software. Chemical shifts (δ) are reported in parts per million (ppm) with respect to internal tetramethylsilane or the residual HOD signal in D₂O. NMR assignments were made with the aid of COSY and HSQCed experiments

Optical rotation values were measured using a Perkin Elmer® Model 341 Polarimeter at 20 °C at a wavelength of 589 nm (sodium D line) unless otherwise noted. Infrared spectra were recorded using a Perkin Elmer® SpectrumBX and UV-vis spectra using a Varian 50 Bio spectrometer.

Low resolution mass spectrometry (LRMS) was employed for monitoring some reactions using an Advion Expression L CMS spectrometer by direct injection or extraction from a TLC plate using an Advion Plate Express, with methanol/formic acid (0.1%) (9:1) used as the mobile phase. For high resolution mass spectrometry (HRMS), the samples were diluted into methanol/formic acid (0.1%) (1:1) and infused into a Synapt G2-Si mass spectrometer (Waters, Manchester, UK) at 5-10 μ L min⁻¹ using a Harvard Apparatus syringe pump. The mass spectrometer was controlled by Masslynx 4.1 software (Waters). It was operated in high resolution and positive ion mode and calibrated using sodium formate. The sample was analysed for 2 min with 1 s MS scan time over the range of 50-1200 m/z with 3.5 kV capillary voltage, 40 V cone voltage, 120°C cone temperature. Leu-enkephalin peptide (1 ng μ L⁻¹,

Waters) was infused at $10 \mu\text{L min}^{-1}$ as a lock mass (m/z 556.2766) and measured every 10 s. Spectra were generated in Masslynx 4.1 by combining a number of scans, and peaks were centred using automatic peak detection with lock mass correction.

Ion exchange chromatography was performed using a Poros[®] HQ 50 strong anion exchange column on a Dionex[™] Ultimate 3000 HPLC system running Chromeleon[™] software. Sugar nucleotide profiling was performed using a Hypercarb[™] Porous Graphitic Carbon LC Column coupled to a Xevo[®] TQ-XS triple quadrupole mass spectrometer running Intellistart and MassLynx software. The column conditions and gradient details are given in the appropriate experimental sections.

Table of Contents

Abstract	iii
Acknowledgements	iv
List of Abbreviations	v
General Experimental Conditions	x
1 Introduction	1
1.1 Pymnesium parvum.....	2
1.1.1 Toxic blooms world-wide.....	2
1.1.2 Threat to fish stocks and food security.....	3
1.2 Toxins reported to be responsible – prymnesins	4
1.2.1 Prymnesin toxins.....	4
1.2.2 Toxicity studies.....	5
1.2.3 The biosynthesis of prymnesin toxins.....	8
1.2.4 Chemistry inspired by prymnesin toxins.....	11
1.3 P. parvum blooms on the Norfolk Broads.....	14
1.3.1 Blooms on Norfolk Broads	14
1.3.2 Spring 2015 P. parvum bloom on the Upper Thurne.....	16
1.3.3 Threat to tourism and leisure industry and local ecosystem.....	17
1.3.4 Current P. parvum mitigation strategy	18
1.4 Overview of the project	18
1.5 References	20
2 The chemoenzymatic synthesis of sugar nucleotides to explore the biosynthesis of prymnesin toxins	23
2.1 Introduction	24
2.1.1 Prymnesin Toxins	24
2.1.2 The origin of carbohydrates on prymnesin toxins	26
2.1.3 Sugar nucleotide profiling.....	28
2.1.4 Sugar nucleotide synthesis.....	29

2.2	D-Galactofuranose on prymnesin-1	31
2.2.1	Biosynthesis of galactofuanose in nature	31
2.2.2	Chemoenzymatic synthesis of UDP-D-galactofuranose	33
2.2.3	LC-MS analysis and profiling of UDP- α -D-Galf.....	36
2.3	Chemical tools for exploring the biosynthesis of L-xylofuranose	39
2.3.1	Possible biosynthetic pathway for L-xylofuranose on prymnesins.....	39
2.3.2	Chemical synthesis of 1,2-trans NDP-sugar standards	41
2.3.3	Preparation of NDP tetrabutyl ammonium salt.....	42
2.3.4	Chemical synthesis of 1,2-trans NDP-sugars.....	42
2.3.5	Sugar nucleotide profiling.....	45
2.4	Summary	48
2.5	Experimental	50
2.5.1	Enzymes	50
2.5.2	NDP-Sugar Purification.....	50
2.5.3	Sugar nucleotide profiling.....	50
2.5.4	Chemical Synthesis.....	51
2.6	References	64
3	Exploring the reactivity and spectroscopy of terminal bis-alkynes	67
3.1	Introduction	68
3.1.1	Alkynes in prymnes in toxins.....	68
3.2	Extracting prymnesin toxins from <i>P. parvum</i> cell cultures	71
3.3	Chemistry	73
3.3.1	Chemical synthesis of hepta-4,6-diyn-1-ol	73
3.3.2	Chemical synthesis of hepta-4,6-diyn-yl- β -D-galactoside	75
3.4	Evaluating the bis-alkyne as a biomarker for prymnesins.	78
3.4.1	Click Chemistry with synthetic toxin analogues.....	78
3.4.2	Click chemistry with prymnesin toxin extracts	82
3.5	Efforts towards the development of a Raman spectroscopy based prymnesin detection system.....	83
3.5.1	Raman spectroscopy and bis-alkynes	83

3.5.2	Raman Spectroscopy of 7-(Triethylsilyl)hepta-4,6-diyne-yl- β -D-galactoside (11)	85
3.5.3	Raman Spectroscopy of prymnesin toxin extracts.....	86
3.6	Summary	87
3.7	Experimental.....	88
3.7.1	Extraction of prymnesin toxins from <i>P. parvum</i> cell cultures.....	88
3.7.2	LC-MS detection of prymnesin toxins.....	88
3.7.3	Raman Spectroscopy.....	88
3.7.4	Chemistry	89
3.7.5	CuAAC coupling of prymnesin extracts with 3-azido-7-hydroxycoumarin	96
3.8	References	96
4	The chemical synthesis of glyceryl glycosides inspired by prymnesin toxins	99
4.1	Introduction	100
4.1.1	Carbohydrates present on reported prymnesin toxins	100
4.1.2	Target glyceryl glycoside fragments.....	105
4.2	Chemistry	106
4.2.1	Choosing a protected glycerol acceptor	106
4.2.2	Synthesis of 1,2-trans glyceryl glycoside fragments	108
4.2.3	Synthesis of 1,2-cis furanosyl glyceryl glycoside fragments	113
4.2.4	Synthesis of 1,2-cis glyceryl pyranoside fragments	123
4.3	Comparison of synthetic glyceryl glycoside fragments with literature toxin NMR values	125
4.4	Summary	126
4.5	Experimental.....	128
4.6	References:	149
5	Synthesis of a glycosylated prymnesin-1 inspired fragment with a view to developing an antibody based prymnesin toxin detection device	151
5.1	Introduction	152
5.1.1	Detection of <i>Prymnesium parvum</i>	152
5.1.2	Detection of polyketide algal toxins	152

5.1.3	Exploring antibody based prymnesin detection	154
5.2	Chemistry	157
5.2.1	Retrosynthetic analysis of toxin fragment	157
5.2.2	Synthesis of (2-R/S-Oxiranyl)methyl 2',3',5'-tri-O-benzoyl- α -L-arabinopyranoside	160
5.2.3	Epoxide ring opening to synthesise 3-(3-azidopropoxy)-2-hydroxypropyl 2,3,4-tri-O-benzoyl- α -L-arabinopyranoside	161
5.2.4	Synthesis of 3-(3-aminopropoxy)-2-(α -D-ribofuranosyloxy)propyl)- α -L-arabinopyranoside	163
5.2.5	Distinguishing between the (R)- and (S)- isomers of (14)	166
5.3	Summary	169
5.4	Experimental	171
5.4.1	Chemistry	171
5.5	References	179
6	Appendices.....	181
6.1	References	193

1 Introduction

1.1 *Prymnesium parvum*

Prymnesium parvum is a marine haptophyte which is ubiquitous in temperate and sub-tropical climates around the globe.¹ It is a unicellular alga which is usually 8-11 μm long and 4-6 μm wide (Figure 1.1).² *P. parvum* has two equal flagella of about 12-15 μm which it uses for mobility, and a haptonema of 3-5 μm which may be used for attachment.^{2,3} It is commonly known as 'golden algae' due to the gold yellow colour of blooms; this is a result of yellow pigments in the chloroplasts, which lie either side of the nucleus.⁴ *P. parvum* utilises chrysolaminarin (a mixed linkage β -1,3/6 glucan)⁵ instead of starch (an α -1,4/6 linked glucan used by plants) as the storage polysaccharide. It is a mixotroph, storing energy photosynthetically when in the euphotic zone (upper layer of a waterbody with sufficient light for photosynthesis) and heterotrophically by phagotrophy when presented with algal prey.⁶

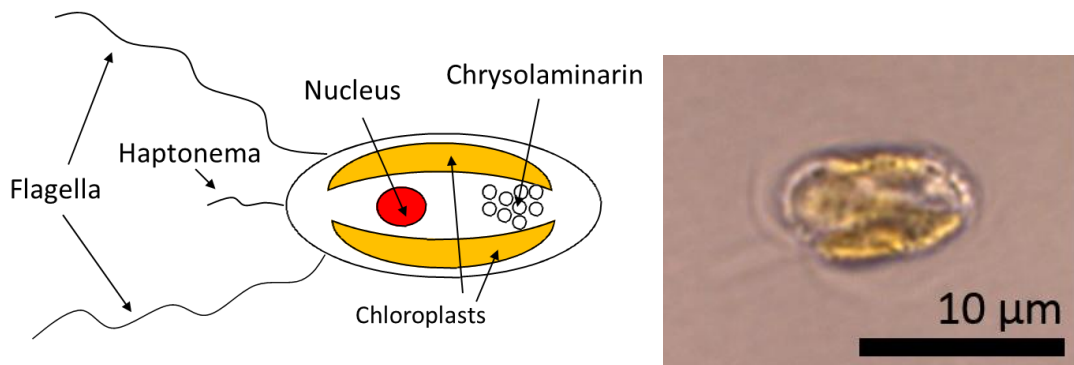


Figure 1.1 - Left: schematic overview of *P. parvum*; Right: Optical microscopy image of *P. parvum* (used with permission from Ben Wagstaff, John Innes Centre)

1.1.1 Toxic blooms world-wide

P. parvum has been linked to harmful algal blooms resulting in large scale fish kills all around the world (Figure 1.2). It is mainly found in cooler marine and brackish waters, and was first identified in Holland by Liebert and Deerns in 1920.⁷ It has since been attributed to numerous large scale fish kills which have been thoroughly reviewed by S. Watson at the Texas Parks and Wildlife department.⁴ What is striking is both the diversity in affected fish species and the geographical range of harmful *P. parvum* blooms. Despite being classified as a marine alga, there is also a steady increase in the occurrence of harmful *P. parvum* blooms in inland brackish water systems.¹ Whilst it is not immediately obvious why *P. parvum* is being found outside of the marine environment, proposed vectors for its introduction to

brackish systems include ship bilge water and encystment (the dispersion of dormant cysts which break down to active microbes under favourable conditions).^{2,8}

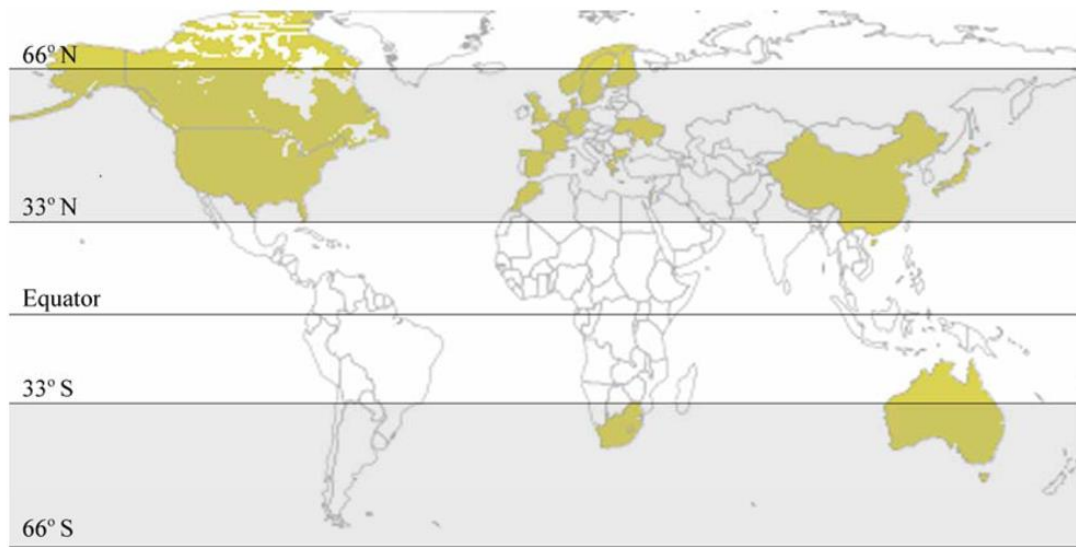


Figure 1.2 – The reported distribution of *P. parvum* around the globe. Image used under a Creative Commons Attribution 3.0 Unported (CC BY 3.0) licence from Manning, S.R.; La Claire, J.W., II. Pymnesins: Toxic Metabolites of the Golden Alga, *Prymnesium parvum* Carter (Haptophyta). *Mar. Drugs* **2010**, *8*, 678-704. Copyright 2010 S. Manning and J. La Claire.

1.1.2 Threat to fish stocks and food security

It is already well known that algal toxins can have serious impacts on food safety. Common examples include okadaic acid and brevetoxins which can cause diarrhetic and neurotoxic shell fish poisoning respectively.^{9,10} Whilst *P. parvum* doesn't appear to pose a direct threat to food safety because the toxin is specific to gill breathers, its ability to devastate fish stocks is alarming. Much recent research into *P. parvum* blooms has been focused on the impact on fish stocks in North America, and especially Texas.¹¹ Here it has had a huge impact on sports fishing, and has been attributed to the death of over 34 million fish and tens of millions of dollars' worth of damage in the one state alone. Moving away from sports fishing, *P. parvum* has the potential to deliver a devastating impact on food security globally. Global aquaculture provided 43% of aquatic animal food consumed by humans in 2007, and had a global value of \$98.5 billion in 2008.¹² Aquaculture is especially important in Asia, which accounts for 79% of the global market by value.¹² As the global population continues to increase, there will continue to be a move towards aquaculture as a way of producing sustainable levels of aquatic animals for human consumption. It is immediately obvious from Figure 1.2 that much of Asia lies within the northern zone where *P. parvum* blooms occur.¹

For this reason it is perfectly feasible that harmful *P. parvum* blooms could prove a real threat to global food security in the future.

1.2 Toxins reported to be responsible – prymnesins

1.2.1 Prymnesin toxins

The toxicity and associated threat to fish stocks in brackish waters of *Prymnesium parvum* has been known for over 50 years.¹³ Yariv and Hestrin coined the name ‘prymnesin’ for the cytotoxic material they noticed was excreted into the growth media of *P. parvum*. Over the subsequent 30 years there was much speculation into the structure of the toxin, with various authors claiming the toxin to be a saponin, proteolipid or carbohydrate.^{4,14} In 1996 Igarashi *et al.*¹⁴ published the first structure of prymnesin-2 isolated from an Israeli strain of *P. parvum*, the structure of which is shown in Figure 1.3. Prymnesin-2 has many noteworthy features, including a lipophilic head terminating in a vinyl chloride, a free amine, 14 polyether rings, several chlorines and a glycosylated tail terminating in a bis-alkyne. Igarashi *et al.*¹⁵ later reported *P. parvum* also produced a second more heavily glycosylated toxin which they named prymnesin-1. This new toxin shared a conserved backbone with prymnesin-2.

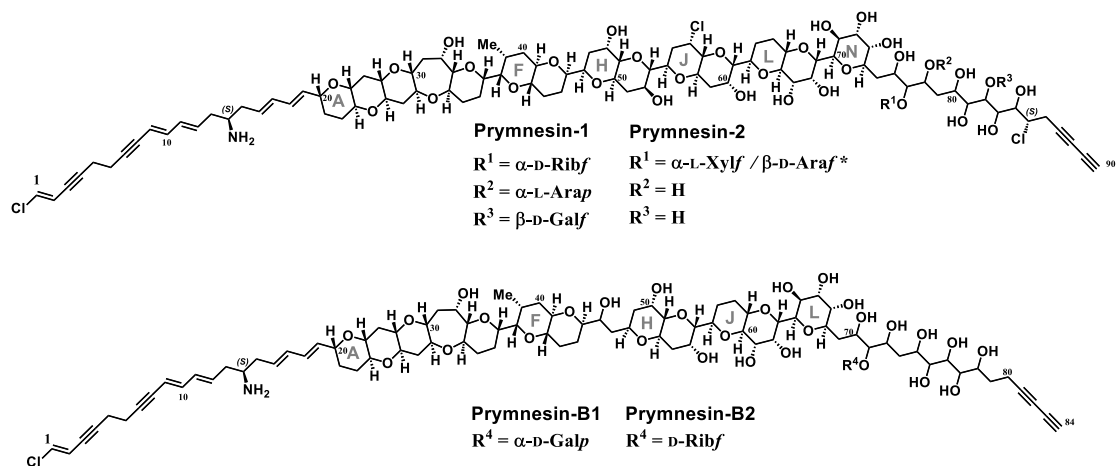


Figure 1.3 - The reported chemical structures of the prymnesin toxins. Prymnesin-1 and prymnesin-2 were originally reported by Igarashi *et al.*^{14,16} The structures of prymnesin-B1 and B2 were published by Rasmussen *et al.*¹⁷ *Rasmussen *et al.*¹⁷ have redrawn prymnesin-2 as being glycosylated with $\beta\text{-D-Araf}$ rather than $\alpha\text{-L-Xylf}$ as originally reported by Igarashi *et al.*¹⁴

It was noted in the literature that the newly published structures of prymnesin-1 and prymnesin-2 were not detectable in subsequent *P. parvum* blooms across the Southern states of the USA. Between 1999 and 2013 the only reported isolation and detection of prymnesin-1 and prymnesin-2 was achieved by La Claire *et al.*¹⁸ using LC-HRMS on *P. parvum* cell extracts from lab grown cultures. The use of toxin extracts of compounds soluble in polar organic solvents, rather than pure compounds for toxicity studies meant there was some debate in the literature as to whether prymnesin-1 and prymnesin-2 were the major toxic components of *P. parvum*; for example, fatty acids¹⁹ and fatty acid amides²⁰ were proposed as the major toxic components of *P. parvum*. However work by Blossom *et al.*²¹ has shown that the fatty acids and fatty acid amides reported were not ichthyotoxic at ecological concentrations. The same group has recently proposed that the reason that prymnesin-1 and prymnesin-2 had not been detected in *P. parvum* blooms in the USA was that there was structural diversity in prymnesin toxins between *P. parvum* strains from different locations.¹⁷ Rasmussen *et al.*¹⁷ went on to isolate and characterise a new set of prymnesin toxins from a Danish strain of *P. parvum* (K-0081), which they named prymnesin-B1 and prymnesin-B2 (Figure 1.3). The prymnesin-B toxins have subtle variations from the original prymnesin toxins: they are glycosylated with a different set of sugars and are missing the H-I polyether rings which are substituted with a -CH(OH)-CH₂ linker and the two alkyl chlorine atoms are replaced with hydroxyl groups. The lipophilic head and bis-alkyne tail are conserved, as are most of the polyether rings. Having isolated and characterised prymnesin-B1 and B2, Rasmussen *et al.*¹⁷ screened 10 strains of *P. parvum* from around the globe by LC-MS and found one produced the prymnesin-1/2 backbone and five produced the prymnesin-B1/B2 backbone. They also indicated that LC-MS suggested the presence of a third type of triply chlorinated prymnesin.¹⁷ Work by our group with natural samples collected during a recent harmful algal blooms has shown that the strain of *P. parvum* present in the Norfolk Broads also produces prymnesin-B1/B2 (ongoing unpublished work).

1.2.2 Toxicity studies

Prymnesins are characterised as extracellular ichthyotoxins, although their physiological purpose is unclear.¹ It has been suggested that it may be defence related.³ For example, Tillmann³ has investigated the interaction between *P. parvum* and the heterotroph *Oxyrrhis marina* and found that under low toxicity conditions (nutrient-deficient cultures, low *P. parvum* cell counts and low light conditions) *O. marina* was able to graze on *P. parvum*.

However under high toxicity conditions (nutrient-normal cultures, higher *P. parvum* cell counts and ambient light) *O. marina* was observed to swell and lyse, and the debris were ingested by *P. parvum*.

The exact mechanism of toxin release into waterways unclear, and it is perhaps strange that both toxic and non-toxic blooms of *P. parvum* have been reported.²² This suggests that there may be an ecological trigger which causes toxin release, and conditions such as light, pH, nutrient availability and temperature have all been explored.^{1,4} It has recently been suggested by Wagstaff *et al.*²³ from our group that this toxicity is due to the mass collapse of a *P. parvum* population by cell lysis caused by viral infection of the algae by the newly discovered megavirus *Prymnesium parvum* DNA virus BW1 (ppDNAV) (Figure 1.4).

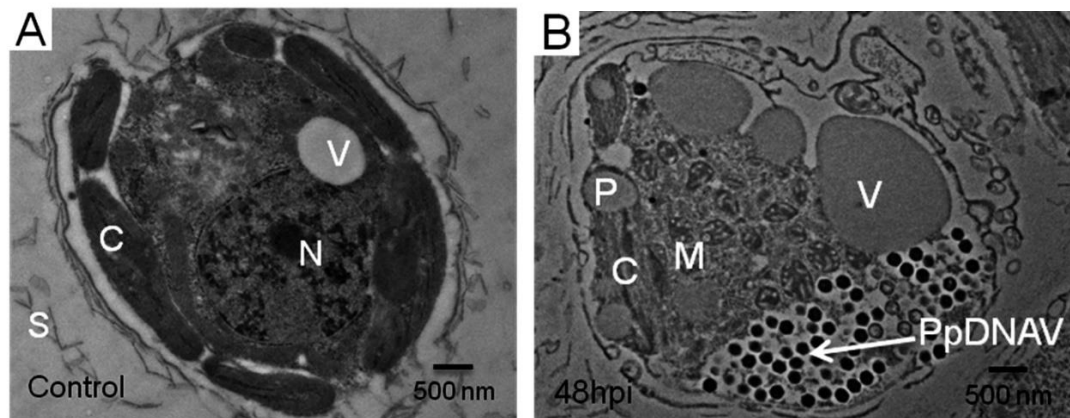


Figure 1.4 - A) thin section of a health *P. parvum* cell; B) Thin section of a *P. parvum* cell 48 hours post infection with PpDNA virus BW1. Figure used under a Creative Commons Attribution 4.0 Unported (CC BY 4.0) licence and adapted from Wagstaff, B.A.; Vladu, I.C.; Barclay, J.E.; Schroeder, D.C.; Malin, G.; Field, R.A. Isolation and Characterization of a Double Stranded DNA Megavirus Infecting the Toxin-Producing Haptophyte *Prymnesium parvum*. *Viruses* **2017**, *9*, 40.

The first study conducted with isolated prymnesin-1 and prymnesin-2 was by Igarashi *et al.*¹⁶ who performed haemolytic and ichthyotoxic assays. They also assessed the intravenous LD₅₀ concentration for mice, as well as Ca²⁺ influx assays and antifungal assays. It was found that that the haemolytic potency HC₅₀ (the toxin concentration required to cause 50% haemolysis as determined by a concentration-absorbance response curve) for PRM-2 ranged from 0.5 nM with dog red blood cells through to 2.5 nM for mice. The ichthyotoxic assay showed a strong enhancement of the toxicity of prymnesin-2 with increased Ca²⁺ concentration and elevated pH. At pH 8.0 and 2 mM Ca²⁺ the LC₅₀ against the fresh water fish *Tanichthys albonubes* was found to be 3 nM, which is twice as potent as brevetoxin-3 (Figure 1.5).¹⁶

Igarashi *et al.* also noted some clues as to the mode of toxicity. First, protonation or acetylation of the free amine group on prymnesin-2 (Figure 1.3) led to a dramatic loss of ichthyotoxicity. They therefore determined that the mode of toxicity required the free amine group to act as a proton acceptor. Second, the addition of the lipids sphingomyelin and cholesterol reduced the haemolytic activity of the toxin, suggesting a direct action on cell membranes by the toxin. Third, the large Ca^{2+} dependence on ichthyotoxicity led the authors to cite the possibility of toxin interaction with Ca^{2+} ATPase which is a Ca^{2+} active-transporter enzyme located in cell membranes. Cation-pore formation²⁴ at elevated pH may lead to the elevated concentration of Ca^{2+} ions in cells affected by prymnesins; the impaired activity of the calcium pump means the cell is unable to lower this ion concentration, leading to cell death.

A more recent toxicity study by Rasmussen *et al.*¹⁷ compared the toxicity of prymnesin-2 with their newly characterised toxin prymnesin-B1. A dose-dependence assay was performed with rainbow trout-gill-W1 cells to assess cell viability with toxin exposure. This showed a half maximal effective concentration (EC_{50}) for prymnesin-2 of 0.92 nM and prymnesin-B1 of 5.98 nM. The authors speculated that all prymnesins are ichthyotoxins, and it is mixtures of several of these toxins that are responsible for many recent global fish kills.¹⁷

Prymnesins are not the only polyketide extracellular algal toxins. Some examples of well documented algal toxins in the literature include okadaic acid,⁹ brevetoxins²⁵ and maitotoxin²⁶ (Figure 1.5). Okadaic acid is a cytotoxin produced by several dinoflagellates which cause diarrhetic shell fish poisoning.⁹ Maitotoxin is a very large and very potent polyketide toxin derived from the dinoflagellate *Gambierdiscus toxicus*. Like prymnesins it is a calcium channel antagonist, and it exhibits mouse toxicity at 0.13 $\mu\text{g}/\text{kg}$.²⁷ Finally brevetoxins which are derived from the dinoflagellate *Karenia brevis* (formerly *Gymnodinium breve*) are a suite of neurotoxins.¹⁰ There is a marked similarity between the rings system A-E in prymnesin-1/2 and brevetoxin-B. Igarashi *et al.*¹⁶ also used brevetoxin-3 (PbTx-3) as an ichthyotoxin control for prymnesin toxicity studies, where they showed that when Ca^{2+} concentrations reached 3 nM, the toxicity of prymnesin-2 was twice that of PbTx-3, with the latter not showing any calcium dependence on toxicity.

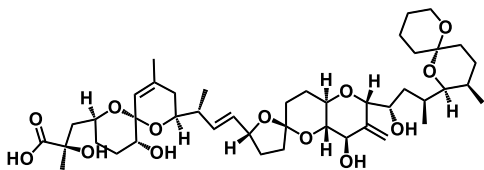
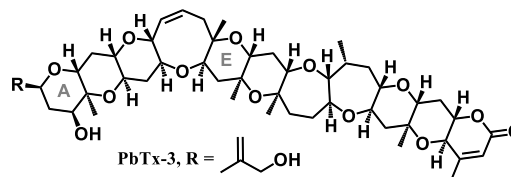
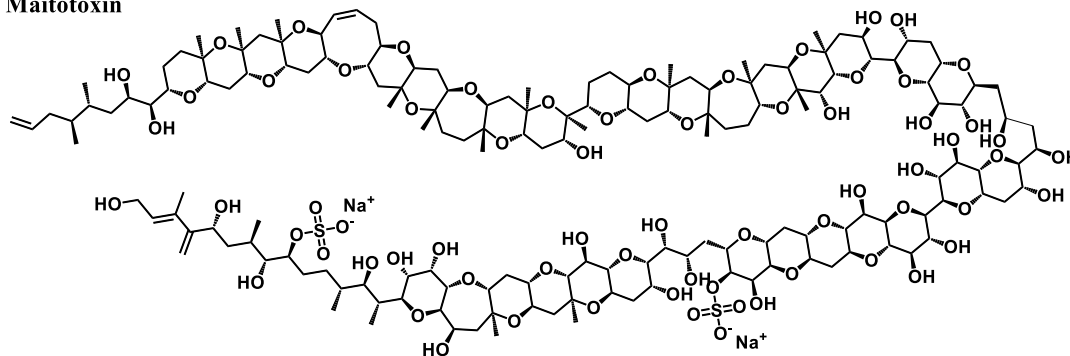
Okadaic Acid**Brevetoxin-B****Maitotoxin**

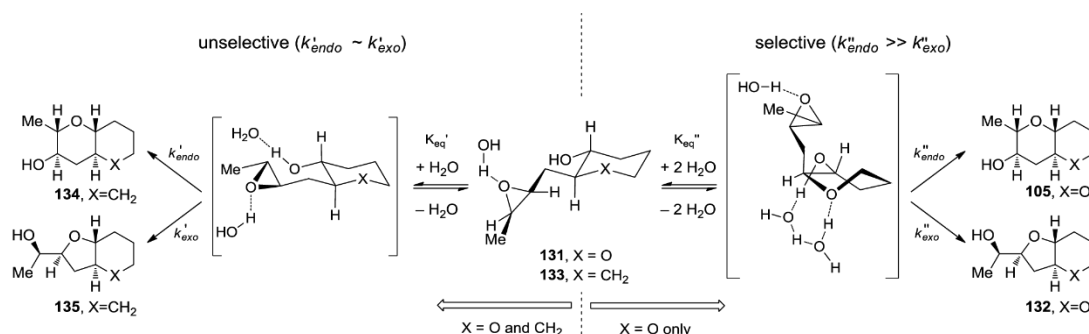
Figure 1.5 – Some examples of other algal polyketide toxins; Okadaic Acid⁹, Brevetoxin-B²⁵ and Maitotoxin.²⁶

1.2.3 The biosynthesis of prymnesin toxins

There is very little information in the literature about the *in vivo* synthesis of prymnesin toxins, although La Claire *et al.*¹ noted that it is ‘very likely’ that prymnesins are derived from acetate-related metabolism based on their structural similarity to other cyclic polyether toxins. Much of what is published is derived from comparison of prymnesins with similar algal polyether ladder toxins such as brevetoxins and maitotoxins. Like these toxins, prymnesins have *trans*-fused cyclic ether rings in the backbone structure, which coupled with the lack of aromatic rings is indicative of polyketides made by type 1 polyketide synthases.^{1,28} Polyketide synthases perform successive condensation reactions of carboxylic acid derived extension units to a growing acyl chain, and may also perform some post-condensation reactions.²⁸

Following the elucidation of the structure of brevetoxin, Nakanashi²⁹ proposed a cascade epoxide ring opening reaction as the biosynthetic mechanism for the polyether ladder in that toxin. This seemed to be in contradiction of Baldwin’s rules of ring closure which, based on stereoelectronic considerations, would favour an epoxide ring opening cascade via the 5-exo-tet intermediate.³⁰ It was not until recently that Vilotijevic and Jamison³¹ noted that neutral water acts as a critical promotor for guiding *endo* selectivity during the ring opening

cascade (Scheme 1.1).³¹ The authors also noted that if the tetrahydropyran (THP) ring oxygen was replaced with CH₂ then the *endo* selectivity was lost



Scheme 1.1 – Mechanism for the *endo* stereoselectivity of cyclisation of templated epoxides in neutral water. Figure used under a Creative Commons Attribution 3.0 Unported (CC BY 3.0) licence and adapted from Vilotijevic and Jamison, Synthesis of marine polycyclic polyethers via *endo*-selective epoxide-opening cascades, *Marine Drugs*, **2010**, *8*, 763-809. © 2010 Vilotijevic and Jamison.

The importance of the THP ring oxygen in ensuring *endo* ring closing selectivity was attributed to two factors.³¹ First the electron withdrawing effect of the ring oxygen is likely to reduce the nucleophilicity of the THP ring alcohol, which electronically biases it towards *endo* attack of the epoxide. Second, as the reaction with the THP ring oxygen present is second order in water, it may be that the THP ring oxygen can facilitate a twist boat intermediate by hydrogen bonding with water, which better sets up the alcohol for *endo* attack of the epoxide.

A tentative epoxide ring opening cascade for the cyclic polyether backbone of prymnesins-1/2 is shown in Figure 1.6. For the ring system A-E, the epoxide opening follows the same mechanism as for brevetoxins. The epoxide at the junction between rings E and F must be *cis* to maintain the corrected stereochemistry.³² This however does not seem correct, given the *trans* orientation of every epoxide on the speculative biosynthesis of brevetoxins, as well as the *trans* orientation of every other epoxide in Figure 1.6. It also leads to the opposite rotamer to that published Sasaki *et al.*³² between the protons on C36 and C37 (at the junction between the E & F rings).

Working back from the reactive epoxide intermediate, a corresponding unsaturated backbone is also proposed in Figure 1.6. Again, note that there is only one *cis*-alkene, whilst all other double bonds are *trans* orientated as might be expected.

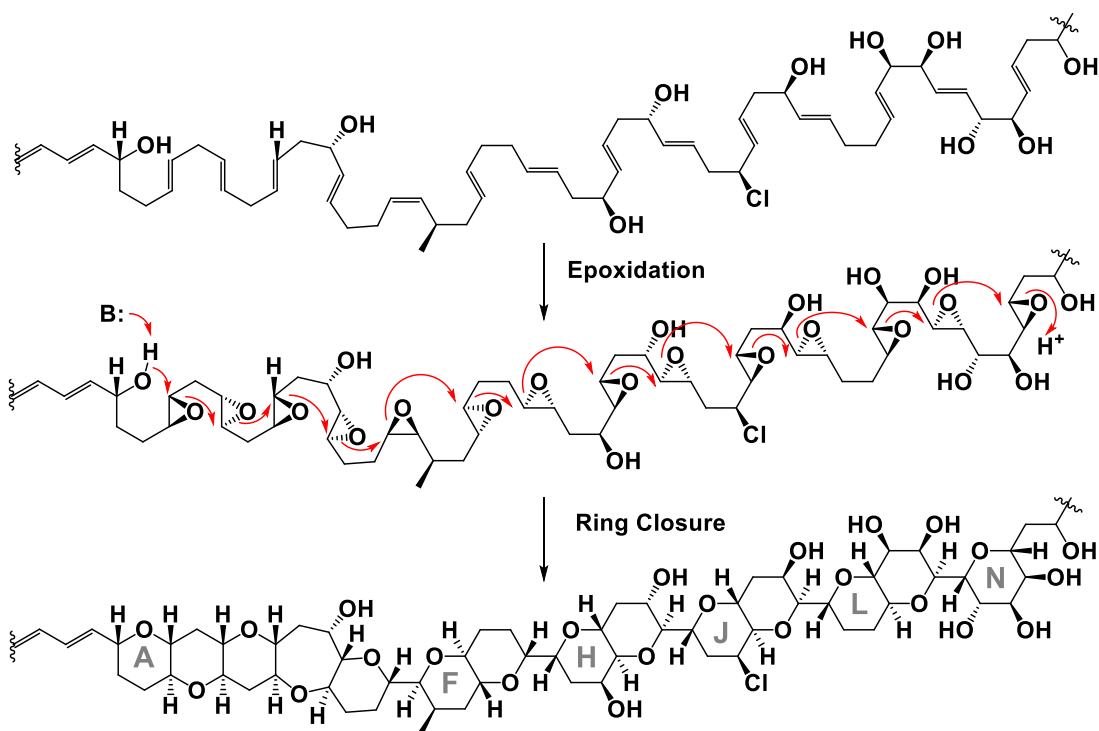
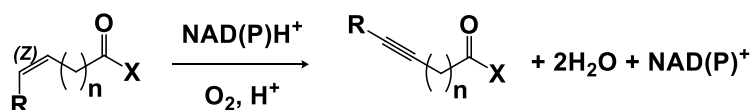


Figure 1.6 - A tentative proposal for an epoxide ring opening cascade which might synthesise the polyether backbone of prymnesins-1/2.^{28,31}

The terminal bis-alkyne found on all prymnesin toxins will be of interest in Chapter 3. Acetylenic bonds in polyketide derived metabolites are usually derived from a reductive pathway as shown in Scheme 1.2.³³ The literature offers very little insight into the biosynthesis of the terminal alkyne found on prymnesins. Zhu *et al.*³⁴ have recently characterised the first protein bound desaturase responsible for the biosynthesis of the terminal alkyne found on jamacamide B, a polyketide cytotoxin produced by the marine cyanobacteria *Moorea producens*. The authors noted that the introduction of ferredoxinase or NADPH increased the activity of the desaturation enzyme (JamB) by about 35%, indicating that ferredoxin is the likely electron donor for the desaturation reaction.



Scheme 1.2 – Iron-catalysed dehydration of the alkene with molecular oxygen.³³

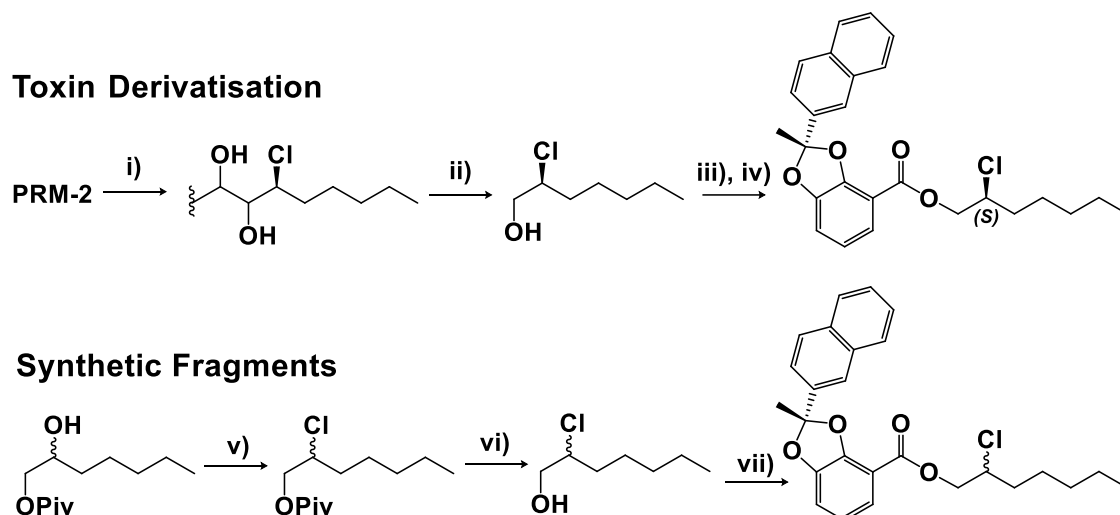
Prymnesins are all reported to be glycosylated with a range of different carbohydrates.^{15,17} Glycosylation can significantly increase the solubility of compounds in water.³⁵ In the case of prymnesins, it might be imagined that the glycosylated end of the toxins leads to a lipophilic head and a polar tail, much like a detergent molecule.¹ As such it has been suggested that prymnesins can form micelles, which in turn can aggregate in cell membranes to create negatively charged pores which are permeable to cations.^{1,13} Glycosylation of the prymnesin backbone is most likely achieved via the Leloir pathway after the biosynthesis of the polyketide backbone is complete. A glycosyltransferase will take an activated sugar nucleotide donor and place the sugar onto the appropriate hydroxyl group on the toxin backbone.³⁶ There is little insight in the literature into the specific enzymes responsible for the glycosylation of prymnesin toxins, and Chapter 2 discusses the synthesis of sugar nucleotide standards for use in a *P. parvum* sugar nucleotide profiling project.

1.2.4 Chemistry inspired by prymnesin toxins.

Initial chemistry relating to prymnesin toxins focused on their modification to assist in the elucidation of their structures. In their initial structural elucidations Igarashi *et al.*^{14,15} acetylated the toxin amine to aid solubility for NMR studies. They also went on to acetylate the free alcohols to locate the hydroxyl groups by changes in ¹³C NMR chemical shifts. The hydrolysed sugars were also trifluoroacetylated for GC analysis. Igarashi *et al.*¹⁶ also used *N*-acetylation during toxicity studies to show that without the free amine, the ichthyotoxic effects of prymnesin-2 were essentially lost.¹⁶

The free amine at C14 which is present on all reported prymnesin toxins has been used as a chemical handle for the semi-quantification of toxin concentration. La Claire *et al.*³⁷ have published a fluorometric assay which covalently labels free amine on prymnesin-1/2 with ninhydrin (NIN) combined with phenylacetaldehyde (PAA). This PRM-NIN-PAA complex is fluorescent and as such can be used to semi-quantify toxin levels. Rasmussen *et al.*¹⁷ have also utilised the direct covalent labelling of the primary amine on prymnesins-1/2 and prymnesin-B1 with 6-aminoquinolyl-*N*-hydroxysuccinimidyl carbamate (Acc-Q tag), and the concentration of the fluorescent toxin derivative was calculated against an external standard.

Synthetic fragments of prymnesin toxins were first made and used by Morrohashi *et al.*³⁸ to elucidate the stereochemistry at the C14 and C85 positions of prymnesin-2. This work was published a couple of years after the initial elucidation of the polyether ring stereochemistry of the toxin backbones was published.¹⁵ The C85 position of prymnesins-1/2 is functionalised with a chlorine atom (Figure 1.3). The stereochemistry of the chlorine atom was determined by comparing HPLC of the chiral fluorescent ester derived from a fragment of authentic toxin with corresponding synthetic compounds (Scheme 1.3).

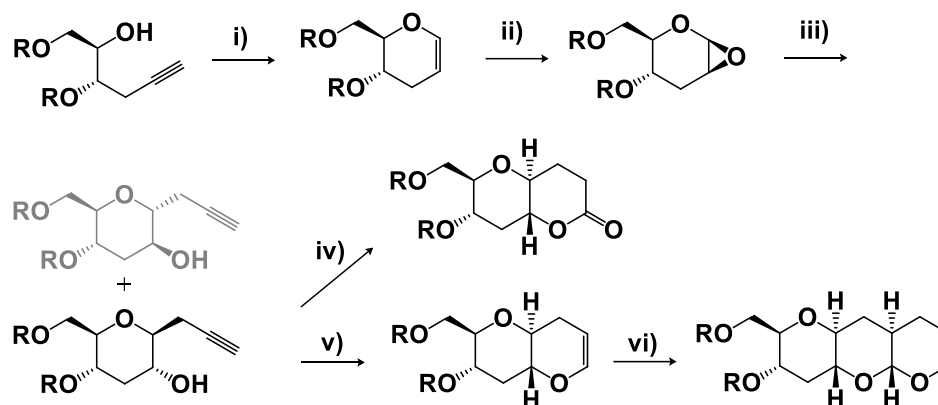


Scheme 1.3 – Key synthetic steps employed by Morrohashi *et al.*³⁸ to determine the absolute stereochemistry of the chlorine atom at position on C85 for prymnesins-1/2. i) H₂, Pd.OH, PrOH/H₂O; ii) NaOCl₄, MeCN; iii) NaBH₄, MeCN; iv) (*S*)-MNB-COOH, EDC, DMF, NEt₃, DCM; v) CCl₄, Ph₃P, DCM, 130 °C; vi) DIBAL, DCM, 0 °C; vii) (*S*)-MNB-COOH, EDC, DMF, NEt₃, DCM.

Morrohashi *et al.*³⁸ also determined the stereochemistry of the free amine at position C14 by amidation with (*S*)- and (*R*)- methoxy-(2-naphtyl)acetic acid (2MNA). They noted that Trost *et al.*³⁹ had reported that the absolute configuration of chiral amines is correlated to the relative change in ¹H NMR shifts observed for the diastereotopic amides formed with (*S*)-2MNA. Building on this work, they compared the ¹H NMR shifts for prymnesin-2 covalently *N*-labelled with (*R*)-2MNA and (*S*)-2MNA and used these to assign the absolute configuration of the amine at C14.

Trost and Rhee⁴⁰ have demonstrated the synthesis of the AB ring fragment in prymnesins using ruthenium catalysed cycloisomerization and oxidative cyclization. The methodology (outlined in Scheme 1.4) is based around the cycloisomerisation of bis-homopropargylic alcohols, which may be used to iteratively build up polycyclic ethers or alternatively oxidised

to a cyclic ketone for further modification.⁴⁰ The authors also utilised their methodology to synthesis a ring fragment from the polyether toxin yessotoxin.



Scheme 1.4 – The key steps in Ru catalysed synthesis of transfused polycyclic ethers from Trost and Rhee.⁴⁰ i) CpRu(PR₃)₂Cl, R₃P, (C₄H₉)₄NPF₆, *N*-hydroxysuccinimide sodium salt, DMF, 85 °c; ii) DMDO, DCM, -78 °c; iii) H₂C=C=C-MgBr; iv) Ru, NHS; v) CpRu(PR₃)₂Cl, R₃P, (C₄H₉)₄NPF₆, *N*-hydroxysuccinimide sodium salt, DMF, 85 °c; vi) repeat ii) – vi). R = 4-fluorophenyl.

Three sets of ring systems inspired by the polyether backbone of pymnesins-1/2 have been chemically synthesised by Sasaki *et al* (Figure 1.7).^{32,41,42} The group started with the synthesis of the HI/JK ring system.⁴¹ The ¹H and ¹³C NMR for HI/JK analogue were found to be in agreement with the literature values for the analogous region of the whole toxin, confirming the earlier assignment. Next the group synthesised the CDE/FG ring system.³² The group noted a difference of around 1 ppm in the ¹³C NMR spectrum between C36 and C37 in the whole toxin and the analogous carbons in the synthetic ring system. By contrast inversion of the stereochemistry at C37 in the synthetic analogue brought the ¹³C NMR shifts to within 0.5 ppm of the published whole toxin spectrum. It was also noted by the authors that this inversion led to coupling constants for the synthetic analogue of $J_{37/38} = 9.0$ Hz and $J_{38/39} = 2.5$ Hz which was in very close agreement with the published spectrum for pymnesin-2.¹⁵ As such the authors recommended the reassignment of the stereochemistry at C37. Finally the group synthesised the JK/LM ring system, with the NMR values for the synthetic confirming the original structural elucidation for the whole toxin.⁴²

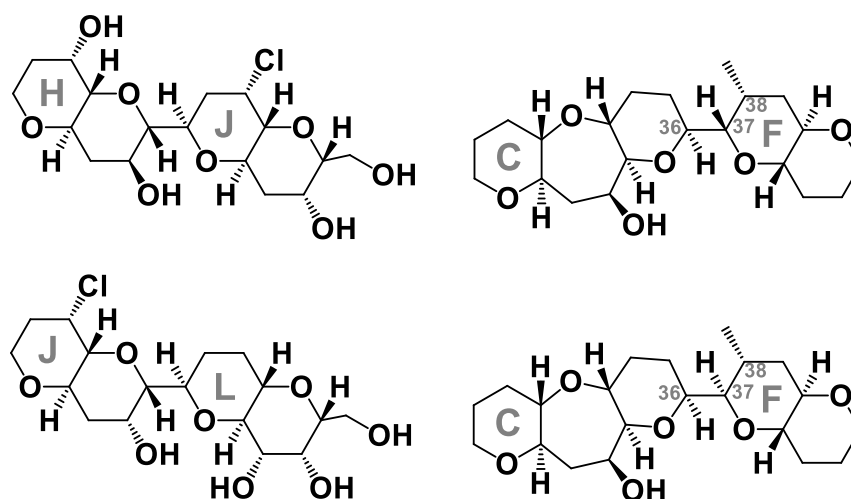


Figure 1.7 - Ring systems inspired by prymnesins-1/2 synthesised by Sasaki *et al.*^{32,42} Clockwise from top left: HI/JK ring system⁴¹; CDE/FG ring system with *anti* linkage between E/F rings; CDE/FG ring system with *syn* linkage between E/F rings,³² JK/LM ring system.⁴²

1.3 *P. parvum* blooms on the Norfolk Broads

1.3.1 Blooms on Norfolk Broads

The Norfolk Broads are the United Kingdom's largest protected inland wetland, and became a national park in 1989. Situated in East Anglia, they cover an area of over 300 km² between Norwich to the west and Great Yarmouth and Lowestoft to the east (Figure 1.8), which drains into seven rivers and over 50 individual shallow lakes or 'broads'.²² The broads are believed to be the result of medieval peat diggings which subsequently flooded, and range in size from a couple of hectares up to Hickling Broad, which is the largest at over 140 hectares.^{43,44}

P. parvum is of concern on The Norfolk Broads which are local to our research group in the East of England. Despite being a marine toxin, *P. parvum* can persist in the Norfolk Broads due to the brackish nature of the waters, which results from regular tidal surges, as well as the drainage to saline marshes for agricultural use.²² There are historic anecdotal records of large scale fish kills on the Thurne system coinciding with a brown colouration of the water (which could be attributed to a *P. parvum* bloom) in 1894, 1911, 1914, 1925, 1934, 1954, 1966, and 1967.²² Bales *et al.*⁴⁵ noted that there were several large-scale fish kills on the Upper Thurne system of the Norfolk Broads attributed to blooms of *P. parvum* between 1969 and 1975. This coincided with a loss of aquatic plant life and an explosion in phytoplankton populations, which was attributed to guano from high populations of blackheaded gulls (*Larus ridibundus*).⁴⁵ There was also a phosphate contribution to the waterways by

agricultural run-off. Since the 1970s there has been an effort to reduced phosphate levels in the Broads by reducing the discharge of sewage effluent into the waterways.⁴⁶ Whilst this has been somewhat successful, it has been noted by Phillips *et al.*⁴⁶ that the release of phosphate into the Broads can be an order of magnitude higher from sediment disturbance than that from catchment sources.

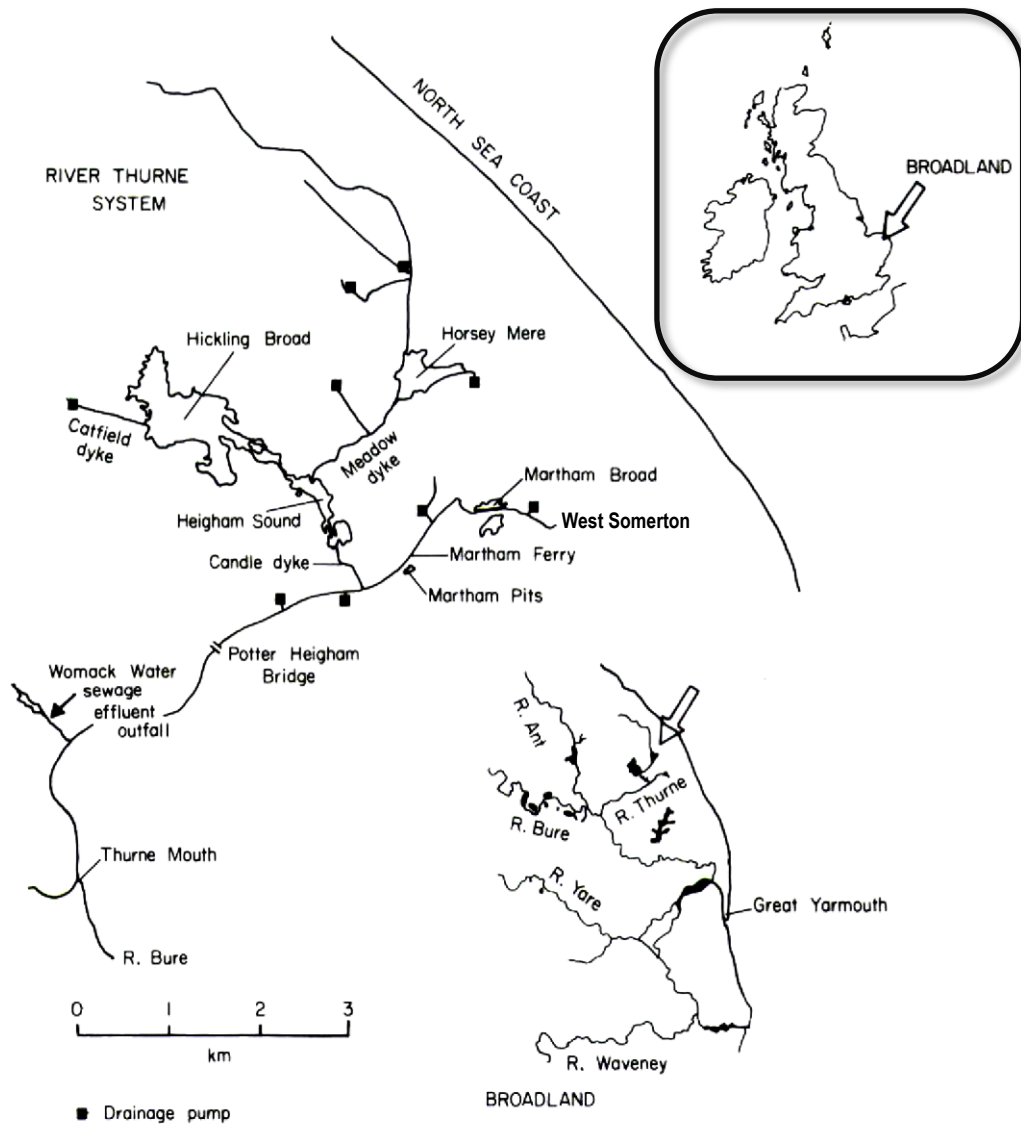


Figure 1.8 – The location of the Norfolk Broads and River Thurne system. Reprinted (adapted) with permission from P. Holdway *et al.*, *Freshwater Biology*, **1978**, 8, 295-311. Copyright 1977 John Wiley and Sons.

Whilst there has been drainage of marshes near to the sea-wall for well over a century, the intensity of pumping has increased significantly with the introduction of electric pumps in the 1960s.⁴⁵ With this came an increase in the salinity of the Broads. The brackish nature of the broads has been beneficial to marine algae in the water system such as *P. parvum*. It has been noted by Igarashi *et al.*¹⁶ that prymnesins are much more potent ichthyotoxins in the presence of elevated Ca^{2+} levels, and so the increased salinity of the Broads may have contributed to an exacerbation of the toxicity of harmful *P. parvum* blooms.

1.3.2 Spring 2015 *P. parvum* bloom on the Upper Thurne

The most recent significant fish kill attributed to *P. parvum* occurred in March 2015 in the Upper Thurne System at West Somerton, Martham, Horsey and Hickling (Figure 1.8). It was estimated that 300-400 fish were killed and 230,000 were relocated to safer waters by the Environment Agency.⁴⁷ When the harmful algal bloom occurred there was no program of actively monitoring *P. parvum* levels in the waterways, with *P. parvum* cell counts only being checked by optical microscopy when the navigable channels were maintained by dredging. The lack of active monitoring meant the Environment Agency was reliant on its public incident telephone number for being made aware of the problem, by which time there were already fish dying in the water.

The mitigation strategy employed in the March 2015 blooms relied solely on the relocation of fish from the affected areas (Figure 1.9). When we attended the site it was noted by Environment Agency staff that the fish were shoaling as though trying to move away from the algae, which resulted in them being trapped in large shoals at the far ends of the staithe. During these blooms optical microscopy of samples taken by us showed the presence of *P. parvum* in the staithe. Furthermore liquid chromatography-mass spectrometry (LC-MS) analysis of extracts prepared from the gills of a deceased pike* (*Esox Lucius*) recovered from Hickling staithe were found to contain the toxin prymnesin-B1.^{17,18}

* The gills were removed at the staithe and taken back to our lab in Norwich. They were freeze ground in liquid nitrogen to a white powder and then extracted in a manner analogous to that described by La Claire *et al.*¹⁸ for extracting prymnesin toxins from harvested *P. parvum* lab cultures. At the time we could not detect prymnesins-1/2 by LC-MS. However the following year Rasmussen *et al.*¹⁷ published the structure of newly discovered prymnesin-B1. On revisiting our LC-MS data we could detect the characteristic peaks for prymnesin-B1.



Figure 1.9 - The relocation of fish from the Upper Thurne river system by the Environment Agency (March 2015). Clockwise from top left: 1) An example of the dead fish found at Hickling Staithe; 2) Netting of fish in the affected area. Note the pump to try to maintain suitable dissolved oxygen levels for the high volume of fish; 3) Environment agency staff moving alive fish into oxygenated tanks on the back of trailers; 4) Road transport of netted fish to safer waters.

1.3.3 Threat to tourism and leisure industry and local ecosystem

In addition to the ecological impact of harmful *P. parvum* blooms in the Norfolk Broads, there are also severe economic impacts for the tourism and leisure industries. The Norfolk Broads were designated a national park in 1989, and in 2017, despite having a permanent population of only 6,350 people, were estimated to draw over 7 million visitors and contribute in excess of £550 million per annum to the local economy, mainly through angling, boating and tourism.⁴⁸ Although the fish found in the Norfolk Broads are no longer commercially caught for food, the Norfolk Broads are a popular leisure destination for anglers. It is therefore obvious from the local economic benefit that it is of great concern locally to maintain healthy fish stocks in the Norfolk Broads.

1.3.4 Current *P. parvum* mitigation strategy

Until recently cell counting has been the only method of measuring *P. parvum* levels in the Norfolk Broads. There is however now ongoing qPCR based monitoring of *P. parvum* populations being carried out by J. Pratscher and co-workers at the University of East Anglia (UEA). However, as it is possible to have non-toxic *P. parvum* blooms,²² elevated cell counts are not necessarily a reason to move fish, and so the Environment Agency can only act once there is clear evidence of dead or dying fish. It would therefore be useful for all parties with a vested interest in maintaining healthy fish populations in the Norfolk Broads to have a portable system for the rapid detection of prymnesin toxins, rather than relying solely on algal cell counts.

1.4 Overview of the project

The emphasis of the project is on the synthesis of toxin fragments and related chemical tools, focussing on the terminal bis-alkyne and glycosylated regions of prymnesin toxins. These tools will then be used to learn more about the biosynthesis of the prymnesin toxins, as well as working towards the development of a portable toxin detection device for use on the Norfolk Broads. The project is split into four main sections.

1. The synthesis of sugar nucleotides relevant to prymnesin toxins for use as standards in an ongoing algal sugar nucleotide profiling project within the group. Prymnesin-1 is reported to be glycosylated with D-galactofuranose, and the synthesis of the corresponding sugar nucleotide as a standard for the project is described.¹⁵ Prymnesin-2 is reported to be glycosylated with L-xylofuranose.¹⁴ The literature offers no insight into the biogenesis of L-xylofuranose, and so a possible biosynthetic pathway for a suitable L-xylofuranose sugar nucleotide was proposed by Ben Wagstaff in the group. The chemical synthesis of the sugar nucleotide intermediates in this proposed pathway is described.
2. An investigation into whether the rare terminal bis-alkyne found on prymnesin toxins could be used as biomarker for the detecting and quantification of toxin levels in waterways without having to use expensive LC-MS equipment was performed.³⁷ Due to the reported difficulties in obtaining large quantities of prymnesin toxins,¹⁷ synthetic bis-alkyne fragments were chemically synthesised as substitutes. These were then used to evaluate the suitability of copper(I) catalysed alkyne-azide

cycloaddition (CuAAC) 'click' reactions of the bis-alkyne with an azide functionalised fluorophore.⁴⁹ Similar experiments were repeated with LC-MS verified toxin extracts. The synthesis of these fragments and fluorescent dye is described, and the suitability of CuAAC as a method of rapid toxin detection is explored. The synthetic bis-alkyne toxin fragments were also used to assess the suitability of the terminal bis-alkyne towards a Raman spectroscopy based detection system.⁵⁰ Bis-alkynes are reported to give very strong Raman signals in otherwise cellular silent regions, and Raman spectroscopy is compatible with aqueous solvent.⁵¹

3. The chemical synthesis of a library of sugar-glycerol compounds inspired by the reported sugars found on prymnesin toxins is described. This relies on a variety of glycosylation techniques, as a range of pyranoses and furanoses with both 1,2-*cis* and 1,2-*trans* glycosidic linkages are required.⁵² Glycerol is chosen as a simplified version of the prymnesin backbone, and is glycosylated at the 2° position with the sugars reported as being present on prymnesin toxins. The synthetic sugar-glycerol fragments are then compared with literature spectra for the whole toxin.
4. Drawing on experience gained in synthesising sugar-glycerol fragments, the synthesis of two larger diglycosylated prymnesin-2 fragments is described. It is hoped that these fragments might prove useful for raising prymnesin-1 specific antibodies, and if so the fragment could also be incorporated into a lateral flow device (dip-stick) for rapid toxin detection in waterways.⁵³ Such a device would be useful to the Environment Agency and those with a vested interest in the ecology of The Broads. Because of the ambiguity in the stereochemistry of the backbone in the glycosylated region of prymnesin toxins, two diastereotopic fragments are required. These fragments need to be glycosylated with L-arabinopyranose and D-ribose, and incorporate a suitable cross-coupling group for conjugation to a carrier protein.

1.5 References

1. S. R. Manning and J. W. La Claire, *Mar. Drugs*, 2010, **8**, 678–704.
2. J. Green, D. Hibberd, and R. Pienaar, *Br. Phycol. J.*, 1982, **17**, 363–382.
3. U. Tillmann, *Aquat. Microb. Ecol.*, 2003, **32**, 73–84.
4. S. Watson, *Literature Review of the Microalga *Prymnesium parvum* and its Associated Toxicity*, Texas Parks and Wildlife Department, 2001.
5. A. Beattie, E. L. Hirst, and E. Percival, *Biochem. J.*, 1961, **79**, 531–537.
6. W. F. Carvalho and E. Granéli, *Harmful Algae*, 2010, **9**, 105–115.
7. F. Liebert and W. . Deerns, *Verhandlungen en Rapp. Uitg. door Rijkinstututen voor Visscher.*, 1920, **1**, 81–93.
8. G. M. Hallegraeff, *Phycologia*, 1993, **32**, 79–99.
9. W. Jawaid, J. P. Meneely, K. Campbell, K. Melville, S. J. Holmes, J. Rice, and C. T. Elliott, *J. Agric. Food Chem.*, 2015, **63**, 8574–8583.
10. J. Naar, A. Bourdelais, C. Tomas, J. Kubanek, P. L. Whitney, L. Flewelling, J. L. Karen Steidinger, and D. G. Baden, *Environ. Health Perspect.*, 2002, **110**, 179–185.
11. B. W. Brooks, J. P. Grover, and D. L. Roelke, *Environ. Toxicol. Chem.*, 2011, **30**, 1955–1964.
12. J. Bostock, B. McAndrew, R. Richards, K. Jauncey, T. Telfer, K. Lorenzen, D. Little, L. Ross, N. Handisyde, I. Gatward, and R. Corner, *Philos. Trans. R. Soc. London B Biol. Sci.*, 2010, **365**, 2897–2912.
13. J. Yariv and S. Hestrin, *J. Gen. Microbiol.*, 1961, **24**, 165–175.
14. T. Igarashi, M. Satake, and T. Yasumoto, *J. Am. Chem. Soc.*, 1996, **118**, 479–480.
15. T. Igarashi, M. Satake, and T. Yasumoto, *J. Am. Chem. Soc.*, 1999, **121**, 8499–8511.
16. T. Igarashi, S. Aritake, and T. Yasumoto, *Nat. Toxins*, 1998, **6**, 35–41.
17. S. A. Rasmussen, S. Meier, N. G. Andersen, H. E. Blossom, J. Ø. Duus, K. F. Nielsen, P. J. Hansen, and T. O. Larsen, *J. Nat. Prod.*, 2016, **79**, 2250–2256.
18. S. R. Manning and J. W. La Claire II, *Anal. Biochem.*, 2013, **442**, 189–195.
19. J. C. Henrikson, M. S. Gharfeh, A. C. Easton, J. D. Easton, K. L. Glenn, M. Shadfan, S. L. Mooberry, K. D. Hambright, and R. H. Cichewicz, *Toxicon*, 2010, **55**, 1396–1404.
20. M. J. Bertin, P. V. Zimba, K. R. Beauchesne, K. M. Huncik, and P. D. R. Moeller, *Harmful Algae*, 2012, **20**, 111–116.
21. H. E. Blossom, S. A. Rasmussen, N. G. Andersen, T. O. Larsen, K. F. Nielsen, and P. J. Hansen, *Aquat. Toxicol.*, 2014, **157**, 159–166.
22. P. A. Holdway, R. A. Watson, and B. Moss, *Freshw. Biol.*, 1978, **8**, 295–311.

23. B. Wagstaff, I. Vladu, J. Barclay, D. Schroeder, G. Malin, and R. Field, *Viruses*, 2017, **9**, 40-51.
24. A. Moran and A. Ilani, *J. Membr. Biol.*, 1974, **16**, 237–256.
25. G. Jeglitsch, K. Rein, D. G. Baden, and D. J. Adams, *J. Pharmacol. Exp. Ther.*, 1998, **284**, 516–525.
26. M. Sasaki, N. Matsumori, T. Maruyama, T. Nonomura, M. Murata, K. Tachibana, and T. Yasumoto, *Angew. Chem. Int. Ed. Engl.*, 1996, **35**, 1672–1675.
27. A. Yokoyama, M. Murata, Y. Oshima, T. Iwashita, and T. Yasumoto, *J. Biochem.*, 1988, **104**, 184–187.
28. R. Kellmann, A. Stüken, R. J. S. Orr, H. M. Svendsen, and K. S. Jakobsen, *Mar. Drugs*, 2010, **8**, 1011–1048.
29. K. Nakanishi, *Toxicon*, 1985, **23**, 473–479.
30. I. Vilotijevic and T. F. Jamison, *Mar. Drugs*, 2010, **8**, 763–809.
31. I. Vilotijevic and T. F. Jamison, *Science*, 2007, **317**, 1189–1192.
32. M. Sasaki, M. Ebine, H. Takagi, H. Takakura, T. Shida, M. Satake, Y. Oshima, T. Igarashi, and T. Yasumoto, *Org. Lett.*, 2004, **6**, 1501–1504.
33. R. E. Minto and B. J. Blacklock, *Prog. Lipid Res.*, 2008, **47**, 233–306.
34. X. Zhu, J. Liu, and W. Zhang, *Nat. Chem. Biol.*, 2014.
35. F. De Bruyn, J. Maertens, J. Beauprez, W. Soetaert, and M. De Mey, *Biotechnol. Adv.*, 2015, **33**, 288–302.
36. L. L. Lairson, B. Henrissat, G. J. Davies, and S. G. Withers, *Annu. Rev. Biochem.*, 2008, **77**, 521–555.
37. J. W. La Claire, S. R. Manning, and A. E. Talarski, *Toxicon*, 2015, **102**, 74–80.
38. A. Morohashi, M. Satake, Y. Oshima, T. Igarashi, and T. Yasumoto, *Chirality*, 2001, **13**, 601–605.
39. B. M. Trost, R. C. Bunt, and S. R. Pulley, *J. Org. Chem.*, 1994, **59**, 4202–4205.
40. B. M. Trost and Y. H. Rhee, *Org. Lett.*, 2004, **6**, 4311.
41. M. Sasaki, T. Shida, and K. Tachibana, *Tetrahedron Lett.*, 2001, **42**, 5725–5728.
42. M. Sasaki, N. Takeda, H. Fuwa, R. Watanabe, M. Satake, and Y. Oshima, *Tetrahedron Lett.*, 2006, **47**, 5687–5691.
43. J. N. Jennings and J. M. Lambert, *Geogr. J.*, 1953, **119**, 91.
44. M. George, *The land use, ecology and conservation of broadland*, Packard Publishing Ltd, Chichester, 1992.
45. K. Irvine, B. Moss, M. Bales, and D. Snook, *Freshw. Biol.*, 1993, **29**, 119–139.

46. G. Phillips, A. Bramwell, J. Pitt, J. Stansfield, and M. Perrow, *Hydrobiologia*, 1999, **395**, 61–76.
47. Environment Agency, <https://www.gov.uk/government/news/quarter-of-a-million-fish-rescued-in-norfolk-broads>, Date Accessed 2017-07-11.
48. The Broads Authority, *Broads Plan 2017*, Norwich, 2017.
49. L. Liang and D. Astruc, *Coord. Chem. Rev.*, 2011, **255**, 2933–2945.
50. V. Tomar, *J. Nanomed. Nanotechnol.*, 2012, **3**, 131–142.
51. H. Yamakoshi, K. Dodo, A. Palonpon, J. Ando, K. Fujita, S. Kawata, and M. Sodeoka, *J. Am. Chem. Soc.*, 2012, **134**, 20681–20689.
52. R. Das and B. Mukhopadhyay, *ChemistryOpen*, 2016, **5**, 401–433.
53. M. Sajid, A. N. Kawde, and M. Daud, *J. Saudi Chem. Soc.*, 2015, **19**, 689–705.

2 The chemoenzymatic synthesis of sugar nucleotides to explore the biosynthesis of prymnesin toxins

Parts of this chapter are in press:

M. Rejzek, L. Hill, E. S. Hems, S. Kuhadomlarp, B. A. Wagstaff, and R. A. Field, in *Methods in enzymology*, Elsevier Inc., 1st edn., 2017, pp. 1–30

2.1 Introduction

2.1.1 Prymnesin Toxins

Prymnesins are reported to be decorated with an interesting set of sugars (Figure 2.1). Prymnesin-1 is decorated with β -D-galactofuranose, α -D-ribofuranose and α -L-arabinopyranose.¹ Prymnesin-2 is decorated with α -L-xylofuranose which has not been reported in the literature before.² Prymnesin-2 has also been drawn (albeit without comment) in a recent paper as glycosylated with α -L-arabinofuranose rather than α -L-xylofuranose.³ The recently discovered prymnesin-B1 is reported to be glycosylated with α -D-galactopyranose.³ Apart from the sugars, the main differences between prymnesins-1/2 and prymnesin-B1 is that the latter is less chlorinated and the polyether backbone has a CH(OH)CH₂ linker in place of the HI ring system. The literature provides no insight regarding the biogenesis of L-xylofuranose, so a tentative biosynthetic pathway is being proposed by our group.

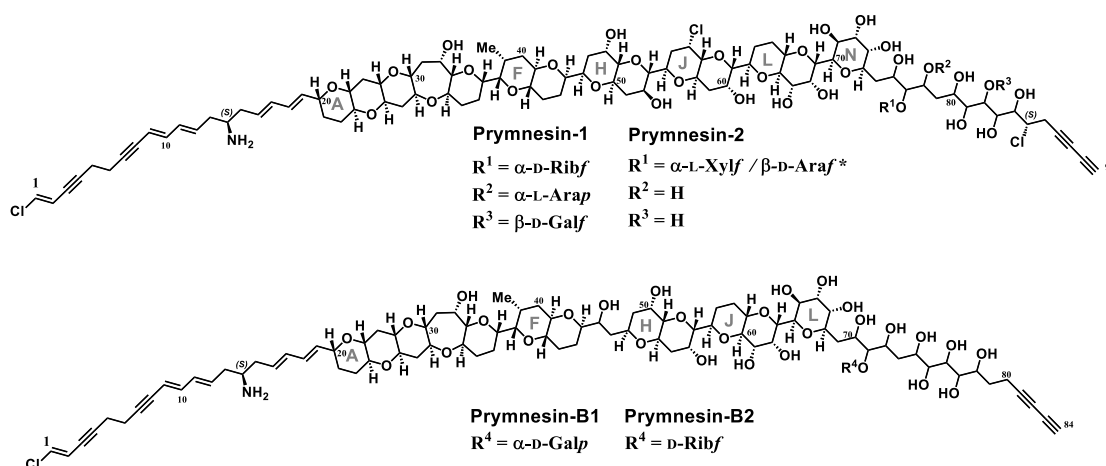


Figure 2.1 - The reported chemical structures of the reported prymnesin toxins. Prymnesin-1 and prymnesin-2 were originally reported by Igarashi *et al.*^{2,4} The structures of prymnesin-B1 and B2 were published by Rasmussen *et al.*³ more recently.

The two main carbohydrates of interest in this chapter are D-galactofuranose found on prymnesin-1 and L-xylofuranose found on prymnesin-2. Both of these sugars were identified by Igarashi *et al.*¹ from chiral GC chromatograms of the carbohydrates hydrolysed from the toxin backbone (Figure 2.2), by comparison with chiral GC of sugar standards; comparison of the retention times was used to identify the carbohydrates on the toxin backbone.

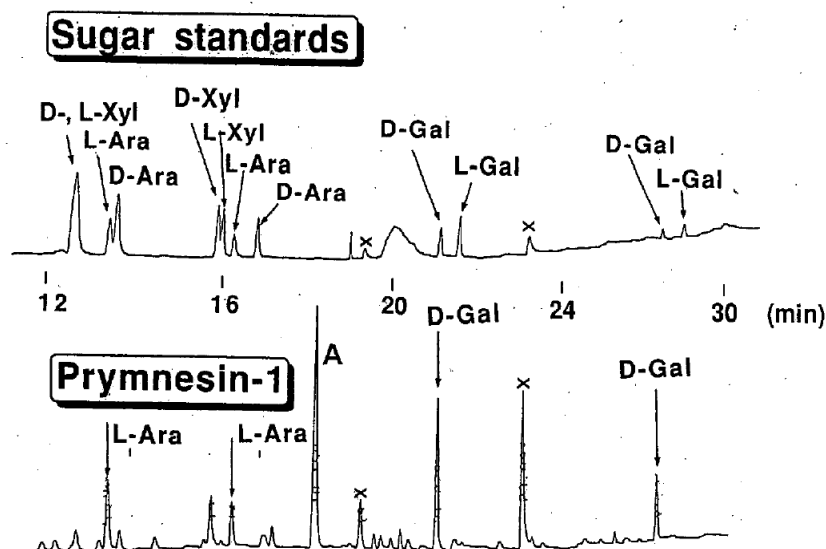


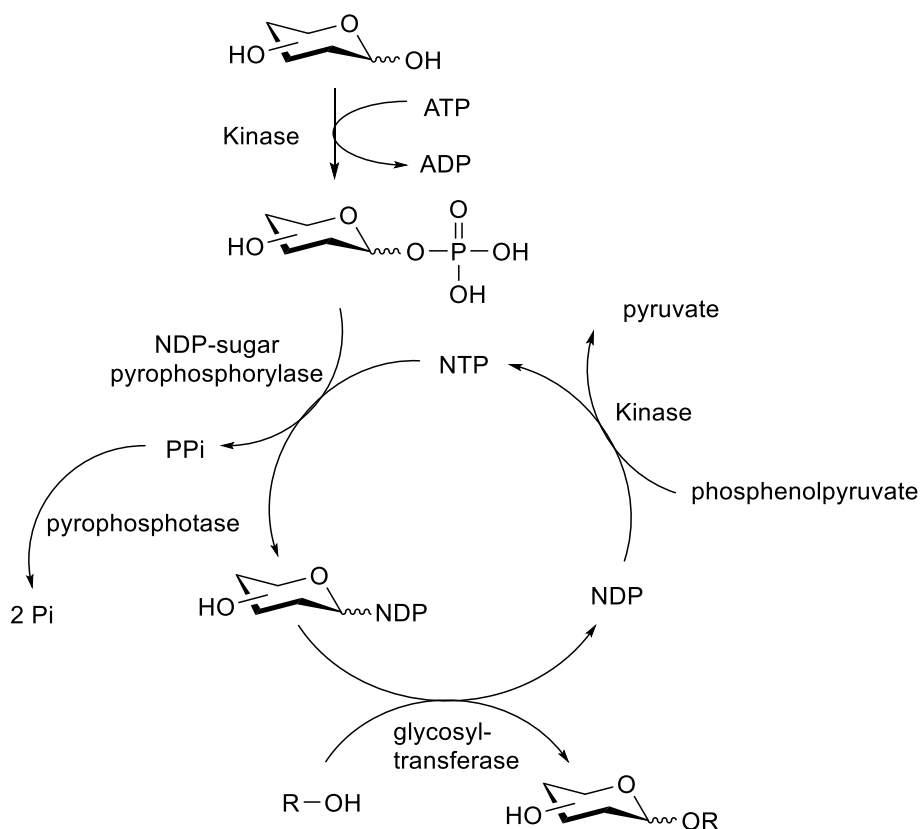
Figure 2.2 - Chiral GC chromatograms showing sugar standards for D- & L-xylose, D- & L-arabinose and D- & L-galactose. On the bottom are the sugars L-arabinose and D-galactose hydrolysed from prymnesin-1. Peaks marked with an X are electrical noises from the instrument. Reprinted (adapted) with permission from T. Igarashi *et al.*, *J. Am. Chem. Soc.*, 1999, **121** (37), pp 8499–8511 (supporting material). Copyright 1999 American Chemical Society.

Of the carbohydrates found on prymnesins-1/2, D-galactose, D-ribose and L-xylose were found to be present on the toxin in the furanose form, whilst L-arabinose was found in the pyranose form. Igarashi *et al.*¹ determined this by comparing the anomeric ¹³C NMR shifts of the sugars with literature values, as shown in Table 2.1. The stereochemistry at the anomeric position was determined by $J_{1,2}$ coupling constants.¹ It may be noted that the literature ¹³C NMR shifts for the anomeric carbons for β -L-xylofuranose and α -D-ribofuranose are ~ 3 ppm smaller than the shift recorded for the sugar on the toxins. These sugars are both furanoses with 1,2-cis anomeric linkages, and this might be attributed to the flexibility of furanose rings when compared with pyranose rings.⁵ By contrast, the difference in ¹³C NMR shifts for the 1,2-trans furanose α -D-galactopyranose and 1,2-trans pyranose α -L-arabinopyranose are much closer to the literature values.

¹³ C NMR shift	β -L-Xylf	α -L-Arap	α -D-Ribf	β -D-Galf
Toxin	106.2	106.1	106.0	110.4
Lit. pyranose	100.6	105.1	100.4	Not given
Lit. furanose	103.0	Not given	103.1	110.0

2.1.2 The origin of carbohydrates on prymnesin toxins

Prymnesin toxins are in part characterised by a range of different sugar moieties which decorate the toxin backbone.^{1,3} Interestingly, different sugars can even be found on the same position of the same backbone, as is the case with prymnesin-1 and prymnesin-2 which are glycosylated at C82 with β -L-xylofuranose and α -D-ribofuranose respectively. Glycosylation of prymnesins is most likely achieved via Leloir glycosylation by enzymes called glycosyltransferases (GTs), using nucleotide diphosphate (NDP) sugars as activated sugar donors (Scheme 2.1).⁶ It follows that the biosynthesis of glycosylated prymnesin toxins necessitates the presence of a range of corresponding NDP-sugars within the cell.



Scheme 2.1 - Overview of an *in vitro* glycosyltransferase cycle.⁶ The sugar-1-phosphate is produced by a kinase, before being converted to the NDP-sugar by NDP-sugar pyrophosphorylase. The by-product of this reaction is pyrophosphate (PPi) which is hydrolysed to inorganic phosphate (Pi) by pyrophosphatase. The NDP-sugar is then used as an activated sugar donor by the glycosyltransferase which transfers the sugar onto the aglycone (R-OH). The residual nucleotide diphosphate (NDP) is regenerated to nucleotide triphosphate (NTP) with phosphoenolpyruvate by a kinase.

Glycosyltransferases may be either retaining or inverting of the stereochemistry at the anomeric position with regards to the initial NDP orientation (Figure 2.3).⁷ For example, prymnesin-1 is glycosylated with β -D-galactofuranose, which would require an inversion of the stereochemistry of the α -linked UDP-galactofuranose donor. By contrast prymnesin-B1 is glycosylated with α -D-galactopyranose, which would require a retention of the stereochemistry of the α -linked UDP-galactopyranose donor. It is therefore clear that there is diversity in the carbohydrate-active enzymes present in *P. parvum*.

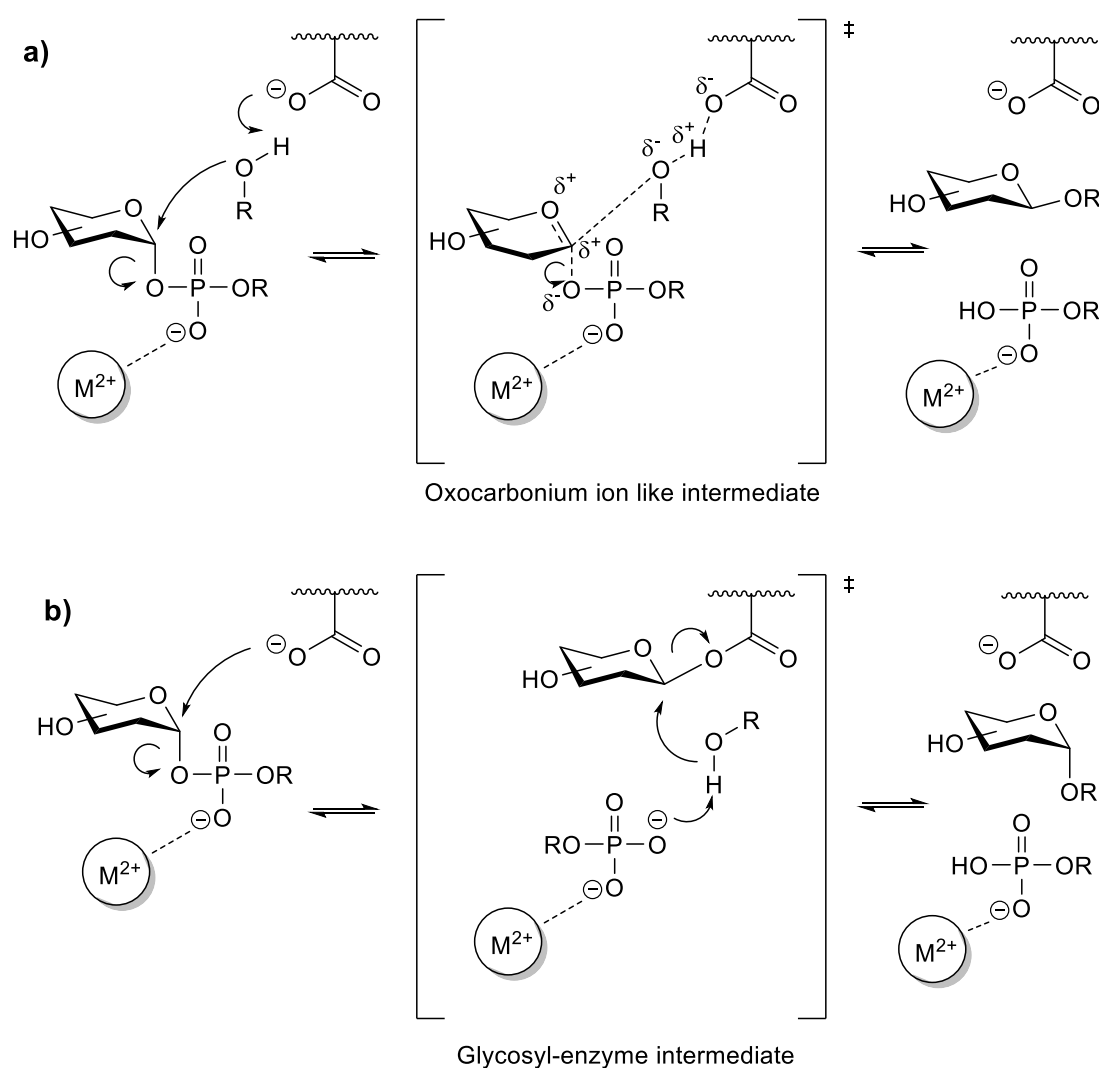


Figure 2.3 – Inverting and non-inverting glycosyl transferase mechanisms, adapted from Lairson *et al.*⁷ The inverting glycosylation mechanism **a)** proceeds through an oxocarbenium like intermediate, while the non-inverting glycosylation mechanism **b)** proceeds through a covalent glycosyl-enzyme intermediate.

2.1.3 Sugar nucleotide profiling

In order to profile the sugar nucleotides present in *P. parvum* it is first necessary to grow an axenic (clean, single species) culture.⁸ The cells can then be easily harvested by centrifugation ready for extraction.⁹ It is important that any extraction technique minimises the degradation of extracted sugar nucleotides. It is also necessary to inactivate carbohydrate-active enzymes from the organism which could degrade the extracted sugar nucleotides to essentially take a 'snap-shot' of the sugar nucleotides present in *P. parvum* at the time of extraction. Fortunately *P. parvum* cell lysis with aqueous ethanol brings about concomitant protein precipitation without serious chemical degradation of the extracted sugar nucleotides.¹⁰

After extraction, it is necessary to separate the sugar nucleotides from one another prior to detection. This is because many sugar nucleotides are isobaric and contain the same chromophore. For example, UDP-D-Glc, UDP-D-Galp and UDP-D-Galf are all indistinguishable by either UV detection or mass spectrometry. Separation techniques broadly rely on liquid chromatography such as anion exchange, capillary electrophoresis, and ion-pair reverse phase methods.¹¹⁻¹³

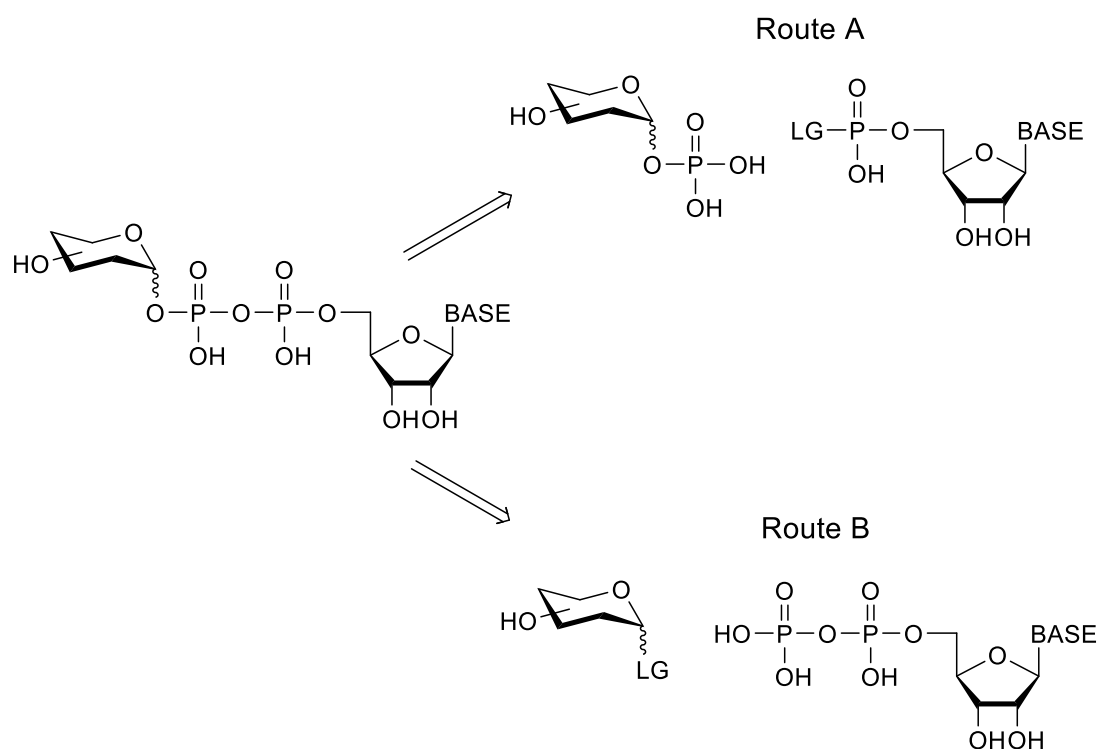
Whichever separation technique is used, it is important that it is compatible with the detection technique to be employed. UV detection is relatively robust with respect to a range of elution solvents and buffers and it is a good method for quantifying the levels of different sugar nucleotides in an extract. For example, Manley and Burns¹¹ made use of anion exchange chromatography coupled with a UV detector to quantify the levels of various NDP-sugars extracted from the red alga *Pterocladia capillacea* when evaluating different extraction techniques. By contrast, mass spectrometry is incompatible with the high salt conditions associated with anion exchange chromatography; Le Bizec *et al.*¹⁴ have discussed how ion pairing in LC-MS systems leads to the suppression of m/z signals by decreasing the evaporation efficiency of analytes so that they cannot enter the gas phase in electrospray ionisation (ESI) mass spectrometry. There may also be neutralisation of ionised species in the gas phase.¹⁴ However, mass spectrometry can offer a much higher level of sensitivity and specificity than UV detection. To alleviate the problems associated with LC-MS systems there has been a move towards volatile buffers working along a pH gradient, coupled with relatively new porous graphitic carbon (PGC) columns.¹⁵

Mass spectrometry can be used for targeting sugar nucleotides using electrospray ionization-tandem mass spectrometry (ESI-MS/MS), using selected reaction monitoring (SRM) for single fragment ions or multiple reaction monitoring (MRM) for multiple daughter ion fragments. The specificity and sensitivity of MRM ESI-MS/MS is particularly high because fragmentation of the parent ion can be performed under optimised conditions, which can be developed using authentic standards of the analyte of interest.¹⁶ For example, MacRae *et al.*¹⁰ utilised LC-ESI MS/MS using MRM transitions to profile sugar nucleotides involved in the biosynthesis of cell surface glycoconjugates of trypanosomatid parasites. If authentic standards cannot be obtained or there is a desire to search more broadly for generic groups (eg UDP-hexoses, GDP-pentoses etc) then MRM transitions can be predicted.¹⁶ The LC-MS/MS method used in this project utilised a PGC column coupled with a triple quadrupole mass spectrometer and is discussed in detail later in this chapter.

2.1.4 Sugar nucleotide synthesis

In order to profile sugar nucleotides from algal cell extracts, it was first necessary to have a set of standards in hand. Not all the sugars found on prymnesin backbones have commercially available NDP-sugar derivatives, and as such they must be made either chemically, enzymatically or by a combination of both techniques. Enzymatic synthesis is useful for synthesising natural NDP-sugars when the correct substrates and enzymes are available. However, the synthesis of unnatural or novel NDP-sugars often requires a chemical approach.

The chemical synthesis of NDP-sugars often relies on one of two pyrophosphate bond disconnections (Scheme 2.2).¹⁷ Route A relies on the pyrophosphate bond being formed by joining two monophosphate groups. In order to enable the coupling to take place at relatively mild conditions and therefore prevent degradation of the NDP-sugar product, and also to prevent the production of dimers, one of the phosphate groups can be activated with a leaving group.¹⁷



Scheme 2.2 - Disconnection strategies for the chemical synthesis of NDP-sugars.¹⁷ Route A breaks the pyrophosphate bond, whilst route B removed the whole NDP group.

Khorana *et al.*¹⁸ developed a reaction between a sugar-1-phosphate and nucleoside phosphomorpholidate which, although commonly used, does suffer from a long reaction time. Bogachev *et al.*¹⁹ developed a quicker method of NDP-sugars using a sugar-1-phosphate and nucleoside *N*-methylimidazolide. An alternative method which does not rely on protecting groups is phosphate activation with carbonyldiimidazole (CDI), which was developed by Tennigkeit *et al.*²⁰ as a method of pyrophosphate bond formation, and subsequently applied to the synthesis of NDP-sugars by Baisch and Öhrlein.²¹ All three methods have been reported in the literature for chemically synthesising UDP- α -D-galactofuranose (UDP-Galf) and are discussed later in this chapter.²²⁻²⁴

Route B relies on the direct glycosylation of a nucleoside diphosphates. This was first reported by Arlt and Hindsgaul²⁵ who coupled per-*O*-benzyl D-glycopyranosyl bromides with organic soluble tetrabutyl ammonium salts of UDP and GDP to give NDP-sugars with mixed α/β stereochemistry at the anomeric position. This method was improved upon by Timmons and Jakeman,²⁶ who utilised neighbouring group participation when reacting ester-protected glycopyranosyl bromides with organic soluble tetrabutyl ammonium salts of UDP and GDP to give NDP-sugars with 1,2-*trans* stereochemistry at the anomeric position.

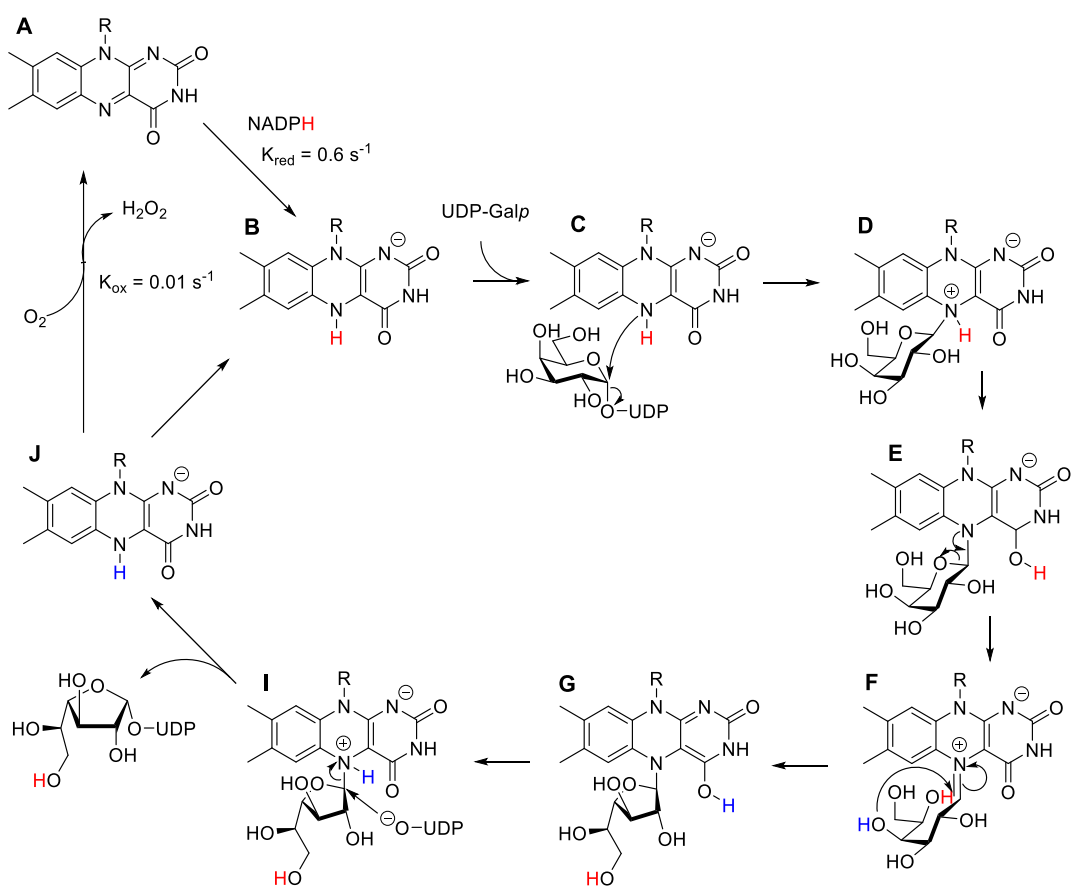
Chemoenzymatic and enzymatic synthesis of NDP-sugars can be a more efficient way of synthesising NDP sugars.²⁷ In some cases it is possible to use enzymes with broad substrate specificity. For example Errey *et al.*²⁸ were able to synthesise a broad range of UDP-sugars from the corresponding sugar-1-phosphate, using galactose-1-phosphate uridylyltransferase (GalPUT). The authors commented on the exceptionally relaxed substrate specificity of this enzyme and were able to turn over a range of sugars, irrespective of the relative or absolute conformation, ring size or substitution pattern.²⁸ Furthermore, work by Wagstaff *et al.*²⁹ has shown that GalPUT will also synthesise nucleobase-modified UDP-sugars, turning over a range of 5-substituted UTP derivatives into the corresponding 5-substituted UDP-galactose. The application of the methodology by Errey *et al.*²⁸ with regards to the chemoenzymatic synthesis of UDP-Galf is discussed in more detail later in this chapter.

My contribution to the profiling of sugar nucleotides from *P. parvum* was the chemoenzymatic synthesis of UDP- α -D-galactofuranose (UDP-D-Galf), as well as the chemical syntheses of UDP- α -D-arabinopyranose (UDP-D-Arap) and UDP- β -L-xylopyranose (UDP-L-Xylp) which are tentatively proposed to be involved in the biogenesis of L-xylofuranose. Finally, a standard of UDP- α -D-mannopyranose (UDP-D-Man) was also synthesised to help account for an unidentified UDP-hexose detected in algal cell extracts.³⁰

2.2 D-Galactofuranose on prymnesin-1

2.2.1 Biosynthesis of galactofuranose in nature

β -D-Galactofuranose, while found on prymnesin-1,¹ is also found in the cell wall or cell surface glycoproteins and glycolipids of many human pathogens,^{31,32} however, galactose is only found in the pyranose form in humans. The corresponding activated furanose sugar donor used by glycosyltransferases is UDP-D-Galf, which is biosynthesised from UDP-D-Galp by the flavoenzyme UDP-galactopyranose mutase (UGM) (Scheme 2.3).³³ The currently accepted main ring contraction step was proposed by Kiessling *et al.*³⁴ The flavin cofactor is only active in the reduced form, and forms a galactose-flavin adduct (Scheme 2.3, E), and interconversion between galacropyranose and galactofuranose proceeds through a flavin-derived iminium species (Scheme 2.3, F).³⁴ UGM has also been shown to catalyse the interconversion between UDP-L-arabinopyranose and UDP-L-arabinofuranose, which only differ structurally from UDP-D-Gal by the absence of the C6 hydroxymethyl group.³⁵



Scheme 2.3 – Flavin dependent UDP-galactopyranose mutase converting UDP-Galp to UDP-Galf (adapted from Tanner *et al.*³³). The UGM is activated by NADPH reduction of flavin (B). Flavin covalently binds with UDP-Galp by attack of C1_{Galp} by N5_{FAD}, which in turn cleaves the anomeric bond (C). Tautomerisation moves the proton shown in red from N5_{FAD} to C4_{FAD=O} (D), which facilitates opening of the Galp ring (E). The proton shown in red is transferred from C4_{FAD=O} to C2_{Gal}, and the proton shown in blue is transferred from C4_{Gal} to C4_{FAD=O} during the key ring contraction step (F-G). Finally direct attack of the FAD-Gal adduct at the C1_{Galp} position liberates UDP-Galf (I-J). The oxidation of the reduced flavin (J-A) is slow and therefore the enzyme can turnover several hundred times before being inactivated by oxidation.

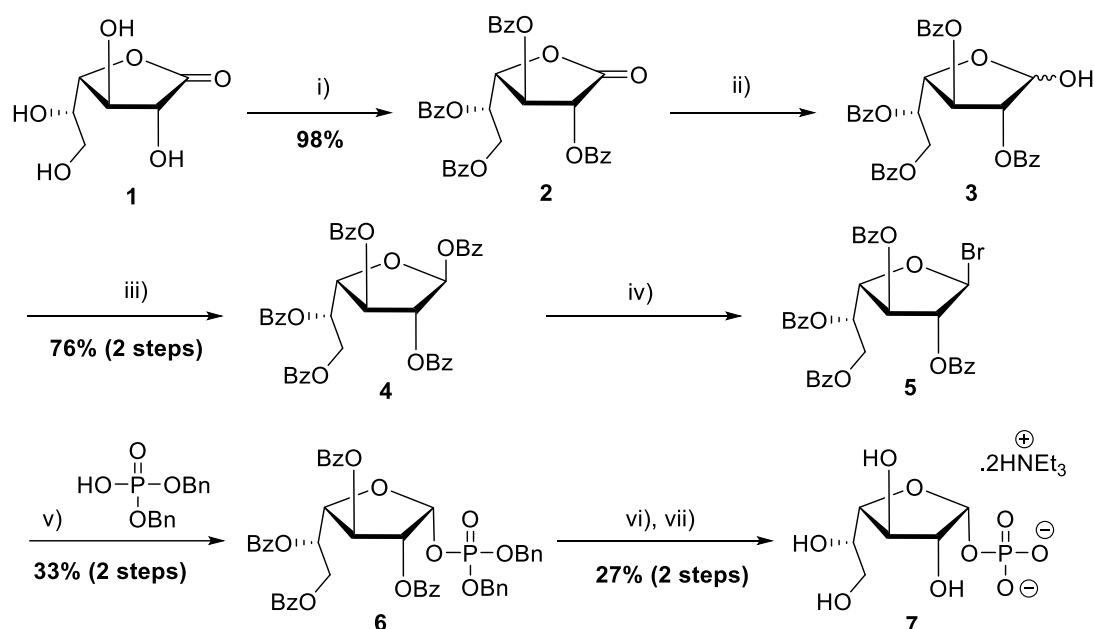
The equilibrium between UDP-D-Galp and UDP- α -D-Galf (**8**) lies very much in favour of the pyranose form, in the ratio 11:1.³⁶ Therefore it would not be feasible to make a useful quantity of UDP- α -D-Galf (**8**), from UDP- α -D-Galp, using UGM. UDP- α -D-Galf (**8**) can, however, be made chemically^{22–24} or chemoenzymatically.²⁸ In both cases α -D-galactofuranosyl phosphate (**7**) (Galf-1-P) must first be chemically synthesised; for the enzymatic synthesis of UDP- α -D-Galf (**8**) this is vital; for the chemical synthesis of UDP- α -D-Galf (**8**) it is a useful starting point as the anomeric stereochemistry of the sugar-nucleotide is predetermined by the anomeric stereochemistry of the sugar phosphate.¹⁷ The chemical synthesis of Galf-1-P (**7**) was first reported by de Lederkremer *et al.*³⁷ The first challenge in

the synthesis is fixing galactose in the five ring furanose form, which can be achieved in a few different ways. The first is by hot benzylation³⁸ or refluxing in methanol in the presence of a Lewis acid.²² Both of these methods do, however, lead to a mixture of pyranose and furanose rings which must be separated before use. An alternative method is the benzylation, reduction and subsequent benzylation of commercially available D-galactono-1,4-lactone (**1**).^{24,38} This second method has the advantage of not forming mixtures of furanosyl and pyranosyl ring which require separation, and has proved effective in the current study for the synthesis of per-*O*-benzoyl galactofuranose (**4**).

2.2.2 Chemoenzymatic synthesis of UDP-D-galactofuranose

The chemical synthesis of Galf-1-P (**7**), shown in Scheme 2.4, essentially as described by Lederkremer *et al.*³⁷ Commercial galactono-1,4-lactone (**1**) was benzyolated with benzoyl chloride in pyridine, which was confirmed by the presence of four new C=O peaks in the ¹³C NMR spectrum between 165.9 and 165.0 ppm. The resulting tetra-*O*-benzoyl-D-galacto-1,4-lactone (**2**) was reduced to the hemiacetal (**3**) using L-selectride®. When the reduction was judged to have gone to completion by TLC, due to consumption of the starting lactone spot (R_f 0.58, hexane/EtOAc 7:3) and a new less mobile spot (R_f 0.48 hexane/EtOAc 7:3), the crude reaction mixture was immediately treated with pyridine, DMAP and benzoyl chloride in the same pot to give per-*O*-benzoyl- β -D-galactofuranose (**4**) with a yield of 76% over two steps. The ¹H NMR showed a new H-1 anomeric signal in the ¹H NMR at 6.78 ppm as a singlet, indicating exclusively the 1,2-*trans* β -anomer had been formed.³⁹ By contrast, Zhang and Liu²⁴ performed the reduction with disiamylborane, followed by benzyolation as two separate steps, with yield of 79% and 84% respectively. Treatment of per-*O*-benzoyl- β -D-galactofuranose (**4**) with 33% w/v HBr/AcOH afforded 2,3,5,6-tetra-*O*-benzoyl- β -D-galactofuranosyl bromide (**5**) which was subjected to a fast work-up using ice cold sat. sodium bicarbonate solution, before being immediately reacted with dibenzyl phosphate in toluene. This condensation gave a mixture of anomers α/β 1.8:1, as judged by integration of H-1' ¹H NMR signals. The 1,2-*cis* α -anomer 2,3,5,6-tetra-*O*-benzoyl- α -D-galactofuranosyl dibenzylphosphate (**6**) was retained more strongly than the 1,2-*trans* β anomer by normal phase chromatography, as reported by Lederkremer *et al.*,³⁷ which allowed the anomers to be separated. The α anomer was identified by the H-1' signal at 6.33 ppm as a doublet of doublets, with a $J_{1,2}$ coupling value of 4.6 Hz and a $J_{1,P}$ coupling value of 5.7 Hz.³⁷ Global deprotection was achieved by hydrogenation of the benzyl groups, followed by

debenzoylation using a mixture of 5/2/1 MeOH:H₂O:Et₃N to give α -D-galactofuranosyl phosphate, bis-triethylammonium salt (**7**) in 27% yield over two steps.



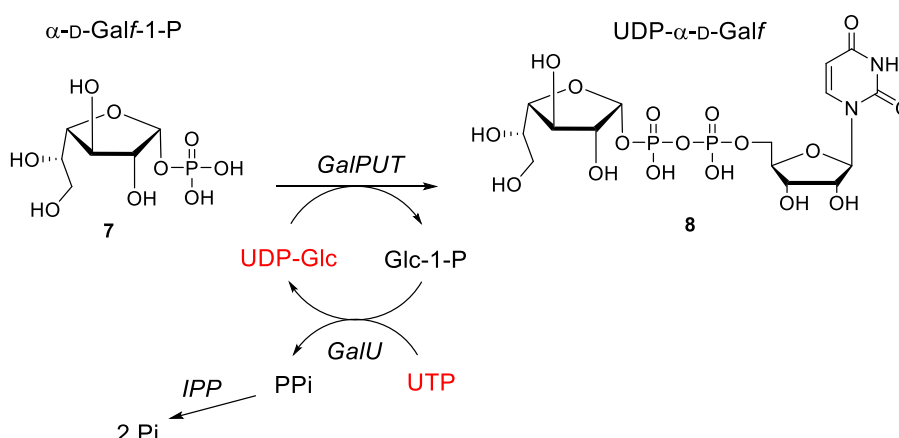
Scheme 2.4 – The chemical synthesis of Galf-1-P; i) BzCl, DMAP, Pyr; ii) L-selectride™, THF; iii) BzCl, DMAP, Pyr; iv) 33% HBR/AcOH, DCM; v) Et₃N, toluene; vi) H₂, Pd/C, Et₃N, EtOAc; vii) MeOH/H₂O/Et₃N (5:2:1)

Although mass spectrometry showed complete deprotection, aromatic signals were still visible in the ¹H NMR spectrum. These were attributed to benzoic acid, the side product of hydrolysis caused by the presence of water during the debenzylation step. An acceptable level of purification of α -D-galactofuranosyl phosphate, bis-triethylammonium salt (**7**) was achieved by simple partitioning between water and diethyl ether, which saved the need to purify by size exclusion or ion exchange chromatography.

With Galf-1-P (**7**) in hand, it was next necessary to consider the synthesis of UDP- α -D-Galf (**8**). The chemical synthesis of UDP- α -D-Galf (**8**) starting from Galf-1-P (**7**) was first reported by Tsvetkov and Nikolaev.²³ The key pyrophosphorylation step in their synthesis was CDI-activated coupling between UMP-imidazole and Galf-1-P (**7**), which gave an overall yield of 23%. Marlow and Kiessling²² subsequently published an improved chemical synthesis of UDP- α -D-Galf (**8**), where the key pyrophosphorylation step in their synthesis was the coupling between UMP-*N*-methylimidazolide and Galf-1-P (**7**), which gave an improved UDP-

α -D-Galf (**8**) yield of 35%. A more recent chemical synthesis of UDP-D-Galf (**8**) reported by Zhang and Liu²⁴ relied on the coupling of Galf-1-P (**7**) with UMP-morpholidate, to give UDP-D-Galf (**8**) with a yield of 20%.

As an alternative route to chemical synthesis, Errey *et al.*²⁸ have shown that it is possible to enzymatically synthesise UDP-D-Galf by using galactose-1-phosphate uridylyltransferase (GalPUT) to transfer uridinediphosphate from UDP- α -D-glucose (UDP-D-Glc) to Gal-1-P (Scheme 2.5). Because UDP-D-Glc and UDP-D-Galf are inseparable by strong anion exchange (SAX) chromatography, a catalytic amount of UDP-glucose was used. UDP-D-Glc was regenerated from glucose-1-phosphate *in situ* with uridylyltransferase using glucose-1-phosphate uridylyltransferase (GalU). The by-product of this regeneration is pyrophosphate, which was enzymatically removed by inorganic pyrophosphatase (IPP) to give inorganic phosphate. It is this phosphate energy sink which drives the overall enzymatic reaction forwards.



Scheme 2.5 – The enzymatic transformation of Galf-1-P to UDP-D-Galf.²⁸ UMP is transferred from UDP-D-Glc onto Galf-1-P by the enzyme *GalPUT*. UDP is then regenerated from Glc-1-P with UTP by the enzyme *GalU*; the by-product of this is PPi which is hydrolysed to Pi by the enzyme *IPP*.

UDP-Galf was enzymatically synthesised following the protocol by Errey *et al.*²⁸ The progression of the biotransformation was followed by SAX HPLC coupled with a UV-detector, using an ammonium bicarbonate buffer to elute the compounds (Figure 2.4). After 24 hours there was a clear partial consumption of UTP, and an increase in the size of the peak relating to UDP- α -D-Galf (**8**) (Figure 2.4). UDP- α -D-Galf (**8**) co-elutes with UDP-D-Glc, which is however only present in the mixture at a catalytic level.

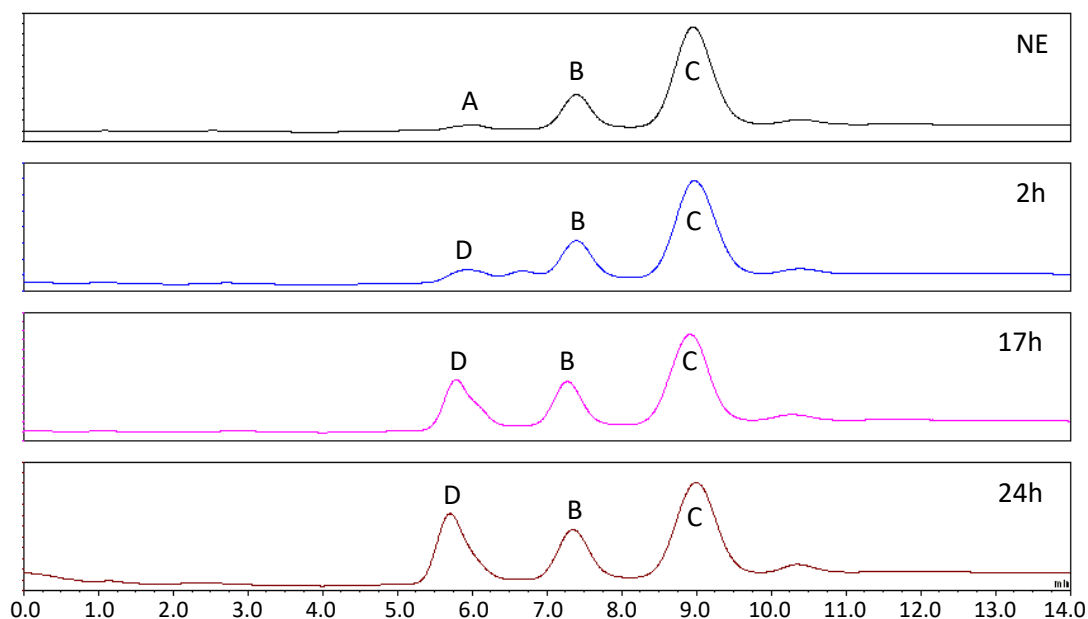


Figure 2.4 – SAX chromatography analysis of the enzymatic synthesis of UDP-Galf. A no enzyme (NE) control as well as time points at 2, 17 and 24 hours were recorded. The peaks on the chromatogram relate to: A) UDP-Glc t_R 5.80; B) UDP, t_R 7.35; C) UTP, t_R 9.00; D) UDP-D-Galf + UDP-D-Glc, t_R 5.70; See experimental section for column conditions.

Whilst SAX coupled with UV-detection proved very convenient, unfortunately there were severe problems with compound degradation when trying to freeze dry UDP- α -D-Galf (**8**) which had been purified by SAX. Fortunately it was possible to observe the characteristic peaks for UDP- α -D-Galf (**8**) in the NMR spectra, with the anomeric ribose H-1' signal at 5.90 ppm as a doublet with a $J_{1',2'}$ coupling value of 4.9 Hz, and the galactofuranose anomeric H-1'' signal at 5.55 ppm as a doublet of doublets with a $J_{1'',2''}$ coupling value of 4.6 Hz and a $J_{1'',p}$ coupling value of 5.2 Hz. There were also two peaks in the ^{31}P NMR at -11.3 ppm and -12.8 ppm. Whilst in the correct region for NDP-sugars, the overlap with UDP-glucose meant they appeared as multiplets. To alleviate the problem of purification by SAX the biotransformation was instead quenched with methanol and centrifuged to remove the precipitated proteins, before being used crude for LC-MS method development.

2.2.3 LC-MS analysis and profiling of UDP- α -D-Galf (**8**)

The UDP- α -D-Galf (**8**) sample was used to determine multiple reaction monitoring (MRM) transitions on a Waters Xevo TQ-S tandem mass spectrometer using a Hypercarb™ porous graphitised carbon column, using a method previously published by us.⁴⁰ The Waters Xevo

TQ-S tandem mass spectrometer is a triple quadrupole spectrometer which is set to search only for specific analytes of interest. The first quadrupole is used as a filter to only allow parent ions of a specific mass/charge ratios through. The second quadrupole is a collision chamber which fragments the parent ions into daughter ions. The third quadrupole then filters again to allow through only daughter ions of specified mass/charge ratios. Using the Intellistart™ function within the MassLynx™ software and electrospray ionisation in negative mode, the instrument searches for a combination of optimised parameters (cone voltage, collision energy) to achieve optimal detection limits for each authentic fragment and its fragments. By only scanning for specified daughter ions, it also has the advantage of long dwell times, further increasing sensitivity. Many sugar nucleotides are isobaric (species of the same mass) and they often produce identical fragment. These species are differentiated based on their retention times. This was achieved by coupling the spectrometer with a liquid chromatography system, using a Hypercarb™ porous graphitised carbon column (PGC).¹⁵ PGCs are good at separating very polar analytes with closely related structures. Compounds are eluted from PGC columns using an acetonitrile gradient against ammonium formate (pH 9.0), a volatile buffer compatible with the LC-MS application.⁴¹

After precipitating the enzymes from the biotransformation (Scheme 2.5) with methanol and removing them by centrifugation (10,000 × g), the crude mixture from the biotransformation of Gal β -1-P (**7**) and UDP- α -D-Gal β (**8**) was used as a standard to find the retention time and optimised mass spectrometry conditions for UDP- α -D-Gal β (**8**). The LC-MS results using a Hypercarb™ PGC column are shown in Figure 2.5; i) shows the result of the injection of the crude mixture giving two isobaric peaks, which was expected as the mixture contains both UDP-Glc and UDP- α -D-Gal β (**8**). ii) shows the UDP-D-Gal β standard which elutes slightly earlier than either UDP-D-Glc or UDP- α -D-Gal β (**8**). As retention times can shift slightly with PGCs, some of the crude biotransformation mixture and UDP-D-Gal β standard were mixed and co-injected which gave iii), showing all three isobaric species. Finally, to determine which peak in the crude biotransformation mixture was which, iv) shows some of the crude mixture was spiked with UDP-D-Glc, and an increase in total ion count for the quicker eluting peak. Coupled with the diagnostic ¹H NMR peaks,²⁴ we were confident that the biotransformation of Gal β -1-P (**7**) into UDP- α -D-Gal β (**8**) had been successful, and that UDP- α -D-Gal β (**8**) eluted after UDP-D-Gal β and UDP-D-Glc.

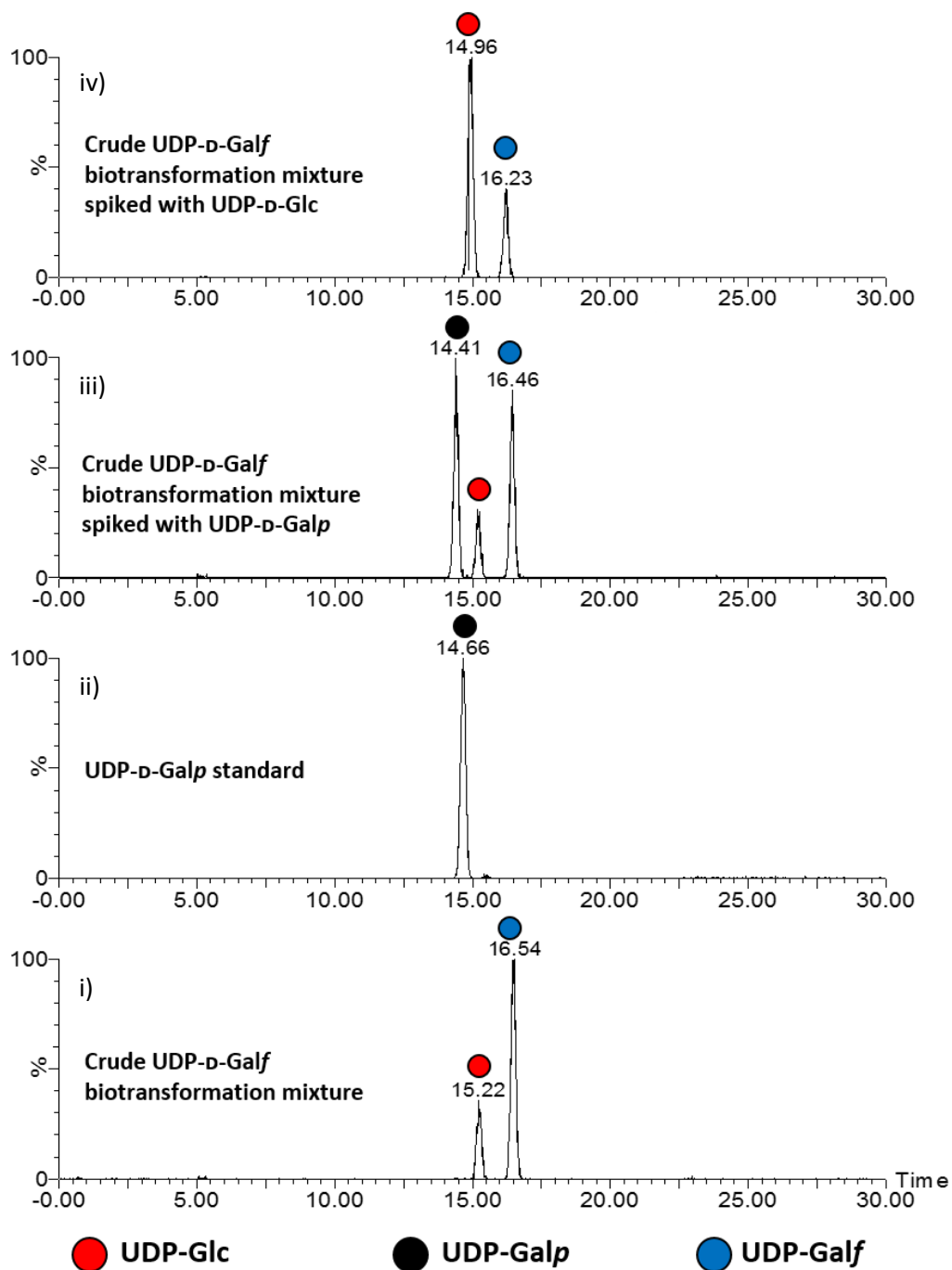


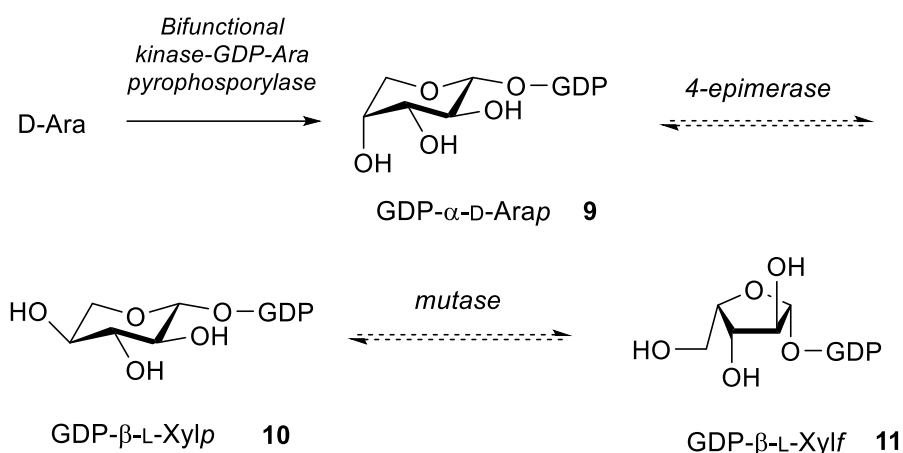
Figure 2.5 –MRM chromatograms of the crude UDP- α -D-Galf (**8**) biotransformation mixture and comparison with authentic standards (UDP-Glc and UDP-Gal). From this it was possible to show that (**8**) was the major species in the crude mixture, and its retention time added to the sugar nucleotide standards database. See experimental section for column conditions.

2.3 Chemical tools for exploring the biosynthesis of L-xylofuranose

2.3.1 Possible biosynthetic pathway for L-xylofuranose on prymnesins

Igarashi *et al.*¹ have reported that prymnesin-2 is glycosylated with α -L-xylofuranose. They first identified the carbohydrate on PRM2 as L-xylose by chiral GC analysis of the trifluoroacetate of the hydrolysed products of PRM2. Igarashi *et al.*¹ then determined that L-xylose was present as a furanoside by comparison of the ¹³C NMR signals with literature values, and the 1,2-*cis* stereochemistry at the anomeric from the $J_{1,2}$ coupling constant of 4 Hz in the ¹H NMR. This is the first time to our knowledge that a natural product has been reported as being glycosylated with L-xylofuranose, and if correct then it follows that *P. parvum* must be producing an NDP-L-Xylf derivative which is being used by a glycosyl transferase to glycosylate the toxin backbone.

Work by Ben Wagstaff in our group produced a possible biosynthetic pathway for L-xylofuranose, shown in Scheme 2.6, using the following reasoning. Xylose and arabinose are interconverting in nature due to epimerase activities. Therefore, the biosynthetic pathway would likely start from either L-xylose or D-arabinose. L-Xylofuranose has not been reported in natural products, but D-arabinose is found in trypanosomes, with GDP- α -D-Arap (**9**) as the sugar nucleotide donor.^{16,42} The next likely step is an inversion of C4 to form GDP- β -L-Xylp (**10**), in a manner analogous to the UDP-Glc/UDP-Gal epimerase mechanism; enzymes performing these C4 epimerisation reactions are abundant, although all known examples require an axial 4-OH group on the sugar, which is absent in GDP- β -L-Xylf (**11**).⁴³ Finally, presuming a similar reaction takes place to UGM, the 4-OH has to be above the plane of the sugar to facilitate top-side attack of the covalent adduct with the flavin cofactor during ring contraction (Scheme 2.3) to form GDP- β -L-Xylf.³³ Therefore the substrate of this reaction has to be GDP- β -L-Xylp (**10**) and not GDP- α -D-Arap (**9**) which has a *syn* configuration between 4-OH and O-GDP.



Scheme 2.6 – a possible biosynthetic pathway for GDP-β-L-xylofuranose (**11**). GDP-α-D-Arap (**9**) is biosynthesised from D-arabinose by a bifunctional kinase-GDP-Ara pyrophosphorylase. A 4-epimerase inverts the 4-OH to give GDP-β-L-Xylp (**10**), and the ring is contracted by a mutase to give GDP-β-L-Xylf (**11**).

Ben Wagstaff used BLASTp analysis to identify a putative trifunctional protein from *P. parvum* (Figure 2.6) (see Appendix for the translated trifunctional protein sequence). A combined transcriptome data set for *Prymnesium parvum* isolated from lake Texoma was acquired from the publicly available MMETSP database,⁴⁴ and UDP-galactopyranose mutase from *Trypanosoma cruzi* (AAX09637.1) was used as a reference sequence. The resulting transcript translates to a 1210 AA protein with 3 clear domains. The N-terminal domain (14AA - 360AA) shares a high sequence identity with UDP-arabinose-4-epimerase isoform X3 from *Ananas comosus* (XP_020109800.1) - 45% sequence identity, 1e-93. The middle domain (390AA - 867AA) shares high sequence identity to UGM from *Trypanosoma cruzi* (AAX09637.1) - 40% sequence identity, 1e-98. There is also a clear third domain in the sequence although the C-terminal domain has no clear homologues in the NCBI dataset which make defining the exact region difficult.



Figure 2.6 – Graphical representation of trifunctional protein from *P. parvum*. A) 14AA – 360AA; B) 390AA – 867AA; C) third domain, with exact region undefined due to a lack of homology with the NCBI dataset

The epimerase shares a higher identity to arabinose 4-epimerases than respective galactose 4-epimerases, suggesting arabinose or xylose as a substrate. So far, only mutases of this protein architecture have been discovered to act on galactose, so all homologues to the middle domain are UDP-galactopyranose mutases. However, Ben Wagstaff speculates an alternative substrate for this enzyme (i.e. UDP-D-Arap or UDP-L-Xylp). The C-terminal domain has no clear homologues with known functions in the NCBI dataset. Due to the occurrence of similar trifunctional proteins in the genomes of other haptophytes *Emiliania huxleyi* and *Chrysochromulina* sp., hits are found to this domain.

Because GDP- α -D-Arap (**9**) is known in trypanosomes it was proposed that the activating nucleotide base would be GDP rather than UDP. This was supported by the fact that Ben Wagstaff noted the trifunctional protein has low homology to GDP-4,6-dehydratases, which suggested a role for GDP in the enzyme function.

The proposed biosynthetic pathway to GDP- β -L-Xylf (**11**) supported by the transcriptome data gave three 1,2-trans sugar nucleotide targets to synthesise for the NDP-sugar standards database (see Appendix, Table 1); GDP- α -D-arabinopyranose (**9**), GDP- β -L-xylopyranose (**10**) and GDP- β -L-xylofuranose (**11**). In addition, sugar nucleotide profiling of algal extracts in the group had also found a UDP-hexose species which didn't match to any standards in the NCBI database. It was therefore also decided to make the 1,2-trans species UDP- α -D-mannose (**12**) as a further UDP-hexose standard.

2.3.2 Chemical synthesis of 1,2-trans NDP-sugar standards

A paper by Timmons *et al.*²⁶ provided a convenient method for synthesising 1,2-trans sugar nucleotides by the direct displacement of glycosyl bromides with the desired NDP. The key parameters for a successful 1,2-trans sugar nucleotide formation are that 1. the pH of the free acid of the NDP to be used should be adjusted to pH 6 for the optimum stability and nucleophilicity; 2. stereo-control at the anomeric position is imparted by the axial participating neighbouring group at C2' (Scheme 2.7); 3. a 1/1/1 ratio of glycosyl bromide : nucleotide 5'-diphosphate : trimethylamine gives the best yield for the coupling reaction at 80 °C in MeCN.

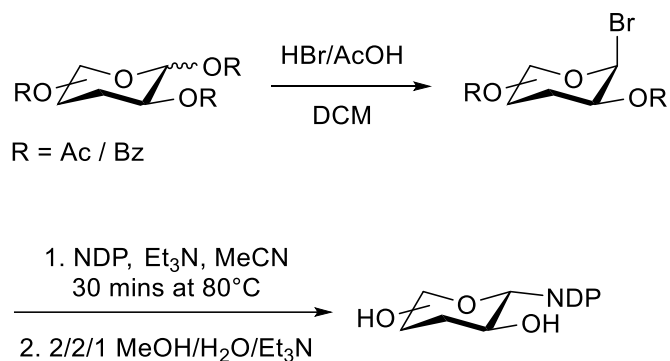


Scheme 2.7 – The influence of neighbouring group participation has been attributed to the stereoselective 1,2-*trans* configuration of sugar nucleotides synthesised from ester protected glycopyranosyl bromides²⁶

2.3.3 Preparation of NDP tetrabutyl ammonium salt

NDP (disodium salt) was converted to the free acid by passing it through Amberlite® IR-120 (H⁺ ion exchange resin. The free acid was then titrated to pH 6 using tetrabutylammonium hydroxide (~40% in water) before being freeze dried for use in the phosphorylation. Integration of ¹H NMR signals showed a ratio of about 2.8 Bu₄N⁺ per equivalent of NDP (lit 2.5 Bu₄N⁺ per equivalent NDP).²⁶ Although there was a slight shift in the peaks on exchanging the counterions, ³¹P NMR did not indicate any significant hydrolysis of NDP as a result of ion exchange.

2.3.4 Chemical synthesis of 1,2-*trans* NDP-sugars



Scheme 2.8 – Generic scheme for the stereoselective synthesis of 1,2-*trans* NDP sugars.²⁶

D-Mannose and L-xylose were separately fully acetylated in acetic anhydride using a catalytic amount (0.7 mol%) of iodine to give per-*O*-acetyl- α -D-mannopyranose (**13**) and per-*O*-acetyl- α,β -L-xylopyranose (**14**) respectively.⁴⁵ Comparison of the ¹H NMR with literature values showed that the per-*O*-acetylated sugars had been synthesised in exclusively the pyranose

forms.⁴⁶⁻⁴⁸ For D-arabinose, iodine-catalysed per-O-acetylation, comparison of the ¹H NMR signals with literature values showed a mixture of pyranose and furanose products had been formed.^{47,49} Therefore a low temperature per-O-benzoylation of D-arabinose using benzoyl chloride in pyridine with 1 mol% DMAP gave per-O-benzoyl-β-D-arabinopyranose (**15**) in >99% pyranose form. Finally tetra-O-acetyl-α,β-L-xylofuranose (**16**) was synthesised by subjecting L-xylose to a hot (70 °C) per-O-acetylation using acetic anhydride in a mixture of acetic and boric acids.⁴⁹ The protected sugars were converted to the corresponding glycosyl bromide donors by treatment with 33% w/v HBr in AcOH immediately before use.

The same general protocol developed by Timmons *et al.*²⁶ was used for the synthesis of 1,2-*trans* sugar nucleotides. In short, tetrabutylammonium NDP salt and trimethylamine were dissolved into MeCN over molecular sieves. The triethylamine was added to neutralise the HBr liberated by the reaction. The sugar bromide was added and the reaction heated to 80 °C for 30 minutes after which time TLC showed consumption of the starting bromide. The solvent was removed under reduced pressure to give the crude reaction mixture. Following Timmons *et al.*,²⁶ at this point the crude mixture was dissolved in water and immediately adjusted to pH 8 with triethylamine. Attempts to use alkaline phosphatase (100U) to remove any unreacted NDP led to degradation of the protected NDP-sugar. Therefore, as unreacted NDP is readily removed from the NDP-sugar by SAX HPLC, I decided to omit the alkaline phosphatase step rather than trying to optimise it.

The crude reaction mixture was then dissolved in a mixture of MeOH/H₂O/Et₃N (5:2:1) and stirred overnight at room temperature to remove the ester protecting groups and give the corresponding NDP-sugar. The reaction mixture was analysed and subsequently purified by HPLC (SAX, UV 265 nm). Strong anion exchange (SAX) separates compounds by their formal charge. The higher the formal charge on a molecule, the more tightly retained it is by the anion exchange matrix. To avoid lengthy desalting steps, for preparative purposes a volatile buffer was used which can be removed by freeze drying. We have had a lot of success in the lab using ammonium bicarbonate as a volatile buffer for SAX HPLC purification of NDP-sugars, as the buffer can be removed by extensive freeze drying.

Any glycosyl bromide donor which had not reacted would have been hydrolysed to the sugar hemiacetal which does not carry a formal charge and as such is not retained by the SAX column. The NDP-sugar carries a formal 2⁻ charge and therefore elutes ahead of any unreacted NDP which carries a formal 3⁻ charge respectively (Figure 2.7).

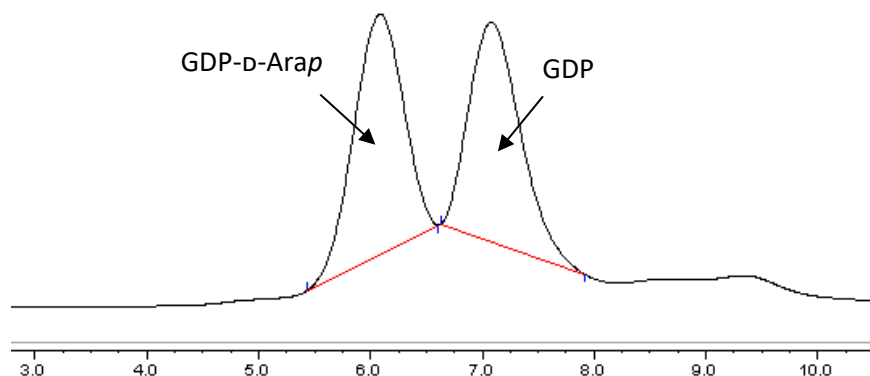


Figure 2.7 - SAX HPLC (UV_{abs} 265 nm) analysis of the crude reaction mixture after the synthesis of GDP-D-arabinopyranose. The more mobile compound has a lower formal charge and is assigned as GDP-D-Arap. The second peak corresponds to a higher formal charge than the first and was assigned as unreacted GDP by comparison with a GDP standard. See experimental section for column conditions.

As both the NDP-sugar and unreacted NDP carry the same chromophore it was possible to compare the relative integration of both peaks in the UV-absorbance chromatogram. It was therefore possible to calculate the conversion of NDP to NDP-sugar (Table 2.2).

Glycosyl bromide	NDP	Conversion
2,3,4-Tri- <i>O</i> -benzoyl-β-D-arabinopyranosyl bromide (17)	GDP	51%*
2,3,4-Tri- <i>O</i> -acetyl-α-L-xylopyranosyl bromide (18)	GDP	23%
2,3,4-Tri- <i>O</i> -acetyl-α-L-xylofuranosyl bromide (19)	GDP	0%
2,3,4,6-tetra- <i>O</i> -acetyl-α-D-mannopyranosyl bromide (20)	UDP	25%

* Of which 16% was the 1,2-*cis* α-anomer as judged by integration of the H-1' ¹H NMR signals.

No GDP-β-L-xylofuranose was detected by SAX HPLC; this was attributed to instability of the 1,2-*trans* NDP-furanoside under the reaction conditions.¹⁷ For the 1,2-*trans* NDP-pyranosides, conversions of between 23% and 51% were obtained.

The NDP-sugars were purified by SAX HPLC using ammonium bicarbonate as a buffer. The buffer was removed by freeze drying to give the NDP-sugar in a form clean enough for NMR analysis and LC-MS profiling.

2.3.5 Sugar nucleotide profiling

There is variation in the absolute retention times of species on the Hypercarb™ column. Pabst *et al.*¹⁵ have shown that there is a drift towards faster elution of NDP-sugar with column reduction. It was therefore important to keep the column earthed to minimise the drift in retention times. We have found that relative retention times compared with an internal UDP-Glc standard offer much better reproducibility. Although only a single chromatogram is shown for each sugar nucleotides, the recorded relative retention time in the published database (Appendix, Table 1) is an average of three readings.⁴⁰

The synthetic GDP-D-Arap was analysed by LC-MS. The Xevo TQ-S tandem mass spectrometer detected two isobaric peaks eluting from the Hypercarb™ PGC column (Figure 2.8) at 19.80 and 20.30 minutes. This could be explained by the presence of either a mixture of pyranose and furanose GDP-sugars, or a mixture of α and β anomers. The small difference in retention times (1 minute) was too small to be attributed to a mixture of pyranose and furanose rings, and it was therefore more likely that a mixture of anomers had been formed.³⁰ ¹H NMR showed a dominant H-1'' signal as a doublet of doublets at 4.82 ppm with a $J_{1'',2''}$ coupling value of 7.5 Hz (1,2-*trans* α -anomer) and a $J_{1'',P}$ coupling value of 7.5 Hz. There was also a minor H-1'' signal as a doublet of doublets at 5.52 ppm with a $J_{1'',2''}$ coupling value of 3.0 Hz (1,2-*cis* β -anomer) with a $J_{1'',P}$ coupling value of 7.0 Hz. This minor anomer was judged to have an abundance of 16% by integration of the H-1'' signals. This ratio was also in agreement with the integrals of the TIC peaks from the Xevo TQ-S mass spectrum. As the two peaks could be distinguished from one another, the larger peak at t_R 20.30 min was added to the sugar nucleotide profiling database as the characteristic peak for GDP- α -D-Arap (**9**).

GDP- β -L-Xylp (**10**) was analysed by LC-MS and the retention time and MRM transitions were added to the database. This time a single peak was detected which meant that either a single anomer had been formed or there were two anomers with the same retention times (Figure 2.8). Analysis of the ¹H NMR showed only a single H-1'' signal at 4.86 ppm as a doublet of doublets with a $J_{1'',2''}$ coupling value of 7.9 Hz (1,2-*trans* β -anomer) and a $J_{1'',P}$ coupling value of 7.9 Hz. The ³¹P NMR spectrum also showed two clean doublets at -11.2 ppm and -13.2 ppm with $J_{P\alpha,P\beta}$ coupling values of 20.2 Hz, which are signals characteristic of NDP-sugars. The NMR spectra, coupled with the LC-MS trace confirmed the presence of just the 1,2-*trans* β -anomer. This is the first time that GDP- β -L-xylopyranose (**10**) has been reported.

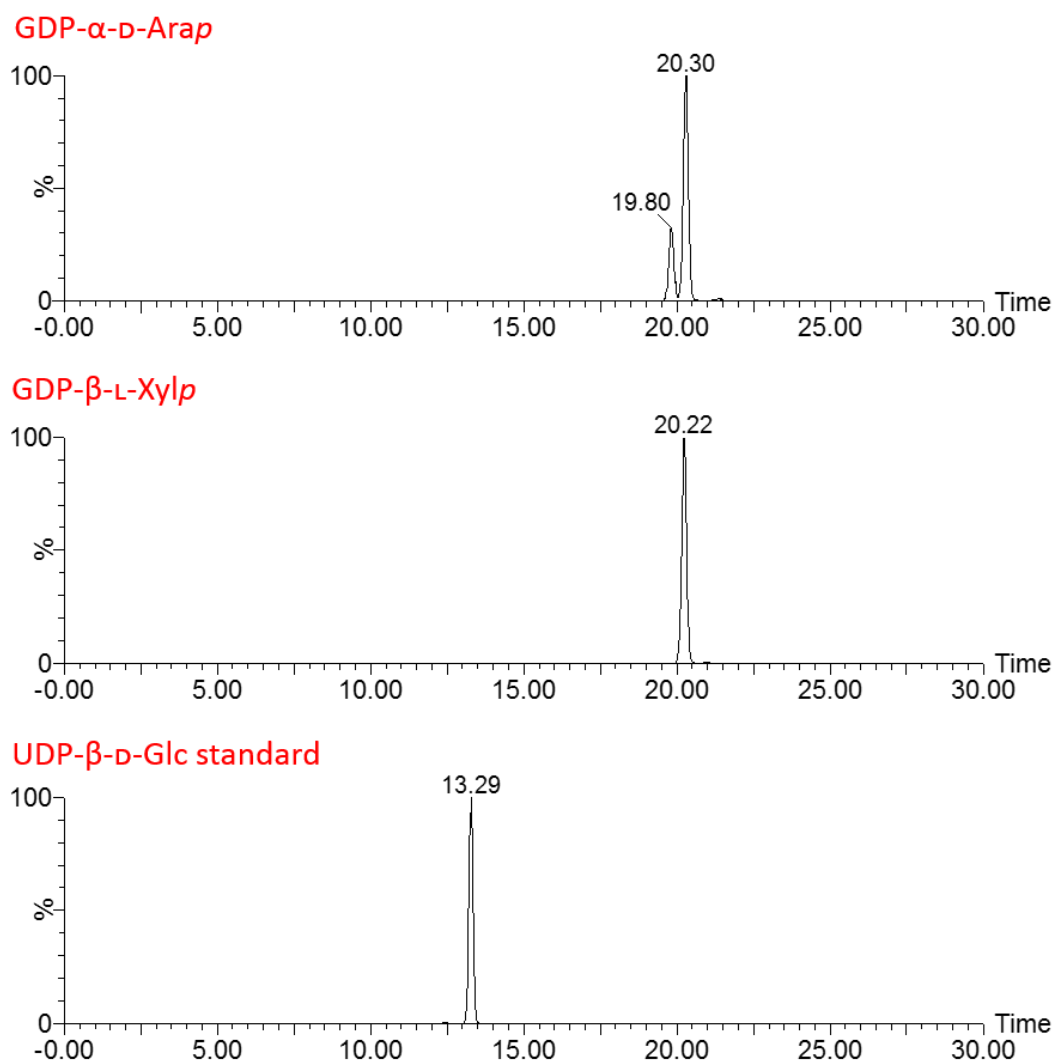


Figure 2.8 – MRM chromatograms (Xevo) for GDP- α -D-arabinopyranose (**9**) and GDP- β -L-xylopyranose (**10**), as well as UDP-Glc against which the retention times are defined. The relative retentions for **10** and **11** were 1.53 and 1.52 respectively. See experimental section for column conditions.

UDP-Man (**12**) was also added to the sugar nucleotide profiling database. Whilst not involved in the proposed biosynthetic pathway of GDP-L-xylofuranose, there was an unaccounted for UDP-hexose species present in some sugar nucleotide profiles of *P. parvum*.³⁰ Although the normal Leloir donor for mannose is GDP-mannose, it was decided worth-while adding UDP-mannose to our database to help narrow down the possibilities for the unidentified UDP-hexose. The LC-MS trace from the Hypercarb™ PGC column coupled to a Xevo Q-TS mass spectrometer showed only a single peak (Figure 2.9). Furthermore there was only H-1'' signal in the ¹H NMR spectrum at 5.42 ppm as a doublet of doublets with a $J_{1'',2''}$ coupling value of 1.8 Hz and a $J_{1'',p}$ coupling value of 8.0 Hz. To confirm the configuration at the anomeric

position a carbon proton-coupled spectrum was recorded which showed a $^1J_{C1'',H1''}$ coupling value of 175.6 Hz which is in keeping with values expected of α -mannosides.⁵⁰ Again the ^{31}P NMR showed two doublets at -11.5 ppm and -13.6 ppm with a $J_{P\alpha,P\beta}$ coupling value of 21.0 Hz, which is in the range characteristic for NDP-sugars.

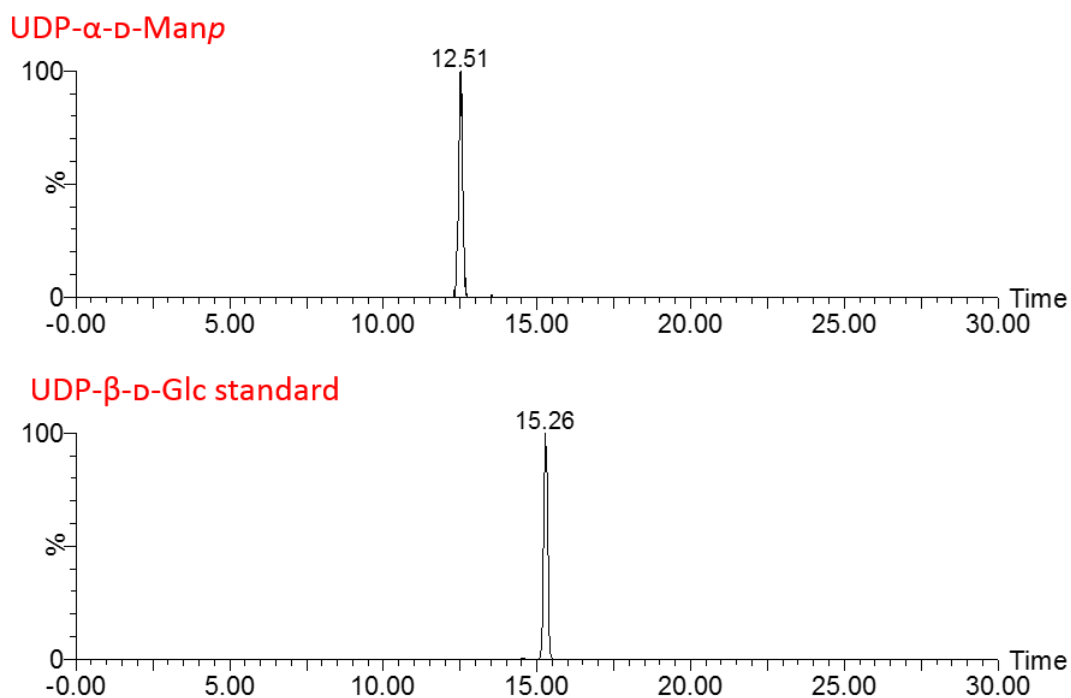


Figure 2.9 - LC-MS (Xevo) TIC chromatogram for UDP- α -D-mannopyranose (**12**) and UDP-Glc reference. The relative retention time of **12** is 0.82. See experimental section for column conditions.

The LC-MS experiments were run three times. The average relative retention times when compared with UDP- α -D-Glc for the sugar nucleotides standards were calculated (Table 2.3). The characteristic MRM transitions were also recorded, and the data was added to our larger database of sugar nucleotides (Appendix, Table 6.1).⁴⁰

Table 2.3 – Average relative retention times and MRM transitions for the sugar nucleotides synthesised in this chapter.⁴⁰

Sugar Nucleotide	Relative Retention time	MRM transitions	Fragment
UDP- α -D-Glucose (standard)	1.00	565 \rightarrow 323	[NMP-H] ⁻
		565 \rightarrow 79	[H ₃ PO ₄ -H ₃ O] ⁻
UDP- α -D-galactofuranose	1.10	565 \rightarrow 323	[NMP-H] ⁻
		565 \rightarrow 159	[H ₄ P ₂ O ₇ -H ₃ O] ⁻
GDP- α -D-arabinopyranose	1.53	574 \rightarrow 442	[NDP-H] ⁻
		574 \rightarrow 362	[NMP-H] ⁻
GDP- β -L-xylopyranose	1.52	574 \rightarrow 442	[NDP-H] ⁻
		574 \rightarrow 424	[NDP-H-H ₂ O] ⁻
UDP- α -D-mannose	0.81	565 \rightarrow 403	[NDP-H] ⁻
		565 \rightarrow 159	[H ₄ P ₂ O ₇ -H ₃ O] ⁻

2.4 Summary

A sugar nucleotide profiling project for *P. parvum* is currently being carried out collaboratively between members of the lab. My contribution to the project was the synthesis of non-commercially available nucleotide standards relating to selected carbohydrates reported as being present on the toxins prymnesin-1 and prymnesin-2. UDP- α -D-Galf (**8**) was synthesised chemoenzymatically from synthetic Galf-1-P (**7**). Although stability of **8** meant that it was not completely purified before use as a standard, it none the less gave a t_R of 1.10 on our porous graphitic column relative to UDP- α -D-Glc, and was used to optimise the MRM transition detection parameters. The 1,2-*trans* sugar nucleotides GDP- α -D-Arap (**9**) and GDP- β -L-Xylp (**10**) which are possible species in the biosynthetic pathway for L-xylofuranose found on prymnesin-2 were synthesised by direct attack of the corresponding glycosyl bromides. GDP -D-Arap was synthesised as a mixture of α/β isomers at the anomeric position, although the 1,2-*trans* sugar nucleotide has the major species and gave a relative t_R of 1.53 for our database; the minor 1,2-*cis* isomer eluted slightly earlier with a relative t_R of 1.49. GDP- β -L-Xylp (**10**) was synthesised with excellent stereochemical control and gave exclusively the 1,2-*cis* β anomer. Again, this standard was added to the sugar nucleotide database and had a relative t_R of 1.52. Finally, UDP- α -D-Manp (**12**) was chemically synthesised to try and pin down an unknown UDP-hexose which was being

detected in *P. parvum* extracts. This was synthesised by direct attack of the mannosyl bromide with UDP which proceeded with excellent stereochemical control to give only the 1,2-trans α anomer, and UDP- α -D-Manp (**12**) was found to have a relative t_R of 0.81. The synthesis of GDP- β -L-Xylf (**11**) is a challenge which still needs to be accomplished as a standard for the sugar-nucleotides profiling project. If the method of synthesising 1,2-*trans* sugar-nucleotides developed by Timmons and Jakeman²⁶ does not lend itself well to furanosyl bromides, one of the alternative methods of chemically synthesising sugar nucleotides discussed earlier in this chapter should be explored.¹⁷ If it were possible to express the trifunctional protein from *P. parvum* (Figure 2.6) then the synthetic 1,2-*trans* sugar nucleotides could also be tested as tentative substrates.

2.5 Experimental

2.5.1 Enzymes

Both galactose-1-phosphate uridylyltransferase (GalPUT, EC2.7.7.12) from *Escherichia coli* and Glucose-1-phosphate uridylyltransferase (GalU) from *Escherichia coli* had been over-expressed and purified previously in the group by Ellis O'Neill.^{28,51} Inorganic pyrophosphatase (IPP) from *Saccharomyces cerevisiae* was purchased from Sigma Aldrich.

2.5.2 NDP-Sugar Purification²⁹

NDP-sugar purification was performed using strong anion-exchange (SAX) HPLC. An aqueous solution of a sample was applied on a Poros[®] HQ 50 column (L/D 50/10 mm, CV = 3.9 mL). The column was first equilibrated with 4.5 CV of 5 mM ammonium bicarbonate buffer, followed by a linear gradient of ammonium bicarbonate from 5 mM to 250 mM in 13.5 CV. The gradient was then held for 4.5 CV, and finally followed a linear gradient back to 5 mM ammonium bicarbonate in 2.7 CV at a flow rate of 7.0 mL/min. Eluted compounds were detected with an on-line detector monitoring absorption at 265 nm. After multiple injections, the column was washed with 3 CV of 1 M ammonium bicarbonate followed by 5 CV of Milli-Q water.

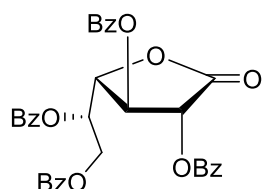
2.5.3 Sugar nucleotide profiling⁴⁰

We have recently reported our LC-MS/MS method for profiling sugar nucleotides.⁴⁰ A Xevo TQ-S tandem quadrupole mass spectrometer (Waters) running in negative ion mode was used. The capillary voltage was 1.5 kV, 500 °C desolvation temperature, 1000 L/h desolvation gas, 150 L/h cone gas, and 7 bar nebulizer pressure. Sugar nucleotide standards (10 µM) were directly infused into the Xevo mass spectrometer at 10 µL/min. The MRM transitions for the sugar nucleotides were generated and optimised using Intellistart software (Waters). Once optimised transitions were in place, the HPLC (Ultimate 3000, Dionex) retention times for the sugar nucleotides standards were determined on a porous graphitised carbon (PGC) column (Hypercarb, Thermo Scientific, dimensions 1 × 100 mm, particle size 5 µm) equipped with a column guard (Hypercarb, 5 µm, 1 × 10 mm). Sugar nucleotides standards (5 µL, 10 µM) were injected onto the column, and a multistep gradient of acetonitrile in water was run at 80 µL/min over 50 minutes. 0 min: 2% MeCN; 20 min: 15% MeCN; 26 min: 50% MeCN; 27 min: 90% MeCN; 30 min: 90% MeCN; 31 min: 2% MeCN; 50 min: 2% MeCN.

The results of the LC-MS/MS were processed using MassLynx software (Waters). We found that there could be significant variations in retention times between runs, but relative retention times compared against a standard of UDP-Glc were fairly stable.

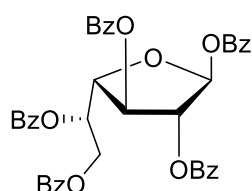
2.5.4 Chemical Synthesis

2,3,5,6-Tetra-*O*-benzoyl- β -D-galacto-1,4-lactone (**1**)²⁴



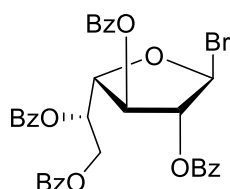
Galactono-1,4-lactone (2.00 g, 11.2 mmol) and DMAP (20mg, 160 μ mol) were dissolved into dry pyridine (30 mL) under N_2 . BzCl (8.0 mL, 68 mmol) was added dropwise to the solution and the reaction mixture was stirred at room temperature for 2 hours. The reaction mixture was diluted into DCM (50 mL) and washed with HCl (1.0 M, 2 \times 10 mL) and brine (10 mL) before being dried over $MgSO_4$, filtered and dried *in vacuo*. The crude residue was purified by FCC to give the title compound (**1**) (6.6 g, 98%) as a yellow oil; R_f 0.45 (hexane/EtOAc 7:3); ν_{max}/cm^{-1} (FTR-IR), 1720 (C=O), 1601 (C=C) 1245 (C-O), 1091 (C-O); δ_H (400 MHz; $CDCl_3$) 8.17-7.26 (m, 20H, Ar), 6.09 (d, $J_{2,3} = 5.7$ Hz, 1H, H-2), 6.08-6.04 (m, 1H, H-5), 5.87 (dd, $J_{2,3} = 5.7$ Hz, $J_{3,4} = 5.7$ Hz, 1H, H-3), 5.06 (dd, $J_{3,4} = 5.7$ Hz, $J_{4,5} = 2.7$ Hz, 1H, H-4), 4.78-4.70 (m, 2H, H-6a,6b); δ_C (100 MHz; $CDCl_3$) 168.7 (C1), 165.9, 165.5, 165.2, 165.0 (4 \times C=O), 134.6, 134.0, 133.8, 133.8, 133.3, 130.6, 130.2, 130.1, 130.0, 129.8, 129.3, 128.9, 128.8, 128.7, 128.6, 128.5, 128.4, 128.1, 127.9 (Ar), 79.5 (C4), 74.3 (C3), 72.3 (C2), 70.1 (C5), 62.4 (C6). The 1H NMR data were in accordance with the literature.⁵²

Per-*O*-benzoyl- β -D-galactofuranose (**4**)³⁹



A solution of 2,3,5,6-tetra-*O*-benzoyl-*D*-galacto-1,4-lactone (**1**) (6.0 g, 10 mmol) in THF (30 mL) was cooled to -78 °C in a bath of dry ice and acetone. L-Selectride® (1M in THF) (15 mL, 1.5 mmol) was slowly added by syringe and the reaction mixture was stirred at -78 °C for 2h, after which time analysis by TLC showed consumption of the starting lactone (R_f 0.58, hexane/EtOAc 7:3) and a new spot (R_f 0.48 hexane/EtOAc 7:3). Pyridine (4 mL) was added in a single portion followed the dropwise addition of benzoyl chloride (5 mL, 43 mmol). The reaction mixture was then removed from the dry ice bath and allowed to warm to room temperature overnight. The solvent was removed under reduced pressure and the crude reaction mixture purified by FCC to give the title compound (5.4 g, 76% over 2 steps) as a white powder; R_f 0.58 (hexane/EtOAc 7:3); δ_H (400 MHz; CDCl₃) 8.12-7.26 (m, 25H, Ar), 6.78 (s, 1H, H-1), 6.15-6.11 (m, 1H, H-5), 5.80 (dd, $J_{2,3} = 0.8$ Hz, $J_{3,4} = 4.1$ Hz, 1H, H-3), 5.77 (d, $J_{2,3} = 0.8$ Hz, 1H, H-2), 4.88 (dd, $J_{3,4} = J_{4,5} = 4.1$ Hz, 1H, H-4), 4.83-4.73 (m, 2H, H-6a,6b) ; 166.0, 165.8, 165.4, 165.2, 164.5 (5 × C=O), 133.7, 133.7, 133.6, 133.3, 133.0, 130.0, 129.9, 129.7, 129.5, 129.4, 129.3, 128.9, 128.6, 128.5, 128.5, 128.4, 128.3, 128.2 (Ar), 99.8 (C1), 84.3 (C4), 81.0 (C2), 77.2 (C3), 70.3 (C5), 63.6 (C6); m/z (MALDI, DHB matrix) calc. for C₄₁H₃₂O₁₁Na⁺ 723.184 ([M+Na]⁺) found 723.116 [M+Na⁺], 739.199 [M+K⁺]; the ¹H NMR data were in accordance with the literature.³⁹

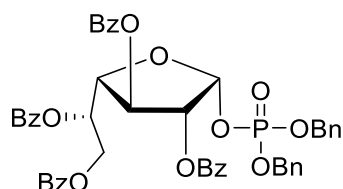
2,3,5,6-Tetra-*O*-benzoyl- β -*D*-galactofuranosyl bromide (**5**)⁵³



Per-*O*-benzoyl- β -*D*-galactofuranose (**4**) (500 mg, 0.71 mmol) was dissolved into dry DCM (5 mL) under N₂. The solution was cooled to 0 °C and HBr (30% w/v in AcOH, 2.0 mL, 7.4 mmol) added dropwise. The reaction mixture was stirred for 1 hour at 0 °C. TLC (hexane/EtOAc 8:2) showed **4** had been consumed and the reaction was diluted with DCM (20 mL) and washed with sat. aqueous sodium bicarbonate solution (3 × 5 mL). The organic layer was then dried over MgSO₄, filtered and dried *in vacuo* to give the title compound as a colourless oil (410 mg, 88%) which was used in the next step without any further purification. R_f 0.33 (hexane/EtOAc 8:2); δ_H (400 MHz; CDCl₃) 8.12-7.23 (m, 20H, Ar), 6.66 (s, 1H, H-1), 6.20 (m, 1H, H-5), 5.90 (s 1H, H-2), 5.70 (d, $J_{3,4} = 4.8$ Hz, 1H, H-3), 4.97 (t, $J_{3,4} = 4.8$ Hz, $J_{4,5} = 4.8$ Hz, 1H, H-4), 4.75-4.73 (m, 2H, H-6); δ_C (100 MHz; CDCl₃) 166.0, 165.7, 165.6, 165.2 (4 × C=O), 133.8,

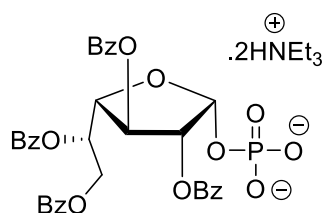
133.7, 133.5, 133.2, 130.1, 130.1, 129.9, 129.7, 128.6, 128.5, 128.4 (Ar), 88.5 (C1), 85.7 (C2), 84.9 (C4), 76.6 (C3), 69.6 (C5), 63.4 (C6).

2,3,5,6-Tetra-O-benzoyl- α -D-galactofuranosyl-dibenzyl phosphate (6)²⁴



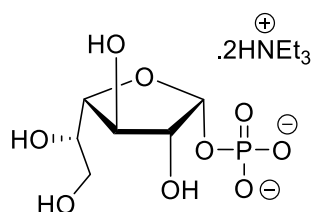
Dibenzyl hydrogen phosphate (300 mg, 1.1 mmol) and Et₃N (0.2 mL, 1.43 mmol) were dissolved into dry toluene (1.7 mL) under N₂. 2,3,5,6-Tetra-O-benzoyl- β -D-galactofuranosyl bromide (5) (410 mg, 0.6 mmol) in dry toluene (4 mL) was added by syringe and the reaction mixture stirred at room temperature for 16 hours. TLC (toluene/EtOAc 9:1) showed both α and β products which were separated by FCC (toluene/EtOAc 9:1) to give α -phosphate (170mg, 33%) as a white powder; R_f 0.26 (toluene/EtOAc 9:1); δ_{H} (400 MHz; CDCl₃) 8.14-7.91 (m, 8H, Ar), 7.55-7.05 (m; 22H, Ar), 6.33, (dd, $J_{1,2} = 4.6$ Hz, $J_{1,P} = 5.7$ Hz, 1H, H-1), 6.17 (dd, $J_{2,3} = J_{3,4} = 7.2$ Hz, 1H, H-3), 5.85-5.82 (m, 1H, H-5), 5.73 (ddd, $J_{1,2} = 4.6$ Hz, $J_{2,3} = 7.2$ Hz, $J_{2,P} = 1.9$ Hz, 1H, H-2), 5.05-4.70 (m, 6H, H-4,6a & 2 \times PhCH₂), 4.61 (dd, $J_{5,6b} = 6.2$ Hz, $^2J_{6a,6b} = 12.0$ Hz, 1H, H-6b); δ_{C} (100 MHz; CDCl₃), 165.9, 165.6, 165.5, 165.4 (4 \times C=O), 133.7, 133.6, 133.2, 133.1, 130.1, 130.0, 129.9, 129.7, 129.5, 129.4, 128.5, 128.5, 128.4, 128.4, 128.3, 127.8, 127.6 (Ar), 97.7 (d, $J_{C1,P} = 4.9$ Hz, C1), 80.0 (C4), 76.5 (d, $J_{C2,P} = 7.1$ Hz, C2), 73.4 (C3), 70.8 (C5), 69.4 (d, $J_{\text{PhCH}_2,P} = 5.4$ Hz, PhCH₂), 69.3 (d, $J_{\text{PhCH}_2,P} = 5.4$ Hz, PhCH₂), 62.7 (C6); LRMS (MALDI, DHB matrix) m/z calc. for C₄₈H₄₁O₁₃PNa⁺ 879.218 ([M+Na]⁺) found 879.308 [M+Na⁺], 865.273 [M.K⁺]; the ¹H NMR data were in accordance with the literature.²⁴

2,3,5,6-Tetra-O-benzoyl- α -D-galactofuranosyl – phosphate, bis-triethylammonium salt²⁴



Triethylamine (0.17 mL) and 2,3,5,6-tetra-*O*-benzoyl- α -D-galactofuranosyl-dibenzyl phosphate (**6**) (170 mg, 0.2 mmol) were dissolved in EtOAc (2.5 mL) under N₂. Pd/C (10%, 20 mg) was carefully added and the system purged with N₂. The system was then purged with and left under H₂ overnight at room temperature. TLC (tol/EtOAc 9:1) showed the consumption of **6** and the catalyst was removed by filtration and the solvent removed under *in vacuo* to give the title compound (73 mg, 41%) as a white powder; δ_{H} (400 MHz; CDCl₃) 8.11-7.17 (m, 8H, Ar), 7.50-7.23 (m, 12H, Ar), 6.23 (dd, $J_{1,2} = J_{1,P} = 7.0$ Hz, 1H, H-1), 6.16 (dd, $J_{2,3} = 7.4$ Hz, $J_{3,4} = 4.4$ Hz, 1H, H-3), 5.87-5.84 (m, 1H, H-5), 5.64 (m, 1H, H-2), 4.90 (dd, $J_{5,6a} = 3.6$ Hz, $J_{6a,6b} = 12.1$ Hz, 1H, H-6a), 4.75 (dd, $J_{5,6b} = 6.5$ Hz, $J_{6a,6b} = 12.1$ Hz, 1H, H-6b), 4.63 (dd, $J_{3,4} = 4.4$ Hz, $J_{4,5} = 5.8$ Hz, 1H, H-4), 3.04 (q, $J_{\text{CH}_2,\text{CH}_3} = 7.3$ Hz, 12H, 2 \times N(CH₂CH₃)₃), 1.31 (q, $J_{\text{CH}_2,\text{CH}_3} = 7.3$ Hz, 18H, 2 \times N(CH₂CH₃)₃); δ_{C} (100 MHz; CDCl₃) 165.9, 165.8, 165.7, 165.4 (4 \times C=O), 133.3, 133.1, 132.9, 131.2, 130.1, 130.1, 129.8, 129.6, 129.5, 129.5, 128.9, 128.4, 128.3, 128.3, 128.2, 127.8, 126.8, 95.9 (d, $J_{\text{C}1,\text{P}} = 4.0$ Hz, C1), 78.3 (C4), 76.6 (d, $J_{\text{C}2,\text{P}} = 7.5$ Hz, C2), 73.9 (C3), 71.8 (C5), 62.9 (C6), 45.7 (2 \times N(CH₂CH₃)₃), 8.6 (2 \times N(CH₂CH₃)₃); δ_{P} (162 MHz; CDCl₃) -1.0 (P); LRMS (ESI⁻) calc for C₃₄H₂₈O₁₃P⁻ 675.1 ([M-H]⁻), found 675.4 [M-H]⁻; the ¹H and ¹³C NMR were in accordance with literature values.²⁴

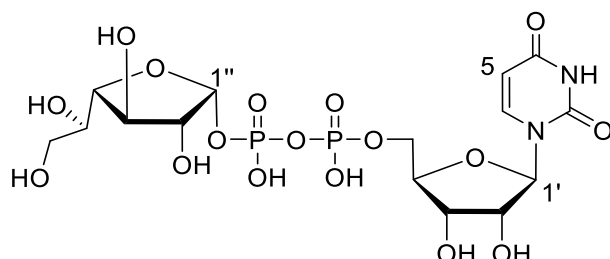
α -D-Galactofuranosyl phosphate, bis-triethylammonium salt (**8**)²⁴



2,3,5,6-tetra-*O*-benzoyl- α -D-galactofuranosyl-phosphate bis-triethylammonium salt (70 mg, 80 μ mol) was dissolved into a solvent system of MeOH/H₂O/Et₃N (5:2:1) (8 mL) and stirred for 4 days at room temperature. The solvent was removed *in vacuo* and the products were partitioned between water and Et₂O to remove benzoic acid. The aqueous layer was separated and dried by lyophilisation to give the title compound (**8**) (24 mg, 66%) as a white powder; δ_{H} (400 MHz; D₂O) 5.36 (dd, $J_{1,2} = J_{1,P} = 4.6$ Hz, 1H, H-1), 4.09 (dd, $J_{2,3} = 8.3$ Hz, $J_{3,4} = 7.3$ Hz, 1H, H-3), 3.97 (dd, $J_{1,2} = 4.6$ Hz, $J_{2,3} = 8.3$ Hz, $J_{2,P} = 2.2$ Hz, 1H, H-2), 3.68-3.45 (m, 4H, H-4,5,6a,6b), 3.03 (q, $J_{\text{CH}_2,\text{CH}_3} = 7.4$ Hz, 12H, 3 \times (NCH₂CH₃)₃), 1.11 (t, $J_{\text{CH}_2,\text{CH}_3} = 7.4$ Hz, 12H, 3 \times (NCH₂CH₃)₃); δ_{C} (100 MHz; D₂O) 96.6 (d, $J_{\text{C}1,\text{P}} = 5.7$ Hz, C1), 81.4 (C4), 76.5 (d, $J_{\text{C}2,\text{P}} = 7.8$ Hz, C2), 73.6 (C3), 71.8 (C5), 62.3 (C6), 46.6 (NCH₂CH₃), 8.2 (NCH₂CH₃); δ_{P} (162 MHz; D₂O) -0.2; HRMS

(ESI⁻) *m/z* calc. for C₆H₁₁O₉P⁻ 259.0224 ([M-H]⁻) found 259.0220 [M-H]⁻. The ¹H and, ¹³C and ³¹P NMR data were in accordance with the literature.²⁴

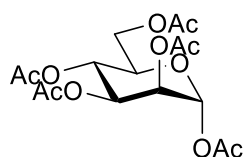
UDP- α -D-Galactofuranose (**9**)²⁸



α -D-Galactofuranosyl phosphate, bis-triethylammonium salt (**8**) (1 mg, 2.2 μ mol), UDP-glucose disodium salt (41 μ g, 65 nmol) and uridine triphosphate trisodium salt (1.2 mg, 2.2 μ mol) were dissolved into 500 μ L of buffer (50 mM HEPES, 10 mM MgCl₂ and 10 mM KCl adjusted to pH 8.0). A small portion (20 μ L) was separated, mixed with methanol (20 μ L) and stored in the freezer as a no enzyme control. Stock solutions of glucose-1-phosphate uridylyltransferase (2.4 mg/ml in 25% glycerol and 75% GF buffer (pH 7.5, 50 mM HEPES, 100 mM NaCl) 5U, 50 μ L), galactose-1-phosphate uridylyl transferase (2.4 mg/ml, GF buffer, 75 U, 50 μ L) and inorganic pyrophosphatase commercial (5U, 50 μ L) were all added and the reaction mixture was stirred at 30 °C for 8 hours.

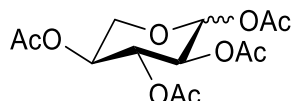
The reaction was subsequently quenched with methanol (500 μ L) and centrifuged at 10,000 \times g for 2 minutes. The supernatant was analysed by strong anion exchange HPLC but was not purified further as it was suitable for use as a sugar nucleotide standard as was. The diagnostic signals are listed. δ_{H} (400 MHz; D₂O) 7.90 (d, $J_{5,6}$ = 8.2 Hz, 1H, H-5), 5.90 (d, $J_{1',2'}$ = 4.9 Hz, 1H, H-1'), 5.86 (d, $J_{5,6}$ = 8.2 Hz, 1H, H-6), 5.55 ($J_{1'',2''}$ = 4.6 Hz, $J_{1'',\text{P}}$ = 5.2 Hz, 1H, H-1''), 4.31-3.96 (m, 7H, H-2'',3'',2',3',4',5'a,5'b), 3.75-3.35 (m, 3H, 4'',5'',6';a,6'b); δ_{P} (162 MHz; D₂O) -11.3 (m, P $_{\beta}$), -12.8 (m, P $_{\alpha}$); HRMS (ESI⁻) *m/z* calc. for C₁₅H₂₃N₂O₁₇P₂⁻ 565.0477 ([M-H]⁻) found 565.0477 [M-H]⁻. The diagnostic ¹H and ³¹P signals were in accordance with literature values.²³

Per-*O*-acetyl- α -D-mannopyranose (**13**)⁵⁴



Iodine (0.7 mol %) was added to a suspension of D-Mannose (1.0 g,) in acetic anhydride (10 mL) under nitrogen. The reaction mixture was stirred overnight at room temperature, before being diluted with EtOAc (100 mL) and washed with sat. Na₂S₂O₃ (3 × 20 mL) and sat. NaHCO₃ (3 × 20 mL). The organic layers were combined and dried over MgSO₄, before being filtered and dried under reduced pressure to give the crude compound (**13**) as a brown oil. This was used without further purification. R_f 0.19 (hexane/EtOAc 7:3); δ_{H} (400 MHz; CDCl₃) 6.09 (d, $J_{1,2} = 1.9$ Hz, 1H, H-1), 5.36-5.34 (m, 2H, H-3,4), 5.26 (dd, $J_{1,2} = 1.9$ Hz, $J_{2,3} = 2.3$ Hz, 1H, H-2), 4.28 (dd, $J_{5,6a} = 4.9$ Hz, $^2J_{6a,6b} = 12.4$ Hz, 1H, H-6a), 4.10 (dd, $J_{5,6b} = 2.5$ Hz, $^2J_{6a,6b} = 12.4$ Hz, 1H, H-6b), 4.09-4.04 (m, 1H, H-5); δ_{C} (100 MHz; CDCl₃) 170.5, 169.9, 169.6, 169.5, 168.0, 166.4 (6 × C=O), 90.5 (C1), 70.5 (C5), 68.7 (C3), 68.3 (C2), 65.5 (C4), 62.0 (C6), 22.1, 20.7, 20.7, 20.6, 20.6, 20.5 (6 × OAc). ¹H and ¹³C NMR were in agreement with literature values.⁴⁸

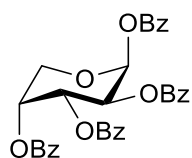
Per-*O*-acetyl- α,β -L-xylopyranose (**14**)⁵⁵



Iodine (0.7 mol %) was added to a suspension of L-xylose (200 mg,) in acetic anhydride (6 mL) under nitrogen.⁴⁵ The reaction mixture was stirred overnight at room temperature, before being diluted with EtOAc (50 mL) and washed with sat. Na₂S₂O₃ solution (3 × 10 mL) and sat. NaHCO₃ solution (3 × 10 mL). The organic layers were combined and dried over MgSO₄, before being filtered and dried under reduced pressure to give the crude compound (**14**) as a yellow oil (α/β 1:5) as judged by ¹H NMR; R_f 0.32 (7:3 Hex:EtOAc); δ_{H} (400 MHz; CDCl₃) 6.27 (d, $J_{1,2} = 3.7$ Hz, 1H, H-1 β), 5.72 (d, $J_{1,2} = 7.0$ Hz, 1H, H-1 α), 5.47 (dd, $J_{2,3} = J_{3,4} = 9.7$ Hz, 1H, H-3 β), 5.21 (dd, $J_{2,3} = J_{3,4} = 8.6$ Hz, 1H, H-3 α), 5.06-4.97 (m, 4H, H-2 α ,4 α ,2 β ,4 β), 4.15 (dd, $J_{4,5a\alpha} = 5.2$ Hz, $^2J_{5a\alpha,5b\alpha} = 12.0$ Hz, 1H, H-5a α), 3.94 (dd, $J_{4,5a\beta} = 6.0$ Hz, $^2J_{5a\beta,5b\beta} = 11.2$ Hz, 1H, H-5a β), 3.71 (dd, $J_{4,5b\beta} = ^2J_{5a\beta,5b\beta} = 11.2$ Hz, 1H, H-5b β), 3.53 (dd, $J_{4,5b\alpha} = 8.5$ Hz, $^2J_{5a\alpha,5b\alpha} = 12.0$ Hz, 1H, H-5b α); δ_{C} (100 MHz; CDCl₃) 170.1, 169.8, 169.7, 169.0 (4 × C=O), 92.1 (C1 α) 89.3 (C1 β), 71.1 (C3 α), 69.6 (C4 α), 69.3 (C3 β), 69.4 (C4 β), 67.9 (C2 α), 68.7 (C2 β), 61.7 (C5 α), 60.7

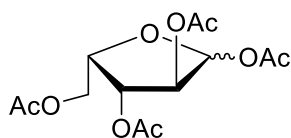
(C5 β), 20.7, 20.7, 20.5, 20.5 (4 \times OAc). The ^1H and ^{13}C NMR signals were in good agreement with literature values for the analogous D-enantiomers; 1,2-cis α -L analogue,⁴⁶ 1,2-trans β -L analogue.⁴⁷

Per-O-benzoyl- β -D-arabinopyranose (**15**)⁵⁶



A solution of D-arabinose (1.0 g, 6.7 mmol) and DMAP (8 mg, 1 mol%) in dry pyridine (15 mL) under nitrogen was cooled in an ice bath. Benzoyl chloride (5.0 mL, 43 mmol) was added dropwise over 30 minutes and the reaction mixture was allowed to warm to room temperature and stirred overnight. The solvent was removed under reduced pressure and the crude mixture was re-dissolved in EtOAc (30 mL) before being washed with 3M HCl (3M, 2 \times 10 mL), sat. NaHCO_3 (2 \times 5 mL) and brine (10 mL). The organic layer was dried over MgSO_4 , filtered and the solvent was removed under reduced pressure to give a crude product as a yellow oil. The crude compound was purified by FCC to give the title compound (**15**) (3.2 g, 85%) as a white powder R_f 0.66 (n-Hex/EtOAc 7:3); δ_{H} (400 MHz; CDCl_3) 8.1 – 7.2 (m, Ar-H, 20H), 6.86 (1H, d, $J_{1,2} = 1.5$ Hz, H-1), 6.07 (2H, m, H-2, H-3), 5.89 (1H, m, H-4), 4.41 (1H, dd, $J_{4,5} = 1.0$ Hz, $^2J_{5a,5b} = 13.4$ Hz, H-5a), 4.18 (1H, dd, $J_{4,5'} = 2.1$ Hz, $^2J_{5a,5b} = 13.4$ Hz, H-5b); δ_{C} (100 MHz; CDCl_3) 165.7, 165.7, 165.6, 164.7 (4 \times C=O), 133.8, 133.6, 133.5, 133.4 (4 \times Ar-C), 129.9 – 128.4 (Ar), 91.1 (C1), 69.5 (C4), 68.2 (C3), 67.8 (C2), 63.0 (C5). The ^1H and ^{13}C NMR signals were in good agreement with literature values for the analogous L-enantiomer.⁵⁶

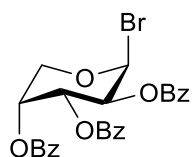
Per-O-acetyl- α,β -L-xylofuranose (**16**)⁴⁹



L-Xylose (1.0 g, 6.6 mmol) was suspended in AcOH (50 mL) under a nitrogen atmosphere. Boric acid (1.86 g, 30 mmol) was added in a single portion and the reaction mixture was heated at 70 $^\circ\text{C}$ for 2 hours.⁴⁹ Acetic anhydride (50 mL) was slowly added over 30 minutes

and the reaction mixture stirred at 70 °C overnight. The reaction mixture was then poured into water (120 mL) and the aqueous mixture was extracted with EtOAc (3 × 40 mL). The organic layers were combined, washed with sat. aqueous NaHCO₃ solution (3 × 30 mL), dried over MgSO₄ and filtered. The solvent was then removed under reduced pressure to give the crude product (**16**) (2.16 g, 52%) (α/β 1:1 as judged by ¹H NMR) as a yellow oil; R_f 0.15 (hexane/EtOAc 7:3); δ_H(400 MHz; CDCl₃) 6.43 (d, $J_{1\alpha,2\alpha} = 4.5$ Hz, 1H, H-1α), 6.12 (s, 1H, H-1β), 5.34 (dd, $J_{2\alpha,3\alpha} = J_{3\alpha,4\alpha} = 6.8$ Hz, 1H, H-3α), 5.38 (dd, $J_{2\beta,3\beta} = 1.6$ Hz, $J_{3\beta,4\beta} = 5.6$ Hz, 1H, H-3β), 5.31 (dd, $J_{1\alpha,2\alpha} = 4.5$ Hz, $J_{2\alpha,3\alpha} = 6.3$ Hz, 1H, H-2α), 5.22 (d, $J_{2\beta,3\beta} = 1.6$ Hz, 1H, H-2β), 4.67-4.61 (m, 2H, H-4β,4α), 4.26-4.21 (m, 3H, H-5aβ, 5bβ, 5aα), 4.13 (dd, $J_{4\alpha,5b\alpha} = 4.3$ Hz, $J_{5a\alpha,5b\alpha} = 12.3$ Hz, 1H, H-5bα), 2.13-2.08 (m, 24H, 8 × OAc); δ_C(100 MHz; CDCl₃) 170.5, 170.4, 170.2, 169.7, 169.5, 169.3, 169.3, 169.2 (8 × C=O), 98.8 (C1β), 92.8 (C2α), 79.9 (C2β), 79.4 (C4β), 75.4 (C4α), 75.2 (C2α), 74.3 (C3β), 73.8 (C3α), 62.4 (5β), 61.6 (C5α), 21.1, 20.9, 20.8, 20.8, 20.7, 20.6, 20.6, 20.4 (8 × OAc); NMR values are in agreement with literature values.⁴⁹

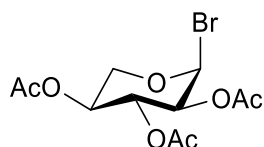
2,3,4-Tri-*O*-benzoyl-β-D-arabinopyranosyl bromide (**17**)



Per-*O*-benzoyl-β-D-arabinopyranose (**15**) (100 mg, 0.18 mmol) was dissolved in dry DCM (3 mL) under a nitrogen atmosphere. 33% w/v HBr in AcOH (0.5 mL) was added and the reaction mixture was stirred at room temperature for 3 hours. Residual HBr was blown out of the reaction flask with a compressed air line, and the solvent was removed under reduced pressure. The crude mixture was re-dissolved in EtOAc (15 mL) and washed with ice cold sat. aqueous NaHCO₃ (3 × 5 mL). The organic layer was dried over MgSO₄, filtered and the solvent evaporated under reduced pressure to give the crude title compound (**17**) as a colourless oil which was used immediately in the next step without further purification. R_f 0.40 (hexane/EtOAc 3:1); δ_H(400 MHz; CDCl₃) 8.11-8.08 (m, 1H, Ar), 8.03-8.01 (m, 1H, Ar), 7.87-7.85 (m, 1H, Ar), 7.63-7.30 (m, 9H, Ar), 6.93 (d, $J_{1,2} = 3.8$ Hz, 1H, H-1), 6.00 (dd, $J_{2,3} = 10.5$ Hz, $J_{3,4} = 3.8$ Hz, 1H, H-3), 5.84-5.83 (m, 1H, H-4), 5.71 (dd, $J_{1,2} = 3.9$ Hz, $J_{2,3} = 10.5$ Hz, 1H, H-2), 4.47 (dbs, $^2J_{5a,5b} = 12.9$ Hz, 1H, H-5a), 4.23 (dd, $J_{4,5b} = 1.9$ Hz, $^2J_{5a,5b} = 12.9$ Hz, 1H, H-5b); δ_H(100 MHz; CDCl₃) 165.6, 165.5, 165.4 (3 × C=O), 133.8, 133.7, 133.4, 130.0, 129.9, 129.8, 128.7,

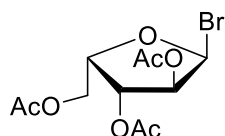
128.6, 128.4 (12 × Ar) 89.8 (C1), 68.9 (C4), 68.7 (C2), 65.0 (C3), 60.4 (C5). The ^1H NMR values were in agreement with those for the analogous L-enantiomer.⁵⁷

2,3,4-Tri-O-acetyl- α -L-xylopyranosyl bromide (**18**)



Per-O-acetyl- α,β -L-xylopyranose (100 mg, 0.3 mmol) was dissolved in dry DCM (3 mL) under a nitrogen atmosphere. 33% w/v HBr in AcOH (0.5 mL) was added and the reaction mixture was stirred at room temperature for 3 hours. Residual HBr was blown out of the reaction flask with a compressed air line, and the solvent was removed under reduced pressure. The crude mixture was re-dissolved in EtOAc (15 mL) and washed with ice cold sat. aqueous NaHCO_3 solution (3 × 5 mL). The organic layer was dried over MgSO_4 , filtered and the solvent evaporated *in vacuo* to give the crude title compound as a colourless oil (**18**) which was used immediately in the next step. R_f 0.55 (hexane/EtOAc 7:3); δ_{H} (400 MHz; CDCl_3) 6.59 (d, $J_{1,2} = 4.0$ Hz, 1H, H-1), 5.57 (dd, $J_{2,3} = 10.0$ Hz, $J_{3,4} = 10.0$ Hz, 1H, H-3), 5.08-5.01 (m, 1H, H-4), 4.78 (dd, $J_{1,2} = 4.0$ Hz, $J_{2,3} = 10.0$ Hz, 1H, H-2), 4.05 (dd, $J_{4,5a} = 6.0$ Hz $^2J_{5a,5b} = 11.4$ Hz, 1H, H-5a), 3.88 (dd, $J_{4,5b} = 11.4$ Hz, $^2J_{5a,5b} = 11.4$ Hz, 1H, H-5b); δ_{C} (100 MHz; CDCl_3); 169.4, 169.4, 169.7 (3 × C=O); 87.5 (C1), 70.9 (C2), 69.5 (C3), 68.1 (C4), 62.5 (C5), 20.7, 20.7, 20.6, (3 × OAc).

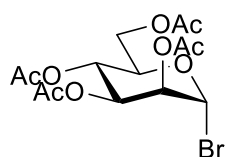
2,3,4-Tri-O-acetyl- α -L-xylofuranosyl bromide (**19**)



Per-O-acetyl- α,β -L-xylofuranose (200 mg, 0.6 mmol) was dissolved in dry DCM (3 mL) under a nitrogen atmosphere. 33% w/v HBr in AcOH (0.5 mL) was added and the reaction mixture was stirred at room temperature for 3 hours. Residual HBr was blown out of the reaction flask with a compressed air line, and the solvent was removed under reduced pressure. The crude mixture was re-dissolved in EtOAc (15 mL) and washed with ice cold sat. aqueous NaHCO_3 solution (3 × 5 mL). The organic layer was dried over MgSO_4 , filtered and the solvent

evaporated *in vacuo* to give the crude title compound (**19**) as a colourless oil which was used immediately in the next step; δ_{H} (400 MHz; CDCl_3) 6.81 (d, $J_{1,2} = 4.7$ Hz, 1H, H-1), 5.62, (dd, $J_{2,3} = J_{3,4} = 6.8$ Hz, 1H, H-3), 5.03 (dd, $J_{1,2} = 4.7$ Hz, $J_{2,3} = 6.8$ Hz, 1H, H-2), 4.75-4.71 (m, 1H, H-4), 4.31 (dd, $J_{4,5a} = 5.5$ Hz, $^2J_{5a,5b} = 12.4$ Hz, 1H, H-5a), 4.15 (dd, $J_{4,5b} = 4.0$, $^2J_{5a,5b} = 12.4$ Hz, 1H, H-5b); δ_{C} (100 MHz; CDCl_3) 170.3, 170.1, 170.0, 169.5 (4 \times C=O), 98.6 (C1), 78.2 (C2), 76.3 (C4), 73.5 (C3), 60.6 (C5), 20.9, 20.8, 20.7, 20.6 (4 \times C=O).

2,3,4,6-penta-O-acetyl- α -D-mannosyl bromide (**20**)



Per-O-acetyl- α -D-mannose (**13**) (100 mg, 0.3 mmol) was dissolved in dry DCM (3 mL) under a nitrogen atmosphere. 33% w/v HBr in AcOH (0.5 mL) was added and the reaction mixture was stirred at room temperature for 3 hours. Residual HBr was blown out of the reaction flask with a compressed air line, and the solvent was removed under reduced pressure. The crude mixture was re-dissolved in EtOAc (15 mL) and washed with ice cold sat. aqueous NaHCO_3 solution (3 \times 5 mL). The organic layer was dried over MgSO_4 , filtered and the solvent evaporated *in vacuo* pressure to give the crude title compound as a colourless oil (**20**) which was used immediately in the next step without further purification; R_f 0.35 (hexane/EtOAc 7:3); δ_{H} (400 MHz; CDCl_3) 6.31 (d, $J_{1,2} = 1.0$ Hz, 1H, H-1), 5.72 (dd, $J_{2,3} = 3.4$ Hz, $J_{3,4} = 10.1$ Hz, 1H, H-3), 5.45 (dd, $J_{1,2} = 1.0$ Hz, $J_{2,3} = 3.4$ Hz, 1H, H-2), 5.37 (dd, $J_{3,4} = 10.1$ Hz, $J_{4,5} = 10.1$ Hz, 1H, H-4), 4.33 (dd, $J_{5,6a} = 5.0$ Hz, $J_{6a,6b} = 12.5$ Hz, 1H, H-6a), 4.25-4.21 (m, 1H, H-5), 4.14 (dd, $J_{5,6b} = 2.1$ Hz, $J_{6a,6b} = 12.5$ Hz, 1H, H-6b), 2.18 (s, 3H, OAc), 2.11 (s, 3H, OAc), 2.08 (s, 3H, OAc), 2.01 (s, 3H, OAc); δ_{H} (100 MHz; CDCl_3) 170.4, 169.6, 169.5, 169.5 (4 \times C=O), 83.1 (C1), 72.8 (C2), 72.1 (C5), 67.9 (C3), 65.3 (C4), 61.1 (C6), 20.7, 20.6, 20.6, 20.5 (4 \times OAc). The ^1H and ^{13}C NMR values were in agreement with published literature values.²⁶

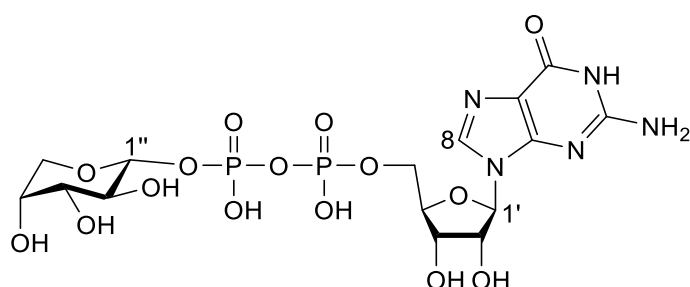
General method: 1,2-trans NDP-sugar synthesis²⁶

NDP-sugar (Bu_4N^+ salt titrated to pH 6, 2.3 – 2.6 eq Bu_4N^+ per eq. of NDP, 0.1 mmol) and trimethylamine (14 μL , 0.1 mmol) was dissolved in anhydrous MeCN (10 mL) under nitrogen in a flask containing ~ 10 \AA MS. Sugar bromide (0.1 mmol) in anhydrous MeCN (5 mL) was

added and the reaction mixture heated at 80 °C for 30 minutes. The molecular sieves were filtered off and the MeCN removed under reduced pressure before the reaction was re-dissolved in water /methanol/triethylamine 2:2:1 (10 mL) and stirred overnight at room temperature. The reaction was again dried under reduced pressure and re-dissolved in water (2 mL). The aqueous solution was passed through a 0.22 μm filter and purified by strong anion exchange HPLC using a gradient of 5 mM – 250 mM NH₄HCO₃ over 10 minutes at a flow rate of 7.0 mL/min. Fractions containing NDP-sugar were combined and the ammonium bicarbonate buffer removed by lyophilisation to give purified NDP-sugar as a white powder.

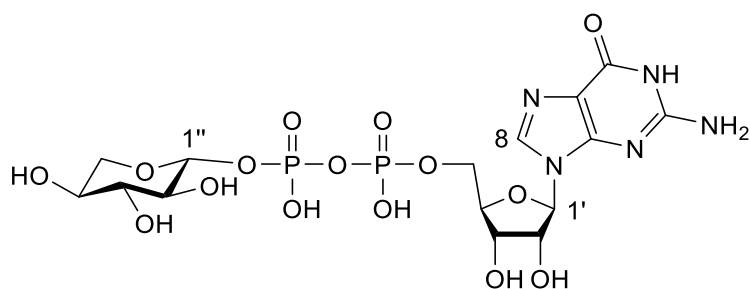
Note that we struggled to record ¹³C NMR without long experiment times which we were keen to avoid due to the unknown stability of these species. Therefore, ¹³C NMR shifts were obtained from HSQCed spectra. As a result, not all the aromatic carbons on the bases could be assigned. The sugar ring carbons are however all present.

GDP- α -D-arabinopyranose (9)⁵⁸



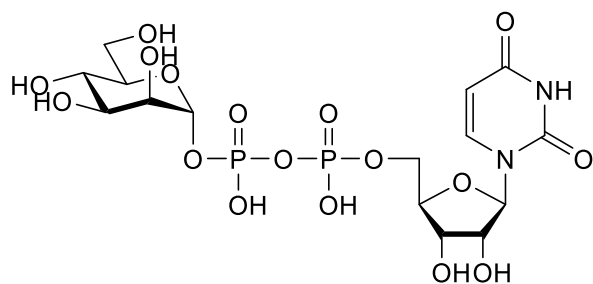
The reaction returned a 5:1 mixture of α : β sugar nucleotides as judged by integration of the H-1'' NMR signals. It was however possible to assign NMR peaks for the major desired α -anomer (9). δ_{H} (400 MHz; D₂O) 8.06 (s, 1H, H-8), 5.86 (d, $J_{1',2'} = 6.4$ Hz, 1H, H-1'), 4.82 (dd, $J_{1'',2''} = 7.5$ Hz, $J_{1'',\text{P}} = 7.5$ Hz, 1H, H-1''), 4.72 (dd, $J_{1',2'} = 6.4$ Hz, $J_{2',3'} = 5.3$ Hz, 1H, H-2'), 4.46 (dd, $J_{2',3'} = 5.3$ Hz, $J_{3',4'} = 3.3$ Hz, 1H, H-3'), 4.29-4.26 (m, 1H, H-4'), 4.14-4.12 (m, 1H, H-5'), 3.87-3.82 (m, 2H, H-4'', 5''a), 3.64-3.54 (m, 3H, H-2'', 3'', 5''b); δ_{C} (100 MHz; D₂O) 114.6 (C6) 98.5 (C1''), 86.7 (C1'), 83.9 (C4'), 73.4 (C2'), 72.0 (C3''), 71.1 (C2''), 70.4 (C3'), 67.5 (C4''), 66.5 (C5''), 65.4 (C5'); δ_{P} (162 MHz; D₂O) -11.2 (d, $J_{\text{P}\alpha,\text{P}\beta} = 19.6$ Hz, P β), -13.0 ((d, $J_{\text{P}\alpha,\text{P}\beta} = 19.6$ Hz, P α); HRMS (ESI⁻) m/z calc. for C₁₅H₂₂N₅O₁₅P₂⁻ 574.0593 ([M-H]⁻) found 574.0597 ([M-H]⁻). ¹H, ¹³C and ³¹P NMR were in agreement with literature values.⁵⁸

GDP- β -L-xylopyranose (10)



$[\alpha]_D - 2.0$ (c 0.1, H₂O), $[\alpha]_{365} = -41$ (c 1.0, H₂O); δ_H (400 MHz; D₂O) 8.03 (s, 1H, H-8), 5.86 (d, $J_{1',2'} = 6.3$ Hz, 1H, H-1'), 4.86 (dd, $J_{1'',2''} = 7.9$ Hz, $J_{1'',P} = 7.9$ Hz, 1H, H-1''), 4.71 (dd, $J_{1',2'} = 6.3$ Hz, $J_{2',3'} = 5.1$ Hz, 1H, H-2'), 4.45 (dd, $J_{2',3'} = 5.1$ Hz, $J_{3',4'} = 3.2$ Hz, 1H, H-3'), 4.28-4.27 (m, 1H, H-4'), 4.14-4.12 (m, 2H, H-5'a,5'b), 3.87 (dd, $J_{4'',5''a} = 5.4$ Hz, 1H, H-5''a), 3.55-3.51 (m, 1H, H-4''), 3.49 (dd, $J_{2'',3''} = 9.2$ Hz, $J_{3'',4''} = 9.2$ Hz, 1H, H-3''), 3.29-3.23 (m, 2H, H-2'',5''b); δ_C (100 MHz; D₂O) 98.5 (C1''), 86.6 (C1'), 83.8 (C4'), 75.1 (C3''), 73.5 (C2'), 73.3 (C2''), 70.4 (C3'), 69.0 (C4''), 65.4 (C5''), 65.2 (C2''); δ_P (162 MHz; D₂O) -11.2 (d, $J_{P\alpha-P\beta} = 20.2$ Hz, P β), -13.1 (d, $J_{P\alpha-P\beta} = 20.2$ Hz, P α); HRMS (ESI⁻) m/z calc. for C₁₅H₂₂N₅O₁₅P₂⁻ 574.0593 ([M-H]⁻) found 574.0594 ([M-H]⁻).

UDP- α -D-mannopyranose (12)²⁶



$[\alpha]_D + 20$ (c 0.1, H₂O); δ_H (400 MHz; D₂O) 7.88 (d, $J_{5,6} = 8.1$ Hz, 1H, H-6), 5.91 (d, $J_{1',2'} = 3.6$ Hz, 1H, H-1'), 5.89 (d, $J_{5',6'} = 8.1$ Hz, 1H, H-5'), 5.42 (dd, $J_{1'',2''} = 1.8$ Hz, $J_{1'',P} = 8.0$ Hz, 1H, H-1''), 4.29-4.27 (m, 2H, H-2',3'), 4.21-4.20 (m, 1H, H-4'), 4.16-4.11 (m, 2H, H-5'a,5'b), 3.97 (dd, $J_{1'',2''} = 1.8$ Hz, $J_{2'',3''} = 3.4$ Hz, 1H, H-2''), 3.85-3.75 (m, 3H, H-3'',5'',6''a), 3.68 (dd, $J_{5'',6''b} = 5.5$ Hz, $J_{6''a,6''b} = 12.4$ Hz, 1H, H-6''b), 3.60 (dd, $J_{3'',4''} = 9.8$ Hz, $J_{4'',5''} = 9.8$ Hz, 1H, H-4''); δ_C (100 MHz; D₂O) 114.6 (C6), 102.7 (C5), 96.2 (C1''), 88.2 (C1'), 83.2 (C4'), 73.8 (C2'), 73.6 (C5''), 70.2 (C2''), 69.8 (C3''), 69.6 (C3'), 66.4 (C4''), 64.9 (C5'), 60.8 (C6''); δ_P (162 MHz; D₂O) -11.5 (d, $J_{P\alpha,P\beta} = 21.0$ Hz, P β), -13.6 (d, $J_{P\alpha,P\beta} = 21.0$ Hz, P α); HRMS (ESI⁻) m/z calc. for C₁₅H₂₄N₂O₁₇P₂⁻

564.0477 ([M-H]⁻) found 564.0477 [M-H]⁻. ¹H and ¹³C NMR were in agreement with literature values.²⁶

2.6 References

1. T. Igarashi, M. Satake, and T. Yasumoto, *J. Am. Chem. Soc.*, 1999, **121**, 8499–8511.
2. T. Igarashi, M. Satake, and T. Yasumoto, *J. Am. Chem. Soc.*, 1996, **118**, 479–480.
3. S. A. Rasmussen, S. Meier, N. G. Andersen, H. E. Blossom, J. Ø. Duus, K. F. Nielsen, P. J. Hansen, and T. O. Larsen, *J. Nat. Prod.*, 2016, **79**, 2250–2256.
4. T. Igarashi, S. Aritake, and T. Yasumoto, *Nat. Toxins*, 1998, **6**, 35–41.
5. J. Kennedy, J. Wu, K. Drew, I. Carmichael, and A. S. Serianni, *J. Am. Chem. Soc.*, 1997, **119**, 8933–8945.
6. F. De Bruyn, J. Maertens, J. Beauprez, W. Soetaert, and M. De Mey, *Biotechnol. Adv.*, 2015, **33**, 288–302.
7. L. L. Lairson, B. Henrissat, G. J. Davies, and S. G. Withers, *Annu. Rev. Biochem.*, 2008, **77**, 521–555.
8. A. Larsen, W. Eikrem, and E. Paasche, *Can. J. Bot.*, 1993, **71**, 1357–1362.
9. J. W. La Claire, S. R. Manning, and A. E. Talarski, *Toxicon*, 2015, **102**, 74–80.
10. J. I. MacRae, S. O. Obado, D. C. Turnock, J. R. Roper, M. Kierans, J. M. Kelly, and M. A. J. Ferguson, *Mol. Biochem. Parasitol.*, 2006, **147**, 126–136.
11. S. L. Manley and D. J. Burns, *J. Phycol.*, 1991, **27**, 702–709.
12. R. Lehmann, M. Huber, A. Beck, T. Schindera, T. Rinkler, B. Houdali, C. Weigert, H.-U. Häring, W. Voelter, and E. D. Schleicher, *Electrophoresis*, 2000, **21**, 3010–3015.
13. J. Rabinä, M. Mäki, E. M. Savilahti, N. Järvinen, L. Penttilä, and R. Renkonen, *Glycoconj. J.*, 2001, **18**, 799–805.
14. J.-P. Antignac, K. de Wasch, F. Monteau, H. De Brabander, F. Andre, and B. Le Bizec, *Anal. Chim. Acta*, 2005, **529**, 129–136.
15. M. Pabst, J. Grass, R. Fischl, R. Léonard, C. Jin, G. Hinterkörner, N. Borth, and F. Altmann, *Anal. Chem.*, 2010, **82**, 9782–8.
16. D. C. Turnock and M. A. J. Ferguson, *Eukaryot. Cell*, 2007, **6**, 1450–1463.
17. G. K. Wagner, T. Pesnot, and R. A. Field, *Nat. Prod. Rep.*, 2009, **26**, 1172.
18. S. Roseman, J. J. Distler, J. G. Moffatt, and H. G. Khorana, *J. Am. Chem. Soc.*, 1961, **83**, 659–663.
19. V. S. Bogachev, *Russ. J. Bioorganic Chem.*, 1996, **21**, 93–119.
20. F. Cramer, H. Neunhoeffler, K. H. Scheit, G. Schneider, and J. Tennigkeit, *Angew. Chem Int. Ed. English*, 1962, **1**, 331–331.
21. G. Baisch and R. Öhrlein, *Bioorg. Med. Chem.*, 1997, **5**, 383–391.

22. A. L. Marlow and L. L. Kiessling, *Org. Lett.*, 2001, **3**, 2517–2519.
23. Y. E. Tsvetkov and A. V. Nikolaev, *J. Chem. Soc. Perkin Trans. 1*, 2000, 889–891.
24. Q. Zhang and H. Liu, *J. Am. Chem. Soc.*, 2000, **122**, 9065–9070.
25. M. Arlt and O. Hindsgaul, *J. Org. Chem.*, 1995, **60**, 14–15.
26. S. C. Timmons and D. L. Jakeman, *Org. Lett.*, 2007, **9**, 1227–1230.
27. J. White-Phillip, C. J. Thibodeaux, and H. Liu, *Methods Enzymol.*, 2009, **459**, 521–544.
28. J. C. Errey, B. Mukhopadhyay, K. P. R. Kartha, and R. A. Field, *Chem. Commun.*, 2004, 2706–2707.
29. B. A. Wagstaff, M. Rejzek, T. Pesnot, L. M. Tedaldi, L. Caputi, E. C. O'Neill, S. Benini, G. K. Wagner, and R. A. Field, *Carbohydr. Res.*, 2015, **404**, 17–25.
30. M. Rejzek, *Personal Communication*.
31. M. Oppenheimer, A. L. Valenciano, K. Kizjakina, J. Qi, and P. Sobrado, *PLoS One*, 2012, **7**, e32918.
32. K. Kizjakina, J. J. Tanner, and P. Sobrado, *Curr. Pharm. Des.*, 2013, **19**, 2561–73.
33. J. J. Tanner, L. Boechi, J. Andrew McCammon, and P. Sobrado, *Arch. Biochem. Biophys.*, 2014, **544**, 128–141.
34. M. Soltero-Higgin, E. E. Carlson, T. D. Gruber, and L. L. Kiessling, *Nat. Struct. Mol. Biol.*, 2004, **11**, 539–543.
35. Q. Zhang and H. Liu, *Bioorg. Med. Chem. Lett.*, 2001, **11**, 145–149.
36. P. M. Nassau, S. L. Martin, R. E. Brown, A. Weston, D. Monsey, M. R. McNeil, and K. Duncan, *J. Bacteriol.*, 1996, **178**, 1047–1052.
37. R. M. de Lederkremer, V. B. Nahmad, and O. Varela, *J. Org. Chem.*, 1994, **59**, 690–692.
38. O. Varela, C. Marino, and R. M. de Lederkremer, *Carbohydr. Res.*, 1986, **155**, 247–251.
39. N. B. D'Accorso, I. M. E. Thiel, and M. Schüller, *Carbohydr. Res.*, 1983, **124**, 177–184.
40. M. Rejzek, L. Hill, E. S. Hems, S. Kuhaudomlarp, B. A. Wagstaff, and R. A. Field, in *Methods in enzymology*, Elsevier Inc., 1st edn., Vol. 1, 2017, pp. 209–238.
41. S. A. Veltkamp, M. J. X. Hillebrand, H. Rosing, R. S. Jansen, E. R. Wickremsinhe, E. J. Perkins, J. H. M. Schellens, and J. H. Beijnen, *J. Mass Spectrom.*, 2006, **41**, 1633–1642.
42. P. Schneider, M. J. McConville, and M. A. Ferguson, *J. Biol. Chem.*, 1994, **269**, 18332–18337.
43. H. M. Holden, I. Rayment, and J. B. Thoden, *J. Biol. Chem.*, 2003, **278**, 43885–43888.
44. P. J. Keeling, F. Burki, H. M. Wilcox, B. Allam, E. E. Allen, L. A. Amaral-Zettler, E. V.

Armbrust, J. M. Archibald, A. K. Bharti, C. J. Bell, B. Beszteri, K. D. Bidle, C. T. Cameron, L. Campbell, D. A. Caron, R. A. Cattolico, J. L. Collier, K. Coyne, S. K. Davy, P. Deschamps, S. T. Dyhrman, B. Edvardsen, R. D. Gates, C. J. Gobler, S. J. Greenwood, S. M. Guida, J. L. Jacobi, K. S. Jakobsen, E. R. James, B. Jenkins, U. John, M. D. Johnson, A. R. Juhl, A. Kamp, L. A. Katz, R. Kiene, A. Kudryavtsev, B. S. Leander, S. Lin, C. Lovejoy, D. Lynn, A. Marchetti, G. McManus, A. M. Nedelcu, S. Menden-Deuer, C. Miceli, T. Mock, M. Montresor, M. A. Moran, S. Murray, G. Nadathur, S. Nagai, P. B. Ngam, B. Palenik, J. Pawlowski, G. Petroni, G. Piganeau, M. C. Posewitz, K. Rengefors, G. Romano, M. E. Rumpho, T. Ryneerson, K. B. Schilling, D. C. Schroeder, A. G. B. Simpson, C. H. Slamovits, D. R. Smith, G. J. Smith, S. R. Smith, H. M. Sosik, P. Stief, E. Theriot, S. N. Twary, P. E. Umale, D. Vaultot, B. Wawrik, G. L. Wheeler, W. H. Wilson, Y. Xu, A. Zingone, and A. Z. Worden, *PLoS Biol.*, 2014, **12**, e1001889.

45. K. P. R. Kartha and R. A. Field, *Tetrahedron*, 1997, **53**, 11753–11766.
46. Y. Su, J. Xie, Y. Wang, X. Hu, and X. Lin, *Eur. J. Med. Chem.*, 2010, **45**, 2713–2718.
47. D. Wahler, O. Boujard, F. Lefèvre, and J. L. Reymond, *Tetrahedron*, 2004, **60**, 703–710.
48. S. M. Andersen, M. Heuckendorff, and H. H. Jensen, *Org. Lett.*, 2015, **17**, 944–947.
49. Y.-J. Kim, S. H. Kwon, I. H. Bae, and B. M. Kim, *Tetrahedron Lett.*, 2013, **54**, 5484–5488.
50. B. Yu, H. van Ingen, S. Vivekanandan, C. Rademacher, S. E. Norris, and D. I. Freedberg, *J. Magn. Reson.*, 2012, **215**, 10–22.
51. Z. Liu, J. Zhang, X. Chen, and P. G. Wang, *ChemBioChem*, 2002, **3**, 348–355.
52. R. M. De Lederkremer and M. I. Litter, *Carbohydr. Res.*, 1971, **20**, 442–444.
53. J. Fuentes Mota, D. Mostowicz, C. Ortiz, M. Angeles Pradera, and I. Robina, *Carbohydr. Res.*, 1994, **257**, 305–316.
54. K. P. R. Kartha and R. Field, *J. Carbohydr. Chem.*, 1998, **17**, 693–702.
55. B. Mukhopadhyay, K. P. R. Kartha, D. A. Russell, and R. A. Field, *J. Org. Chem.*, 2004, **69**, 7758–7760.
56. C. Gauthier, J. Legault, S. Lavoie, S. Rondeau, S. Tremblay, and A. Pichette, *Tetrahedron*, 2008, **64**, 7386–7399.
57. H.-S. Dang, B. P. Roberts, J. Sekhon, and T. M. Smits, *Org. Biomol. Chem.*, 2003, **1**, 1330–1341.
58. U. B. Gokhale, O. Hindsgaul, and M. M. Palcic, *Can. J. Chem.*, 1990, **68**, 1063–1071.

3 Exploring the reactivity and spectroscopy of terminal bis-alkynes

3.1 Introduction

3.1.1 Alkynes in prymnesin toxins

Multiple large scale fish kills have been attributed to the particularly bioactive prymnesin ichthyotoxins (Figure 3.1).¹⁻³ Igarashi *et al.*⁴ have shown that the concentration of prymnesin-1 and prymnesin-2 required to cause 50% lethality (LC₅₀ values) are 8 nM and 9 nM respectively towards the fresh water fish *Tanichthys albonubes*. Furthermore Rasmussen *et al.*³ have demonstrated that prymnesin-B1 and prymnesin-2 will lyse rainbow trout gill-W1 cells with EC₅₀ values of 5.98 nM and 0.92 nM respectively. The low concentrations of prymnesins required to cause fish kills makes their detection in waterways a challenge. Current toxin detection methods rely on LC-MS analysis of *P. parvum* cell extracts.^{5,6} This requires expensive and specialist lab-based equipment, which makes detection difficult for fisheries management staff in either the public or private sectors. We have therefore been exploring whether it would be possible to develop a sensitive portable toxin detection system which could be easily used by fisheries staff. Any system needs to be able to detect toxins in field samples at sub-nanomolar concentrations to be of practical use.

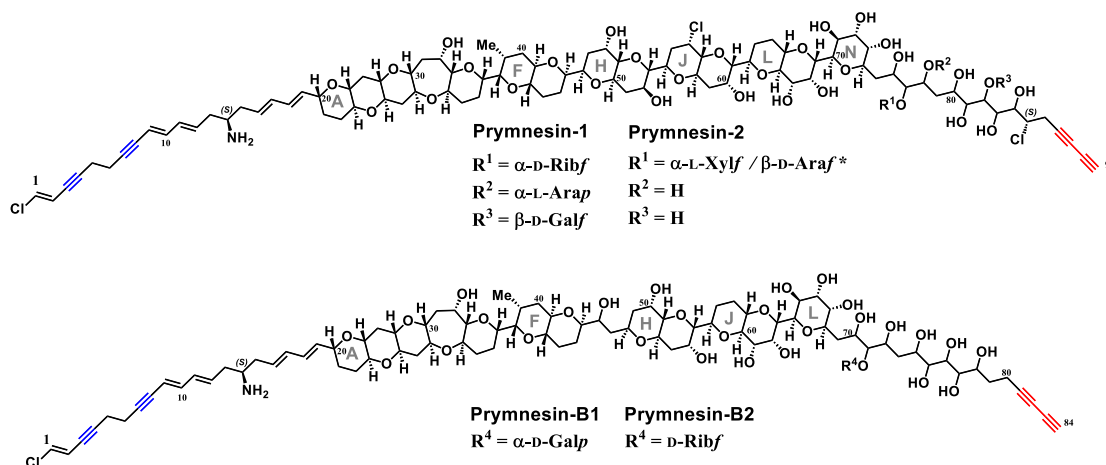


Figure 3.1 – The reported structures of the known prymnesin toxins.^{3,4} The internal alkynes are shown in blue, and the terminal bisalkynes are shown in red. Note that despite the variation between prymnesin and prymnesin-B toxins, the number and relative locations of the alkynes are conserved.

Prymnesin toxins all conserve a terminal bis-alkyne in their backbone structures.^{2,3} The presence of a terminal bis-alkyne in prymnesin-2 was first deduced by Igarashi *et al.*⁷ in their initial elucidation of the planar structure of this part of the toxin (Figure 3.2), where they found three quaternary carbons by ¹³C NMR, which showed HMBC cross-peaks with H-86. They also found a terminal acetylenic proton which gave a signal in acidic solvent (CD₃OD/

CD₃OOD 19:1) at 2.63 ppm (t, $^6J_{86,90} = 1.2$ Hz, H-90), but which slowly disappeared in basic solvent (CD₃OD/C₅D₅N 1:1) over 12 hours. By comparing the chemical shift of the terminal acetylenic proton with literature values, along with the coupling which is appropriate for $^6J_{H-H}$ through two triple bonds, they assigned the terminal bis-alkyne region of the toxin backbone. Due to the similarity in NMR spectra for the backbones of prymnesin-1 and prymnesin-2, Igarashi *et al.*² also found the same terminal bis-alkyne moiety conserved in PRM-1 too.

The internal alkynes at the other end of the toxin were found by disconnections in the spin system between C1 and C10 due to found quaternary carbons. HMBC correlations shown in Figure 3.2, along with long range $^5J_{2,5}$ coupling of 2 Hz and $^5J_{6,9}$ coupling of 3 Hz, UV maxima and 1H and ^{13}C NMR shifts were indicative of the presence of the reported internal alkynes.⁷

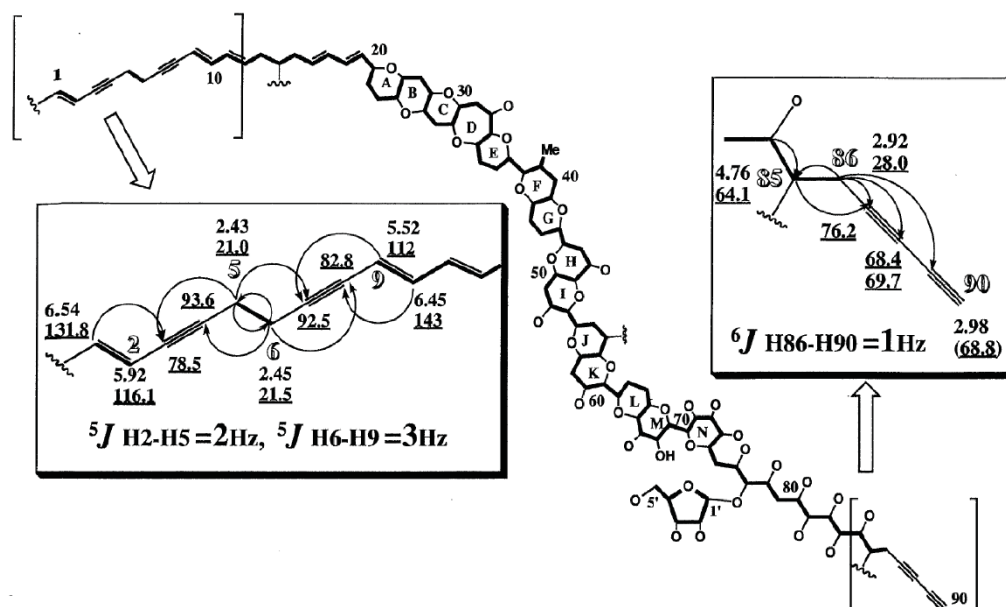


Figure 3.2 – The structure of the termini of prymnesin-2 were elucidated by Igarashi *et al.*⁷ using HMBC and chemical shifts. The arrows represent the long-range coupling between the carbon atom (arrow head) and the protons (arrow tail). Normal numbers are proton shifts and underlined numbers are the carbon shifts. Reprinted (adapted) with permission from T. Igarashi *et al.* *J. Am. Chem. Soc.*, 1996, 118 (2), pp 479–480. Copyright 1996 American Chemical Society.

More recently Rasmussen *et al.*³ have also reported the presence of a terminal bis-alkyne in the newly characterised toxin prymnesin-B1 as well as the tentatively characterised toxin prymnesin-B2. However, they did not have enough compound in solution to detect the quaternary C81, 82, 83 or the acetylenic C84 C-H in the HMBC spectrum. Their assignment

is therefore partially inferred from the high-resolution mass spectrum and comparison with published prymnesin structures.

Terminal bis-alkynes are not unique to prymnesin toxins (Figure 3.3). For example, the marine sponge *Callyspongia* sp. produces the C₂₁ polyacetylene callyberyne A.⁸ PQ-8 is produced by the American white ginseng plant (*P. quinquefolius*),⁹ and the wood rotting fungus *Sistotrema raduloides* produces sistodiolyne which is a very unstable polyketide metabolite.¹⁰

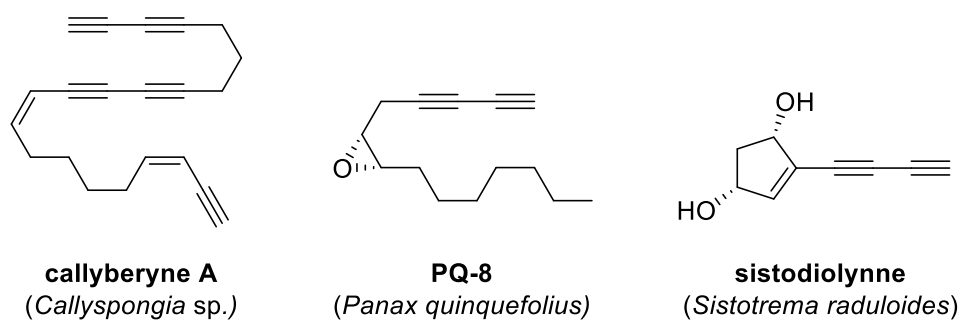


Figure 3.3 - From left, examples of marine, plant and microbe bis-alkynes.¹¹

Nevertheless, terminal bis-alkynes are sufficiently rare moieties in natural products to offer a biomarker with interesting chemical and spectroscopic properties.^{11,12} The first thing we explored was the possibility of labelling these terminal bis-alkynes via the ubiquitous bio-orthogonal copper-catalysed alkyne-azide cycloaddition (CuAAC) ‘click’ reaction.^{13,14} We also found some previous research which showed that bis-alkynes are good targets for Raman spectroscopy.¹⁵ For example, Yamakoshi *et al.*¹⁵ explored a structure – Raman shift/intensity relationship for a series of alkynes, and showed that bis-alkynes gave stronger Raman signals than single alkynes, with shifts in the cellular silent region of the Raman spectrum.

To explore the possibility of using a CuAAC click reaction or Raman-based methods for the detection of prymnesin toxins in water ways, it was first necessary to have either the authentic toxin or a suitable analogue in hand. Lab grown *P. parvum* cultures were grown to extract authentic samples of the prymnesin toxins. It is very challenging to obtain more than trace quantities of prymnesin toxin on a laboratory scale.^{2,3} Therefore it was also decided to perform detection method development using synthetic terminal bis-alkyne analogues. These analogues were prepared chemically, and the authentic toxin extracts were used where an experiment with the synthetic bis-alkyne analogue showed potential.

3.2 Extracting prymnesin toxins from *P. parvum* cell cultures

Prymnesin toxins were extracted from lab grown *P. parvum* cell cultures following a protocol developed by La Claire *et al.*⁵ (Figure 3.4). Healthy three-week-old *P. parvum* cell cultures were harvested by centrifugation and the supernatant discarded. The pellet was washed with cold acetone, and extracted with MeOH and n-PrOH. The solvent extracts were combined and dried before being re-suspended in water. The aqueous suspension was defatted with EtOAc before being freeze dried to give the crude prymnesin extract for LC-MS analysis.

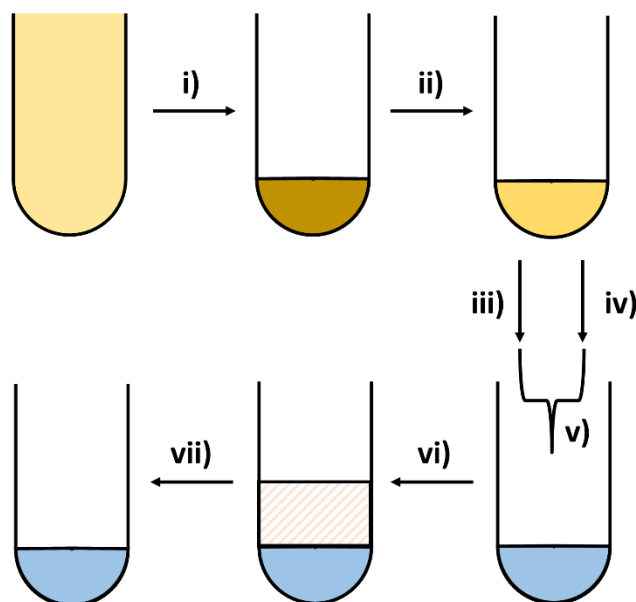


Figure 3.4 - Extraction of prymnesin toxins, following the protocol developed by La Claire *et al.*⁵ i) A *P. parvum* culture is harvested by centrifugation; ii) The cell pellet is lysed and washed with acetone ($\times 3$); iii) The cell pellet is extracted with MeOH ($\times 3$); iv) The cell pellet is extracted with n-PrOH ($\times 3$); v) The MeOH and n-PrOH extracts are combined and dried, before being re-suspended in water; vi) The aqueous suspension is de-fatted with EtOAc ($\times 3$); vii) The aqueous layer is recovered and dried.

The extracted-ion chromatogram (EIC) for m/z of 919.9 ($[\text{PRM}_{\text{aglyc}} + 2\text{H}^+]$, $[\text{C}_{91}\text{H}_{130}\text{Cl}_3\text{NO}_{31}]^{2+}$ calcd. 919.88²⁺) shows two peaks originating from PRM-1 and PRM-2 toxins (Figure 3.5). In both cases, some of the toxin has fragmented to the aglycone form. Because of the conserved backbone structure, this gives the same mass to charge ratio for both toxins. Figure 3.6 shows the m/z spectra under the EIC peak for PRM-1 and Figure 3.7 shows the m/z spectra under the EIC peak for PRM-2.

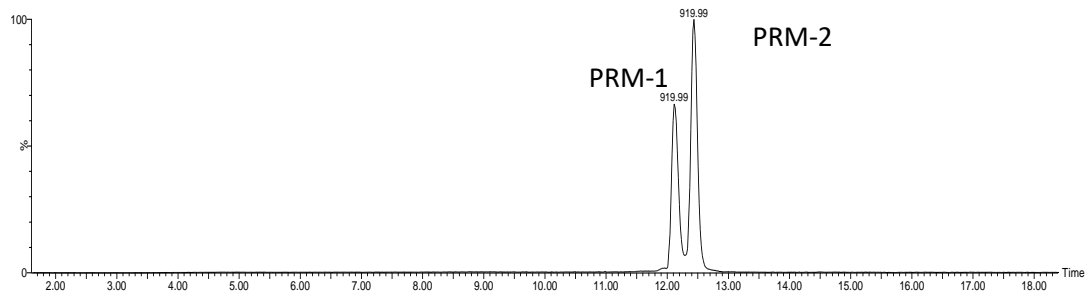


Figure 3.5 – Mass spectra for the *P. parvum* extracts confirms the presence of PRM-1 and PRM-2; the EIC for m/z 919.9 relates to $[\text{PRM}_{\text{aglc}} + 2\text{H}]^{2+}$.⁵ The assignment of PRM-1 and PRM-2 is based on the distribution of partially glycosylated toxin fragments under each of the peaks.

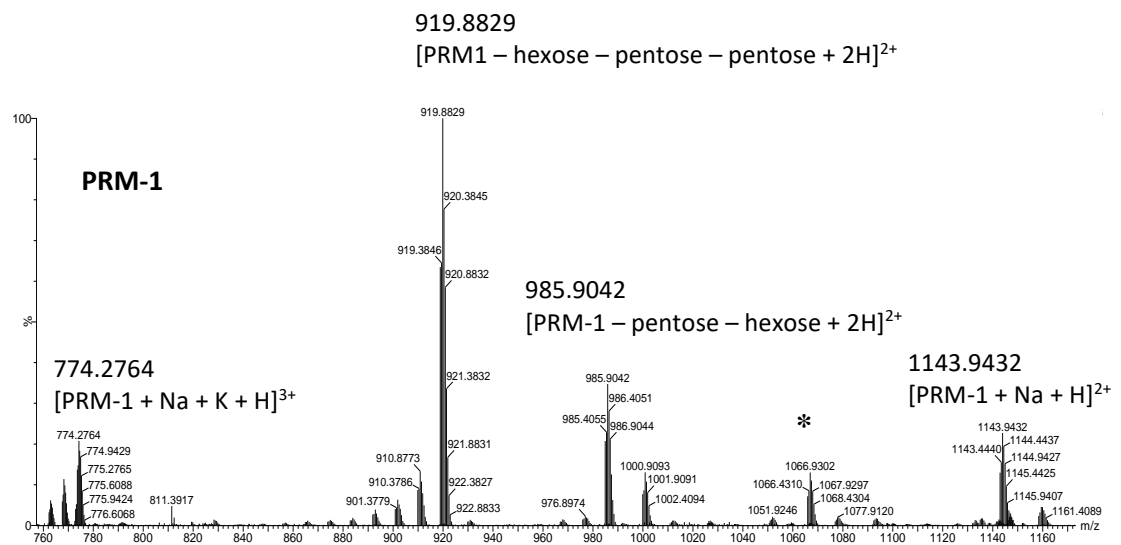


Figure 3.6 - m/z under the two EIC peaks relating to PRM-1 shown in Figure 3.5; the spectra show characteristic ion fragments for PRM-1 as described by La Claire *et al.*⁵; The peak marked * is not mentioned in the literature, but could correspond to $[\text{PRM-1} - \text{pentose} + 2\text{H}]^{2+}$.

The peak marked with an asterisk (*) is not reported as a diagnostic peak in the literature, but it does align with the assignment $[\text{PRM-1} - \text{pentose} + 2\text{H}]^{2+}$. This would make it an additional good characteristic peak for distinguishing between PRM-1 and PRM-2. Overall the LC-MS showed that both PRM-1 and PRM-2 had been successfully extracted from lab grown *P. parvum* cultures.

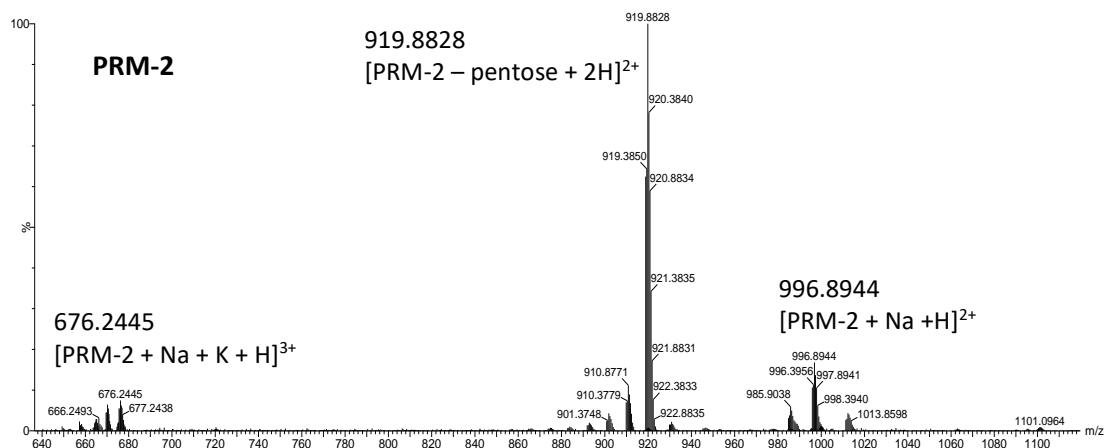
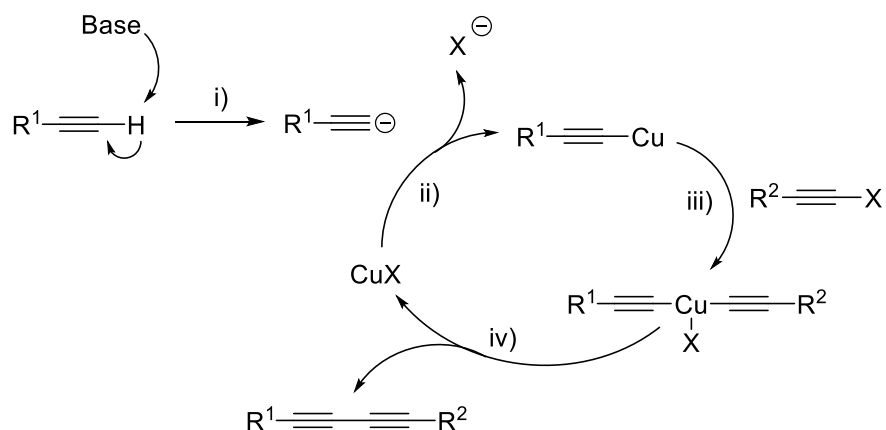


Figure 3.7 – m/z under the two EIC peaks shown in Figure 3.5; the spectra show characteristic ion fragments for PRM-1 and PRM-2 as described by La Claire *et al.*⁵

3.3 Chemistry

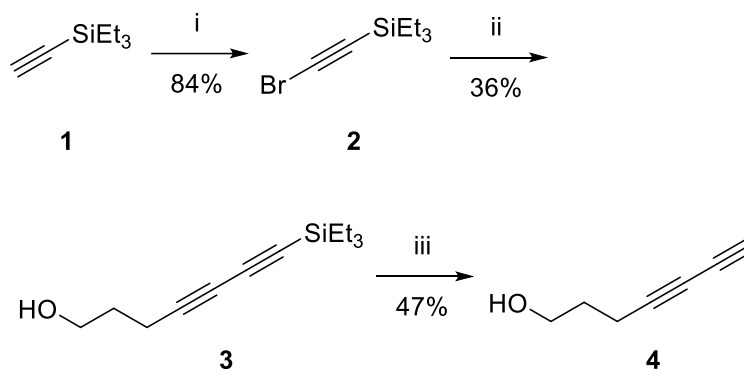
3.3.1 Chemical synthesis of hepta-4,6-diyne-1-ol (**4**)

A glycosylated bis-alkyne was synthesised to act as a toxin substitute for CuAAC click chemistry and Raman spectroscopy studies. A simple bis-alkyne (**4**) was synthesised in 3 steps with an overall yield of 15% (Scheme 3.2). Triethylsilyl acetylene was selected as an acetylene donor, as a previous literature report had suggested that the more common protecting group trimethylsilane was liable to base catalysed cleavage under Cadiot–Chodkiewicz conditions.¹⁶ Triethylsilyl acetylene (**1**) was treated with *N*-bromosuccinimide in the presence of silver nitrate to give (bromoethynyl) triethylsilane (**2**) in good yield, as confirmed by the loss of the acetylenic proton at 2.35 ppm by ¹H NMR. The commercial alkyne 4-propyn-1-ol was chosen because like prymnesins this has 3 carbons between the alkynes and first hydroxyl groups. We omitted the chlorine atom found on prymnesins for simplicity. Coupling was carried out under Cadiot–Chodkiewicz reaction conditions (Scheme 3.1), to give 7-(triethylsilyl)hepta-4,6-diyne-1-ol (**3**).¹⁶ This was confirmed by a loss of the acetylenic proton from 4-propan-1-ol and the addition of ethyl groups from the TES protecting group as a quartet at 0.61 ppm and triplet at 0.99 ppm by ¹H NMR.



Scheme 3.1 – mechanism for the copper(I) catalyzed Cadiot-Chodkiewicz coupling reaction.¹⁷ i) removal of the acetylenic proton with a base; ii) formation of a copper-acetylide; iii) oxidative addition; iv) reductive elimination.

Tetrabutylammonium fluoride (TBAF) was used to remove the triethylsilyl protecting group. After purification, the removal of the silyl protecting group to give hepta-4,6-diyne-1-ol (**4**) was confirmed by ¹H NMR by the presence of an acetylenic proton at 2.00 ppm as a triplet with ⁶J_{H-H} coupling value of 1.2 Hz, which is reasonable for coupling through two triple bonds.⁷ Furthermore, comparison of the ¹³C NMR with the HSQCed spectra confirmed the presence of three quaternary carbons which make up the bis alkyne system.



Scheme 3.2 – The chemical synthesis of hepta-4,6-diyne-1-ol: i) AgNO₃, NBS, 3h. ii) 4-propyn-1-ol, Cu(I)Cl, BuNH₂. iii) TBAF, THF.

It was found that the free bis-alkyne proceeded to rapidly decompose to a red oil. A similar phenomenon was reported by Tykwinski *et al.*¹⁸ who noted that a range of terminal bis-alkynes they had synthesised decomposed if concentrated to dryness. The same group also showed with terminal tri-ynes that decomposition greatly increases once a protecting group

is removed to leave an acetylenic proton.¹⁹ Some work has been carried out by Bryce *et al.*²⁰ exploring the stability of terminal bis-alkynes, which found that the shelf life of bis-alkynes can be increased by keeping them as a dilute solution. However there is ambiguity in the literature about the ‘decomposition’ pathway for such compounds. It could tentatively be attributed to UV-catalysed 1,4-addition polymerisation as shown in Figure 3.8.²¹

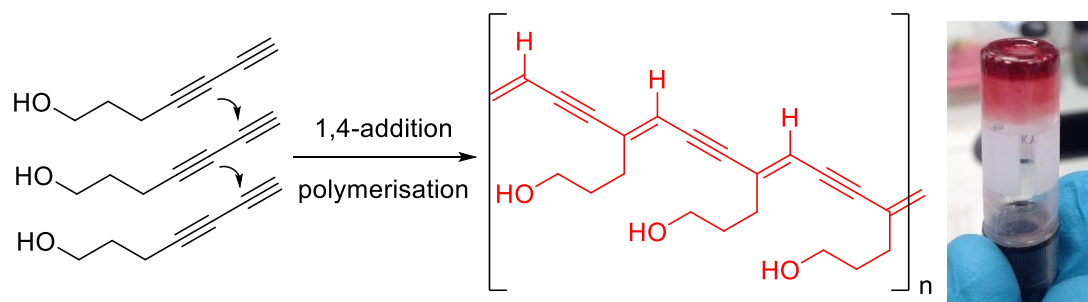
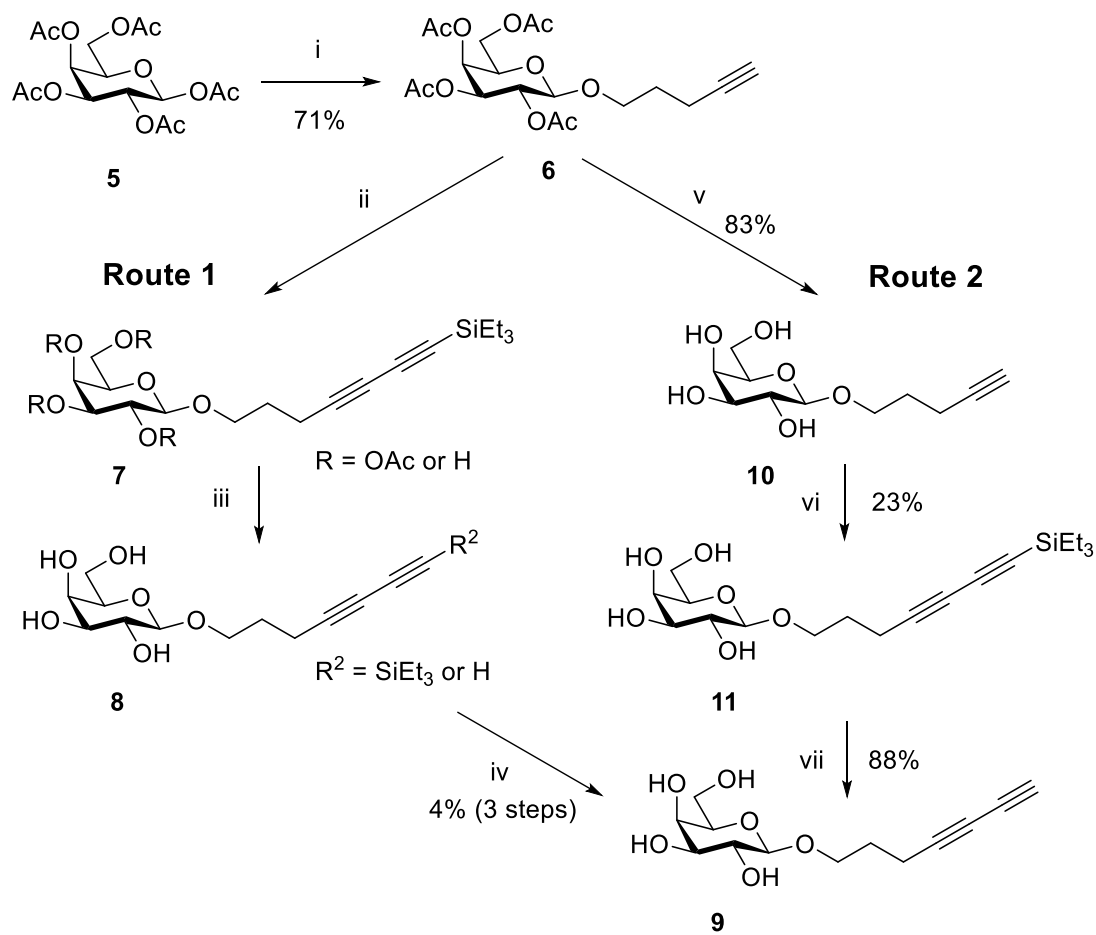


Figure 3.8 – A possible bis-alkyne decomposition pathway (from Nie and Wang)²¹ and the red bis-alkyne sample (hepta-4,6-diyne-1-ol) after it had arrived at our collaborator’s lab.

3.3.2 Chemical synthesis of hepta-4,6-diyne-yl- β -D-galactoside

Following on from the experience gained in synthesising and handling hepta-4,6-diyne-1-ol (**4**), a more water soluble substrate for Raman spectroscopy studies was synthesised (Scheme 3.3). This was achieved by synthesising a glycosylated form of hepta-4,6-diyne-1-ol (**4**). A survey of the literature showed that some 4-pentyn-1-yl glycosides had been reported.^{22,23} In these examples, $\text{BF}_3 \cdot \text{OEt}_2$ -promoted glycosylation of 4-pentyn-1-ol was achieved directly from the per-*O*-acetylated sugar. Due to the problems experienced with the degradation of hepta-4,6-diyne-1-ol (**4**) it was decided to perform the glycosylation step with a bench stable terminal alkyne, and then install the second alkyne unit via the Cadiot-Chodkiewicz coupling reaction, rather than attempt a direct glycosylation of hepta-4,6-diyne-1-ol (**4**). This order of reactions is in keeping with similar literature examples.²³

β -D-Galactose pentacetate was used to glycosylate pentyn-1-ol using $\text{BF}_3 \cdot \text{OEt}_2$ as the promotor. This gave pent-4-yn-1-yl 2',3',4',6'-tetra-*O*-acetyl- β -D-galactopyranoside (**6**) with the stereochemistry at the anomeric position confirmed by the ¹H NMR H-1' anomeric signal (doublet with a $J_{1',2'}$ coupling value of 8.0 Hz). From this point forward, two different synthetic pathways were evaluated as shown in Scheme 3.3.



Scheme 3.3 - i) 4-pentyn-1-ol, $\text{BF}_3 \cdot \text{Et}_2\text{O}$. ii) $\text{Br}-\text{C}\equiv\text{C}-\text{TES}$, $\text{Cu}(\text{I})\text{Cl}$, BuNH_2 , MeOH iii) Na , MeOH . iv) $\text{NEt}_3 \cdot 3\text{HF}$. v) Na , MeOH . vi) $\text{Br}-\text{C}\equiv\text{C}-\text{TES}$, $\text{Cu}(\text{I})\text{Cl}$, BuNH_2 , MeOH . vii) $\text{Et}_3\text{N} \cdot 3\text{HF}$

Route 1 covers steps ii – iv. The Cadiot–Chodkiewicz coupling reaction was first employed to synthesise the triethyl silyl protected bis-alkyne (**7**).^{11,23} It was found that this worked well in dry methanol, which dispensed with the need to degas water to use as a solvent in the reaction. Low resolution mass spectrometry direct from TLC analysis showed that whilst the coupling had been successful, a range of partially deacetylated compounds had been formed. This was attributed to the presence of BuNH_2 which would have served as a nucleophile to produce AcNHBu . Rather than try and separate all the components, it was felt more useful to combine them and place them in a methoxide solution overnight to remove all of the remaining acetate groups (Step iii, Scheme 3.3). Whilst this was successful in removing the acetate groups, it also led to partial removal of the triethylsilyl protecting group from the bis-alkyne. This isn't a problem if the globally deprotected compound hepta-4,6-diyne-1-yl- β -D-galactoside (**9**) is required for immediate use. If, however, the compound needs to be stored for a period of time, it is best to do so with the terminal TES protecting groups still on the

bis-alkyne, as this prevents the polymerisation described earlier.²⁰ The mixtures of protected and deprotected bis-alkyne were again pooled and the remaining triethylsilyl protecting group removed with Et₃N.3HF to give hepta-4,6-diyn-yl-β-D-galactoside (**9**). It was clear at this point that Route 1 was not a particularly useful synthetic route to synthesise hepta-4,6-diyn-yl-β-D-galactoside (**9**) because of the mixtures of compounds being synthesised, as well as the problem with decomposition of the terminal bis-alkyne.

An alternative synthetic approach is shown in Route 2 (Scheme 3.3, steps v – vii). Here the acetate protecting groups were removed from galactose *before* the modified Cadiot–Chodkiewicz coupling, as they were no longer required after the initial glycosylation. The successful coupling with triethylsilyl acetylene was confirmed by the additional ethyl signals in the ¹H NMR spectrum as well as the new C6 and C7 signals in the ¹³C NMR at 67.6 ppm and 65.0 ppm respectively. This gave a TES protected bis-alkyne (**11**) which required only a single deprotection step prior to use.

Silyl protecting groups are routinely removed using a fluoride source, the high affinity between silicon and fluorine driving the reaction. TBAF or NaF are both common fluoride sources for this reaction, but these present the problem of having to desalt the reaction mixture.²⁴ As an alternative to fluoride salts, Et₃N.3HF was used. This has the advantage that work-up is achieved simply by evaporation and chromatography.²⁴ Et₃N.3HF also has the advantage of being much less aggressive than Pyr.HF, and as such it may be used with borrosilicate glassware up to 150 °C.²⁵ This final deprotection step worked well, to give hepta-4,6-diyn-yl-β-D-galactoside (**9**), and the presence of the terminal bis-alkyne as confirmed by the acetylenic proton at 2.41 ppm as a triplet with ⁶J_{H-H} coupling of 1.2 Hz.⁷ Hepta-4,6-diyn-yl-β-D-galactoside (**9**) also degraded to a red/brown oil on standing, and so the TES group was only removed immediately before use.

Two different routes were explored to synthesise hepta-4,6-diyn-yl-β-D-galactoside (**9**) (Scheme 3.3). Route 1 was problematical; the acetate protecting groups on the sugar were incompatible with the BuNH₂ used in the Cadiot–Chodkiewicz coupling reaction, and the deacetylation of the sugar also partially deprotected the bis-alkyne, leading to rapid decomposition. By contrast, route 2 solved these problems by removing the acetate protecting groups from the sugar before installing the bis-alkyne. Route 2 had an overall yield of 17%, which is four times greater than the 4% overall yield recorded for route 1.

3.4 Evaluating the bis-alkyne as a biomarker for prymnesins.

3.4.1 Click Chemistry with synthetic toxin analogues

La Claire *et al.*⁶ recently described a semi-quantitative chemical assay for the detection of prymnesin toxins. This fluorometric assay relied on the specific binding of ninhydrin (NIN) and phenylacetaldehyde (PAA) to the primary amine groups present on all reported prymnesin toxins.^{2,3} This creates a fluorescent compound which could be used to semi-quantify the total amount of prymnesin toxins in a sample (Figure 3.9). Manning and La Claire⁵ have also shown that it is possible to stain prymnesin toxins run up a TLC plate with ninhydrin. A draw back to this method is that there will likely be other compounds with amine groups in the *P. parvum* cell extracts.

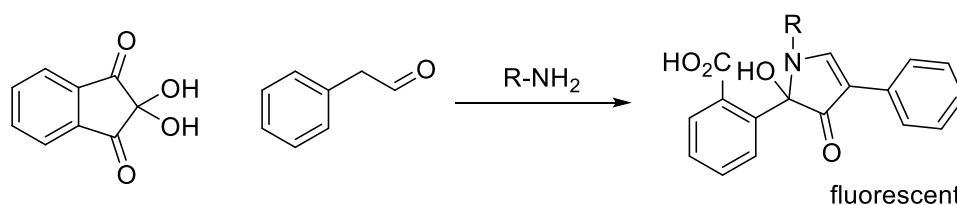


Figure 3.9 – Reaction of ninhydrin (NIN), phenylacetaldehyde (PAA) and the primary amine on prymnesin toxins (R-NH₂).²⁶

Following on from this work, we were interested to see whether the terminal bis-alkynes present on prymnesin toxins could be utilised for covalent binding an azide functionalised fluorophore via a CuAAC reaction.^{13,14} Given the instability of terminal bis-alkynes, we were also interested to see whether they were more reactive than terminal alkynes with regards to azide-alkyne cycloaddition click reactions. If so, this could lead to a simple chemical method of selectively labelling the terminal bis-alkyne conserved across all prymnesin toxins with a reporter molecule for detection. Previous work by Tykwinski *et al.*¹⁸ has shown that CuAAC reactions of poly-alkynes with benzyl azide gave regioselective coupling at the terminal alkyne only (Figure 3.10).

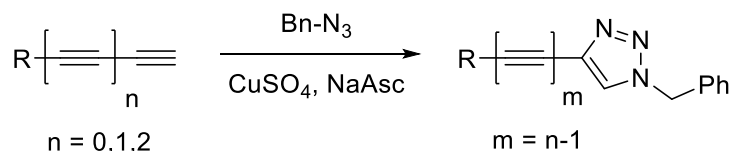
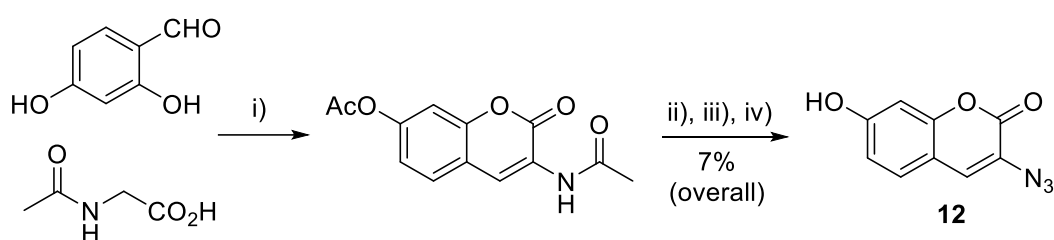


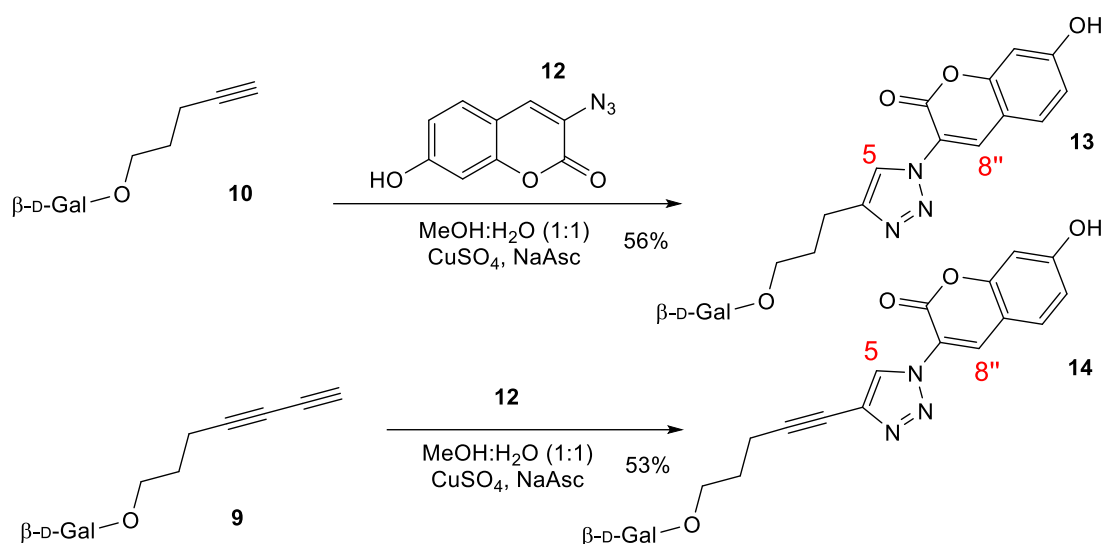
Figure 3.10 – Tykwinski *et al.*¹⁸ have shown that CuAAC with poly-alkynes is regioselective, only generating a triazole ring at the terminal alkyne. They did not find multiple azide addition to the poly-alkyne framework.

3-Azido-7-hydroxycoumarin (**12**) was chosen as a clickable reporter molecule as it is a dye which only fluoresces after it has been clicked with an alkyne to form a triazole ring.²⁷ A similar approach has been used in our group before by Ivanova *et al.* who used **12** to quantify alkyne labelled mannosides.²⁸ 3-Azido-7-hydroxycoumarin was synthesised following the protocol published by Sivakumar *et al.*²⁷ (Scheme 3.4). The presence of the azide group was confirmed by ATR-IR, with a strong peak at 2107 cm⁻¹, and the ¹H NMR agreed with published literature values.²⁷



Scheme 3.4 – the chemical synthesis of 3-azido-7-hydroxycoumarin (**12**).²⁷ i) NaOAc, Ac₂O, reflux; ii) EtOH/HCl (1:1), reflux; iii) NaNO₂, 0 °C; iv) NaN₃.

3-Azido-7-hydroxycoumarin (**12**) was coupled pent-4-yn-1-yl β-D-galactoside (**10**) and hepta-4,6-diyn-yl-β-D-galactoside (**9**) separately under CuAAC conditions to give 3-[1-(7-hydroxycoumarin)-1H-1,2,3-triazol-4-yl] propyl β-D-galactopyranoside (**13**) and 5-[1-(7-hydroxycoumarin)-1H-1,2,3-triazol-4-yl] pent-4-yn-1-yl β-D-galactopyranoside (**14**) respectively (Scheme 3.5). The new ‘clicked’ products (**13** & **14**) showed a loss of the acetylenic protons and the formation of diagnostic triazole signals between 8.5 ppm and 8.7 ppm (H-5, Scheme 3.5). There was also a diagnostic downfield shift in the ¹H NMR signal for H-8'' on the coumarin chromophore. Importantly, mass-spectrometry analysis of the crude mixture after the reaction of the terminal bis-alkyne (**9**) with the azide (**12**) showed that CuAAC had occurred selectively and exclusively at the terminal alkyne, which is in agreement with details published by Tykwinski *et al.*¹⁸ Both the H-5' and H-8'' shifts for (**14**) were shifted further down field than for (**13**), which may be attributed to the anisotropic effect of the p-electrons in the residual alkyne system.



Scheme 3.5 – The chemical synthesis of 3-[1-(7-hydroxy-coumarin)-1H-1,2,3-triazol-4-yl] propyl β -D-galactopyranoside (**13**) and 5-[1-(7-hydroxy-coumarin)-1H-1,2,3-triazol-4-yl] pent-4-yn-1-yl β -D-galactopyranoside (**14**).

In order to assess whether there was a marked difference in the rates of CuAAC between the terminal mono- and bis-alkyne galactosides, a mixture of mono-alkyne (**10**)/bis-alkyne (**9**)/dye (**12**) of 1:1:0.9 was dissolved into DMSO (700 μ L) in an NMR tube. The ratios of the starting materials were checked by integration in the ^1H NMR spectrum of the acetylenic protons on the alkyne galactosides (**9** & **10**) and the aromatic H-5 signal on the dye (**12**) (**Figure 3.11**). The ratio of the components was judged to be alkyne (**10**)/bis-alkyne (**9**)/dye (**12**) 1.0:0.95:0.91.

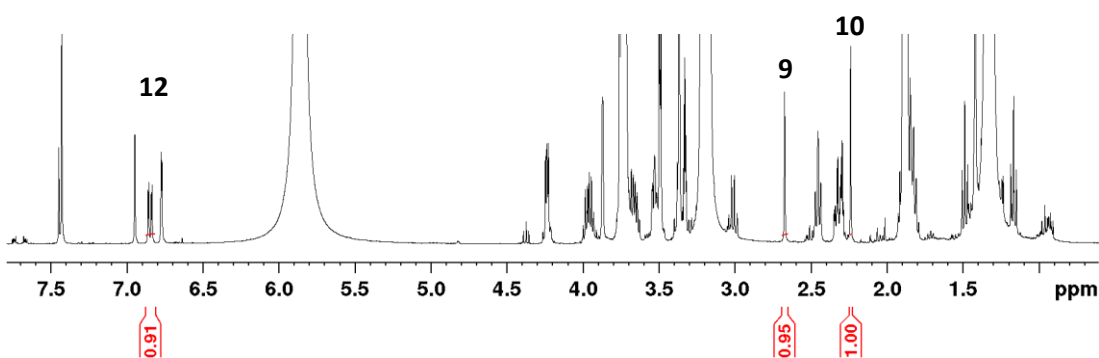


Figure 3.11- Judging the ratios of the starting materials (9, 10, 12) by integration of the ^1H NMR signals.

A freshly prepared solution of 0.1 M aqueous copper sulfate and 0.2 M aqueous sodium ascorbate (10 μ L) was added to start the coupling reaction (Scheme 3.5). After 2 hours, the azide (**12**) was judged to have been consumed by a loss of the H-5 signal at 6.82 ppm in the ^1H NMR spectrum. A quantitative ^1H NMR was recorded and the spectra compared with the ^1H NMR spectra of 3-[1-(7-hydroxy-coumarin)-1H-1,2,3-triazol-4-yl]propyl β -D-galactopyranoside (**13**) and 5-[1-(7-hydroxy-coumarin)-1H-1,2,3-triazol-4-yl]pent-4-yn-1-yl β -D-galactopyranoside (**14**) standards (Scheme 3.5).

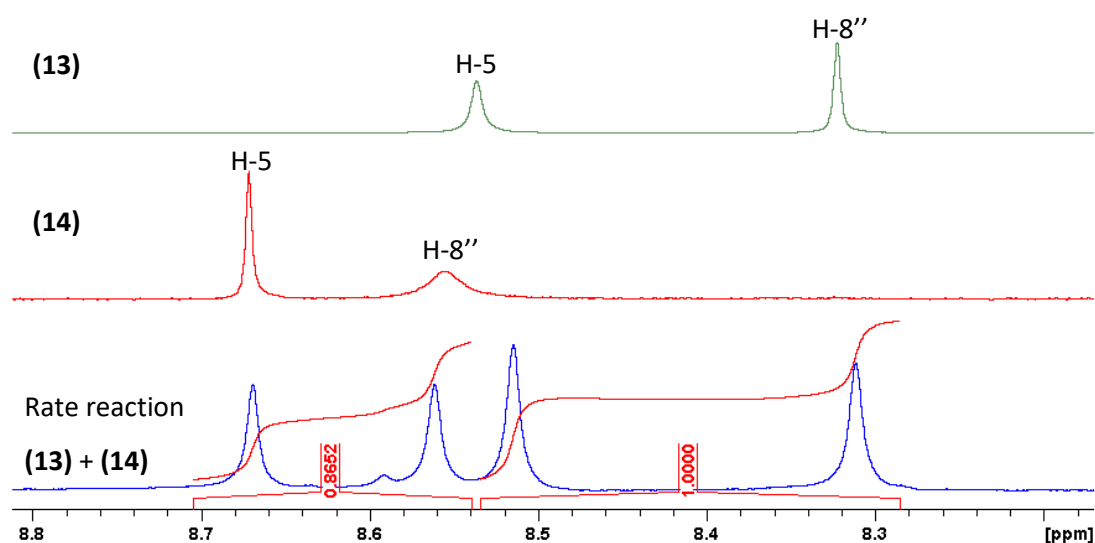


Figure 3.12 - ^1H NMR spectra showing the H-5 and H-8'' signals of 3-[1-(7-hydroxy-coumarin)-1H-1,2,3-triazol-4-yl]propyl β -D-galactopyranoside (**13**) (green), 5-[1-(7-hydroxy-coumarin)-1H-1,2,3-triazol-4-yl]pent-4-yn-1-yl β -D-galactopyranoside (**14**) (red) and a mixture of both compounds from the CuAAC rate reaction shown in **Scheme 3.5** (blue).

Integration of the H-5 and H-8'' signals showed that the ratio of (**13**)/(**14**) was 1.0:0.87. Correcting for the initial concentration ratios of the terminal alkyne (**10**) and terminal bis-alkyne (**9**) analogues, this suggested that the terminal alkyne analogue (**10**) had reacted about 5% faster than the terminal bis-alkyne analogue (**9**) with 3-azido-7-hydroxycoumarin (**12**) under CuAAC conditions. As such it was found that there was no notable difference in the rate between terminal alkynes and terminal bis-alkynes reacting with azides under CuAAC conditions.

3.4.2 Click chemistry with prymnesin toxin extracts

Ivanova *et al.*²⁸ have recently shown that the limit of detection for 1,2,3-triazol-7-hydroxycoumarins (T-7-HC) is pH dependent, with the intensity of fluorescence doubling from pH 6 to pH 9. They found a detection limit from a TLC plate visualised by UV irradiation at 365 nm was ca 160 pmol, and ca 100 nM when detected in solution by fluorimeter.²⁸ Whilst the detection limit for 1,2,3-triazole-7-hydroxycoumarins is too high as is for detecting prymnesin toxins at sub-lethal concentrations in water samples,⁴ solid phase extraction may be a way to concentrate the toxins from a known volume of water.

Preliminary testing was performed using LC-MS verified prymnesin extracts. A CuAAC reaction was performed with 3-azido-7-hydroxycoumarin (**12**) and toxin extracts. The crude mixture was then run on a TLC plate using the conditions described by Igarashi *et al.*² and the TLC plate visualised under a UV-light (Figure 3.13).

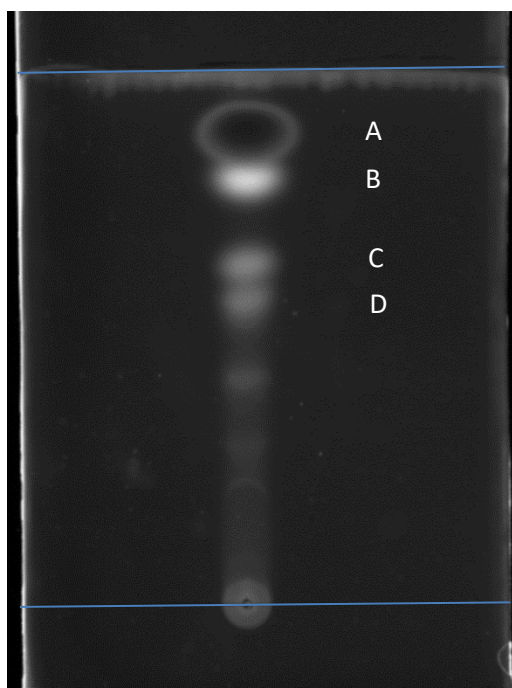


Figure 3.13 – TLC plate visualised under a UV lamp showing the crude products of a CuAAC of prymnesin extracts 3-azido-7-hydroxycoumarin. A. unreacted 3-azido-7-hydroxycoumarin; B. PRM_(aglyc)- (T-7-HC); C. PRM-2-(T-7-HC); D. PRM-1-(T-7-HC).

In Figure 3.13, spot A is unreacted 3-azido-7-hydroxycoumarin (**12**), and spots B, C and D showed pale blue under a UV-light. The R_f values of the fluorescent spots were compared with the literature values for prymnesins, and due to the added lipophilicity of the aromatic coumarin fluorophore for the fluorescent spots, all ran slightly faster than the free toxins.⁵ Spot B (R_f 0.78) was possibly an unrelated alkyne containing metabolite or perhaps more plausibly the aglycone form of prymnesin-(T-7-HC) (lit.⁵ for PRM_{aglyc} R_f 0.7). Spot C (R_f 0.64) probably relates to prymnesin-2-(T-7-HC) (lit.⁵ for PRM-2 R_f 0.6) and Spot D (R_f 0.57) probably relates to prymnesin-1-(T-7-HC) (lit.⁵ for PRM-1 R_f 0.5).

It would make sense that the more carbohydrate moieties there are on the toxin backbone, the more tightly it is retained by silica gel due to the increased polarity of the glycosylated compound. It would be useful to confirm the identities of each of the three major fluorescent species at least by LC-MS, and work is currently underway in the lab to extract the fluorescent compounds and obtain HRMS for these compounds. Overall the CuACC coupling of 3-azido-7-hydroxycoumarin (**12**) with prymnesins shows promise for developing a cheap and rapid chemical method of detecting prymnesin toxins.

3.5 Efforts towards the development of a Raman spectroscopy based prymnesin detection system

3.5.1 Raman spectroscopy and bis-alkynes

Raman spectroscopy measures the frequency shift of inelastically scattered light.²⁹ When a photon hits a molecule it may excite an electron to a higher energy state. The excited molecule may relax straight back to the original ground state by emitting a photon of the same energy, which is described as Rayleigh scattering, and is not observed by Raman spectroscopy. Alternatively, the emitted photon may fall to a higher or lower energy state than it started in, which may be described as Stokes or anti-Stokes scattering respectively (Figure 3.14).

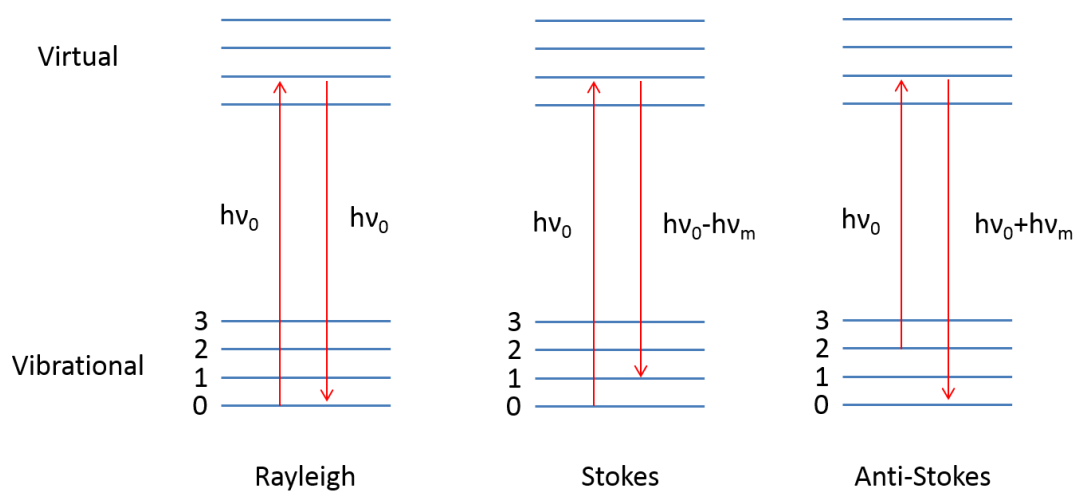


Figure 3.14 - The excitation and relaxation of electrons between vibrational and virtual energy levels.

One of the endearing features of Raman spectroscopy is that it requires very little sample preparation and is almost completely insensitive to aqueous absorption bands.³⁰ This makes it a potentially useful tool for the detection of analytes in water samples.³¹ For example, Raman spectroscopy has been used to identify algal species and even locate biomolecules in algal cells.³² It has also been used to detect and quantify levels of the algal neurotoxin domoic acid in shell fish tissue.³³

Alkynes have recently been used as tags for imaging small molecules using Raman microscopes.³⁰ As well as their small size and low molecular weight when compared with many fluorescent dyes, alkynes have an advantage of giving signals in the normally cellular silent region of a Raman spectrum. Yamakoshi *et al.*¹⁵ recently explored the suitability of a range of alkynes and bis-alkynes for use as Raman tags to track the mobility of small molecule in living cells. The authors showed that bis-alkynes give much higher intensities (approximately 5 times greater) than comparable single alkyne units.¹⁵ They also noted a characteristic shift for bis-alkynes of around 2200 cm^{-1} . However, the limit of detection for the bis-alkynes most sensitive to Raman spectroscopy was found to be about $0.1\text{-}0.2\text{ mM}$,¹⁵ which is about three orders of magnitude too high for the detection of prymnesin toxins.^{3,4} If these limits of detection can be enhanced, Raman spectroscopy an interesting candidate for the detection of the rare terminal bis-alkyne biomarker found on prymnesins.

Raman signals can be greatly improved by using techniques such as Surface-Enhanced Raman Scattering (SERS),³⁴ which uses the excitement of surface plasmon electrons on metal nanoparticles to enhance Raman signals. The principals of SERS are reviewed in great detail

by Stiles *et al.*³⁵ From a pragmatic standpoint, it is important to note that SERS can offer Raman signal enhancements in the order of ten orders of magnitude, which can be sufficient for single molecule detection. So long as a well-defined and consistent SERS substrate is used,³⁵ we were hopeful that this might be a useful means to detect and quantify prymnesin toxin levels in waterways, by using the terminal bis-alkyne as toxin bio-marker. SERS is compatible with a range of handheld Raman spectrometers which could feasibly be used for taking field measurements. There are also a range of commercially available gold and silver substrates deposited onto disposable silicon or paper 'chips', which could be used by an end user with very little training.

3.5.2 Raman Spectroscopy of 7-(Triethylsilyl)hepta-4,6-diyn-yl- β -D-galactoside (**11**)

Hepta-4,6-diyn-yl- β -D-galactoside (**9**) was not stable enough to survive the time required to courier it to our collaborator's lab (Duncan Graham, University of Strathclyde) and had decomposed to a red oil by the time it arrived. Bis-alkynes are notorious for being unstable to decomposition or polymerisation.³⁶

To circumnavigate this problem 7-(triethylsilyl)hepta-4,6-diyn-yl- β -D-galactoside (**11**) was sent to our collaborator as the bis-alkyne was much more stable with a terminal triethylsilyl protecting group in place. However, as our collaborator did not have the facilities to perform the fluoride mediated removal of the TES group, a spectrum was obtained with triethylsilyl protecting group still in place using 1 μ g of bis-alkyne in 100 μ l of MeOH + 900 μ l AuNP suspension in water which after background subtraction gave the Raman spectrum shown in Figure 3.15.

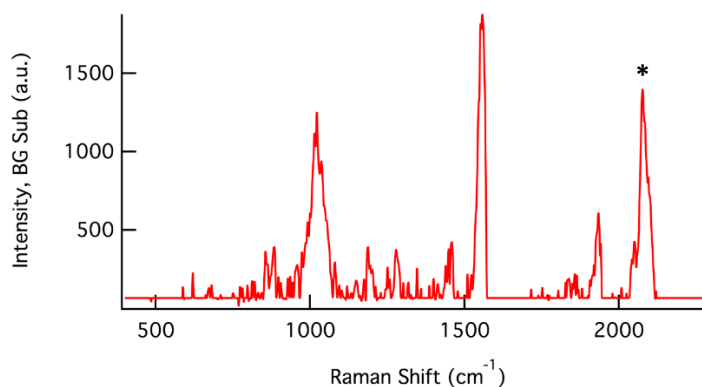


Figure 3.15 - Background subtracted SERS Raman spectrum of the TES protected bis-alkyne (**11**) at 2.5 mmol/mL. The * denotes the peak that was assigned to the terminal bis-alkyne.

3.5.3 Raman Spectroscopy of prymnesin toxin extracts

The LC-MS verified prymnesin toxin extracts were used to try and record surface enhanced Raman spectra (SERS). The spectra were first recorded using a Snowy Range Instruments Benchtop Raman spectrometer. Alkyne Raman bands appear at around 2250 cm^{-1} .¹⁵ The only benchtop spectrometers available at our collaborator's lab that could read above 2000 cm^{-1} used a 532 nm excitation laser. This green light caused the Raman signals to be quenched by fluorescence caused by organic pigments from the alga such as chlorophylls,³² meaning a Raman spectrometer with a longer wavelength excitation laser was required.

The substrate based experiments were later repeated using a Raman microscope with an excitation wavelength of 633 nm. Both gold and silver nanoparticle slide mounted P-SERSTM substrates from Diagnostic anSERS_{INC} were tried, as well as gold and silver nanoparticle slide mounted RAM-SERS substrates from OceanOptics. Despite there being less fluorescence, it still wasn't possible to detect any bis-alkyne bands in the spectrum due to quenching of the signals by fluorescence.

Experiments were also carried out by adding toxin extract to aqueous gold nanoparticle suspensions. However, even at very low extract concentrations, the nanoparticles flocculated and fell out of suspension, meaning that no useable Raman spectrum could be recorded. To this end, it was obvious that with the equipment available to us it would unfortunately not be possible to use Raman spectroscopy as a viable method of detecting prymnesin toxins.

3.6 Summary

This chapter aimed to explore whether it was possible to develop a pragmatic chemical answer to the problem faced by fisheries and environmental staff in monitoring the levels of prymnesin toxins in water ways. Cultures of *P. parvum* were grown and the presence of prymnesin toxins from the harvested cell extracts were confirmed by LC-MS. Two bis-alkyne containing toxin analogues (hepta-4,6-diyne-1-ol (**4**) and hepta-4,6-diyne-yl- β -D-galactoside (**9**)) were chemically synthesised, and the synthetic pathway of hepta-4,6-diyne-yl- β -D-galactoside (**9**) was optimised after it was found that the alkyne coupling conditions were not compatible with acetate protecting groups. It was also found that the terminal bis-alkynes were prone to quick degradation once the silicone protecting groups had been removed from them, which made work with collaborators in a different institute challenging. Leading on from the apparent instability of the terminal bis-alkynes when compared with bench stable terminal alkynes, the question of reactivity towards azides under CuACC conditions was explored, and it was found that there was very little difference in reaction rates, with terminal alkyne reacting about 5% more quickly. How terminal bis-alkynes react with azides was explored, and it was found that only a single terminal triazole ring was formed at the terminal alkyne under CuACC conditions. After the experiments with synthetic bis-alkyne analogues, 3-azido-7-hydroxycoumarin (**12**) was added to *P. parvum* cell extracts which had been verified as containing prymnesin-1 and prymnesin-2 by LC-MS. TLC analysis of this click reaction showed three fluorescent spots which R_f values slightly higher than those reported for PRM-1, PRM-2 and PRM_{aglycone}. Attempts to extract these compounds for LC-MS analysis were unsuccessful, but nevertheless, given the very low limit of detection for the UV-fluorescence detection of 1,2,3-triazole-7-hydroxycoumarin labelled compounds on TLC plates, this shows some promise as a method for rapid chemical detection of prymnesin toxins in waterways. Finally work with collaborators at the University of Strathclyde was conducted to explore the possibility of SERS based Raman detection of prymnesin toxins in waterways. Problems with fluorescent compounds in *P. parvum* cell extracts along with the degradation of terminal bis-alkynes in transit, meant that it was not possible to obtain a useable set of reference spectra with a view to developing a Raman based toxin detection system.

3.7 Experimental

3.7.1 Extraction of prymnesin toxins from *P. parvum* cell cultures

Prymnesin toxin extractions were performed using the protocol developed by La Claire *et al.*⁵ Cultures of *Prymnesium parvum* (100 mL) were grown in 5PSU f/2 media at room temperature in a 16/8 h (light/dark) cycle. After 3 weeks, the cells were harvested by centrifugation (4000 × g for 5 minutes) and the supernatant discarded. The cells were suspended in cold acetone (20 mL, -20 °C) and subject to vortex mixing for two minutes. The resulting suspension was split into two equal portions and centrifuged at 4000 × g for 5 minutes. The supernatant was discarded, being careful not to disturb the cell debris, and the pellets were subject twice more to the same acetone wash. The cell pellets were then suspended in MeOH (10 mL) and vortex mixed for two minutes, after which time the cell debris was pelleted by centrifugation (4000 × g for 5 minutes) and the supernatant was collected. This methanol extraction was repeated twice more, followed by three rounds of analogous extraction using n-PrOH. The MeOH and n-PrOH extracts were combined, dried *in vacuo* and re-suspended in Milli-Q® water (10 mL) before being defatted with EtOAc (3 × 5 mL).⁵ The aqueous fraction was then dried by lyophilisation to give the prymnesin toxins extract.

3.7.2 LC-MS detection of prymnesin toxins

The *P. parvum* extracts were analysed by LC-MS on a Synapt G2-Si mass spectrometer coupled to an Acquity UPLC system (Waters, Manchester, UK). The extracts were first dissolved into 50 µL of Milli-Q water. Aliquots of 2 µL sample were injected onto an Acquity UPLC® BEH C18 column, 1.7 µm, 1x100 mm (Waters) and eluted with a gradient of 10-90% acetonitrile in 0.1% formic acid in 12 min at a flow rate of 80 µL min⁻¹. The mass spectrometer was controlled using Masslynx 4.1 software (Waters) and operated in positive MS-Tof and resolution mode with a capillary voltage of 2.5 kV and a cone voltage of 40 V in the m/z range of 200-2000. Leu-enkephalin peptide (1 ng mL⁻¹, Waters) was infused at 3 µl min⁻¹ as a lock mass and measured every 20 s.

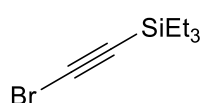
3.7.3 Raman Spectroscopy

Raman spectroscopy of 7-(triethylsilyl)hepta-4,6-diy-yl-β-D-galactoside (**11**) was performed using a hand-held Snowy Range instruments 638 nm Raman spectrometer. The spectrum

was recorded by dissolving 1 μg of **11** in 100 μL of MeOH, before adding this to 900 μL AuNP suspension in water. Raman spectroscopy of toxin extracts from SERS substrates were attempted using a Renishaw spectrometer coupled with a Leica DMLM microscope, using a 633 nm excitation laser. Toxin extract was dissolved into 100 μL of water, and 10 μL was then deposited on the test SERS substrates.

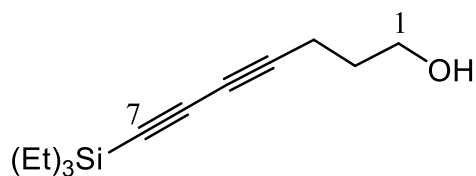
3.7.4 Chemistry

(Bromoethynyl) triethylsilane (**2**)³⁷



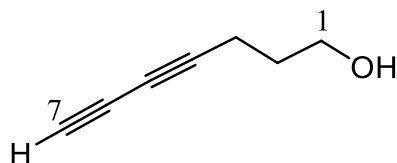
Triethylsilyl ethyne (**1**) (1.0 mL, 5.58 mmol) and AgNO_3 (190 mg, 1.1 mmol) were dissolved into dry acetone (30 mL) under N_2 . The reaction mixture was stirred vigorously in the dark for 20 minutes after which time the reaction mixture had turned a milky white colour. *N*-Bromosuccinimide (1.1g, 6.1 mmol, 1.1 eq) was added and the reaction mixture was stirred for a further 3 hours in the dark. TLC (neat hexane) showed complete consumption of the starting material and the reaction mixture was filtered and the solvent was removed under reduced pressure. The crude mixture was purified on a short silica column using pure *n*-hexane to give (bromoethynyl) triethylsilane (**2**) (1.0 g, 84%) as a colourless oil; R_f 0.84 (neat hexane); δ_{H} (400 MHz; CDCl_3) 0.99 (t, $J = 8.1$ Hz, 9H, $\text{Si}(\text{CH}_2\text{CH}_3)_3$), 0.61 (q, $J = 8.1$ Hz, 6H, $\text{Si}(\text{CH}_2\text{CH}_3)_3$); δ_{C} (100 MHz; CDCl_3) 84.6 ($\text{Si}-\text{C}\equiv\text{C}-\text{Br}$), 61.6 ($\text{Si}-\text{C}\equiv\text{C}-\text{Br}$), 7.3 ($\text{Si}(\text{CH}_2\text{CH}_3)_3$), 4.3 ($\text{Si}(\text{CH}_2\text{CH}_3)_3$). The ^1H and ^{13}C NMR data were in accordance with the literature.

7-(Triethylsilyl)hepta-4,6-diyne-1-ol (**3**)³⁷



CuCl (40 mg) and BuNH₂ (4.5 mL) were added to degassed water (15 mL) under N₂. Whenever the water started to turn blue a spatula tip of NH₂OH.HCl was added to reduce any Cu(II). The suspension was cooled in an ice bath and 4-pentyn-1-ol (0.41 mL, 0.38 g, 4.47 mmol) was added, at which point the reaction mixture went bright yellow. (Bromoethynyl) triethylsilane (**2**) (1.0g, 4.9 mmol) in Et₂O (2.5 mL) was added by syringe over 5 minutes. After 30 minutes, TLC showed consumption of the terminal alkyne. The reaction mixture was washed with Et₂O (3 × 15 mL), and the organic layers were combined and dried over MgSO₄, filtered and the solvent removed *in vacuo*. The crude product was purified by FCC (8:2 n-hex:EtOAc) to give the title compound (**3**) (355 mg, 36%) as a brown oil (n.b. if deprotecting with fluoride in the next step there is no need to purify as excess bromo ethyne is a gas at room temperature and so will evaporate). R_f 0.45 (hexane/EtOAc 8:2); δ_H(400 MHz; CDCl₃) 3.77-3.73 (m, 2H, H-1), 2.42 (t, *J*_{2,3} = 6.5 Hz, 2H, H-3), 1.82-1.76 (m, 2H, H-2), 1.58 (bs, 1H, OH), 0.99 (t, *J* = 7.7 Hz, 9H, Si(CH₂CH₃)₃), 0.61 (q, *J* = 7.7 Hz, 6H, Si(CH₂CH₃)₃); δ_C(100 MHz; CDCl₃) 89.2 (C6), 81.4 (C7), 78.4 (C4), 66.1 (C5), 61.3 (C-1), 30.8 (C-2), 15.8 (C-3), 7.3 (Si(CH₂CH₃)₃), 4.2 (Si(CH₂CH₃)₃); (MALDI-TOF) *m/z* calc. for C₁₃H₂₃OSi 223.152 ([M.H]⁺) found 223.138 [M.H]⁺. The ¹H and ¹³C NMR data were in accordance with the literature.³⁷

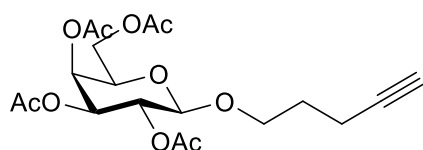
Hepta-4,6-diyn-1-ol (**4**)³⁷



7-(Triethylsilyl)hepta-4,6-diyn-1-ol (**3**) (360 mg, 1.6 mmol) was dissolved into dry THF (5 mL) under N₂ and cooled in an ice bath. 1M TBAF (in THF) (1.9 mL, 1.9 mmol) was added and the reaction mixture was allowed to warm to room temperature and was stirred for 1 hour. TLC showed consumption of **3**. The reaction mixture was quenched with saturated NH₄Cl and extracted with DCM (3 × 5 mL). The organic layers were combined and dried over MgSO₄, filtered and the solvent was removed *in vacuo*. Purification by FCC (10-25% n-Hex/EtOAc) returned hepta-4,6-diyn-1-ol (**4**) (80 mg, 46%) as a colourless oil. R_f 0.29 (hexane/EtOAc 8:2); δ_H(400 MHz; CDCl₃) 3.73 (t, *J*_{1,2} = 7.0 Hz, 2H, H-1); 2.40 (*J*_{2,3} = 7.0 Hz, ⁵*J*_{3,7} = 1.2 Hz, 2H, H-3), 2.38 (br, 1H, OH), 2.00 (t, ⁶*J*_{3,7} = 1.2 Hz, 1H, H-7), 1.82-1.76 (m, 2H, H-2), δ_C(100 MHz; CDCl₃)

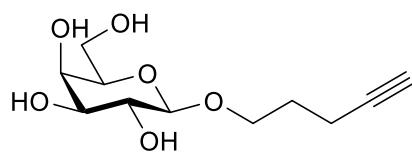
77.6 (C4), 68.3 (C6), 65.1 (C5), 64.8 (C7), 61.1 (C-1), 30.6 (C-2), 15.5 (C-3); $\nu_{\max}/\text{cm}^{-1}$ (ATR-IR) 3286 (O-H), 2360, 2339, 2225 (C≡C), 1054 (C-OH), 621 (C≡C); HRMS (TOF MS ESI⁻) m/z calc. for $\text{C}_7\text{H}_7\text{O}^-$ 107.0502 ([M-H]⁻) found 107.0640 [M-H]⁻. (n.b. this oil very quickly turns into a brown syrup if left neat. The compound should be stored as a dilute ether solution or preferably with the protecting TES group being removed immediately before subsequent use.)

Pent-4-yn-1-yl 2',3',4',6'-tetra-O-acetyl- β -D-galactopyranoside (**6**)²²



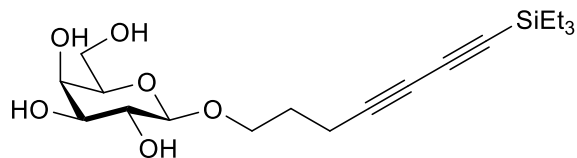
β -D-Galactose pentaacetate (**5**) (1.0 g, 2.6 mmol) and 4-pentyn-1-ol (1 mL, 10.7 mmol) were dissolved in anhydrous DCM (20 mL) and the solution was cooled to 0 °C. $\text{BF}_3 \cdot \text{Et}_2\text{O}$ (2 mL, 16 mmol) was slowly added and the reaction mixture was stirred overnight at room temperature. TLC (hexane/EtOAc 8:2) showed complete consumption of the donor and the reaction mixture was quenched with sat. aqueous NaHCO_3 (20 mL). The reaction mixture was extracted with DCM (3 \times 10 mL) and the organic layers were combined and dried over MgSO_4 , before being filtered and concentrated *in vacuo* to give crude product which was purified by FCC to give the title compound (**6**) (450 mg, 71%) as a yellow oil. R_f 0.1 (hexane/EtOAc 8:2); $[\alpha]_D +2.8$ (c 1.0 CHCl_3); δ_H (400 MHz; CDCl_3) 5.40 (dd, $J_{3',4'} = 3.4$ Hz, $J_{4',5'} = 1.1$ Hz, 1H, H-4'), 5.21 (dd, $J_{1',2'} = 8.0$ Hz, $J_{2',3'} = 10.5$ Hz, 1H, H-2'), 5.03 ($J_{2',3'} = 10.5$ Hz, $J_{3',4'} = 2.3$ Hz, 1H, H-3'), 4.47 (d, $J_{1',2'} = 8.0$ Hz, 1H, H-1'), 4.22-4.11 (m, 2H, H-6'a,b), 3.99 (dt, $J_{1a,1b} = 9.7$ Hz, H-1a, $J_{1a,2a} = 5.2$ Hz, 1H, H-1a), 3.93-3.90 (m, 1H, H-5'), 3.67-3.61 (m, 1H, H-1b), 2.29-2.25 (m, 2H, H-3), 2.16 (s, 3H, OAc), 2.08 (s, 3H, OAc), 2.06 (s, 3H, OAc), 1.99 (s, 3H, OAc), 1.95 (t, $^4J_{3,5} = 2.7$ Hz, 1H, H-5), 1.89-1.71 (2H, m, 2a,b); δ_C (100 MHz; CDCl_3) 170.4, 170.3, 170.2, 169.5 (4 \times C=O), 101.6 (C1'), 83.4 (C4), 70.9 (C3'), 70.6 (C5'), 68.9 (C2'), 68.8 (C5), 68.3 (C1), 67.0 (C4'), 61.3 (C6'), 28.2 (C2), 20.7, 20.7, 20.6, 20.6 (4 \times Ac), 14.8 (C3); HRMS (ESI⁺) m/z calc. for $\text{C}_{19}\text{H}_{26}\text{O}_{10}\text{Na}^+$ 437.1418 ([M+Na]⁺) found 437.1421 [M+Na]⁺. ¹H and ¹³C NMR values were in agreement with literature values.²²

Pent-4-yn-1-yl β -D-galactoside (**10**)²²



A piece of sodium metal (5 mg, 0.2 mmol) was placed in dry MeOH (10 mL). After the cessation of effervescence, the solution of sodium methoxide was added by syringe to a solution of pent-4-yn-1-yl 2',3',4',6'-tetra-O-acetyl- β -D-galactopyranoside (**6**) (750 mg, 1.8 mmol) in MeOH (10 mL) under N₂ and the reaction mixture was left to stir overnight. Low resolution mass spectrometry showed only the desired product, and the reaction mixture was neutralised to pH 7.0 with Amberlite® 120 H+ resin, before being filtered and concentrated under reduced pressure to give the title compound (**10**) (370 mg, 83%) as a yellow oil; $[\alpha]_D$ -13.0 (*c* = 1.0, MeOH) (lit.³⁸ $[\alpha]_D$ -24.6 (*c* = 0.85, MeOH)); δ_H (400 MHz; CD₃OD) 4.23 (d, $J_{1',2'}$ = 7.2 Hz, 1H, H-1'), 3.98 (dt, $^2J_{1a,1b}$ = 12.4 Hz, $J_{1a,2}$ = 6.3 Hz, 1H, H-1a), 3.86 (dd, $J_{3',4'}$ = 3.1 Hz, $J_{4',5'}$ = 1.0 Hz, 1H, H-4'), 3.77-3.75 (m, 2H, H-6'a,b), 3.67 (dt, $^2J_{1a,1b}$ = 12.4 Hz, $J_{1a,2}$ = 6.3 Hz, 1H, H-1b), 3.55-3.46 (m, 3H, H-2',3',5'), 2.35-2.30 (m, 2H, H-3), 2.22 ($^4J_{3,5}$ = 2.8, 1H, H-5), 1.86-1.81 (m, 1H, H-2); δ_C (100 MHz; CD₃OD) 103.7 (C1'), 83.4 (C4), 75.2 (C3'), 73.6 (C5'), 71.2 (C2'), 68.9 (C4'), 68.2 (C5), 67.9 (C1), 61.1 (C6'), 28.7 (C2), 14.4 (C3); HRMS (ESI⁺) *m/z* calc. for C₁₁H₁₈O₆Na⁺ 269.0996 ([M+Na]⁺) found 269.0990 [M+Na]⁺. The ¹H and ¹³C NMR spectra were in agreement with literature values.²²

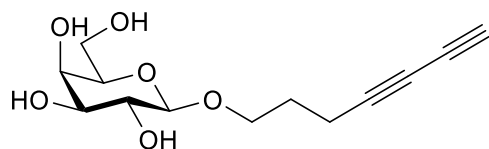
7-(Triethylsilyl)hepta-4,6-diyn-yl- β -D-galactoside (**11**)



4-Pentyn-yl- β -D-galactoside (**10**) (370 mg, 1.5 mmol), BuNH₂ (7 mL), H₂O (3 mL) and NH₂OH.HCl (35 mg, 0.5 mmol) were dissolved in MeOH (20 mL). The reaction mixture was cooled to 0 °C and CuCl (15 mg, 0.15 mmol) was added in a single portion. (Bromoethynyl)(triethyl)silane (**2**) (1.0 g, 4.9 mmol) was added dropwise by syringe. The

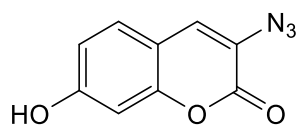
reaction mixture immediately went bright orange, and after stirring at 0 °C for 1 hour the reaction mixture was a dark blood red. The reaction mixture was diluted with EtOAc (50 mL) and washed with sat. aqueous NH₄Cl solution (3 × 10 mL). The aqueous layer was then extracted with EtOAc (3 × 5 mL) and the organic layers were combined, dried over MgSO₄, filtered and concentrated *in vacuo*. The crude residue was purified by FCC (gradient of 0% to 20% MeOH in DCM) to return the title compound (**11**) (135 mg, 23%) as a yellow powder; R_f 0.44 (DCM/MeOH 9:1); [α]_D = +10 (c 1.0, MeOH); δ_H(400 MHz; CD₃OD) 4.12 (d, *J*_{1',2'} = 7.2 Hz, 1H, H-1'), 3.86 (dt, ²*J*_{1a,1b} = 10.1 Hz, *J*_{1a,2} = 4.1 Hz, 1H, H-1a), 3.74 (dd, *J*_{3',4'} = 3.1 Hz, *J*_{4',5'} = 1.0 Hz, 1H, H-4'), 3.68-3.60 (m, 2H, H-6'a,b), 3.55 (dt, ²*J*_{1a,1b} = 10.1 Hz, *J*_{1a,2} = 4.1 Hz, 1H, H-1b), 3.43-3.35 (m, 3H, H-2',3',5'), 2.36 (t, *J*_{2,3} = 7.1 Hz, 2H, H-3), 1.77-1.71 (m, 2H, H-2), 0.91 (t, *J*_{8,9} = 8.0 Hz, 9H, 3 × CH₃), 0.52 (t, *J*_{8,9} = 8.0 Hz, 6H, 3 × CH₂) δ_C(100 MHz; CD₃OD) 101.3 (C1'), 87.1 (C6), 77.2 (C4), 76.18 (C7), 72.8 (C3'), 71.2 (C5'), 68.8 (C2'), 66.5 (C4'), 65.4 (C1), 62.8 (C5), 58.7 (C6'), 26.0 (C2), 12.8 (C3) 3.9 (CH₃), 1.4 (CH₂); HRMS (ESI⁺) *m/z* calc for C₁₉H₃₂O₆SiNa⁺ 407.1861 ([M+Na]⁺) found 407.1859 [M+Na]⁺.

Hepta-4,6-diyn-yl-β-D-galactoside (**9**)



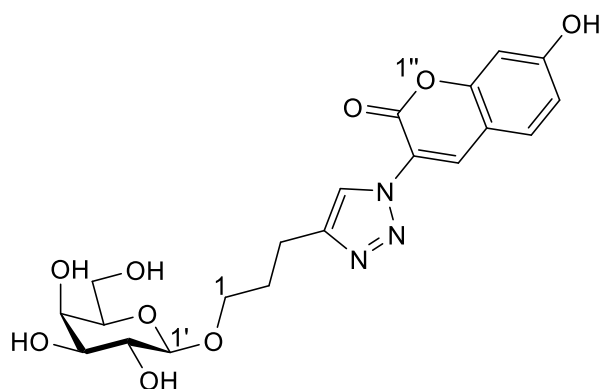
To a solution of 7-(triethylsilyl)hepta-4,6-diyn-yl-β-D-galactoside (**11**) (34 mg, 90 μmol) in anhydrous THF (3 mL) was added Et₃N·3HF (145 μL, 0.9 mmol). The reaction mixture was stirred over night at room temperature, after which time TLC (DCM/MeOH 9:1) showed the reaction had gone to completion. The crude mixture was dried under reduced pressure and purified by FCC to give the title compound (**9**) (20 mg, 88%) as a pink powder. R_f 0.16 (DCM/MeOH 9:1); [α]_D = -13.0 (c = 1.0, MeOH); δ_H(400 MHz; CD₃OD) 4.11 (d, *J*_{1',2'} = 7.1 Hz, 1H, H-1'), 3.85 (dt, ²*J*_{1a,1b} = 10.2 Hz, *J*_{1a,2} = 6.0 Hz, 1H, H-1a), 3.73 (dd, *J*_{3',4'} = 3.1 Hz, *J*_{4',5'} = 1.0 Hz, 1H, H-4'), 3.65-3.63 (m, 2H, H-6'a,b) 3.54 (dt, ²*J*_{1a,1b} = 10.2 Hz, *J*_{1a,2} = 6.0 Hz, 1H, H-1b), 3.43-3.34 (m, 3H, H-2',3',5'), 2.41 (t, ⁶*J*_{3,7} = 1.2 Hz, 1H, H-7), 2.33 (t, *J*_{2,3} = 7.1 Hz, 2H, H-3), 1.77-1.70 (m, 2H, H-2); δ_C(100 MHz; CD₃OD) 103.7 (C1'), 76.8 (C4), 75.2 (C3'), 73.6 (C5'), 71.2 (C2'), 68.9 (C4'), 67.7 (C1), 67.6 (C6), 65.0 (C7), 64.4 (C5), 61.0 (C6'), 28.3 (C3), 14.9 (C2); HRMS (ESI⁺) *m/z* for C₁₃H₁₈O₆Na⁺ 293.0996 ([M+Na]⁺), found 293.0995 [M+Na]⁺.

3-azido-7-hydroxycoumarin (**12**)²⁷



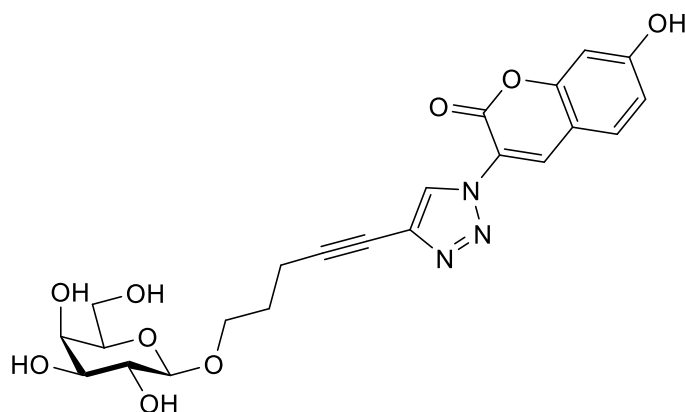
A suspension of 2,4-hydroxybenzaldehyde (4.2 g, 30 mmol), *N*-acetylglycine (3.5 g, 30 mmol) and sodium acetate (12.5 g, 150 mmol) in acetic anhydride (100 mL) was heated to reflux overnight. The reaction mixture was poured onto ice and the resulting yellow solid was filtered off and dissolved in a 1:1 mixture of EtOH/HCl (conc.) (50 mL) and heated to reflux for 1 hour. The resulting mixture was then cooled in an ice bath and NaNO₂ (4.2 g, 61 mmol) in ice cold water (40 mL) was added in a single portion. After 10 minutes NaN₃ (6.5 g, 100 mmol) was added in small portions and the reaction mixture was stirred for 1 hour. The resulting precipitate was filtered off, washed with ice cold water and dried *in vacuo* before being purified by FCC to give crude 3-azido-7-hydroxycoumarin (**12**) (410 mg, 7%) as a brown powder. *R*_f 0.53 (hexane/EtOAc 6:4); $\nu_{\max}/\text{cm}^{-1}$ (ATR-IR) 3292 (br, OH), 2107 (s, N₃), 1676 (m, C=O), 1621, 1594, 1342 (m, Ar-O), 1317 (s, C=O), 1258, 1220, 1120, 926, 836, 624; δ_{H} (400 MHz; DMSO-*d*₆) 10.53 (s, 1H, OH), 7.61 (s, 1H, H-4), 7.49 (d, *J*_{5,6} = 8.5 Hz, 1H, H-6), 6.82 (dd, *J*_{5,8} = 2.2 Hz, *J*_{5,6} = 8.5 Hz, 1H, H-5), 6.76 (d, *J*_{5,8} = 2.2 Hz, 1H, H-8); δ_{C} (100 MHz; DMSO-*d*₆) 106.2 (C7), 152.7 (C2), 129.1 (C6), 127.8 (C4), 121.1 (C3), 113.8 (C5), 111.3 (C5), 111.3 (C10), 102.0 (C8); The ¹H NMR data were in accordance with the literature.²⁷

3-[1-(7-Hydroxy-coumarin)-1H-1,2,3-triazol-4-yl] propyl β-D-galactopyranoside (**13**)



4-Pentyn-yl- β -D-galactoside (**10**) (25 mg, 0.1 mmol) and 3-azido-7-hydroxycoumarin (**12**) (32 mg, 0.1 mmol) were dissolved in MeOH/H₂O (1:1) (2 mL). The reaction was initiated by adding 1M aqueous copper sulfate solution (20 μ L) and 1M aqueous sodium ascorbate solution (50 μ L) and then stirred at room temperature for 2 hours before being concentrated *in vacuo*. The crude residue was purified by semi-prep TLC (CHCl₃/MeOH 85:15) to give the title compound (**13**) as a yellow powder (25 mg, 56%); R_f 0.53 (CHCl₃/MeOH 85:15); [α]_D -12.6 (*c* = 0.5, MeOH); UV-vis (DMSO) λ_{abs} = 393 nm; δ_{H} (400 MHz; CD₃OD) 8.36 (s, 1H, H-5), 8.27 (1H, s, H-8''), 7.54 (d, $J_{6'',7''}$ = 8.8 Hz, 1H, H-7''), 6.80 (dd, $^4J_{4''6''}$ = 2.4 Hz, $J_{6'',7''}$ = 8.8 Hz, 1H, H-6''), 6.72 (d, $J_{4'',6''}$ = 2.4 Hz, 1H, H-4''), 4.14 (d, $J_{1',2'}$ = 7.6 Hz, 1H, H-1'), 3.87 (dt, $J_{1a,1b}$ = 9.9 Hz, $J_{1a,2}$ = 6.3 Hz, 1H, H-1a), 3.74 (dd, $J_{3',4'}$ = 3.1 Hz, $J_{4',5'}$ = 1.0 Hz, H-4'), 3.69-3.62 (m, 2H, H-6'a,b), 3.52 (dt, $J_{1a,1b}$ = 9.9 Hz, $J_{1b,2}$ = 6.3 Hz, 1H, H-1b), 3.48-3.36 (m, 3H, H-5',2',3'), 2.83 (t, $J_{2,3}$ = 7.4 Hz, 2H, H-3), 1.96-1.90 (m, 2H, H-2); δ_{C} (100 MHz; DMSO) 156.9 (C=O), 155.2 (C4), 147.2 (Ar), 136.7 (C5), 131.3 (C7''), 123.5 (C8''), 115.0 (C6''), 104.0 (C1'), 102.7 (C4''), 75.6 (C3'), 73.8 (C5'), 71.0 (C2'), 68.7 (C4'), 68.1 (C1), 60.9 (C6'), 29.6 (C2), 22.0 (C3); HRMS (ESI⁺) *m/z* calcd. for C₂₀H₂₄N₃O₉⁺ 450.1507 ([M.H]⁺) found 450.1505 [M.H]⁺.

5-[1-(7-Hydroxy-coumarin)-1H-1,2,3-triazol-4-yl] pent-4-yn-1-yl β -D-galactopyranoside (14)



Hepta-4,6-diy-yl- β -D-galactoside (**9**) (27 mg, 0.1 mmol) and 3-azido-7-hydroxycoumarin (**12**) (32 mg, 0.1 mmol) were dissolved in MeOH/H₂O (1:1) (2 mL). The reaction was initiated by adding 1M aqueous copper sulfate solution (20 μ L) and 1M aqueous sodium ascorbate

solution (50 μ L) and then stirred at room temperature for 2 hours before the mixture was concentrated *in vacuo*. The crude residue was purified by semi-prep TLC ($\text{CHCl}_3/\text{MeOH}$ 85:15) to give the title compound (**14**) as a yellow powder (25 mg, 53%); R_f 0.72 ($\text{CHCl}_3/\text{MeOH}$ 85:15); $[\alpha]_D = -1.0$ ($c = 1.0$, MeOH), $[\alpha]_{436} = -27.4$ ($c = 1.0$, MeOH); UV-vis (DMSO) $\lambda_{\text{abs}} = 349$ nm; δ_{H} (400 MHz; CD_3OD) 8.49 (s, 1H, H-5), 8.41 (1H, s, H-8''), 7.55 (d, $J_{6'',7''} = 8.3$ Hz, 1H, H-7''), 6.80 (dd, $^4J_{4'',6''} = 2.4$ Hz, $J_{6'',7''} = 8.3$ Hz, 1H, H-6''), 6.73 (d, $J_{4'',6''} = 2.4$ Hz, 1H, H-4''), 4.15 (d, $J_{1',2'} = 7.5$ Hz, 1H, H-1'), 3.99-3.92 (m, 1H, H-1), 3.74 (dd, $J_{3',4'} = 3.2$ Hz, $J_{4',5'} = 1.0$ Hz, H-4'), 3.70-3.60 (m, 4H, H-1b,5',2',3'), 2.53 (t, $J_{2,3} = 7.4$ Hz, 2H, H-3), 1.88-1.81 (m, 2H, H-2); δ_{C} (100 MHz; DMSO) 156.8 (C=O), 137.9 (C8''), 131.4 (C7''), 130.4 (C6), 128.4 (C7), 115.4 (C6''), 104.0 (C1'), 102.8 (C4''), 94.4 (C4), 75.6 (C5'), 73.9 (C2'), 71.1 (C3'), 70.5 (C5), 68.6 (C4'), 67.6 (C1), 60.9 (C6), 28.8 (C2), 15.9 (C3); HRMS (ESI⁺) m/z calcd. for $\text{C}_{22}\text{H}_{24}\text{N}_3\text{O}_9^+$ 474.1507 ([M.H]⁺) found 474.1510 [M.H]⁺.

3.7.5 CuAAC coupling of prymnesin extracts with 3-azido-7-hydroxycoumarin

The crude prymnesin extract was mixed with 3-azido-7-hydroxycoumarin (100 μ g) in a mixture of $\text{H}_2\text{O}/\text{EtOH}$ 1:1 (100 μ L). A freshly prepared solution of 0.1M aqueous copper sulfate and 0.2M aqueous sodium ascorbate (10 μ L) was added to start the coupling reaction. After 2 hours, the crude reaction mixture was separated by TLC under the conditions described by Igarashi *et al.*² The TLC plate was dried and visualised under a UV lamp.

3.8 References

1. S. R. Manning and J. W. La Claire, *Mar. Drugs*, 2010, **8**, 678–704.
2. T. Igarashi, M. Satake, and T. Yasumoto, *J. Am. Chem. Soc.*, 1999, **121**, 8499–8511.
3. S. A. Rasmussen, S. Meier, N. G. Andersen, H. E. Blossom, J. Ø. Duus, K. F. Nielsen, P. J. Hansen, and T. O. Larsen, *J. Nat. Prod.*, 2016, **79**, 2250–2256.
4. T. Igarashi, S. Aritake, and T. Yasumoto, *Nat. Toxins*, 1998, **6**, 35–41.
5. S. R. Manning and J. W. La Claire II, *Anal. Biochem.*, 2013, **442**, 189–195.
6. J. W. La Claire, S. R. Manning, and A. E. Talarski, *Toxicon*, 2015, **102**, 74–80.
7. T. Igarashi, M. Satake, and T. Yasumoto, *J. Am. Chem. Soc.*, 1996, **118**, 479–480.
8. A. Umeyama, C. Nagano, and S. Arihara, *J. Nat. Prod.*, 1997, **60**, 131–133.
9. Y. Fujimoto, H. Wang, M. Satoh, and N. Takeuchi, *Phytochem*, 1994, **35**, 1255–1257.
10. A. K. Amegadzie, W. A. Ayer, and L. Sigler, *Can. J. Chem.*, 1995, **73**, 2119–2125.

11. A. L. K. Shi Shun and R. R. Tykwinski, *Angew. Chem - Int. Ed.*, 2006, **45**, 1034–1057.
12. R. E. Minto and B. J. Blacklock, *Prog. Lipid Res.*, 2008, **47**, 233–306.
13. V. V. Rostovtsev, L. G. Green, V. V. Fokin, and K. B. Sharpless, *Angew. Chem - Int. Ed.*, 2002, **41**, 2596–2599.
14. C. W. Tornøe, C. Christensen, and M. Meldal, *J. Org. Chem.*, 2002, **67**, 3057–3064.
15. H. Yamakoshi, K. Dodo, A. Palonpon, J. Ando, K. Fujita, S. Kawata, and M. Sodeoka, *J. Am. Chem. Soc.*, 2012, **134**, 20681–20689.
16. J. P. Marino and H. N. Nguyen, *J. Org. Chem.*, 2002, **67**, 6841–6844.
17. K. S. Sindhu, A. P. Thankachan, P. S. Sajitha, and G. Anilkumar, *Org. Biomol. Chem.*, 2015, **13**, 6891–6905.
18. T. Luu, R. McDonald, and R. R. Tykwinski, *Org. Lett.*, 2006, **8**, 6035–6038.
19. T. Luu and R. R. Tykwinski, *J. Org. Chem.*, 2006, **71**, 8982–8985.
20. K. West, C. Wang, A. S. Batsanov, and M. R. Bryce, *J. Org. Chem.*, 2006, **71**, 8541–8544.
21. X. Nie and G. Wang, *J. Org. Chem.*, 2006, **71**, 4734–4741.
22. F. Pertici and R. J. Pieters, *Chem. Commun.*, 2012, **48**, 4008–4010.
23. B. W. Gung and R. M. Fox, *Tetrahedron*, 2004, **60**, 9405–9415.
24. M. C. Pirrung, S. W. Shuey, D. C. Lever, and L. Fallon, *Bioorg. Med. Chem. Lett.*, 1994, **4**, 1345–1346.
25. A. L'Heureux, F. Beaulieu, C. Bennett, D. R. Bill, S. Clayton, F. LaFlamme, M. Mirmehrabi, S. Tadayon, D. Tovell, and M. Couturier, *J. Org. Chem.*, 2010, **75**, 3401–3411.
26. M. Weigele, S. L. DeBernardo, J. P. Tengji, and W. Leimgruber, *J. Am. Chem. Soc.*, 1972, **94**, 5927–5928.
27. K. Sivakumar, F. Xie, B. M. Cash, S. Long, H. N. Barnhill, and Q. Wang, *Org. Lett.*, 2004, **6**, 4603–4606.
28. I. M. Ivanova, S. A. Nepogodiev, G. Saalbach, E. C. O'Neill, M. D. Urbaniak, M. A. J. Ferguson, S. S. Gurcha, G. S. Besra, and R. A. Field, *Carbohydr. Res.*, 2017, **438**, 26–38.
29. P. Rostron, S. Gaber, and D. Gaber, *Int. J. Eng. Tech. Res.*, 2016, **1**, 50–64.
30. L. Wei, F. Hu, Y. Shen, Z. Chen, Y. Yu, C.-C. Lin, M. C. Wang, and W. Min, *Nat. Methods*, 2014, **11**, 410–412.
31. T. Murphy, S. Lucht, H. Schmidt, and H.-D. Kronfeldt, *J. Raman Spectrosc.*, 2000, **31**, 943–948.
32. V. Tomar, *J. Nanomed. Nanotechnol.*, 2012, **3**, 131–142.

33. H. Neson and J. F. Sperry, *Proc. SPIE*, 2002, **4577**, 193–204.
34. Y. Chen, J.-Q. Ren, X.-G. Zhang, D.-Y. Wu, A.-G. Shen, and J.-M. Hu, *Anal. Chem.*, 2016, **88**, 6115–6119.
35. P. L. Stiles, J. A. Dieringer, N. C. Shah, and R. P. Van Duyne, *Annu. Rev. Anal. Chem.*, 2008, **1**, 601–626.
36. Y. Morisaki, T. Luu, and R. R. Tykwinski, *Org. Lett.*, 2006, **8**, 689–692.
37. K. P. Wang, E. J. Cho, S. Y. Yun, J. Y. Rhee, and D. Lee, *Tetrahedron*, 2013, **69**, 9105–9110.
38. W. Y. Lu, X. W. Sun, C. Zhu, J. H. Xu, and G. Q. Lin, *Tetrahedron*, 2010, **66**, 750–757.

4 The chemical synthesis of glyceryl glycosides inspired by prymnesin toxins

4.1 Introduction

4.1.1 Carbohydrates present on reported prymnesin toxins

There are currently two different prymnesin backbone structures reported in the literature;^{1,2} with variation in glycosylation patterns, there are four different reported prymnesin toxins (Figure 4.1).

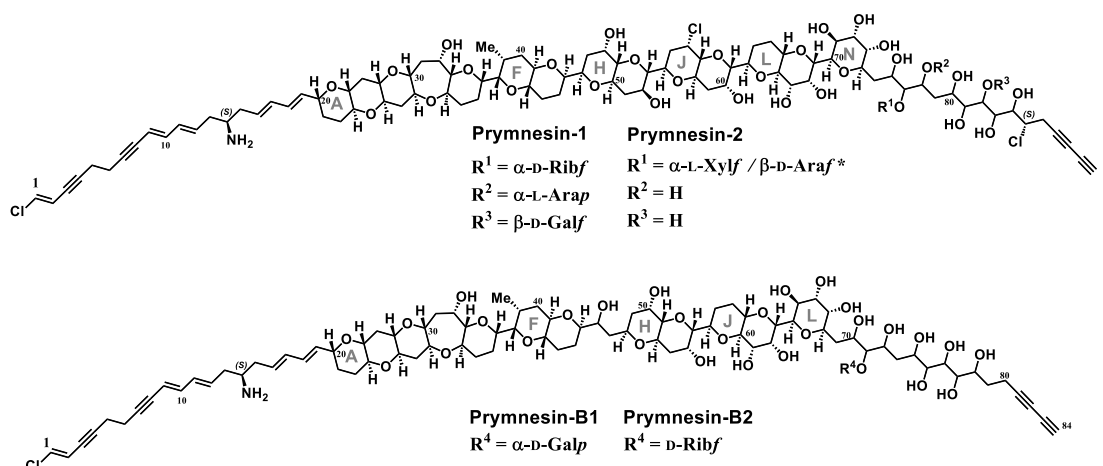


Figure 4.1 – The reported structures of the prymnesin toxins. Prymnesins-1 (PRM-1) and prymnesin (PRM-2) have a conserved backbone with a variation in sugars. Prymnesin-B1 (PRM-B1) and prymnesin-B2 (PRM-B2) also share a conserved backbone which is slightly shorter than that for PRM-1 and PRM-2, and are each decorated with a single sugar at the same position.

Igarashi et al.³ first deduced that the backbone of prymnesin-2 is glycosylated at C77 with α -L-xylofuranose. The glycosylation position on the backbone and the pentose ring size were elucidated by HMBC NMR cross peaks between H1'/C4' and H1'/C77. The carbohydrate on prymnesin-2 was then hydrolysed, trifluoroacetylated and identified as L-xylose by chiral GC. The carbohydrate moieties on prymnesin-1 were identified in a later paper by Igarashi et al.¹ When comparing the ^1H and ^{13}C NMR spectra for PRM-1 and PRM-2, they noticed that all of the chemical shifts were within 0.1 ppm (for proton NMR) and 1.0 ppm (for carbon NMR), with the exception of the region C78 – C82. From this, it was deduced that PRM-1 and PRM-2 shared a conserved backbone but were glycosylated with different sugars. The two extra carbon sequences due to the sugar rings, plus an additional molecular mass of 294 MU when compared with PRM-2, suggested that PRM-1 was glycosylated with an additional hexose and pentose.¹ Chiral GC of the sugars from the hydrolysed toxins was compared with sugar

standards and as such L-arabinose, D-galactose were assigned from the GC chromatogram (Figure 2.2).

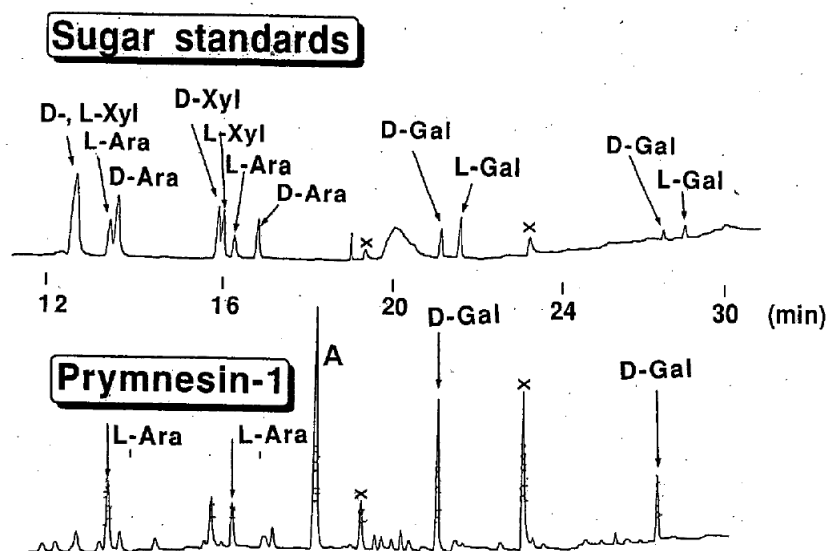


Figure 4.2 – The top chiral GC chromatogram shows the sugar standards for D- & L-xylose, D- & L-arabinose and D- & L-galactose. The bottom chiral GC chromatogram show the sugars L-arabinose and D-galactose which were hydrolysed from prymnesin-1. Peaks marked with an X are electrical noises from the instrument. Reprinted (adapted) with permission from T. Igarashi et al., *J. Am. Chem. Soc.*, 1999, **121** (37), pp 8499–8511 (supporting material). Copyright 1999 American Chemical Society.

The remaining pentose was identified as ribose by chiral GC. Because the standards for D-ribose and L-ribose have very similar retention times under the column conditions Igarashi et al.¹ were using, it was necessary to co-inject the unidentified pentose hydrolysed from prymnesin-1 with D-ribose and a mixture of D- & L-ribose. The co-injection with D-ribose led to an increase of the intensity of the prymnesin-1 hydrolyte peaks, whilst the addition of a mixture of D- & L-ribose led to both an enhancement of the prymnesin-1 hydrolyte peaks and an additional (L-ribose) peak (Figure 4.3). From this information, the final assignment for this pentose on prymnesin-1 was D-ribose.

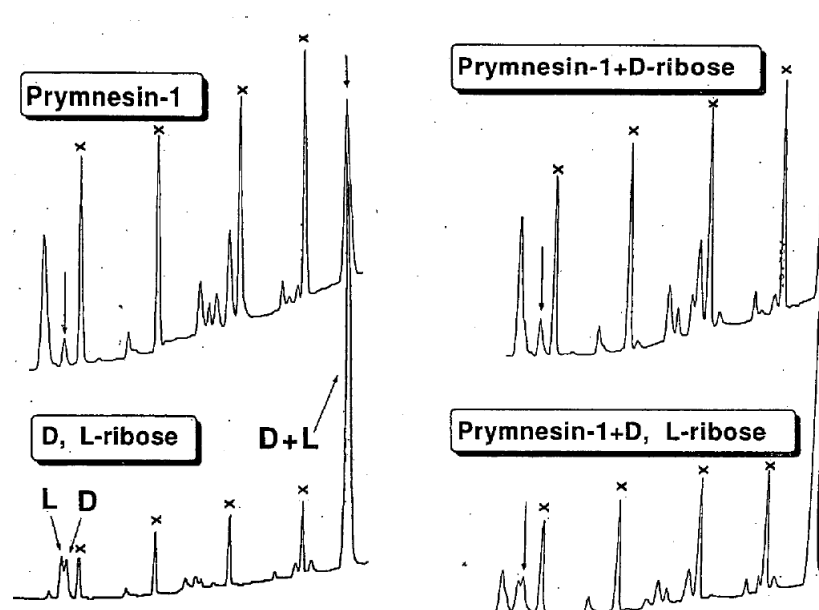


Figure 4.3 - GC chromatograms used to identify D-ribose on prymnesin-1. Clockwise from top left: GC chromatogram of the unidentified sugar in prymnesin-1; hydrolysed sugars spiked with D-ribose; hydrolysed sugars spiked with D- & L-ribose; standards for D- & L-ribose. Peaks marked with an X are electrical noises from the instrument. Reprinted (adapted) with permission from T. Igarashi et al., *J. Am. Chem. Soc.*, 1999, **121** (37), pp 8499–8511 (supporting material). Copyright 1999 American Chemical Society.

The position of the carbohydrates on the backbone of prymnesin-1 was determined by HMBC and nOe coupling, and the stereochemistry at the anomeric position and the ring size were determined by comparison of ^{13}C NMR chemical shifts and ^1H NMR coupling constants with literature values, to identify α -L-arabinopyranose, α -D-galactopyranose and α -D-ribofuranose (Table 4.1). As already discussed in Chapter 2, the literature ^{13}C shifts for the anomeric carbons of the 1,2-*cis* sugars for β -L-xylofuranose and α -D-ribofuranose are ~ 3 ppm smaller than the shift recorded for the sugar on the toxins. This might be attributed to the flexibility of furanose rings when compared with pyranose rings.⁴ The difference in ^{13}C NMR for the 1,2-*trans* sugars α -D-galactopyranose and α -L-arabinopyranose are much closer to the literature values.

Table 4.1 - ^{13}C NMR shifts for the anomeric carbons found on prymnesins-1/2 and the literature values Igarashi *et al.*¹ used as comparison to assign the ring as either furanose or pyranose form.

^{13}C NMR shift	$\alpha\text{-L-Xylf}$	$\alpha\text{-L-Arap}$	$\alpha\text{-D-Ribf}$	$\beta\text{-D-Galf}$
Toxin	106.2	106.1	106.0	110.4
Lit. pyranose	100.6	105.1	100.4	Not given
Lit. furanose	103.0	Not given	103.1	110.0

More recently Rasmussen *et al.*² have reported two new prymnesin toxins, prymnesin-B1 and prymnesin-B2, which share a conserved backbone. These toxins have a slightly different backbone to the original prymnesin-1/2 toxins; they are missing the H and I polyether rings which are replaced by a $-\text{CH}(\text{OH})-\text{CH}_2-$ linker, and have two less chlorine atoms than PRM-1/2. Prymnesin-B1 has been fully characterised and the carbohydrate was identified as a hexose by the difference in mass between the glycosylated and aglycone forms of the toxin. Chiral GC was used to identify the sugar as D-galactose, and the ring identified as being in the pyranose form by ^{13}C NMR values (Figure 4.4). The stereochemistry at the anomeric position was found to be 1,2-*cis* by the $J_{1,2}$ coupling value of 4 Hz. Finally, the toxin was found glycosylated at C-71 by HSQC NMR, and this was reinforced by nOe and a deshielded ^{13}C NMR shift for C-71. Prymnesin-B2 was only present in trace amounts and so could not be fully characterised by the authors. They also found an additional carbohydrate had been liberated by hydrolysis in the chiral GC, which was assigned as D-ribose (Figure 4.4). The chiral GC-MS conditions used by Rasmussen *et al.*² removed the ambiguity between D-ribose and L-ribose which was a problem encountered by Igarashi *et al.*¹ when assigning a pentose on prymnesin-1. The authors suggested that prymnesin-B2 is also glycosylated at C-71, which would be analogous with the position D-ribose is found on prymnesin-1.¹ It is also worth noting that Rasmussen *et al.*² have re-drawn prymnesin-2 as being glycosylated with $\beta\text{-D}$ -arabinofuranose. However, they offer no written remark or explanation for this in either their paper or supplementary material, and this anomaly is dealt with later in this chapter.

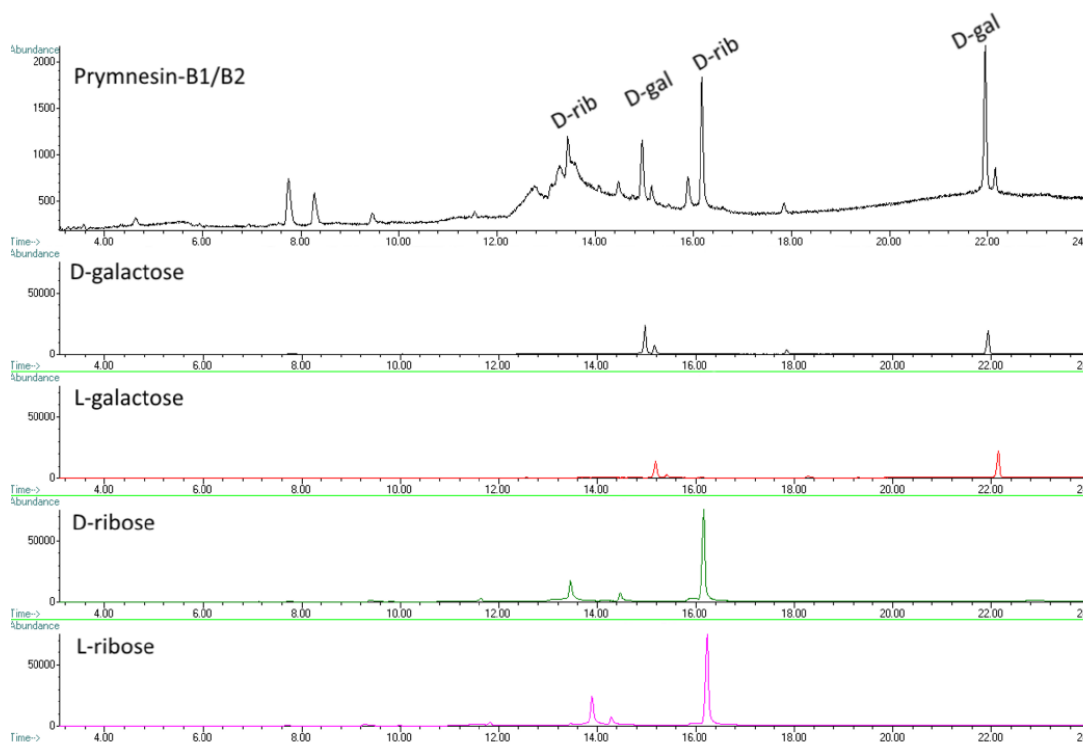


Figure 4.4 - Chiral GC-MS trace for prymnesin-B1/B2 hydrolyte along with standards of D-galactose, L-galactose, D-ribose and L-ribose. Reprinted (adapted) with permission from S. Rasmussen et al., *J. Nat. Prod.*, 2016, **79** (9), pp 2250–2256 (supporting material). Copyright 2016 American Chemical Society and American Society of Pharmacognosy. <http://pubs.acs.org/doi/full/10.1021/acs.jnatprod.6b00345>

Prymnesin-1 and prymnesin-2 have a conserved backbone, and the region between C76 – C84 is heavily hydroxylated. Determining the position of the hydroxyl groups was achieved by Igarashi et al.³ by comparison of proton shifts before and after per-*O*-acetylation. In a later paper by Igarashi et al.¹ where the stereochemistry of the toxin backbones was derived, they were unable to specify the specific stereochemistry for the hydroxylated region C-76 – C-84, most likely due to the flexibility in the backbone structure in this region. A similar story is true for Rasmussen et al.² who, in their much more recent paper characterising prymnesin-B1, were also unable to specify the stereochemistry in the flexible hydroxylated region of the toxin. This means that there is an ambiguity in desired structure if synthesising chemical fragments of prymnesins inspired by this region of the toxin.

4.1.2 Target glyceryl glycoside fragments

In order to gain insight into the structure and properties of prymnesin toxins, a library of glyceryl glycosides was synthesised as model fragments of the prymnesin toxins (Figure 4.5). The glyceryl glycoside 2-O-(α -D-glucopyranosyl) glycerol is known and is an osmolyte used by cyanobacteria to combat the effects of salt-stress and drought.⁵ Glyceryl glycosides have also found use as moisturising ingredients in cosmetics.⁶ Two of the glyceryl glycosides in our library have previously been reported in the literature. The first isolated algal glyceryl glycoside was 'floridoside' (1,3-dihydroxypropan-2-yl α -D-galactopyranoside) (**7**) from the red alga *Mastocarpus stellatus*.⁷ Floridoside has been found to be a potent activator of the classical complement pathway,⁷ and this chemical synthesis has been reported in the literature.^{8,9} 1,3-Dihydroxypropan-2-yl α -L-arabinopyranoside (**2**) has been synthesised as a reference compound in an old project determining the glycosidic linkages of disaccharides. However, (**2**) has only been characterised by melting point and optical rotation.^{10,11} The other glyceryl glycosides have not been reported before.

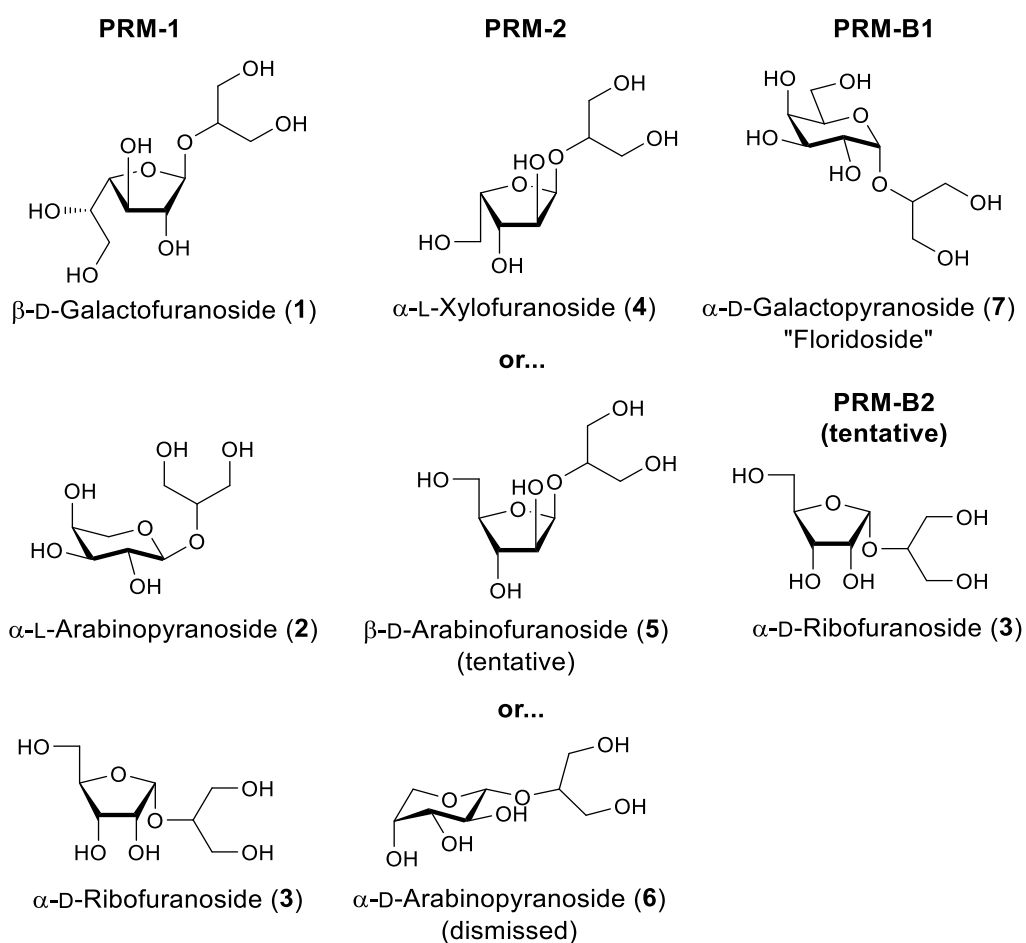


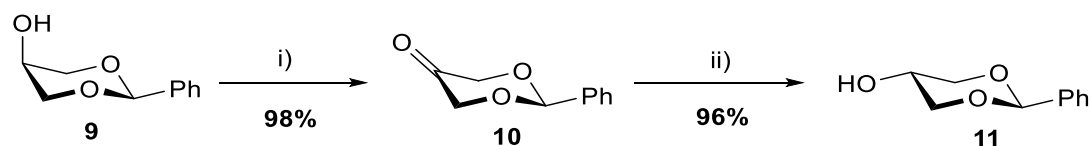
Figure 4.5 – Target sugar glycerol fragments inspired by PRM-1, PRM-2, PRM-B1 and PRM-B2.

4.2 Chemistry

4.2.1 Choosing a protected glycerol acceptor

Glycerol was glycosylated at the 2° hydroxyl position to synthesise small analogues of the prymnesin toxins glycosylated backbones. Due to flexibility in the backbone of the glycosylated region of prymnesin toxins, the stereochemistry in this region is so far undefined. Using glycerol as a small fragment of the toxin backbone eliminated the need to define the stereochemistry at the 2-*O*- position of the acceptor after glycosylation. A second benefit of synthesising the library shown in Figure 4.5 was that it helped to develop glycosylation techniques for larger diglycoside fragments inspired by the toxins (Chapter 5). Due to the increased reactivity of 1° alcohols compared with 2° alcohols, it was necessary to have protecting groups on the glycerol 1,3-*O* positions for the glycosylation step. Using the same protecting groups on the glycerol 1,3-*O*- positions ensured symmetry across the acceptor. This prevents the complication of purifying mixtures of isomers which differ at the stereochemistry of the acceptor as well as the anomeric position after glycosylation.

cis-1,3-*O*-Benzylidene glycerol (**9**) is commercially available and was considered as a protected glycerol acceptor. It has also been used by Perlin *et al.*¹¹ to synthesise 3-dihydroxypropan-2-yl α -L-arabinopyranoside (**2**). However, preliminary attempts to glycosylate *cis*-1,3-*O*-benzylidene glycerol (**9**) using acetobromo D-glucose (**12**) under Koenigs-Knorr conditions were unsuccessful.¹² This is perhaps because of the axial orientation of the hydroxyl group makes *cis*-1,3-*O*-benzylidene glycerol a relatively unreactive donor. The hydroxyl group was therefore inverted from an axial to an equatorial orientation by sequential oxidation and reduction.¹³ (Scheme 4.1).



Scheme 4.1 – Chemical synthesis of *trans*-1,3-*O*-benzylidene glycerol (**11**) by inversion of the hydroxyl group on *cis*-1,3-*O*-benzylidene glycerol via oxidation and reduction.¹³ i) DMP, DCM. ii) NaBH₄, THF/H₂O.

Cis-1,3-*O*-benzylidenglycerol (**9**) was treated with Dess-Martin periodinane (DMP) in DCM to give 2-phenyl-1,3-dioxan-5-one (**10**) in very good yield. The oxidation of the alcohol to a ketone was confirmed by loss of the 2H proton by ^1H NMR and a new carbonyl signal in the ^{13}C NMR at 204.2 ppm. Reduction of the ketone was performed using sodium borohydride which gave *trans*-1,3-*O*-benzylidenglycerol (**11**) in very good yield. This reduction requires hydride attack the ketone from the *more* hindered face of **10**. Houk *et al.*¹⁴ have used computational modelling to explain that axial attack reduces torsional strain in the transition state, whilst equatorial attack of the ketone would require rotation of the $\text{C}_\alpha\text{-C}_{\text{CO}}$ bond leading to torsional strain (Figure 4.6). The successful reduction was accompanied by a loss of the carbonyl signal in the ^{13}C NMR and the ^1H and ^{13}C NMR values agreed with the published literature for *trans*-1,3-*O*-benzylidenglycerol (**11**).¹⁵

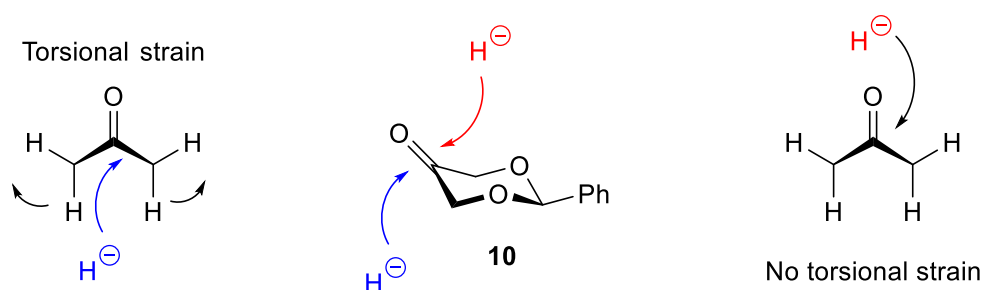
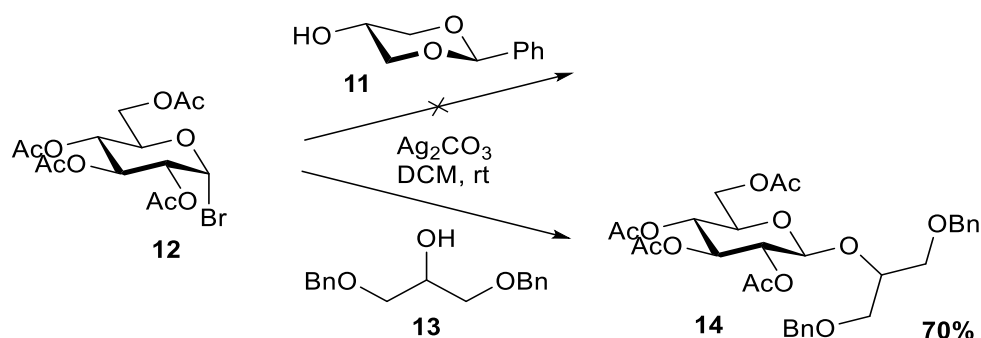


Figure 4.6 – Steric effects leading to the axial attack of the ketone **10**, which lead to the equatorial hydroxyl group on **11**.

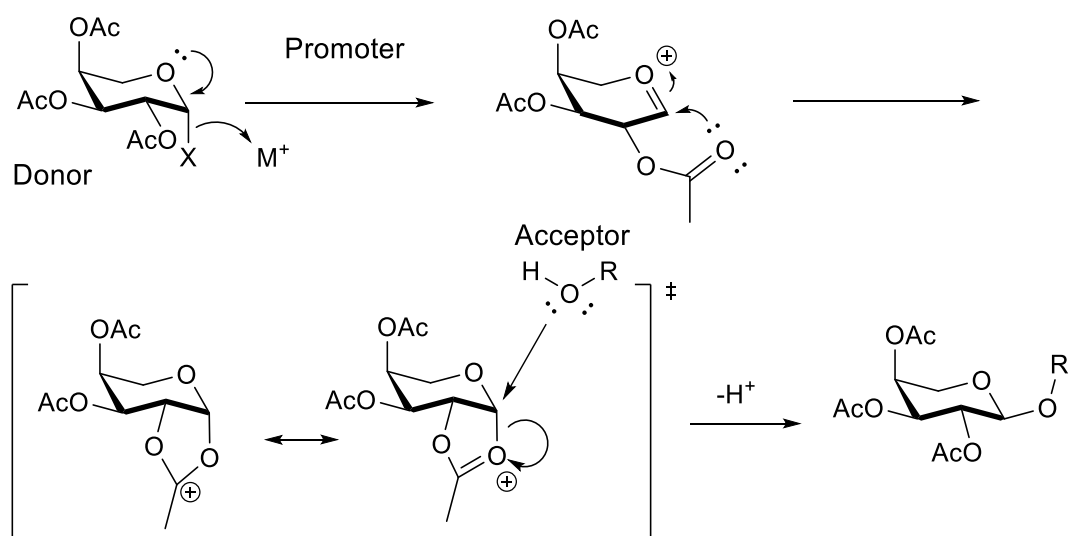
trans-1,3-Di-*O*-benzylidenglycerol (**11**) acceptor was mixed with acetobromo D -glucose (**12**) and silver carbonate in DCM. Again, no glycosylation was seen, which may be due to the noted instability of **11**.¹³ As such it was decided a better acceptor needed to be found. 1,3-Di-*O*-benzyl glycerol (**13**) is a commercially available symmetrical glycerol acceptor. It is relatively inexpensive, stable at room temperature, and the lack of acid labile groups make it compatible with a range of glycosylation conditions. 1,3-Di-*O*-benzyl glycerol (**13**) was mixed with acetobromo D -glucose (**12**) and silver carbonate in DCM to give 1,3-bis(benzyloxy)propan-2-yl 2',3',5',6'-tetra-*O*-acetyl- β - D -glucopyranoside (**14**) as exclusively the 1,2-*trans* β -anomer, as judged by the ^1H NMR H-1' signal which was a doublet at 4.80 ppm with a $J_{1,2'}$ coupling of 8.0 Hz (Scheme 4.2). 1,3-Di-*O*-benzyl glycerol (**13**) was therefore used as the protected glycerol acceptor for the synthesis of the sugar glycerol fragments.



Scheme 4.2 - Trialling protected glycerol acceptors by glycosylation with acetobromo D-glucose under Koenigs–Knorr conditions.¹²

4.2.2 Synthesis of 1,2-*trans* glyceryl glycoside fragments

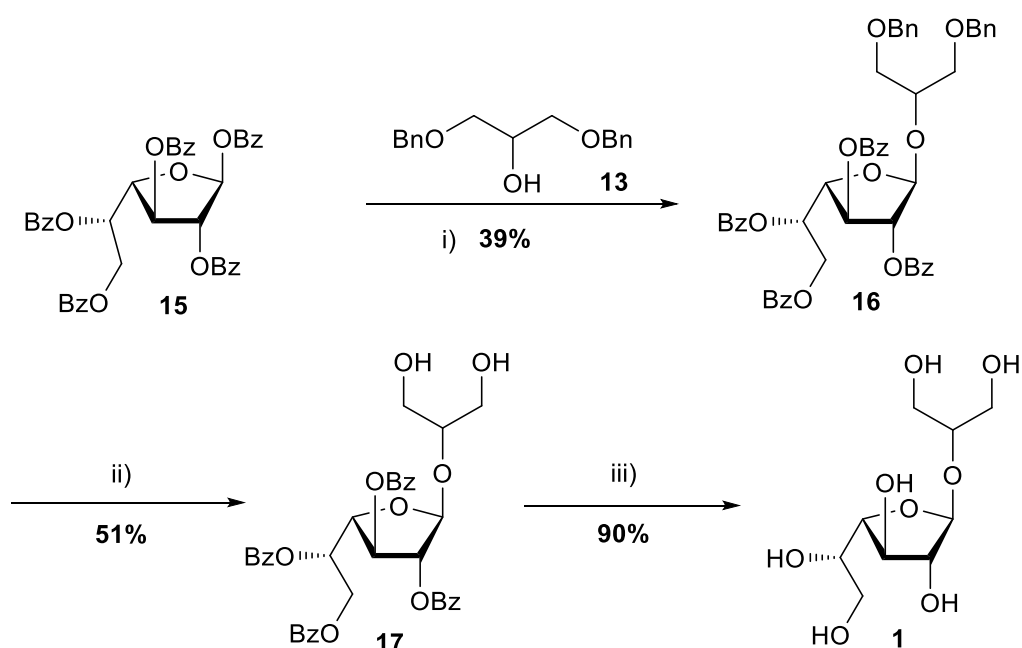
The synthesis of 1,2-*trans* glycosides is often achieved by utilising neighbouring group participation.¹⁶ Here the oxocarbenium cation is formed by abstraction of a leaving group at the anomeric position of the sugar. This can be achieved by the abstraction of bromide with silver carbonate as per the Koenig-Knorr reaction, or direct abstraction of an ester from the anomeric position using a Lewis acid.^{12,17} The oxocarbenium cation is then stabilised by the carbonyl oxygen lone pairs of the ester protecting group at C2, which in turn sterically blocks attack by the acceptor alcohol from the same face as the protecting group, leading to exclusively 1,2-*trans* product (Scheme 4.3).



Scheme 4.3 – Mechanism by which neighbouring group participation by an ester group at the 2 position on a glycosidic donor leads to 1,2-*trans* glycosylation.¹⁶

4.2.2.1 1,3-Dihydroxypropan-2-yl-β-D-galactofuranoside (1)

The synthesis of per-*O*-benzoyl-β-D-galactofuranose (**15**) was described earlier on in the project (Chapter 2), using a modified protocol by Zhang and Liu.¹⁸ As there are no acid labile groups present on either the donor or the acceptor, SnCl₄ promoted glycosylation of 1,3-di-*O*-benzyl glycerol (**13**) with per-*O*-benzoyl-β-D-galactofuranose (**15**) was employed for the initial reaction step (Scheme 4.4).^{17,19}



Scheme 4.4 – The chemical synthesis of 1,3-dihydroxypropan-2-yl β-D-galactofuranoside (**1**). i) SnCl₄, DCM. ii) H₂, 10% Pd/C, EtOAc. iii) MeOH/H₂O/Et₃N (5:2:1)

Neighbouring group participation by the benzoyl ester protecting group ensured that only the 1,2-*trans* β-anomer (**16**) was produced, and the configuration at the anomeric position was confirmed by the presence of a single H-1' signal as singlet in the ¹H NMR at 5.61 ppm.¹⁹ It was decided to remove the benzyl protecting groups by hydrogenation first as this left the lipophilic benzoyl protecting groups *in situ* to aid recovery of the compound from the palladium on activated charcoal (Pd/C) catalyst. After hydrogenation, the benzoyl protecting groups were removed using a mixture of MeOH/H₂O/Et₃N (5:2:1). ¹H NMR spectra recorded after global deprotection showed the presence of aromatic signals, despite the fact mass spectrometry indicated that the global deprotection had gone to completion. Due to the water present in the methoxide catalysed debenzylation step, it was possible for both base

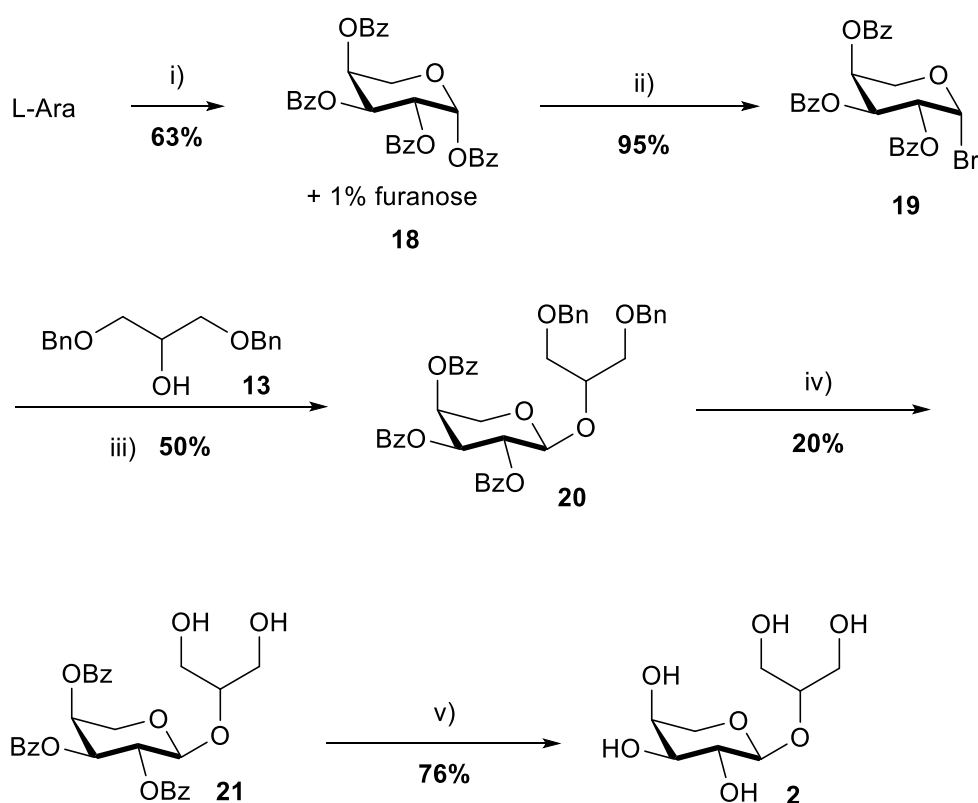
catalysed hydrolysis and trans-esterification of the benzyl ether protecting groups to occur, leading to both methyl benzoate and benzoic acid. While the former is volatile, the latter may have remained in the mixture. As **(1)** contains no acidic groups, the crude mixture was dissolved in methanol and passed through Dowex® 1X2-400 resin (OH⁻ form) which bound any benzoic acid but allow 1,3-dihydroxypropan-2-yl-β-D-galactofuranoside (**1**) to pass through. The ¹H NMR was run again and the aromatic signals were no longer present in the spectrum. The stereochemistry at the anomeric position was confirmed by the H-1' signal as at 4.99 ppm, with a small $J_{1',2'}$ coupling value of 1.7 Hz. Due to overlapping peaks in the ¹H NMR, a COSY and HSQCed spectrum were used to assign the ¹³C NMR peaks, as well as give a better indication as to where the varying proton signals are on the ¹H NMR spectrum. The HSQCed spectrum is shown in Appendices, Figure 6.1.

4.2.2.2 1,3-Dihydroxypropan-2-yl α-L-arabinopyranoside (**2**)

The synthesis of 1,3-dihydroxypropan-2-yl α-L-arabinopyranoside (**2**) has previously been described by Perlin et al.¹¹ in 1957. Here the authors accessed (**2**) via a Koenigs–Knorr condensation using acetobromo L-arabinopyranose (**19**) as the donor, 1,3-di-*O*-benzylidene glycerol (**13**) as the acceptor and silver carbonate as a promotor.¹² The final deprotected compound was, however, only characterised by optical rotations.

Initial attempts to acetylate L-arabinose with acetic anhydride in pyridine led to significant quantities of per-*O*-acetyl L-arabinofuranose which were inseparable from per-*O*-acetyl L-arabinopyranose. Therefore L-arabinose was per-*O*-benzoylated with benzoyl chloride in pyridine to give (**18**) (Scheme 4.5).²⁰ To minimise the formation of per-*O*-benzoyl L-arabinofuranose, it was found necessary to carry out this benzoylation in the presence of DMAP, with the addition of benzoyl chloride being performed dropwise at 0 °C. After benzoylation and workup the ¹H NMR spectrum showed a H-1 signal at 6.87 ppm as a broad singlet which confirmed 1,2,3,4-tetra-*O*-benzoyl-β-L-arabinopyranose (**18**) was the major species (99% by integration of ¹H NMR anomeric signals).²⁰ Treatment of (**18**) with 33% HBr in acetic acid gave the glycosyl bromide donor (**19**) which was immediately used in the silver carbonate promoted glycosylation of 1,3-di-*O*-benzylglycerol (**13**). Neighbouring group participation ensured that only the 1,2-*trans* α-anomer (**20**) was formed, and this was confirmed by the presence of a single H-1' signal at 5.06 ppm as a doublet, albeit with a slightly low $J_{1',2'}$ coupling value of 5.9 Hz. This lower coupling value was attributed to twisting of the sugar ring by the bulky benzoyl protecting groups. The glycerol benzyl ether protecting

groups were removed by hydrogenation over a Pd/C catalyst and sodium-methoxide catalysed transesterification was employed to remove the benzoyl protecting groups, and to give 1,3-dihydroxypropan-2-yl α -L-arabinopyranoside (**2**) as a white powder. After global deprotection, ^1H NMR of the (**2**) showed the presence of aromatic signals at 7.4-7.2 ppm, despite mass spectrometry showing that both reaction steps had gone to completion. Despite using a fresh sodium methoxide solution, it is evident that there was some moisture present during the debenzoylation step, which led to the formation of some benzoic acid. This was removed as previously described by passing the crude mixture containing (**2**) through Dowex[®] 1X2-400 resin (OH^- form).



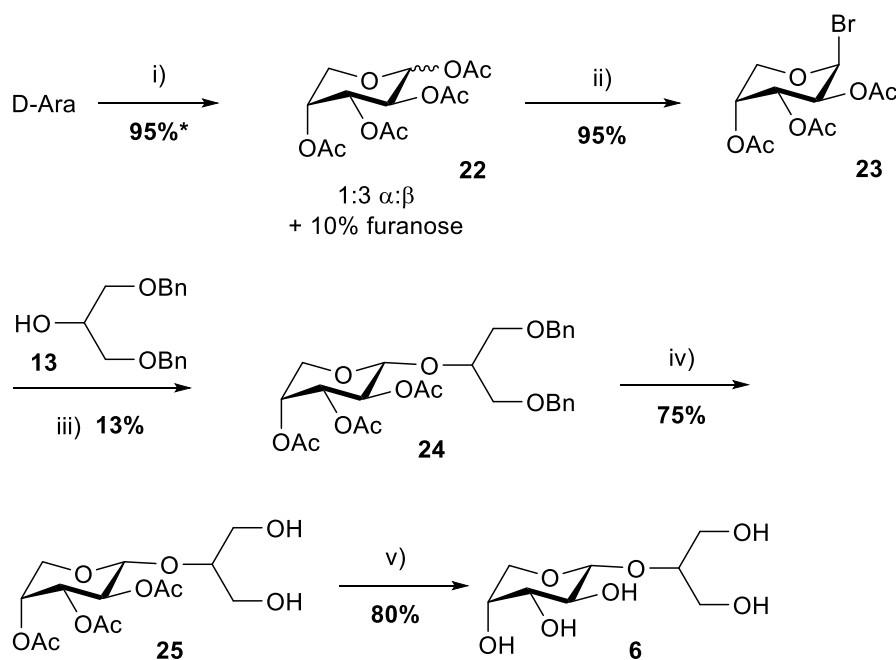
Scheme 4.5 – The chemical synthesis of 1,3-dihydroxypropan-2-yl α -L-arabinopyranoside. i) BzOH, DMAP, Pyr, 0 °C. ii) 33% v/v HBr/AcOH, DCM. iii) Ag_2CO_3 , Drierite[™], toluene. iv) H_2 , 10% Pd/C, EtOAc, Et_3N . v) Na, MeOH.

With the protecting groups removed, the ^1H NMR of (**2**) showed a single H-1' signal at 4.35 ppm as a doublet with a larger $J_{1',2'}$ coupling value of 7.5 Hz, which confirmed the presence of the 1,2-*trans* α -anomer. Apart from the H-1' signal, most of the proton peaks for (**2**) overlapped in the ^1H NMR spectrum. Much more information was gained from the HSQC

spectrum, and by combining this with data from the COSY 2D spectrum and comparison with other sugar glycerol fragments it was possible to assign all peaks in the HSQC spectrum and therefore the ^{13}C NMR spectrum (Appendices, Figure 6.2).

4.2.2.3 1,3-Dihydroxypropan-2-yl α -D-arabinopyranoside (**6**)

1,3-Dihydroxypropan-2-yl α -D-arabinopyranoside (**6**) was synthesised following informal discussions with delegates at the 2015 European Conference on Marine Natural Products (Strathclyde, Scotland). These had suggested that there was a new prymnesin toxin decorated with D-arabinose. However, since synthesising this compounds the delegates have published their work, where prymnesin-2 is drawn as being glycosylated with D-arabinofuranose at C77,² rather than L-xylofuranose as had been previously reported.^{1,3}



Scheme 4.6 – The chemical synthesis of 1,3-dihydroxypropan-2-yl α -D-arabinopyranoside (**6**). i) I_2 , Ac_2O . ii) 33% v/v HBr/AcOH, DCM. iii) AgOTf, DCE. iv) H_2 , 10% Pd/C, MeOH. v) Na, MeOH. * Based on total mass recovered.

D-Arabinose was acetylated using acetic anhydride and iodine as a Lewis acid catalyst.²¹ The acetylation resulted in mainly the desired pyranose ring configuration (**22**), with about 10% acetylated furanose seen by NMR. This was found to give much better control of the ring size than using acetic anhydride in pyridine, as was described earlier with L-arabinose. Because of the problems experienced earlier with the removal of benzoyl protecting groups

which led to the formation of benzoic acid, it was decided to try and continue with a mixture of per-*O*-acetyl α -arabinoses (**22**). The sugar bromide (**23**) was synthesised from (**22**) using 33% HBr/AcOH, and was subsequently used as the glycosyl donor for the silver triflate promoted glycosylation of 1,3-di-*O*-benzyl glycerol (**13**). The glycosylation was very low yielding, possibly due to orthoester formation due to the 1,2-*trans* configuration of the anomeric bromide and neighbouring acetate group, as well as additional furanose products in the crude mixture. However enough compound was isolated for use in the next steps, with the stereochemistry of the isolated compound being confirmed as 1,2-*trans* (α -anomer) (**25**) by ^1H NMR; the H-1' signal at 4.69 ppm was a doublet with a $J_{1',2'}$ coupling value of 6.9 Hz. Removal of the benzyl ether protecting groups by hydrogenation over a Pd/C catalyst was deliberately performed before deacetylation. This was because the hydrogenation step of other glyceryl glycoside compounds in this series had given very low yields. Informal discussions with a delegate at the 'Carbohydrate Active Enzymes in Industrial Biotechnological Applications' conference in St Andrews (August 2015), had revealed she too was having problems with the recovery of similar sugar glycerol compounds from the palladium catalyst after hydrogenation. By leaving the acetate groups *in situ* on the sugar, it was hoped the increased lipophilicity of the compound would make it easier to wash (desorb) (**25**) from the surface of the Pd/C catalyst. This gave (**25**) with 75% yield, which was the joint highest yield for any hydrogenation in this series. The acetate groups were removed by methoxide-catalysed transesterification to give 1,3-dihydroxypropan-2-yl α - D -arabinopyranoside (**6**). The 1,2-*trans* orientation of the anomeric linkage in (**6**) was confirmed by ^1H NMR, with the H-1' signal at 4.35 ppm present as a doublet with a $J_{1',2'}$ coupling value of 7.5 Hz. Whilst there was not as much overlap of signals in the ^1H NMR spectrum as with some of the other glyceryl glycoside fragments, a combination of COSY and multiplicity information from the HSQCed spectrum allowed the full assignment of the ^{13}C NMR peaks, as well as more precise information about in which regions of the ^1H NMR spectrum multiplets the individual proton signals were located (Appendices, Figure 6.3).

4.2.3 Synthesis of 1,2-*cis* furanosyl glyceryl glycoside fragments

Synthesis of 1,2-*cis* furanoses can prove challenging as it can be difficult to control the stereochemistry at the anomeric centre. It was important to use non-participating protecting groups for the glycosylation steps to minimise the formation of 1,2-*trans* glycosylation products.^{22,23} The same general methodology was used for the glycosylation

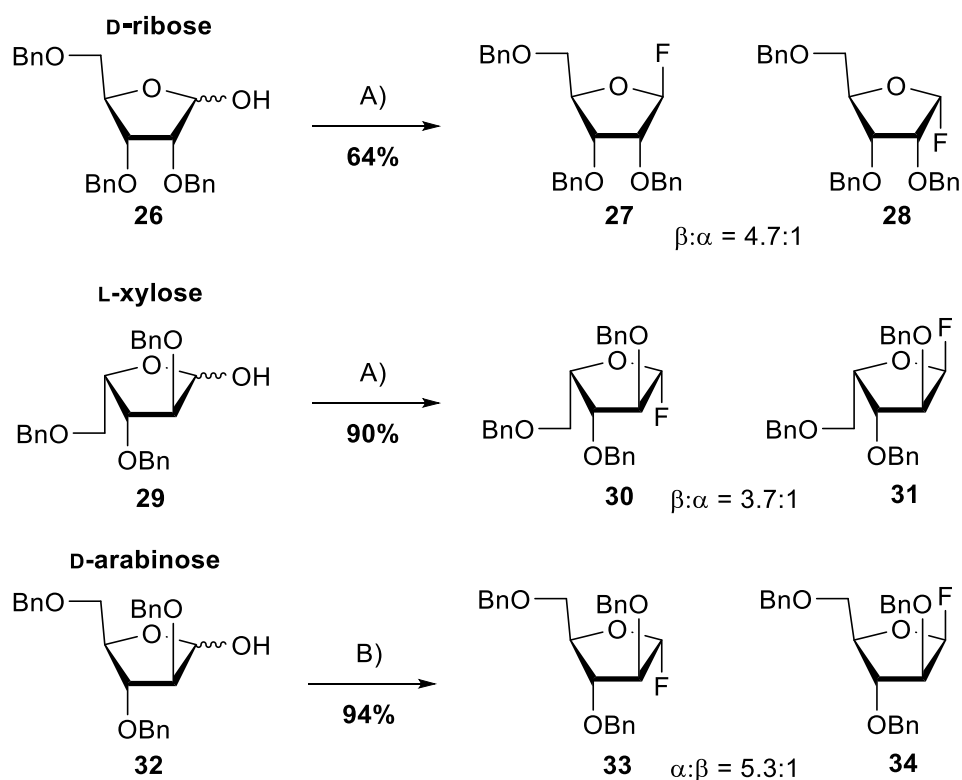
step to synthesise α -D-ribofuranoside (**3**), α -L-xylofuranoside (**4**) and β -D-arabinofuranoside (**5**) fragments. The first two sugars are reported as decorating the backbone of prymnesin-1 and prymnesin-2, respectively.¹ A recent paper by Rasmussen et al.² draws the structure of prymnesin-2 as being decorated with the third sugar, α -D-arabinofuranose instead of β -L-xylofuranose.

4.2.3.1 Synthesis of fluoro furanoside sugar donors

Work by Shoda et al.²² showed that the SnCl₂-promoted glycosylation of a range of alcohols with 1,2-*trans* glycosyl fluorides gave good stereoselectivity for 1,2-*cis* glycosides.²² Furthermore, it was found that with ribofuranosides, both yield and stereoselectivity could be improved with the addition of trityl perchlorate.²² Before exploring this methodology it was first necessary to synthesise the corresponding glycosyl fluoride donors.

All three 2,3,5-tri-*O*-benzyl glycosylfuranoside hemi-acetals (D-ribofuranose (**26**), L-xylofuranose (**29**) and D-arabinofuranose (**32**)) necessary for the library of prymnesin toxin fragments are commercially available from Carbosynth (UK). Both Lartey et al.²⁴ and Haines et al.²⁵ simultaneously published methodology showing that anomeric hydroxyl groups could be conveniently replaced with fluorine using the mild fluorinating reagent diethylaminosulfur trifluoride (DAST) (Scheme 4.7).

Haines et al.²⁵ in particular explored solvent effects on DAST fluorination of anomeric hydroxyl groups. They found that a polar solvent such as THF gave the best stereoselectivity for β -fluorides with D-sugars. As it is reported to be desirable to have the 1,2-*trans* fluoride for glycosylation, this meant that in each case the β -fluoride would be the target compound.²²



Scheme 4.7 - Fluorination of the 2,3,5-tri-*O*-benzyl glycosyl fluorides using DAST.^{24,25} A) DAST, THF, 0 °C to r.t., 20 minutes. B) DAST, DCM, r.t., 20 minutes. Note: yield refer to the total α/β mixture recovered.

The synthesis of 2,3,5-tri-*O*- β -D-ribofuranosyl fluoride (**27**) was performed following the literature protocol.^{24,25} Comparison of the ¹H NMR with literature values showed the 1,2-*trans* β -fluoride (**27**) was the major anomer, with ¹H NMR showing the H-1 signal as a doublet at 5.67 ppm with $J_{1,F}$ coupling value of 63.3 Hz and no observed $J_{1,2}$ coupling. By comparison the ¹H NMR H-1 signal for the 1,2-*cis* α -fluoride (**28**) showed an H-1 signal as a doublet of doublet with a similar $J_{1,F}$ coupling value of 65.8 Hz and also a $J_{1,2}$ coupling value of 3.4 Hz. ¹⁹F NMR was also found to be very useful in identifying and characterising the two anomers, with the α -ribosyl fluoride having a F-1 signal as a doublet of doublet at -131.7 ppm with $J_{1,F}$ and $J_{2,F}$ splitting; the β -ribosyl fluoride having a F-1 signal as a doublet of multiplet at -115.3 ppm.

2,3,5-Tri-*O*- β -L-xylofuranosyl fluoride (**30**) was synthesised using the same DAST fluorination methodology as for the ribosyl fluoride (**27**). The anomers were inseparable by normal phase chromatography. It was however still possible to characterise the two anomers in the mixture by ¹H, ¹³C and ¹⁹F NMR. The anomers were readily distinguished by the coupling

constants of the H-1 signals. The 1,2-*cis* α -fluoride (**31**) H-1 signal appeared as a doublet of doublets with both $J_{1,F}$ coupling and also a $J_{1,2}$ coupling value of 3.5 Hz. The 1,2-*trans* β -fluoride (**30**) H-1 signal however appeared as doublet, with only $J_{1,F}$ coupling be observed. ^{19}F NMR (Figure 4.7) showed the β anomer (**30**) had large $J_{2,F}$ coupling value of 18.9 Hz, whilst the α anomer (**31**) had a much smaller $J_{2,F}$ coupling value of 6.8 Hz, but also exhibited $J_{4,F}$ coupling of 6.8 Hz.

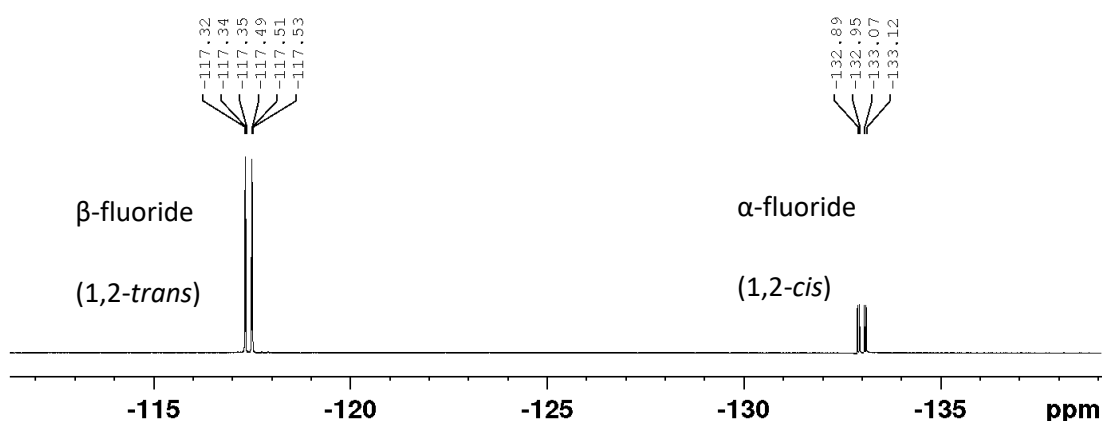


Figure 4.7 - ^{19}F NMR spectrum of 2,3,5-tri-*O*-benzyl- β/α -L-xylofuranosyl fluorides (**30,31**)

Interestingly, ^{13}C NMR also showed $\text{C}_{4\alpha,F}$ coupling whilst there was no coupling between fluorine and the C4 carbon for the β -fluoride (**30**) (Figure 4.8).

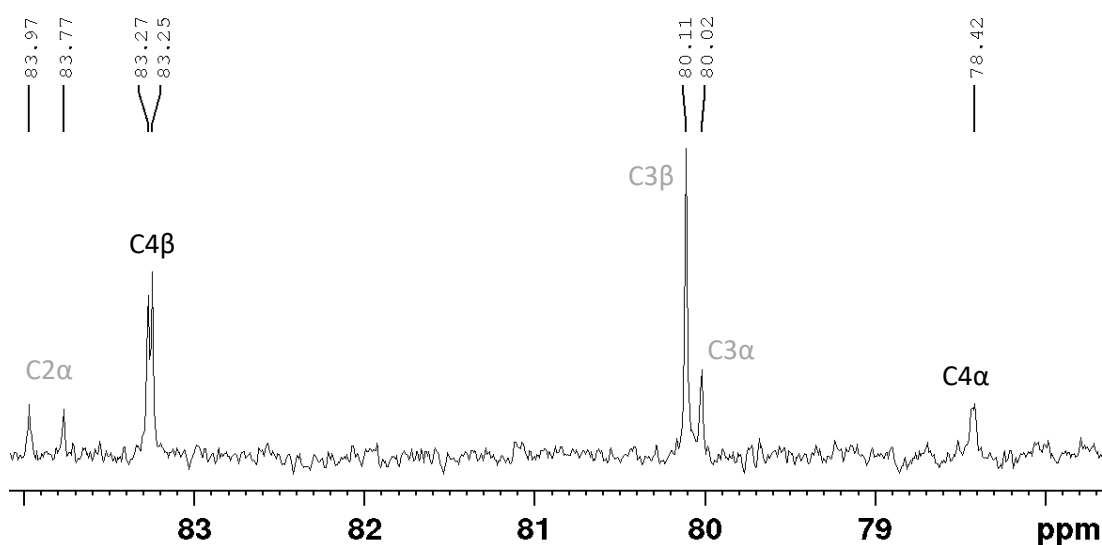
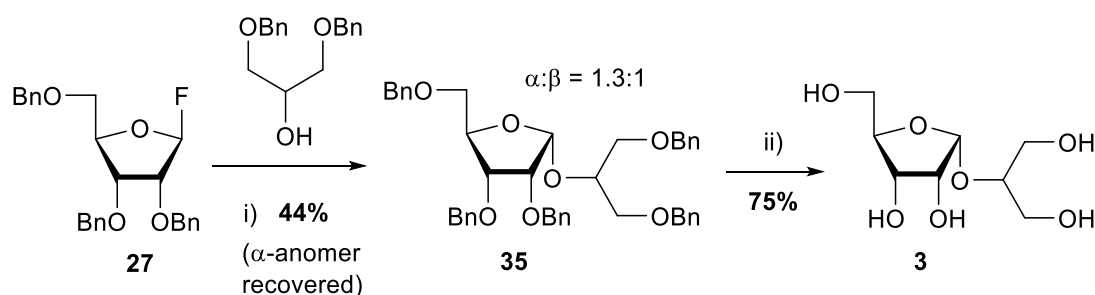


Figure 4.8 - ^{13}C NMR spectrum for the mixture of 2,3,5-tri-*O*-benzyl- β/α -L-xylofuranosyl fluoride (**30,31**) highlighting the difference in carbon-fluorine coupling at the C4 position between the two anomers.

Finally, 2,3,5-tri-*O*- β -D-arabinofuranosyl fluoride (**33**) was considered. DAST fluorination worked well, and the ratio of α/β fluoride was judged to be 5.3:1 by integration of the H-1 NMR signals. The 1,2-*trans* α -fluoride (**33**) gave an H-1 signal at 5.78 ppm as a doublet with a $J_{1,F}$ coupling value of 61.6 Hz and no observed $J_{1,2}$ coupling; the 1,2-*cis* β -fluoride (**34**) was identified by an H-1 signal at 5.62 ppm as a doublet of doublets with a $J_{1,2}$ coupling value of 3.5 Hz. Although the anomers separated on a TLC plate they were not separated for the following glycosylation step.

4.2.3.2 1,3-Dihydroxypropan-2-yl α -D-ribofuranoside (**3**)

1,2-*cis* Selective glycosylation of 1,3-di-*O*-benzyl glycerol (**13**) was performed using 2,3,5-tri-*O*-benzyl- β -D-ribofuranosyl fluoride (**27**) as the donor (Scheme 4.8). SnCl_2 was used as a promotor due to the high affinity of the tin-fluorine bond, and trityl perchlorate was also used as a Lewis acid additive to try to increase 1,2-*cis* selectivity.²² It was found however that for this glycosylation trityl perchlorate made a negligible difference to the stereochemical outcome of glycosylation, with an α/β ratio of 1.3:1 as judged by integration of the ^1H NMR H-1' signals.



Scheme 4.8 – The chemical synthesis of 1,3-dihydroxypropan-2-yl α -D-ribofuranoside. (**3**) i) SnCl_2 , $\text{Ph}_3\text{C}^+\text{ClO}_4^-$, Et_2O . ii) H_2 , 10% Pd/C, MeOH/EtOH (5:1)

The stereochemistry of the glycosidic linkages was determined by comparison with literature NMR values of ribofuranosides, with α -ribosides having $J_{1,2}$ couplings of 3-5 Hz and C-1' values of 96-102 ppm; β -ribosides having $J_{1,2}$ couplings of 0-2.8 Hz and C-1' values of 100-107 ppm.²² In the case of a mixture of ribofuranoside anomers, HSQC NMR along with ^1H NMR J

couplings can be an expedient way to quickly determine which isomer is which, as shown in Figure 4.9.

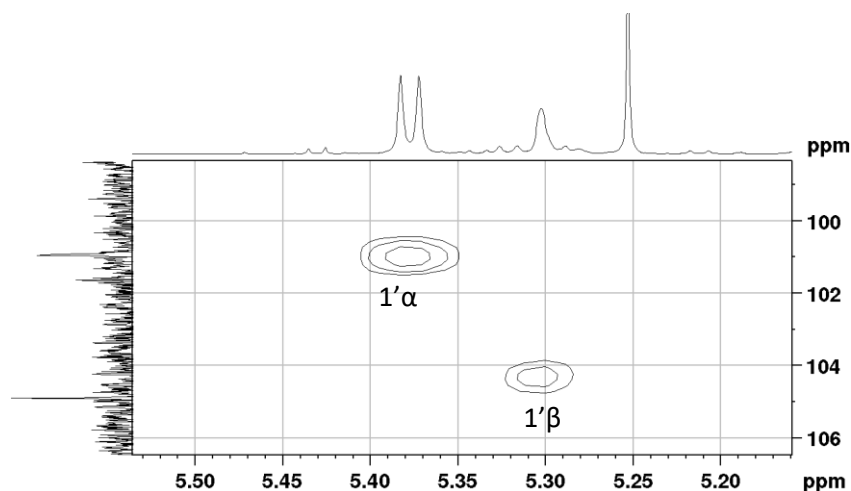
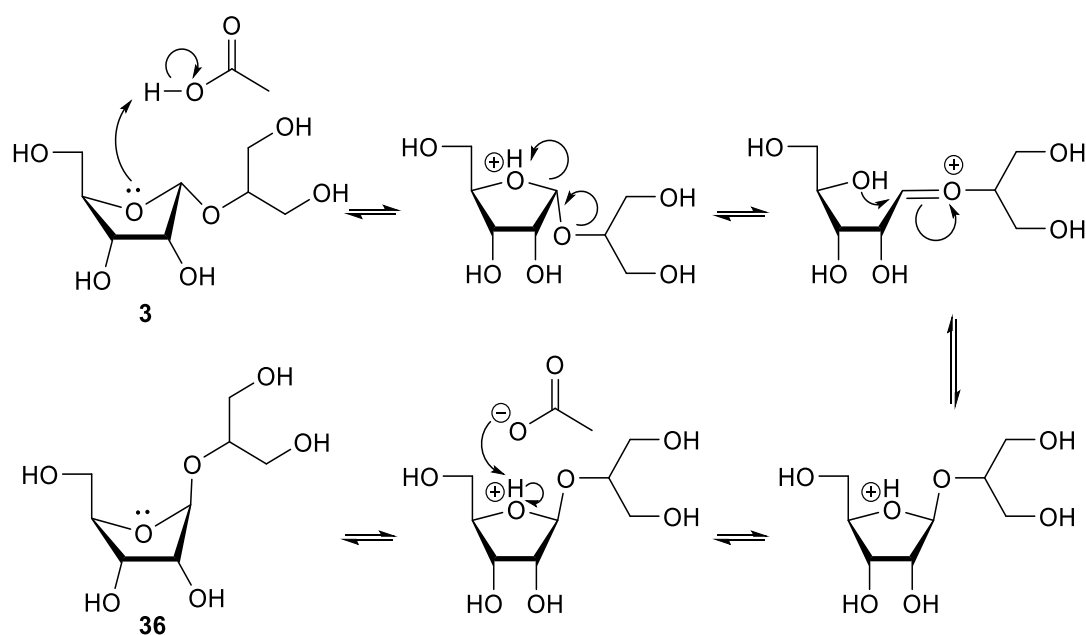


Figure 4.9 - HSQCed NMR spectrum of a crude mixture containing 1,3-bis(benzyloxy)propan-2-yl 2,3,5-tri-*O*-benzyl- α/β -D-ribofuranosides (**3,36**)

1,3-Bis(benzyloxy)propan-2-yl 2,3,5-tri-*O*-benzyl- α -D-ribofuranoside (**35**) was isolated by normal phase chromatography and the 1,2-*cis* stereochemistry at the α -anomeric position confirmed by the H-1' signal at 5.38 ppm as a doublet with a $J_{1,2}$ coupling value of 4.3 Hz. Further confirmation of the anomeric stereochemistry was obtained by running a NOESY NMR which showed long range interactions between the H-1' α , H-2' α and H-3' α protons, but no long-range nOe interactions for the H-1' β proton. By contrast the 1,2-*trans* β -anomer showed a H-1' signal in the ^1H NMR at 5.30 ppm as a singlet; the ^{13}C NMR showed a C1' signal at 104.9 ppm.

The benzyl ether protecting groups were removed by hydrogenation of (**35**) over a Pd/C catalyst in AcOH. The H-1' signal after hydrogenation appeared as a singlet at 5.07 ppm and the C-1' signal at 106.5 ppm. These signals were characteristic of a 1,2-*trans* furanose (**36**), which suggested that anomerisation had occurred during the hydrogenation.²² Acetic acid had been used as the solvent as it is able to dissolve both the protected and deprotected products. However this may have caused acid catalysed anomerisation via the pathway shown in Scheme 4.9.⁴ Kennedy et al.⁴ have shown that protonation of the ring oxygen leads to structural changes in the furanose ring, one of which is a significant change in the length of the C1-O5 bond which breaks during ring opening. The energy barriers between conformers of furanose rings are much smaller than those for pyranoses. Therefore

protonation of the ring oxygen in furanoses is able to bring about larger conformational changes than might be the case with pyranoses. The authors explained that protonation of the ring oxygen “enhances ring-opening by inducing structural changes in the furanose ring that move the reactant closer to the transition states” than the original reactants.⁴ As the mechanism of inversion at the anomeric position is at equilibrium it would make sense that the equilibrium lies in favour of the thermodynamic product. Dubois et al.²⁶ have suggested that this may be due to the flexibility in furanose rings allows the best overlap of the endo oxygen lone pair and the C1-O1 σ^* orbital when the anomeric substituent is in the axial position.



Scheme 4.9 – A proposed mechanism for the inversion of stereochemistry at the anomeric position under acidic conditions; protonation of the ring oxygen lengthens the C1-O5 bond and brings about a conformation change in the furanose ring that brings the reactant state closer to the transition states.⁴

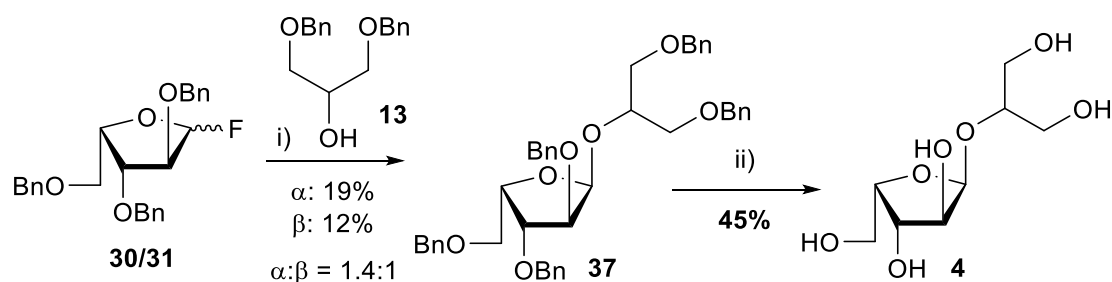
The hydrogenation was repeated in a mixture of MeOH/EtOH (5:1) to give 1,3-dihydroxypropan-2-yl α -D-ribofuranoside (**3**). Following reports by Filippov et al.²⁷ we were keen to check that hydrogenation had not caused an intramolecular side reaction forming anhydro ribfuranose and glycerol. Fortunately, there was no NMR or mass spectrometry evidence for this happening.

The ¹H NMR signals of **3** were not particularly well resolved after deprotection, but the HSQCed NMR (Appendices, Figure 6.4) gave much more information, and coupled with COSY

NMR it was possible to fully assign the ^{13}C NMR spectrum as well as gain more insight about which regions of the ^1H NMR correlated with which protons on the compound.

4.2.3.3 1,3-Dihydroxypropan-2-yl α -L-xylofuranoside (**4**)

1,3-Bis(benzyloxy)propan-2-yl 2,3,5-tri-*O*-benzyl- α -L-xylofuranoside (**37**) was synthesised by using 2,3,5-tri-*O*- α,β -D-xylofuranosyl fluoride (**30/31**) to glycosylate 1,3-di-*O*-benzyl glycerol (**13**) (Scheme 4.10). Glycosylation was promoted using SnCl_2 and gave a mixture of α/β 1.0 : 0.8. The mixture of anomers proved to be challenging to separate but after several rounds of FCC there was enough of each anomer isolated for full characterisation. The anomers were identified by ^{13}C and ^1H NMR, with the 1,2-*cis* α -anomer (**37**) giving an H-1' signal at 5.35 ppm as a characteristic doublet showing a $J_{1',2'}$ coupling value of 4.3 ppm; by contrast the 1,2-*trans* β -anomer gave an H-1' signal at 5.31 ppm with a lower $J_{1',2'}$ coupling value of 1.9 Hz. As expected the 1,2-*cis* anomer (**37**) gave a lower C-1' shift at 99.9 ppm compared with the higher 1,2-*trans* C-1' shift at 107.1 ppm.²²



Scheme 4.10 – The chemical synthesis of 1,3-dihydroxypropan-2-yl α -L-xylofuranoside (**4**). i) SnCl_2 , Et_2O . ii) H_2 , $\text{Pd}(\text{OH})_2/\text{C}$, MeOH/EtOAc (9:1).

The desired 1,2-*cis* α -anomer (**37**) was debenzylated by hydrogenation but this time over a 20% $\text{Pd}(\text{OH})_2/\text{C}$ catalyst to try and avoid isomerisation at the anomeric position as seen with ribose, to give 1,3-dihydroxypropan-2-yl- α -L-xylofuranoside (**4**). The 1,2-*cis* stereochemistry of the deprotected compound gave an anomeric H-1' signal at 5.09 ppm as a characteristic doublet with a $J_{1',2'}$ coupling value of 4.4 Hz and a C1' signal at 101.3 ppm. There was an overlap of the H-2a,2b and H-5' signals in the ^1H NMR, but by using HSQCed (Appendices, Figure 6.5) and COSY spectra it was possible to assign all peaks in the ^{13}C NMR. As further confirmation of the stereochemistry at the anomeric position a NOSEY NMR spectrum was

recorded which showed long range coupling between H-1' and H-2' & H-5' but *not* between H-3' & H-4' (Figure 4.10).

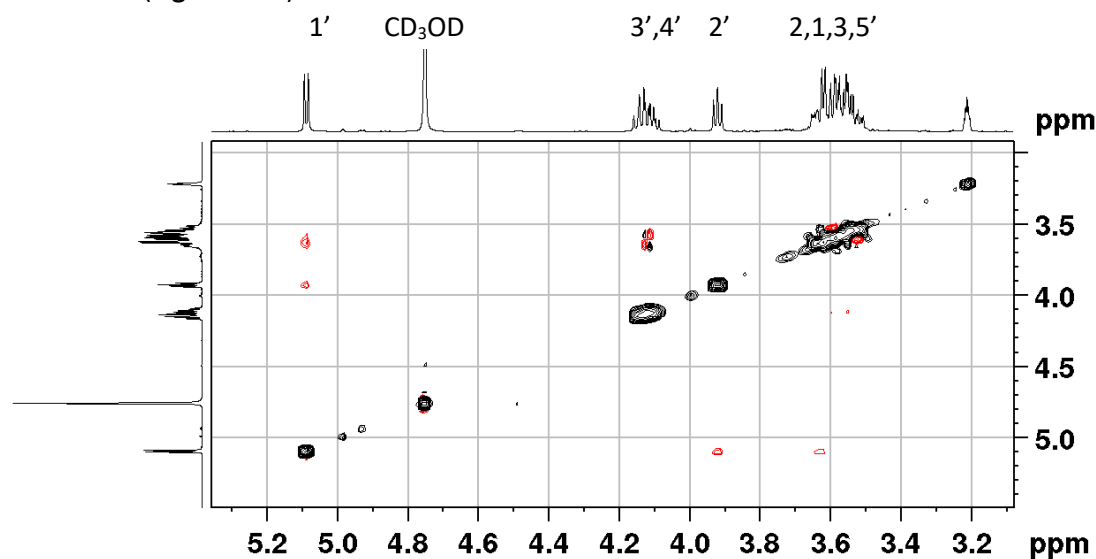
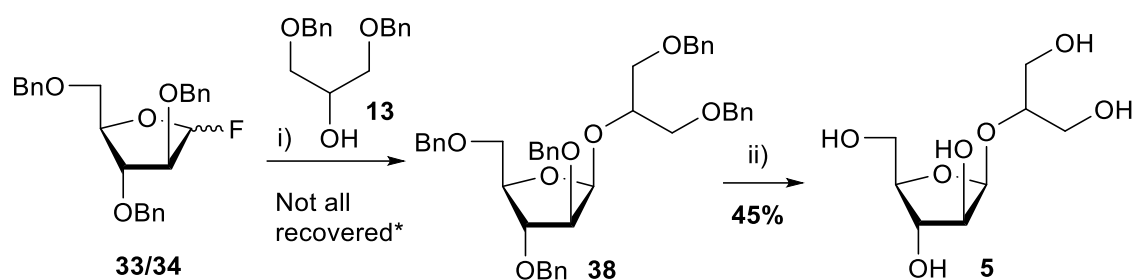


Figure 4.10 – NOESY 2D NMR spectrum of 1,3-dihydroxypropan-2-yl α -L-xylofuranoside (**5**). The cross-peaks (1',2') and (1',5'), reinforced by the lack of a cross-peak (1',3') or (1',4') confirm the 1,2-*cis* stereochemistry at the anomeric position.

4.2.3.4 1,3-Dihydroxypropan-2-yl β -D-arabinofuranoside (**5**)

2,3,5-Tri-*O*-benzyl- α,β D-arabinofuranosyl fluoride (**33/34**) was used as a glycosyl fluoride donor to glycosylate 1,3-di-*O*-benzyl glycerol (**13**), using SnCl₂ was used as a promotor. Shoda et al.²² included an example in their paper 'Stereoselective synthesis of 1,2-*cis*-glycofuranosides using glycofuranosyl fluorides' using 2,3,5-tri-*O*-benzyl-L-arabinofuranosyl fluoride as an example, and showed that they obtained very good 1,2-*cis* selectivity without the addition of trityl perchlorate. It was therefore decided to try the glycosylation without trityl perchlorate, which gave a α/β ratio of 1:2.2 as judged by integration of the H-1' NMR signals. The 1,2-*cis* β -anomer (**38**) was identified by the C-1' signal at 100.8 ppm and the H-1' signal at 5.32 ppm as a characteristic doublet with a $J_{1',2'}$ coupling value of 4.4 Hz. By contrast the 1,2-*trans* α -anomer gave a higher C-1' signal at 106.1 ppm and the H-1' signal at 4.08 ppm as a broad singlet. The anomers had very similar R_f values and so several rounds of FCC were required to separate enough of each for characterisation from the crude glycosylation mixture. The desired 1,2-*cis* β -anomer was subject to debenylation by hydrogenation over Pd/C catalyst to give 1,3-dihydroxypropan-2-yl β -D-arabinofuranoside (**5**).



Scheme 4.11 – The chemical synthesis of 1,3-dihydroxypropan-2-yl β-D-arabinofuranoside (**5**). i) SnCl₂, Et₂O. ii) H₂, 10% Pd/C, MeOH:EtOAc (9:1). * Note due to the difficulty in separating the anomers, once a useable amount of (**38**) had been isolated (560 mg, 37%) no further rounds of FCC purification were performed. Therefore, not all material was recovered and so a yield is not given.

As expected, there was a lot of overlap of proton signals in the ¹H NMR, and as such the HSQCed NMR spectrum (Appendices, Figure 6.6) is much more informative, and by combining the HSQCed with COSY NMR it was possible to completely assign the ¹³C NMR spectrum.

A NOESY NMR spectrum was also run (Figure 4.11) which showed long range coupling between H-1' and H-2' & H-4' but *not* between H-1' and H-3', which confirmed the presence of the 1,2-*cis* isomer.

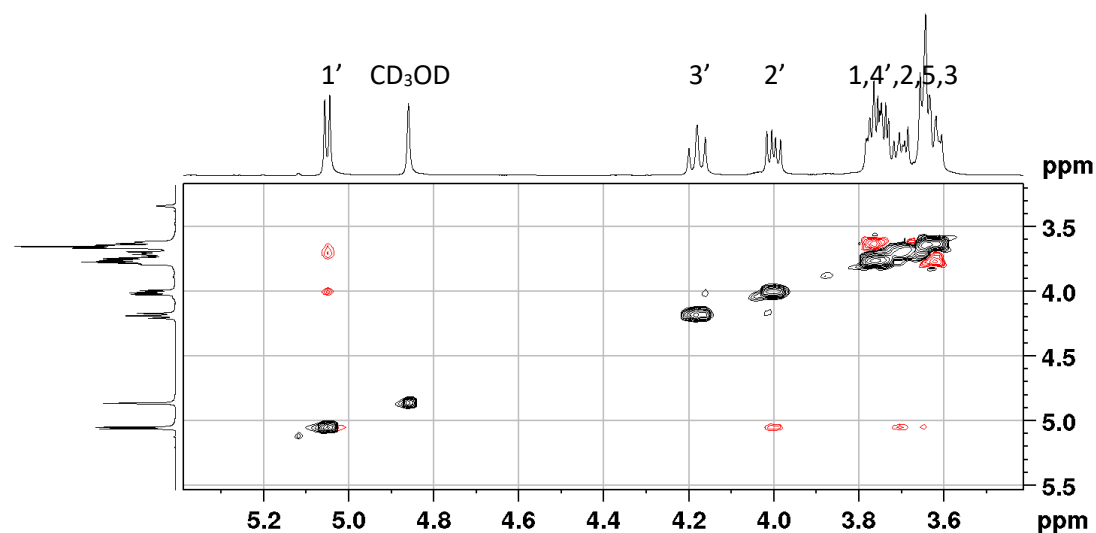
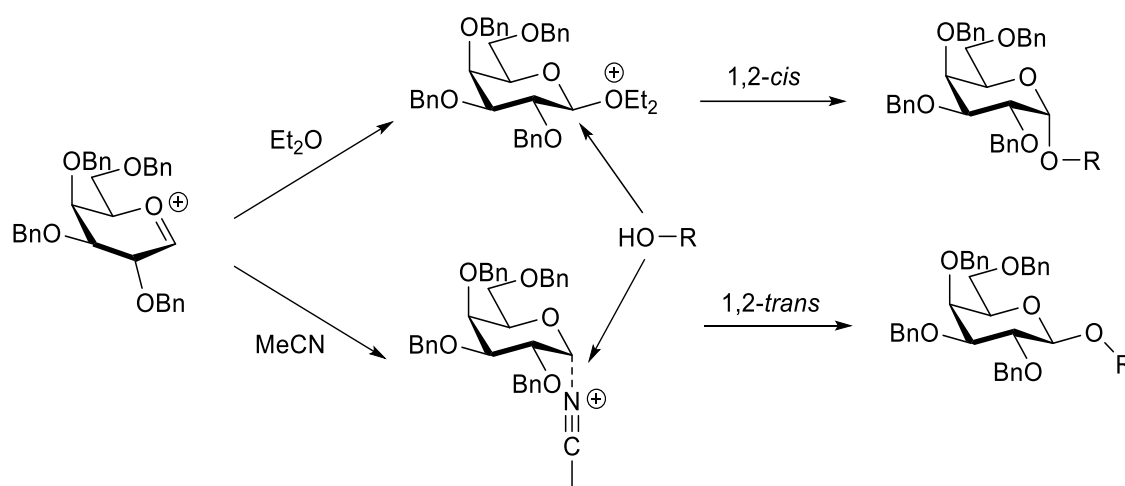


Figure 4.11 - NOESY 2D NMR spectrum of 1,3-dihydroxypropan-2-yl β-D-arabinofuranoside (**5**). The cross-peaks (1',2') and (1',4'), reinforced by the lack of a cross-peak (1',3') confirm the stereochemistry as 1,2-*cis* (β-D-arabinofuranoside)

4.2.4 Synthesis of 1,2-*cis* glyceryl pyranoside fragments

Ethereal solvents have been shown to promote 1,2-*cis* axial glycosylation, with diethyl ether giving predominantly (but not exclusively) the equatorial intermediate as shown in Scheme 4.12.²⁸ By contrast, acetonitrile forms a nitrilium intermediate species which due to stabilisation by the anomeric effect sits in exclusively the axial position; this leads to exclusively top side attack of the sugar.²⁸



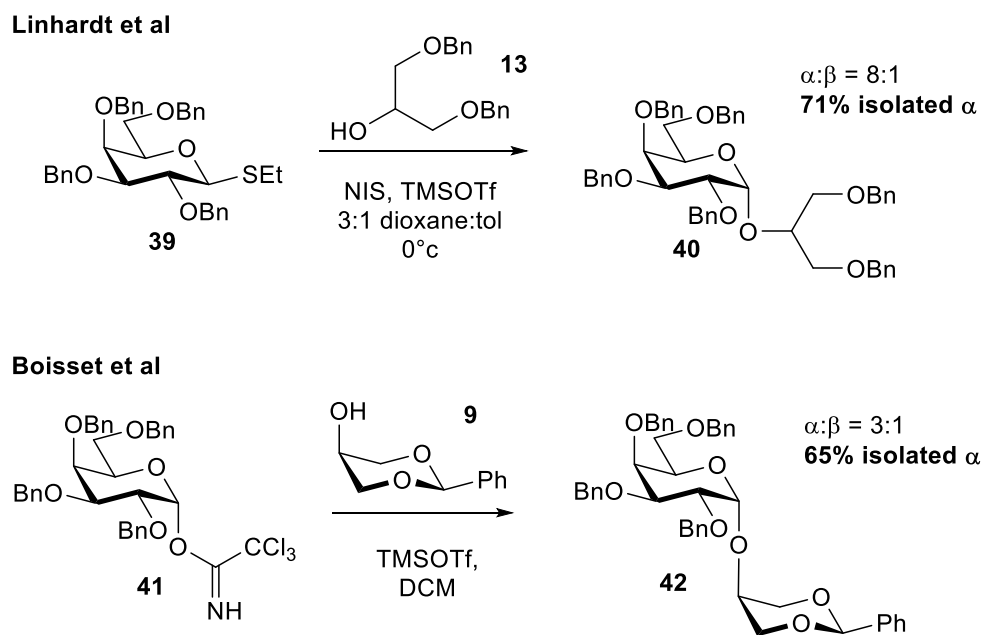
Scheme 4.12 – Solvent effect on glycosylation using pyranoses with non-participating protecting groups. Ethereal solvents sit equatorial to the intermediate directing attack from the bottom face of the sugar, whilst acetonitrile forms a 1,2-*cis* nitrilium species which directs attack from the top face.²⁸

1,3-Dihydroxypropan-2-yl α -D-galactopyranoside (**7**)

The newly reported toxin prymnesin-B1 has been shown to be glycosylated with α -D-galactopyranose.² Although published recently, it was decided prudent to synthesise a glycerol inspired toxin fragment to add to the library of glyceryl glycoside compounds. The synthesis of 1,3-dihydroxypropan-2-yl α -D-galactopyranoside (**7**) has been reported in two previous papers, and is better known as fluoridoside.^{7,9}

The key literature glycosylation steps are shown in Scheme 4.13, where Linhardt et al.⁹ choose to use a thioglycoside donor (**39**) which afforded them good stereochemical control at the anomeric position, especially when employing a mixture of dioxane and toluene as solvents. By contrast Boisset et al.⁸ used a glycosyl imidate (**41**) as the sugar donor and *cis*-1,3-benzylidenglycerol (**9**) as the acceptor (Scheme 4.13). However, we have experienced

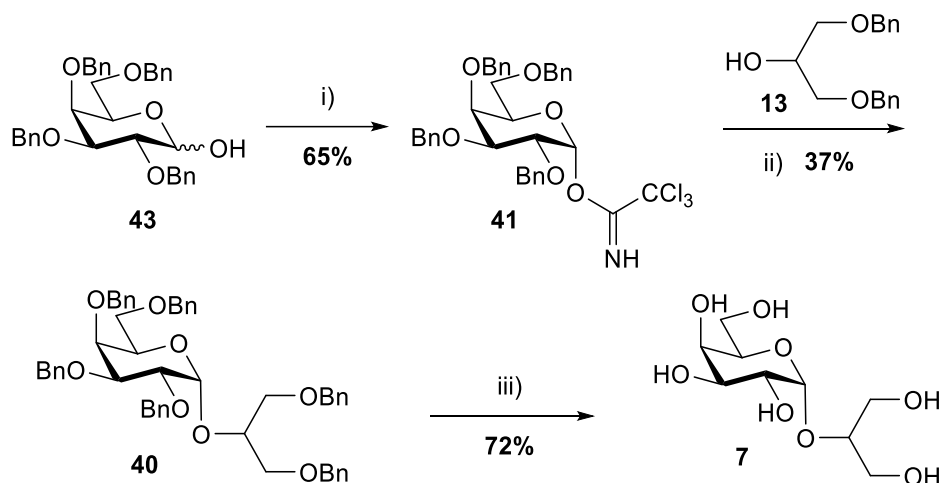
problems using **(9)** in other glycosylations (see 4.2.1), which were attributed to the low reactivity of the axial OH group. We therefore decided to try using an amalgamation of both glycosylations, using 1,3-di-*O*-benzyl glycerol (**13**) as the acceptor and **41** as the donor to try and improve on the stereocontrol at the anomeric position.



Scheme 4.13 – A comparison of the published literature glycosylation steps in the synthesis of floridoside. Linhardt et al.⁹ relied on a thiol donor with NIS/TMSOTf promoted glycosylation which gave much better stereocontrol than Boisset et al.⁸ who employed an imidate glycosyl donor with TMSOTf promoted glycosylation of *cis*-1,3-*O*-benzylidene glycerol (**13**).

In keeping with previous methodology in this work, 1,3-dibenzyl glycerol (**13**) was used as the acceptor. This would allow access to the target compound in a single deprotection step (Scheme 4.14). Tetra-*O*-benzyl- α -D-galactopyranosyl trichloroacetimidate (**41**) was selected as the glycosyl donor, and the glycosylation promoted with TMSOTf.²⁹ A mixture of toluene and diethyl ether was selected as the solvent system. The yield was low, probably due to moisture in the solvents but the stereocontrol was excellent and the 1,2-*cis* α anomer (**40**) was easily separated from the crude reaction mixture, with the H-1' anomeric signal at 4.11 ppm having a slightly high $J_{1',2'}$ coupling value of 5.2 Hz, which might be attributed to some distortion of the sugar ring by the large benzyl ether protecting groups on the molecule. Debenzylation was carried out in a single step by hydrogenation over a Pd/C catalyst to give 1,3-dihydroxypropan-2-yl α -D-galactopyranoside (**7**), which without the benzyl protecting

groups gave an H-1' signal at 5.02 ppm with a $J_{1,2'}$ coupling value of 3.8 Hz which is reasonable for a 1,2-*cis* orientated glycosidic bond. Both the ^1H and ^{13}C NMR were in agreement with the published literature values.^{8,9}



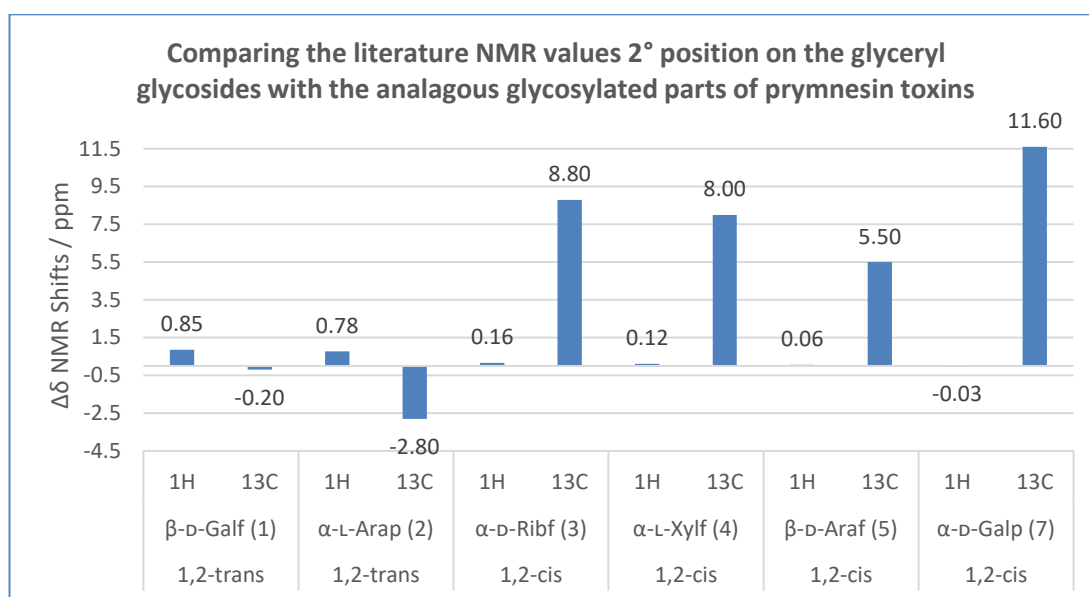
Scheme 4.14 – The chemical synthesis of 1,3-dihydroxypropan-2-yl α-D-galactopyranoside (**7**). i) CCl₃CN, DBU, DCM, 0 °C to r.t. ii) TMSOTf, toluene/Et₂O (4:1), 0 °C to r.t. iii) H₂, 10% Pd/C, MeOH.

4.3 Comparison of synthetic glyceryl glycoside fragments with literature toxin NMR values

The ^1H and ^{13}C NMR values for the 2° position on glycerol (H-2 and C2) for the glycosylated fragments were compared with literature values for the corresponding signals from the prymnesins (Chart 4.1, Table 2 Supporting Information). For the synthetic glyceryl glycoside fragments, in many cases the H-2 signal was part of a larger multiplet of peaks in the 1D ^1H NMR spectrum, and so a more accurate H-2 shift was extracted from the HSQCed spectrum instead. For PRM-1 and PRM-2, the literature NMR values were obtained using a mixture of CD₃OD/C₅D₅N 1:1, with the machine locked onto d₄-methanol as the reference solvent.¹ It is immediately obvious that there are large differences in the literature and the synthetic glyceryl glycoside fragment ^{13}C NMR values for α-L-Xylf (**4**) and α-D-Ribf (**3**). Interestingly these are both 1,2-*cis* anomeric linkages to the backbone. By comparison the difference between the ^{13}C NMR values of the toxin backbone and analogous 2° position on the glyceryl glycoside fragments for α-L-Arap (**2**) and β-D-Galf (**1**) is much smaller. These two species have a 1,2-*trans* configuration with regards to the anomeric position. Regarding the new carbohydrate assignment of β-D-Araf on PRM-2 by Rasmussen *et al.*² the ^1H and ^{13}C NMR shifts for our synthetic β-D-Araf (**6**) and α-L-Xylf (**4**) glycerol fragment (**6**) were compared with the literature NMR shifts for the carbohydrate on PRM-2. It was noted that the NMR shifts

for our synthetic β -D-Araf glycerol fragment (**6**) were closer to the literature NMR shifts for the carbohydrate in PRM-2 than for the α -L-Xylf glycerol fragment (**4**). However, there is still a large difference between the 2° position on glycerol (H-2 and C2) and H-77/C77 values for PRM-2 when compared to either fragment (**6**) or fragment (**4**).

Chart 4.1 - Comparing the literature NMR values 2° position on the glyceryl glycosides with the analogous glycosylated parts of prymnesin toxins. Raw data and solvent conditions are shown in Appendices, Table 6.2.



4.4 Summary

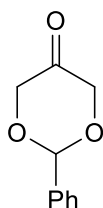
A library of glyceryl glycoside fragments inspired by the published prymnesin toxins has been synthesised. The 1,2-*trans* glyceryl pyranoside fragments (α -L-Arap (**2**), α -D-Arap (**6**)) were synthesised using Koenigs-Knorr methodology, with excellent stereocontrol at the anomeric position.¹² The 1,2-*trans* glyceryl furanoside fragment (β -D-Galf (**1**)) was synthesised using SnCl₄ promoted glycosylation, again with excellent stereocontrol. 1,2-*cis* Glyceryl furanoside fragments (α -D-Ribf (**3**), α -L-Xylf (**4**), β -D-Araf (**5**)) were synthesised from the corresponding glycofuranosyl fluoride donor, with moderate stereoselectivity. By contrast the 1,2-*cis* glyceryl pyranoside fragment (α -D-Galp (**7**)) was synthesised from the corresponding glycosyl imidate with excellent stereocontrol, which may be attributed to the anomeric effect leading to formation of the thermodynamic product. Removal of ester protecting groups was relatively straight forward, and in the case of benzoyl protecting groups any benzoic acid by-

product from hydrolysis was easily removed using Dowex® 1X2-400 hydroxide form anion exchange resin. Removal of benzyl groups by hydrogenation was problematical; in the case of 1,3-bis(benzyloxy)propan-2-yl 2,3,5-tri-*O*-benzyl- α -D-ribofuranoside (**3**) a change of solvent was required to prevent isomerisation at the anomeric position. Some hydrogenation yields were also low, albeit with no by-products seen by NMR or mass spectrometry, which suggested particularly strong adsorption of the deprotected compounds onto the hydrogenation catalyst.

Comparison of the ^{13}C and ^1H NMR shifts between the synthetic glyceryl glycoside fragments and the carbohydrate NMR shifts reported by Igarashi *et al.*^{1,3} showed that the synthetic fragments with a 1,2-*trans* configuration with respect to the anomeric position had NMR shifts that were much closer to those reported for carbohydrates on the prymnesin toxins. By contrast, fragments with a 1,2-*cis* orientation with respect to the anomeric position deviated in their NMR chemical shifts at the anomeric position when compared with the values published by Igarashi *et al.*¹ It was also noted that some ambiguity about the carbohydrate present on PRM-2 had been caused by Rasmussen *et al.*² who had drawn the toxin as being glycosylated with β -D-Araf, rather than α -L-Xylf as reported by Igarashi *et al.*³ Comparison of the anomeric chemical shifts for the anomeric positions of the glyceryl glycoside fragments β -D-Araf (**6**) and α -L-Xylf (**4**) were compared with the published shifts for the carbohydrate on PRM-2 by Igarashi *et al.*¹ and it was found that the literature chemical shifts were closer to those of the β -D-Araf glyceryl glycoside fragment (**6**).

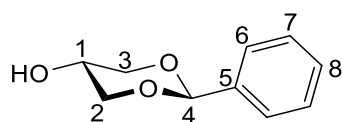
4.5 Experimental

2-Phenyl-1,3-dioxan-5-one (**10**)¹⁵



cis-1,3-*O*-Benzylidene glycerol (600 mg, 3.3 mmol) and Dess-Martin periodinane (2.1 g, 5.0 mmol) were dissolved into DCM (50 mL) and stirred overnight at room temperature. TLC (hexane/EtOAc 1:1) showed complete consumption of the alcohol and the reaction mixture was quenched with a mixture of aqueous Na₂S₂O₅/NaHCO₃ solution (1:1, 40 mL). The organic layer was separated and the aqueous layer was washed with Et₂O (3 × 20 mL). The organic layers were combined and dried over MgSO₄, before being filtered and dried *in vacuo* to give 2-phenyl-1,3-dioxan-5-one (**10**) (580 mg, 98%) as a yellow oil; R_f 0.40 (hexane/EtOAc 1:1); δ_H(400 MHz; CDCl₃) 7.54-7.52 (m, 2H, Ar), 7.43-7.38 (m, 3H, Ar), 5.89 (s, 1H, H-2), 4.53 (d, *J*_{1a,1b} = *J*_{3a,3b} = 18.0 Hz, 2H, H-1a,3a), 4.46 (d, *J*_{1a,1b} = *J*_{3a,3b} = 18.0 Hz, 2H, H-1b,3b); δ_C(100 MHz; CDCl₃) 204.2 (C=O), 136.8, 129.4, 128.5, 126.1 (6 × Ar), 99.0 (C2), 72.4 (C1,C3). ¹H and ¹³C NMR values were in agreement with literature values.¹⁵

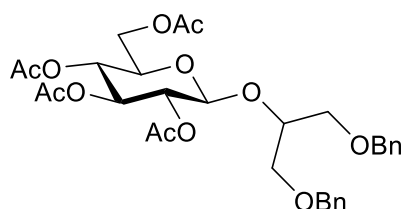
Trans-1,3-*O*-benzylidene glycerol (**11**)¹⁵



2-Phenyl-1,3-dioxan-5-one (**10**) (580 mg, 3.3 mmol) was dissolved into a mixture of THF/H₂O (3:1, 40 mL) and cooled in an ice bath. Sodium borohydride (250 mg, 6.6 mmol) was added in a single portion and the reaction mixture was stirred for 30 minutes. The reaction mixture was then allowed to warm to room temperature before being washed with Et₂O (5 × 10 mL). The organic layers were combined and dried over MgSO₄, before being filtered and dried *in vacuo* to give *trans*-1,3-*O*-benzylidene glycerol (**11**) (560 mg, 96%) as a colourless oil; R_f 0.59 (hexane/EtOAc 1:1); δ_H(400 MHz; CDCl₃) 7.48-7.45 (m, 2H, Ar), 7.39-7.34 (m, 3H, Ar), 5.41 (s, 1H, H-4), 4.28 (dd, *J*_{1a,1b} = 11.2 Hz, *J*_{1a,5} = 5.0 Hz, 1H, H-1a), 4.28 (dd, *J*_{3a,3b} = 11.2 Hz, *J*_{3a,5} = 5.0 Hz, 1H, H-3a), 3.99-3.90 (m, 1H, H-2), 3.76-3.73 (m, 1H, OH), 3.58 (dd, *J*_{1a,1b} = 11.2 Hz, *J*_{1a,5} =

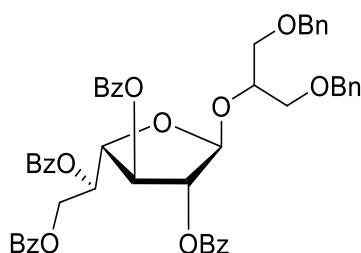
9.8 Hz, 1H, H-1b), 3.55 (dd, $J_{1a,1b} = 11.2$ Hz, $J_{1a,5} = 9.8$ Hz, 1H, H-1b); δ_c (100 MHz; CDCl₃) 137.5 (C5), 129.1 (C8), 128.4 (C6), 126.1 (C7), 101.0 (C4), 71.7 (C1, C3), 61.3 (C2). The ¹H and ¹³C NMR values were in agreement with literature values.¹⁵

1,3-Bis(benzyloxy)propan-2-yl 2',3',5',6'-tetra-O-acetyl- β -D-glucopyranoside (**14**)⁶



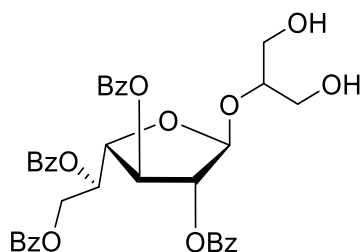
2,3,4,6-Tetra-O-acetyl- α -D-glucopyranosyl bromide (**12**) (200 mg, 0.5 mmol) and 1,3-O-di-benzyloxypropan-2-yl bromide (**13**) (250 μ L, 1.0 mmol) were dissolved into dry DCM (5 mL). Silver carbonate (200 mg, 0.75 mmol) was added in a single portion and the reaction mixture was stirred overnight. TLC showed consumption of the glycosyl bromide donor (R_f 0.42 (hexane/EtOAc 8:2)). The reaction mixture was filtered and the solvent removed under reduced pressure. Purification by FCC gave the title compound (**14**) (210 mg, 70%) as a white powder; R_f 0.22 (hexane/EtOAc 8:2); $[\alpha]_D -4.7$ (c 1.0, CHCl₃) (lit.⁶ -5.0 (c 1.0, CHCl₃)); δ_H (400 MHz; CDCl₃) 7.37-7.26 (m, 10H, Ar), 5.20 (dd, $J_{2',3'} = 10.0$ Hz, $J_{3',4'} = 10.0$ Hz, 1H, H-3'), 5.07 (dd, $J_{3',4'} = 10.0$ Hz, $J_{4',5'} = 10.0$ Hz, 1H, H-4'), 5.00 (dd, $J_{1',2'} = 8.1$ Hz, $J_{2',3'} = 10.0$ Hz, 1H, H-2'), 4.80 (d, $J_{1',2'} = 8.1$ Hz, 1H, H-1'), 4.52 (s, 2H, PhCH₂), 4.51 (s, 2H, PhCH₂), 4.21 (dd, $J_{5',6'a} = 4.8$ Hz, $J_{6'a,6'b} = 12.2$ Hz, 1H, H-6'a), 4.08 (dd, $J_{5',6'b} = 2.4$ Hz, $J_{6'a,6'b} = 12.2$ Hz, 1H, H-6'b), 4.05-4.03 (m, 1H, H-2), 3.69-3.61 (m, 3H, H-1,5'), 3.52-3.50 (m, 2H, H-3), 2.04 (s, 3H, Ac), 2.01 (s, 3H, Ac), 2.00 (s, 3H, Ac), 1.93 (s, 3H, Ac); δ_c (100 MHz; CDCl₃) 170.6, 170.3, 169.4, 169.4 (4 \times C=O), 138.2, 138.0, 128.4, 128.4, 127.7, 127.6, 127.6, 127.6 (Ar), 100.8 (C1'), 78.4 (C2), 73.5 (CH₂Ph), 73.4 (CH₂Ph), 72.9 (C3'), 71.7 (C1), 71.5 (C3), 71.0 (C5'), 70.1 (C2'), 68.5 (C4'), 62.0 (C6'), 20.7, 20.6, 20.6, 20.6 (4 \times Me). NMR were in agreement with literature values.⁶

1,3-Bis(benzyloxy)propan-2-yl 2',3',5',6'-tetra-O-benzoyl-β-D-galactofuranoside (**14**)



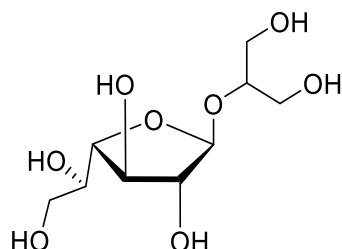
A solution of per-*O*-benzoyl-β-D-galactofuranose (**15**) (250 mg, 0.36 mmol) dissolved in DCM (4 mL) was cooled in an ice bath. SnCl₄ solution (1M in DCM, 400 μL, 0.4 mmol) was slowly added by syringe. After 15 minutes at 0 °C 1,3-*O*-di-benzyl-glycerol (**13**) (80 μL, 0.32 mmol) was added by syringe and the mixture was allowed to warm and was stirred for 18 hours at room temperature after which TLC analysis (hexane/EtOAc 7:3) showed consumption of **15**. The mixture was diluted with DCM (30 mL) and washed with sat. aqueous NaHCO₃ (2 × 10 mL). The organic layers were combined, dried over MgSO₄, filtered and dried *in vacuo* to give a crude residue which was purified by FCC to give the title compound (**14**) (120 mg, 39%) as a colourless oil; R_f 0.61 (hexane/EtOAc 7:3); [α]_D -1.2 (c 1.0, CHCl₃); δ_H(400 MHz; CDCl₃) 8.07-8.04 (m, 2H, Bz), 7.97-7.95 (m, 1H, Bz), 7.90-7.88 (m, 1H, Bz), 7.57-7.20 (m, 25H, Ar), 6.03-5.99 (m, 1H, H-5'), 5.61 (s, 1H, H-1'), 5.59 (d, *J*_{3',4'} = 5.4 Hz, 1H, H-3'), 5.55 (s, 1H, H-2'), 4.75 (dd, *J*_{3',4'} = 5.4 Hz, *J*_{4',5'} = 3.4 Hz, 1H, H-4'), 4.73 (dd, *J*_{5',6'a} = 7.7 Hz, ²*J*_{6'a,6'b} = 12.0 Hz, 1H, H-6'a), 4.58-4.52 (m, 3H, H-6'b, PhCH₂), 4.51 (d, ²*J* = 11.9 Hz, PhCHH), 4.45 (d, ²*J* = 11.9 Hz, PhCHH), 4.25-4.20 (m, 1H, H-2), 3.71-3.67 (m, 2H, H-1), 3.62 (d, *J*_{2,3} = 5.3 Hz, 2H, H-3); δ_C(100 MHz; CDCl₃) 166.1, 165.8, 165.7, 165.4 (4 × C=O), 138.2, 138.1, 133.4, 133.3, 133.2, 133.0, 130.0, 129.9, 129.8, 129.7, 129.6, 129.2, 129.1, 128.4, 128.4, 128.3, 127.7, 127.6 (Ar), 105.0 (C1'), 82.1 (C2'), 81.4 (C4'), 77.8 (C3'), 74.6 (C2), 73.5, 73.5 (2 × PhCH₂), 70.6 (C1), 70.3 (C5'), 70.2 (C3), 63.9 (C6'); HRMS (ESI⁺) *m/z* calc. for C₅₁H₄₆O₁₂Na⁺ 873.2887 ([M+Na]⁺) found 873.2875 [M+Na]⁺.

1,3-Dihydroxypropan-2-yl 2,3,5,6-tetra-O-benzoyl-β-D-galactofuranoside (**17**)



To a solution of 1,3-bis(benzyloxy)propan-2-yl 2,3,5,6-tetra-*O*-benzoyl- β -D-galactofuranoside (**15**) (115 mg, 140 μ mol) in EtOAc/EtOH (10:1) (20 mL) was added activated 10% palladium on charcoal (10 mg). The system was flushed with N₂ (\times 3) followed by H₂ (\times 3) and stirred overnight at room temperature. After the system had been flushed with N₂ (\times 3) the catalyst was filtered off and the solvent removed under reduced pressure to give the title compound (**17**) (60 mg, 64%) as a colourless oil; R_f 0.18 (hexane/EtOAc 1:1); $[\alpha]_D = -1.1$ (c 1.0, CHCl₃); δ_H (400 MHz; CDCl₃) 8.09-8.06 (m, 2H, Ar), 8.02-7.97 (m, 4H, Ar), 7.93-7.90 (m, 2H, Ar), 7.59-7.51 (m 4H, Ar), 7.49-7.30 (m, 8H, Ar), 6.00-5.96 (m 1H, H-5'), 5.73 (dd, $J_{2',3'} = 2.1$ Hz, $J_{3',4'} = 5.7$ Hz, 1H, H-3'), 5.52 (s, 1H, H-1'), 5.49 (d, $J_{2',3'} = 2.1$ Hz, 1H, H-2'), 4.85 (dd, $J_{3',4'} = 5.7$ Hz, $J_{4',5'} = 3.8$ Hz, 1H, H-4'), 4.79 (dd, $J_{5',6'a} = 4.6$ Hz, $^2J_{6'a,6'b} = 11.8$ Hz, 1H, H-6'a), 4.72 (dd, $J_{5',6'b} = 6.6$ Hz, $^2J_{6'a,6'b} = 11.8$ Hz, 1H, H-6'b), 3.94-3.89 (m, 1H, H-2), 3.78-3.72 (m 4H, H-2,3), 2.56 (bs, 1H, OH), 2.47 (bs, 1H, OH); δ_C (100 MHz; CDCl₃) 166.2, 166.2, 165.7, 165.6 (4 \times C=O), 133.7, 133.7, 133.4, 133.2, 130.0, 129.9, 129.8, 129.5, 129.3, 128.8, 128.6, 128.5, 128.5, 128.4 (Ar), 106.5 (C1'), 83.3 (C2'), 81.1 (C4'), 80.8 (C2), 77.3 (C3'), 70.3 (C5'), 63.1 (C1), 63.1 (C6'), 62.4 (C3); HRMS (ESI⁺) m/z calc. for C₃₇H₃₄O₁₂Na⁺ 693.1948 ([M+Na]⁺) found 693.1956 [M+Na]⁺.

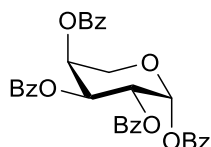
1,3-Dihydroxypropan-2-yl β -D-galactofuranoside (**1**)



1,3-Dihydroxypropan-2-yl 2,3,5,6-tetra-*O*-benzoyl- β -D-galactofuranoside (**17**) (55 mg, 82 μ mol) was dissolved into a solution of MeOH/H₂O/NEt₃ (5:2:1, 8 mL) and stirred vigorously for 18h at room temperature. The solvent was removed *in vacuo* and the crude mixture was dissolved in MeOH (5 mL) and passed through Dowex[®] 1X2-400 hydroxide form ion exchange resin (1 g). The eluted compound was dried *in vacuo* to give the title compound (**1**) (7 mg, 51%) as a colourless oil; R_f 0.06 (tol/MeOH, 8:2); $[\alpha]_D = -144$ (c 0.5, MeOH); δ_H (400 MHz; MeOH); 4.99 (d, $J_{1',2'} = 1.7$ Hz, 1H, H-1'), 3.93-3.92 (m, 2H, H-3',4'), 3.90 (dd, $J_{1',2'} = 1.7$ Hz, $J_{2',3'} = 4.0$ Hz, 1H, H-2'), 3.65-3.58 (m, 2H, H-5',2), 3.56-3.48 (6H, H-1,3,6'a,6'b); δ_C (100 MHz; MeOH) 107.8 (C1'), 83.4 (C3'), 81.6 (C2'), 78.8 (C2), 77.3 (C4'), 71.0 (C5'), 63.0 (C6'),

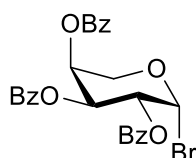
61.9 (C1), 61.1 (C3); HRMS (ESI⁺) calc. for C₉H₁₈O₈Na⁺ 277.0899 ([M+Na]⁺) found 277.0895 [M+Na]⁺.

per-*O*-benzoyl-β-*L*-arabinopyranose (**18**)²⁰



A solution of *L*-arabinose (1.0 g, 6.7 mmol) and DMAP (1 mol %) in dry pyridine (15 mL) was cooled in an ice bath and benzoyl chloride (5.0 mL, 43 mmol) was added dropwise over 30 minutes. The reaction was allowed to warm and stirred overnight at room temperature. The solvent was removed *in vacuo* and the crude mixture was dissolved in EtOAc (20 mL) and washed with 1M HCl solution (3 × 5 mL) to remove any residual pyridine. The organic layer was dried over MgSO₄ and the solvent was removed under reduced pressure before the crude mixture was purified by FCC to give the title compound (**18**) (3.40 g, 90%) as a white foam, R_f 0.4 (hexane/EtOAc 3:1); [α]_D +301 (c 1.0, CHCl₃) (lit.²⁰ +291.2 (c 0.1, CHCl₃)); δ_H(400 MHz; CDCl₃) 8.14-8.12 (m, 4H, Ar), 7.90-7.87 (m, 4H, Ar), 7.65-7.61 (m, 2H, Ar), 7.55-7.45 (m, 6H, Ar), 7.32-7.28 (m, 4H, Ar), 6.87 (bs, 1H, H-1), 6.07-6.06 (2H, m, H-2,3), 5.91-5.89 (m, 1H, H-4), 4.42 (dd, *J*_{4,5a} = 1.0 Hz, ²*J*_{5a,5b} = 13.5 Hz, 1H, H-5a), 4.18 (dd, *J*_{4,5b} = 2.1 Hz, ²*J*_{5a,5b} = 13.5 Hz); δ_C(100 MHz; CDCl₃) 165.8, 165.7, 165.6, 164.7 (4 × C=O), 133.8, 133.6, 133.5, 133.4, 129.9, 129.8, 129.4, 129.1, 128.9, 128.8, 128.8, 128.6, 128.4, 128.4 (Ar), 91.1 (C1), 69.5 (C4), 68.2 (C3), 67.8 (C2), 63.0 (C5). ¹H and ¹³C NMR values were in agreement with literature values²⁰

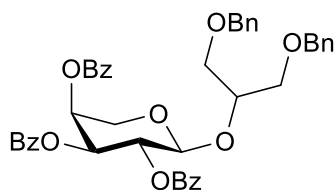
2,3,4-Tri-*O*-benzoyl-β-*L*-arabinopyranosyl bromide³⁰



Per-*O*-benzoyl-β-*L*-arabinopyranose (**18**) (2.4 g, 4.2 mmol) was dissolved into dry DCM (10 mL) under N₂. A solution of 33% HBr in AcOH (2.5 mL) was added in a single portion and the reaction mixture stirred for 3 hours at room temperature after which time TLC showed

consumption of the start material. The solvent was removed under reduced pressure and the reaction mixture was re-dissolved into EtOAc (10 mL) before being washed with ice cold saturated NaHCO₃ (3 × 3 mL). The organic layer was dried over MgSO₄ and the solvent removed under reduced pressure to give the title compound (**19**) (2.1 g, 95%) as an oil which was immediately used in the next step, R_f 0.42 (hexane/EtOAc 3:1); δ_H(400 MHz; CDCl₃) 8.11-8.08 (m, 1H, Ar), 8.03-8.01 (m, 1H, Ar), 7.87-7.85 (m, 1H, Ar), 7.63-7.30 (m, 9H, Ar), 6.94 (d, $J_{1,2} = 3.9$ Hz, 1H, H-1), 6.00 (dd, $J_{2,3} = 10.5$ Hz, $J_{3,4} = 3.9$ Hz, 1H, H-3), 5.84-5.83 (m, 1H, H-4), 5.71 (dd, $J_{1,2} = 3.9$ Hz, $J_{2,3} = 10.5$ Hz, 1H, H-2), 4.47 (dm, $^2J_{5a,5b} = 12.9$ Hz, 1H, H-5a), 4.23 (dd, $J_{4,5b} = 1.9$ Hz, $^2J_{5a,5b} = 12.9$ Hz, 1H, H-5b); δ_H(100 MHz; CDCl₃) 165.6, 165.6, 165.4 (3 × C=O), 133.8, 133.7, 133.4, 130.0, 129.9, 129.8, 128.7, 128.6, 128.4 (12 × Ar) 89.8 (C1), 68.9 (C4), 68.7 (C2), 65.0 (C3), 60.4 (C5). The ¹H NMR were in agreement with literature values.³⁰

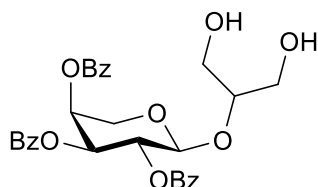
1,3-Bis(benzyloxy)propan-2-yl 2,3,4-tri-*O*-benzoyl- α -L-arabinopyranoside (**20**)



2,3,4-Tri-*O*-benzoyl- β -L-arabinopyranosyl bromide (**19**) (2.1 g, 4.0 mmol), was dried azeotropically with dry toluene (3 × 20 mL). The glycosyl bromide (**19**) was then dissolved into dry toluene (10 mL) under N₂ and 1,3-*O*-di-benzyl-glycerol (**13**) (0.9 mL, 3.8 mmol, 0.9 eq), and Ag₂CO₃ (1.8 g, 6.4 mmol, 1.5 eq) were added. The reaction was stirred at 55 °C under N₂ for 4 hours after which time TLC (hex:EtOAc 3:1) showed complete consumption of the glycosyl bromide. The reaction mixture was filtered and the solvent removed under reduced pressure. Purification by FCC gave the title compound (**20**) (1.5 g, 50%) as a colourless oil, R_f 0.48 (toluene/EtOAc 9:1); [α]_D +94.4 (c 1.0, CHCl₃); δ_H(400 MHz; CDCl₃) 8.05-7.94 (m, 5H, Ar), 7.58-7.17 (m, 20H, Ar), 5.71 (dd, $J_{1',2'} = 5.9$ Hz, $J_{2',3'} = 8.3$ Hz, 1H, H-2'), 5.67-5.65 (m, 1H, H-4'), 5.60 (dd, $J_{2',3'} = 8.3$ Hz, $J_{3',4'} = 3.5$ Hz, 1H, H-3'), 5.06 (d, $J_{1',2'} = 5.9$ Hz, 1H, H-1'), 4.35 (s, 2H, PhCH₂), 4.37-4.32 (m, 3H, H-5a', PhCH₂), 4.15-4.12 (m, 1H, H-2), 3.82 (dd, $J_{4',5'} = 2.3$ Hz, $^2J_{5a',5b'} = 12.6$ Hz, 1H, H-5b'), 3.69 (dd, $J_{1a,2} = 5.3$ Hz, $^2J_{1a,1b} = 10.3$ Hz, 1H, H-1a), 3.63-3.59 (m, 2H, H-1b,3a), 3.50 (dd, $J_{2,3b} = 6.4$ Hz, $J_{3a,3b} = 10.3$ Hz, 1H, H-3b); δ_C(100 MHz; CDCl₃); 165.7, 165.6, 165.2 (3 × C=O), 138.2, 138.1, 133.4, 133.3, 129.9, 129.8, 129.5, 129.2, 128.5, 128.4, 128.3, 127.7, 127.6, 127.5, 127.5 (Ar), 100.4 (C1'), 77.6 (C2), 73.4, 73.4 (2 × PhCH₂), 70.8 (C1), 70.4

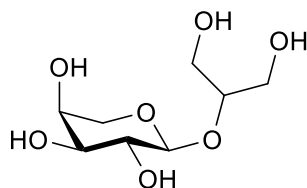
(C3'), 70.4 (C3), 70.2 (C2'), 68.3 (C4'), 62.0 (C5'); HRMS (ESI⁺) m/z calc. for C₄₃H₄₀O₁₀Na⁺ 739.2519 [M+Na]⁺ found 739.2513 [M+Na]⁺.

1,3-Dihydroxypropan-2-yl 2,3,4-tri-*O*-benzoyl- α -L-arabinopyranoside (**21**)



To a solution of 1,3-bis(benzyloxy)propan-2-yl 2,3,4-tri-*O*-benzoyl- α -L-arabinopyranoside (**20**) (1.50 g, 2.1 mmol) in EtOAc/EtOH 10:1 (50 mL) was added palladium on activated charcoal (10% Pd basis) (50 mg). The system was flushed with N₂ (×3) followed by H₂ (×3) and stirred overnight at room temperature. After the system had been flushed with N₂ (×3) the catalyst was filtered off and the solvent removed under reduced pressure to give the title compound (**21**) (182 mg, 22%) as a white powder. R_f 0.21 (EtOAc/hexane 6:4); [α]_D +261 (c 1.0, CHCl₃); δ _H(400 MHz; CDCl₃) 8.10-8.08 (m, 2H, Ar), 8.01-7.99 (m, 2H, Ar), 7.89-7.87 (m, 2H, Ar), 7.62-7.27 (m, 9H, Ar), 5.80 (dd, $J_{1',2'} = 7.3$ Hz, $J_{2',3'} = 9.7$ Hz, 1H, H-2'), 5.73-5.71 (m, 1H, H-4'), 5.62 (dd, $J_{2',3'} = 9.7$ Hz, $J_{3',4'} = 3.4$ Hz, 1H, H-3'), 4.90 (d, $J_{1',2'} = 7.3$ Hz, 1H, H-1'), 4.36 (dd, $J_{4',5'a} = 2.8$ Hz, $^2J_{5'a,5'b} = 13.2$ Hz, 1H, H-5'a), 3.96 (dd, $J_{4',5'b} = 1.5$ Hz, $^2J_{5'a,5'b} = 13.2$ Hz, 1H, H-5'b), 3.86-3.83 (m, 1H, H-2), 3.69-3.67 (m, 2H, H-1), 3.58-3.55 (m, 2H, H-3), 2.85 (bs, 1H, OH), 2.05 (bs, 1H, OH); δ _C(100 MHz; CDCl₃) 165.7, 165.6, 165.6 (3 × C=O), 133.7, 133.6, 133.5, 129.9, 129.8, 129.7, 129.3, 129.0, 128.9, 128.6, 128.6, 128.4, (12 × Ar), 102.0 (C1'), 83.9 (C2), 71.0 (C3'), 70.4 (C2'), 68.7 (C4'), 64.0 (C5'), 62.7 (C1), 62.4 (C3); HRMS (ESI⁺) calc. for C₂₉H₂₈O₁₀Na⁺ 559.1580 [M+Na]⁺ found 559.1577 [M+Na]⁺.

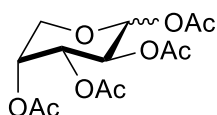
1,3-Dihydroxypropan-2-yl α -L-arabinopyranoside (**2**)



Sodium (20 mg) was added to dry methanol (18 mL) under N₂. After the cessation of effervescence 1,3-Dihydroxypropan-2-yl 2,3,4-tri-*O*-benzoyl- α -L-arabinopyranoside (**21**)

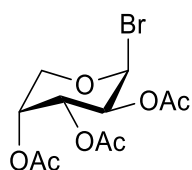
(180 mg, 0.3 mmol) was added in dry MeOH (8 mL) and the mixture was vigorously stirred overnight at room temperature. The reaction mixture was neutralised using Amberlite IR-120 resin, filtered and the solvent removed under *in vacuo*. The crude mixture was dissolved in H₂O and passed through Dowex® 1X2-400 (OH⁻ form) ion exchange resin (1 g) to give 1,3-dihydroxypropan-2-yl α -L-arabinopyranoside (**2**) (62 mg, 76%) as a colourless oil. $[\alpha]_D + 6.8$ (c 1.0, H₂O); δ_H (400 MHz; D₂O) 4.35 (d, $J_{1',2'} = 7.5$ Hz, 1H, H-1'), 3.83-3.78 (m, 2H, H-4',5'a), 3.77-3.73 (m, 1H, H-2), 3.65-3.62 (m, 6H, H-1,2,5'b,3'), 3.45 (dd, $J_{1',2'} = 7.5$ Hz, $J_{2',3'} = 9.4$ Hz, 1H, H-2'); δ_C (100 MHz; D₂O) 103.4 (C1'), 81.1 (C2), 72.9 (C3'), 71.3 (C2'), 68.4 (C4'), 66.2 (C5'), 61.4 (C1), 61.0 (C3); HRMS (ESI⁺) *m/z* calc. for C₈H₁₆O₇Na⁺ 247.0794 [M+Na]⁺ found 247.0798 [M+Na]⁺.

Per-*O*-acetyl- α/β -D-arabinopyranose (**22**)³¹



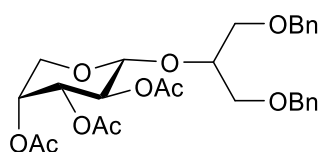
D-Arabinose (1.0 g, 6.7 mmol) was suspended in acetic anhydride (20 mL) under a N₂ atmosphere, iodine (100 mg, 0.4 mmol) was added in a single portion and the reaction mixture was left to stir over night. The reaction mixture was diluted with DCM (150 mL) and washed with saturated aqueous Na₂S₂O₃ solution (3 × 15 mL) and saturated NaHCO₃ solution (3 × 15 mL). The organic layer separated and was dried over MgSO₄, filtered and the solvent was removed under reduced pressure to give the title compound (**22**) as a yellow syrup (2.0 g, 95%); *R_f* = 0.42 (Hexane/EtOAc 7:3); δ_H (400 MHz; CDCl₃) 6.88 (1H, d, $J_{1,2} = 6.9$ Hz, H-1 α), 6.35 (1H, d, $J_{1,2} = 3.0$ Hz, H-1 β); δ_C (100 MHz; CDCl₃) 90.2 (C1 β), 85.7 (C1 α). ¹H and ¹³C NMR spectra are in good agreement with data extracted from spectra of an anomeric mixture.³¹

2,3,4-Tri-*O*-acetyl- β -D-arabinopyranosyl bromide (**23**)³²



Per-*O*-acetyl-D-arabinopyranose (**22**) (1.0 g, 3.1 mmol) was dissolved in DCM (10 mL) under a N₂ atmosphere. 33% v/v HBr in AcOH (2 mL) was added in a single portion and the reaction mixture stirred at room temperature for 3 hours, after which time TLC showed consumption of the start material. The reaction mixture was diluted with DCM (50 mL) and poured into ice cold saturated NaHCO₃ solution (10 mL). The organic layer was separated and further washed with saturated NaHCO₃ solution (2 × 15 mL) before being dried over MgSO₄. Following filtration, the solvent was removed under reduced pressure to give the title compound (**23**) as a yellow oil (1.0 g, 95%) which was immediately used in the next step; R_f 0.50 (hexane/EtOAc 7:3); δ_{H} (400 MHz; CDCl₃) 6.70 (d, $J_{1,2}$ = 3.8 Hz, 1H, H-1'), 5.42-5.28 (m, 2H, H-3,4), 5.11-5.07 (m, 1H, H-2), 4.12 (d, $J_{5a,5b}$ = 13.3 Hz, 1H, H-5a), 3.94 (dd, $J_{4,5b}$ = 1.7 Hz, $J_{5a,5b}$ = 13.3 Hz, 1H, H-5b), 2.16, 2.12, 2.03 (3 × OAc); δ_{C} (100 MHz; CDCl₃) 170.0, 170.0, 169.8 (3 × C=O), 89.7 (C1), 67.9 (C4), 67.8 (C2), 67.7 (C3), 64.7 (C5), 20.8, 20.7, 20.6 (3 × OAc). The ¹H and ¹³C NMR were in agreement with literature values.³²

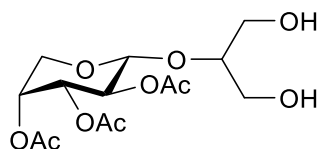
1,3-Bis(benzyloxy)propan-2-yl 2',3',4'-tri-*O*-acetyl- α -D-arabinopyranoside (**24**)



Freshly prepared 4Å MS (2 g) were added to a solution of 2,3,4-tri-*O*-acetyl- α -D-arabinopyranosyl bromide (**24**) (1.0 g, 2.9 mmol) and 1,3-di-*O*-benzyl glycerol (**13**) (740 μ L, 3.0 mmol) dissolved in DCE (20 mL) under a N₂ atmosphere. The mixture was stirred at room temperature for 30 minutes to ensure anhydrous conditions. The reaction mixture was then cooled to 0 °C and AgOTf (1.1 g, 4.4 mmol) was added in a single portion. The reaction mixture was allowed to warm to room temperature and was stirred overnight in the dark. The resulting white precipitate and 4Å MS were removed by filtration through Celite, and the solvent was removed under reduced pressure. The crude reaction mixture was then purified by FCC (hexane/EtOAc 9:1 to 6:4) to give the title compound (**24**) as a colourless oil

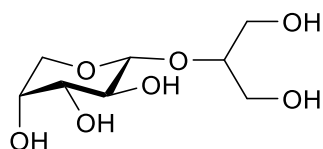
(200 mg, 13%); R_f 0.22 (hexane/EtOAc 7:3); $[\alpha]_D -4.4$ (c 1.0, CHCl_3); δ_H (400 MHz; CDCl_3) 7.37-7.27 (m, 10H, ArH), 5.24 (m, 1H, H-4'), 5.20 (dd, $J_{2',3'} = 9.5$ Hz, $J_{1',2'} = 6.9$ Hz, 1H, H-2'), 5.02 (dd, $J_{2',3'} = 9.5$ Hz, $J_{3',4'} = 3.6$ Hz, 1H, H-3'), 4.69 (d, $J_{1',2'} = 6.9$ Hz, 1H, H-1'), 4.52 (d, $J = 6.1$ Hz, 1H, PhCH_2), 4.04 (m, 1H, H-2), 4.01 (dd, $^2J_{5'a,5'b} = 13.1$ Hz, $J_{4',5'a} = 3.3$ Hz, 1H, H-5'a), 3.68-3.65 (m, 2H, H-1), 3.58 – 3.53 (m, 3H, H-3,5'b); δ_C (100 MHz; CDCl_3) 170.4, 170.2, 169.5 ($3 \times \text{C=O}$), 128.4, 128.4, 127.7, 127.6 (Ar), 100.9 (C1'), 77.75 (C1) 173.5, 173.4 ($2 \times \text{PhCH}_2$), 70.9 (C2), 70.9 (C3), 70.2 (C3'), 69.4 (C2'), 67.7 (C4'), 63.1 (C5'), 21.0, 20.7, 20.7 ($3 \times \text{OAc}$); HRMS (ESI⁺) m/z calc. for $\text{C}_{28}\text{H}_{34}\text{O}_{10}\text{Na}$ 553.2050 ($[\text{M}+\text{Na}]^+$) found 553.2044 $[\text{M}+\text{Na}]^+$.

1,3-Dihydroxypropan-2-yl 2',3',4'-tri-O-acetyl- α -D-arabinopyranoside (25)



1,3-Bis(benzyloxy)propan-2-yl 2',3',4'-tri-O-acetyl- α -D-arabinopyranoside (**24**) (200 mg, 0.4 mmol) was dissolved in MeOH (10 mL) and palladium on activated charcoal (10% Pd basis) (50 mg) was added. The system was flushed with N_2 ($\times 3$) followed by H_2 ($\times 3$) and stirred overnight at room temperature. After the system had been flushed with N_2 ($\times 3$) the catalyst was filtered through Celite and the filter was washed with MeOH (20 mL). The organic washes were combined and the solvent was removed under reduced pressure to give the title compound (**25**) (100 mg, 75%) as a white powder; R_f 0.15 (9:1 EtOAc:Hex) $[\alpha]_D -9.8$ (c 1.0, MeOH); δ_H (400 MHz; CDCl_3) 5.29 (bs, 1H, H-4'), 5.23 (dd, $J_{2',3'} = 9.8$ Hz, $J_{1',2'} = 7.8$ Hz, 1H, H-2'); 5.07 (dd, $J_{2',3'} = 9.8$ Hz, $J_{3',4'} = 3.4$ Hz, 1H, H-3'), 4.57 (d, $J_{1',2'} = 7.8$ Hz, 1H, H-1'), 4.06 (dd, $^2J_{5'a,5'b} = 13.2$ Hz, $J_{4',5'a} = 1.8$ Hz, 1H, H-5'a), 3.81-3.76 (m, 1H, H-2), 3.71 (d, $^2J_{5'a,5'b} = 13.2$ Hz, 1H, H-5'b), 3.69-3.66 (m, 4H, H-1,3), 2.93 (bs, 1H, OH), 2.33 (bs, 1H, OH), 2.17 (s, 3H, OAc), 2.10 (s, 3H, OAc), 2.03 (s, 3H, OAc); δ_C (100 MHz; CDCl_3) 170.3, 170.1, 170.1 ($3 \times \text{C=O}$), 101.9 (C1'), 83.5 (C2), 70.3 (C3'), 69.6 (C2'), 67.7 (C4'), 64.1 (C5'), 62.7 (C1), 62.4 (C3), 20.9, 20.8, 20.7 ($3 \times \text{OAc}$); HRMS (ESI⁺) m/z calc. for $\text{C}_{14}\text{H}_{22}\text{O}_{10}\text{Na}$ 373.1111 ($[\text{M}+\text{Na}]^+$) found 373.1107 $[\text{M}+\text{Na}]^+$.

1,3-Dihydroxypropan-2-yl α -D-arabinopyranoside (6)

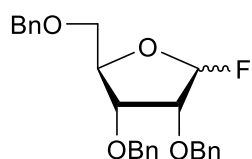


1,3-Dihydroxypropan-2-yl 2',3',4'-tri-*O*-acetyl- α -D-arabinopyranoside (**25**) (100 mg, 0.29 mmol) was dissolved into MeOH (10 mL) under N₂. A solution of sodium metal (5 mg, 0.2 mmol) in dry MeOH (10 mL) was added by syringe and the reaction mixture was left to stir overnight. Low resolution mass spectrometry showed only the desired product, and the reaction mixture was neutralised to pH 7.0 with Amberlite® 120 (H⁺) resin, before being filtered and the solvent removed under reduced pressure to give the title compound (**6**) as an oil (52 mg, 80%); $[\alpha]_D$ -4.6 (*c* 1.0, MeOH); δ_H (400 MHz; MeOH) 4.25 (d, $J_{1',2'} = 7.0$ Hz, 1H, H-1'), 3.78 (dd, $^2J_{5'a,5'b} = 12.5$ Hz, $J_{5'a,4} = 2.6$ Hz, 1H, H-5'a), 3.72-3.69 (m, 1H, H-4'), 3.66-3.62 (m, 1H, H-2), 3.59-3.53 (m, 4H, H-1,3), 3.50-3.42 (m, 3H, H-2', H-5'b, H-3'); δ_C (100 MHz; MeOH) 103.5 (C1'), 81.1 (C2), 72.8 (C3'), 71.3 (C2'), 68.4 (C4'), 65.8 (C5'), 61.7 (C1), 61.3 (C3); HRMS (ESI⁺) *m/z* calc. for C₈H₁₆O₇Na 247.0794 [M+Na]⁺ found 247.0794 [M+Na]⁺

Trityl perchlorate (Ph₃C⁺.ClO₄⁻)³³

Triphenyl methanol (500 mg, 1.9 mmol) was dissolved into acetic anhydride (8 mL) and in an ice bath. 70% w/w Perchloric acid (700 μ L, 8.2 mmol) was added dropwise and the reaction mixture immediately turned dark yellow. The reaction mixture was stirred for 1 hour at 0 °C before the solvent was carefully filtered off and the remaining yellow powder was rinsed with dry Et₂O (5 \times 2 mL). The reaction mixture was then dried in the dark on a high vacuum line overnight to give the title compound (455 mg, 69%) as a yellow powder; ν_{max}/cm^{-1} (FTR-IR) 1579 (s), 1483 (m), 1447 (m), 1353 (s), 1294 (m), 1191 (w), 1166 (w), 1073 (broad, vs), δ_H (400 MHz; CD₃CN) 7.37-7.27 (m, 15H, Ar), δ_C (100 MHz; CD₃CN) 148.1 (Ph₃C⁺), 128.4 (6 \times Ar), 128.3 (6 \times Ar), 127.6 (3 \times Ar). The infrared spectrum is in good agreement with literature values.³³

2,3,5-Tri-*O*-benzyl-*D*-ribofuranosyl fluoride (27/28)²⁵



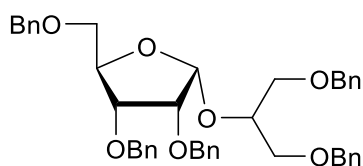
2,3,5-Tri-*O*-benzyl-*D*-ribofuranose (**26**) (1.0 g, 2.4 mmol) was dissolved into dry THF (10 mL) and cooled to -30 °C. DAST (0.4 mL, 2.9 mmol, 1.2 eq) was added in a single portion and the reaction mixture was allowed to warm to room temperature. After 20 minutes TLC indicated all starting material had been consumed. The reaction mixture was cooled back down to -30 °C and the residual DAST was quenched with MeOH (0.5 mL). The solvent was removed under reduced pressure and the glycosyl fluorides separated by FCC to give the title compound (645 mg, 64%),

(**27**) (α -anomer) R_f 0.70 (hexane/EtOAc 9:1); δ_H (400 MHz; CDCl₃) 7.34-7.17 (m, 15H, Ar), 5.69 (dd, $J_{1,2} = 3.4$ Hz, $J_{1,F} = 65.8$ Hz, 1H, H-1), 4.71-4.57 (m, 4H, 2 \times PhCH₂), 4.49-4.39 (m, 3H, PhCH₂ & H-4), 3.91 (m, 1H, H-3), 3.89 (ddd, $J_{2,F} = 25.9$, $J_{1,2} = 3.4$ Hz, $J_{2,3} = 6.4$ Hz, 1H, H-2), 3.43 (dd, $J_{4,5a} = 3.9$ Hz, $^2J_{5a,5b} = 10.5$ Hz, 1H, H-5a), 3.38 (dd, $J_{4,5b} = 3.5$ Hz, $^2J_{5a,5b} = 10.5$ Hz, 1H, H-5b); δ_C (100 MHz; CDCl₃) 137.9, 137.7, 137.4 (3 \times Ar), 128.5, 128.5, 128.4, 128.3, 128.1, 128.0, 127.8, 127.6 (Ar), 108.6 (d, $J_{C1,F} = 234$ Hz, C1), 85.1 (C4), 78.6 (d, $J_{C2,F} = 20.7$ Hz, C2), 74.3 (C3), 73.5, 72.7, 72.5 (3 \times CH₂Ph), 69.7 (C5); δ_F (376 MHz; CDCl₃) -131.7 (dd, $J_{1,F} = 234$ Hz, $J_{2,F} = 20.7$ Hz).

(**28**) (β -anomer) R_f 0.82 (hexane/EtOAc 9:1) [α]_D +49.4 (c 1.0, CHCl₃); δ_H (400 MHz; CDCl₃) 7.35-7.29 (m, 15H, Ar), 5.67 (d, $J_{1,F} = 63.3$ Hz, 1H, H-1), 4.64-4.44 (m, 6H, PhCH₂), 4.46-4.41 (m, 1H, H-4), 4.14-4.10 (m, 1H, H-3), 3.99 (dd, $J_{2,3} = 4.2$ Hz, $J_{2,F} = 4.2$ Hz, 1H, H-2), 3.68 (dd, $J_{4,5a} = 3.4$ Hz, $^2J_{5a,5b} = 11.1$ Hz, 1H, H-5a), 3.58 (dd, $J_{4,5b} = 5.3$ Hz, $^2J_{5a,5b} = 11.1$ Hz, 1H, H-5b); δ_C (100 MHz; CDCl₃) 138.1, 137.5, 137.4 (3 \times Ar), 128.6, 128.5, 128.4, 128.1, 128.0, 128.0, 127.7, 127.6 (Ar), 112.6 (d, $J_{C1,F} = 224$ Hz, C1), 82.4 (C4), 78.9 (d, $J_{C2,F} = 30.1$ Hz, C2), 77.1 (C3), 73.4, 72.8, 72.8 (3 \times CH₂Ph), 70.2 (C5); δ_F (376 MHz; CDCl₃) -115.3 (dm, $J_{1,F} = 63.3$ Hz).

The diagnostic NMR signals for both anomers are in agreement with literature values.²²

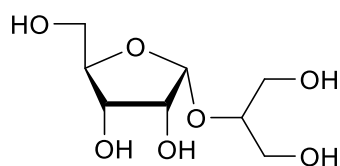
1,3-Bis(benzyloxy)propan-2-yl 2,3,5-tri-O-benzyl- α -D-ribofuranoside (**35**)



2,3,5-Tri-O-benzyl- β -D-ribofuranosyl fluoride (**28**) (210 mg, 0.5 mmol), SnCl₂ (95 mg, 0.5 mmol) and trityl perchlorate (170 mg, 0.5 mmol) were dissolved into a suspension of 4Å MS (1.0 g) in dry Et₂O (5 mL) under N₂. The reaction mixture was wrapped with aluminium foil to exclude light and cooled to -15 °C. 1,3-Di-O-benzyl glycerol (**13**) (100 μ L, 0.40 mmol, 0.8 eq) was added in a single portion and the reaction mixture was stirred for 6 hours before being placed in the fridge overnight. When TLC (hexane/EtOAc 7:3) showed consumption of the acceptor, the reaction mixture was diluted with Et₂O (50 mL), filtered and washed with saturated aqueous NH₄Cl solution (3 \times 10 mL). The organic layer was separated, dried over MgSO₄ and filtered before the solvent was removed under reduced pressure. The anomers were separated by FCC to give the title compound (**35**) (148 mg, 44%) as a colourless oil: R_f 0.10 (hexane/Et₂O 7:3); [α]_D +52.5 (c 1.0, CHCl₃); δ _H(400 MHz; CDCl₃) 7.32-7.18 (m, 25H, Ar), 5.38 (d, $J_{1',2'}$ = 4.3 Hz, 1H, H-1'), 4.73-4.38 (m, 10H, 5 \times PhCH₂), 4.26-4.24 (m, 1H, H-4'), 4.23-4.17 (m, 1H, H-2), 3.82 (dd, $J_{2',3'}$ = 7.1 Hz, $J_{3',4'}$ = 3.9 Hz, 1H, H-3'), 3.75 (dd, $J_{1',2'}$ = 4.3 Hz, $J_{2',3'}$ = 7.1 Hz, 1H, H-2'), 3.74-3.59 (m, 4H, H-1,3), 3.41 (dd, $J_{4',5'a}$ = 3.9 Hz, $^2J_{5'a,5'b}$ = 10.6 Hz, 1H, H-5'a), 3.34 (dd, $J_{4',5'b}$ = 4.2 Hz, $^2J_{5'a,5'b}$ = 10.6 Hz, 1H, H-5'b); δ _C(100 MHz; CDCl₃) 138.6, 138.6, 138.4, 138.1, 138.0 (5 \times Ar), 128.3, 128.3, 128.2, 128.0, 127.9, 127.6, 127.6, 127.6, 127.5, 127.5, 127.4 (Ar), 101.5 (C1'), 81.5 (C4'), 77.2 (C2'), 75.6 (C2), 75.5 (C3'), 73.4, 73.4, 73.3 72.2, 72.0 (5 \times CH₂Ph), 71.7 (C1), 70.7 (C3), 69.9 (C5'); HRMS (ESI⁺) m/z calc. for C₄₃H₄₆O₇Na⁺ 697.3141 [M+Na]⁺ found 697.3129 [M+Na]⁺.

The β -anomer was a colourless oil: R_f 0.20 (hexane/Et₂O 7:3); [α]_D + 42.4 (c 1.0, CHCl₃); δ _H(400 MHz; CDCl₃) 7.31-7.22 (m, 25H, Ar), 5.30 (s, 1H, H-1'), 4.65-4.39 (m, 10H, PhCH₂), 4.36-4.30 (m, 1H, H-4'), 4.05-4.01 (m, 1H, H-2), 4.03 (dd, $J_{2',3'}$ = 4.8 Hz, $J_{3',4'}$ = 7.4 Hz, 1H, H-3'), 3.92 (d, $J_{2',3'}$ = 4.8 Hz, 1H, H-2'), 3.65-3.42 (m, 6H, H-1,3,5'a,5'b); δ _C(100 MHz; CDCl₃) 138.4, 138.3, 138.3, 138.0, 138.0, 128.4, 128.4, 128.3, 128.0, 127.8, 127.7, 127.6, 127.6, 127.5, 127.5 (Ar), 104.9 (C1'), 80.4 (C4'), 79.7 (C2'), 78.5 (C2), 74.8 (C3'), 73.4, 73.2, 73.0, 72.4, 72.1 (5 \times PhCH₂), 71.5 (C5'), 70.2 (C1), 70.2 (C3).

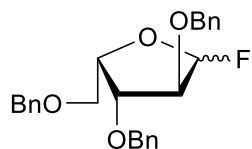
1,3-Dihydroxypropan-2-yl α -D-ribofuranoside (**3**)



1,3-Bis(benzyloxy)propan-2-yl 2,3,5-tri-O-benzyl- α -D-ribofuranoside (**35**) (80 mg, 120 μ mol) was dissolved in MeOH/EtOH (5:1, 12 mL) and palladium on activated charcoal (10% Pd basis) (50 mg) was added. The system was flushed with N₂ (\times 3) followed by H₂ (\times 3) and stirred overnight at room temperature. After the system had been flushed with N₂ (\times 3) the catalyst was filtered through Celite and the filter was washed with AcOH (50 mL). The organic washes were combined and the solvent was removed under reduced pressure to give the title compound (**3**) (20 mg, 75%); $[\alpha]_D +68.2$ (*c* 1.0, MeOH); δ_H (400 MHz; CD₃OD) 5.11 (d, $J_{1',2'} = 4.3$ Hz, 1H, H-1') 4.01-3.89 (m, 3H, H-4',2',3'), 3.72-3.47 (m, 7H, H-2,5'a,5'b,1,3); δ_C (100 MHz; CD₃OD) 102.0 (C1'), 85.9 (C4'), 79.0 (C2), 71.9 (C2'), 70.1 (C3'), 61.9 (C5'), 61.5 (C1), 60.8 (C3); HRMS (ESI⁺) *m/z* calc for C₈H₁₆O₇Na⁺ 247.0794 [M+Na]⁺ found 247.0798 [M+Na]⁺.

The 1,2-*trans* β -anomer 1,3-dihydroxypropan-2-yl β -D-ribofuranoside (**36**): δ_H (400 MHz; CD₃OD) 5.07 (s, 1H, H-1'), 4.22 (dd, $J_{2',3'} = 4.3$ Hz, $J_{3',4'} = 6.9$ Hz, 1H, H-3'), 4.03 (d, $J_{2',3'} = 4.3$ Hz, 1H, H-2'), 3.96-3.93 (m, 1H, H-4), 3.78-3.49 (m, 7H, H-2,1,3,5'a,5'b); δ_C (100 MHz; CD₃OD) 106.5 (C1'), 82.5 (C4'), 79.4 (C2), 74.7 (C2'), 70.0 (C3'), 61.7 (C1), 61.3 (C3), 60.6 (C5').

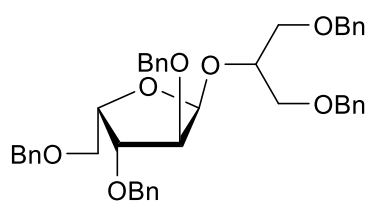
2,3,5-Tri-O-benzyl- β / α -L-xylofuranose fluoride (**30/31**)



2,3,5-Tri-O-benzyl-L-xylofuranose (**29**) (500 mg, 1.2 mmol) was dissolved in dry THF (10 mL), the solution was cooled to -30 °C and DAST (0.2 mL, 1.5 mmol) was added in a single portion. The reaction mixture was allowed to warm to room temperature and stirred for 20 minutes, after which time TLC (hexane/EtOAc indicated **29** had been consumed. The reaction mixture was cooled back to -30 °C and quenched with MeOH (0.5 mL). The solvent was removed under reduced pressure and the crude mixture of anomers was passed through a short silica

plug and the solvent was removed under reduced pressure to give the mixture of fluoride anomers (**31/30**) (450 mg, 90%) as a colourless oil. The ratios of anomers was judged to be α/β 1.0:0.3 by integration of the anomeric ^1H NMR signals; R_f 0.31 (hexane/EtOAc 8:2); δ_{H} (400 MHz; CDCl_3) 7.38-7.25 (m, 26H, Ar), 5.74 (d, $J_{1\beta,F} = 64.6$ Hz, 1H, H-1 β), 5.67 (dd, $J_{1\alpha,F} = 64.8$ Hz, $J_{1\alpha,2\alpha} = 3.5$ Hz, 0.3H, H-1 α), 4.68-5.90 (m, 11.7H, H-4 α ,4 β ,PhCH $_2$), 4.35 (dd, $J_{2\alpha,3\alpha} = 6.5$ Hz, $J_{3\alpha,4\beta} = 6.5$ Hz, 0.3H, H-3 α), 4.15 (d, $J_{2\beta,F} = 6.8$ Hz, 1H, H-2 β), 4.13 (ddd, $J_{2\alpha,F} = 18.9$ Hz, $J_{1\alpha,2\alpha} = 3.5$ Hz, $J_{2\alpha,3\alpha} = 6.5$ Hz, 0.3H, H-2 α) 4.07 (d, $J_{3\beta,4\beta} = 5.7$ Hz, 1H, H-3 β), 3.84 (dd, $J_{4\alpha,5a\alpha} = 5.1$ Hz, $J_{5a\alpha,5b\alpha} = 10.3$ Hz, 1H, H-5a α), 3.76 (dd, $J_{4\alpha,5b\alpha} = 7.0$ Hz, $^2J_{5a\alpha,5b\alpha} = 10.3$ Hz, 1H, H-5b α), 3.70 (dd, $J_{4\beta,5a\beta} = 3.9$ Hz, $J_{5a\beta,5b\beta} = 10.9$ Hz, 1H, H-5a β), 3.60 (dd, $J_{4\beta,5b\beta} = 5.8$ Hz, $^2J_{5a\beta,5b\beta} = 10.9$ Hz, 1H, H-5b β); δ_{C} (100 MHz; CDCl_3) 138.2 (C=O β), 138.1 (C=O α), 137.8 (C=O α), 137.5 (C=O β), 134.4 (C=O α), 137.0 (C=O β), 128.6, 128.6, 128.5, 128.5, 128.4, 128.2, 128.1, 128.0, 127.9, 127.8, 127.8, 127.8, 127.7, 127.7, 127.7, 127.6 (Ar), 113.3 (d, $J_{\text{C}1\beta,F} = 225$ Hz, C1 β), 107.5 (d, $J_{\text{C}1\alpha,F} = 230$ Hz, C1 α), 85.1 (d, $J_{2\beta,F} = 31.0$ Hz, C2 β), 83.9 (d, $J_{2\alpha,F} = 21.0$ Hz, C2 α), 83.3 (d, $J_{4,F} = 2.4$ Hz, C4 β), 80.1 (C3 β), 80.0 (C3 α), 78.4 (C4 α), 73.5 (PhCH $_2$ β), 73.5 (PhCH $_2$ α), 72.9 (PhCH $_2$ α), 72.8 (PhCH $_2$ α), 72.5 (PhCH $_2$ β), 72.2 (PhCH $_2$ β), 69.3 (C5 β), 68.7 (C5 α); δ_{F} (376 MHz; CDCl_3) -177.4 (ddd, $J_{1,F} = 64.6$, $J_{2,F} = 6.8$ Hz, $J_{4,F} = 6.8$ Hz, F β), -133.0 (dd, $J_{1,F} = 64.8$ Hz, $J_{2,F} = 18.9$ Hz, F α); HRMS (ESI $^+$) m/z calc. for $\text{C}_{26}\text{H}_{27}\text{FO}_4\text{Na}^+$ 445.1786 [M+Na] $^+$ found 445.1791 [M+Na] $^+$.

1,3-Bis(benzyloxy)propan-2-yl 2,3,5-tri-O-benzyl- α -L-xylofuranoside (**37**)

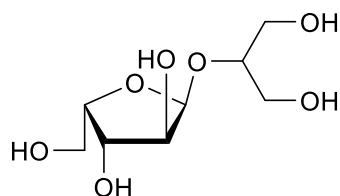


2,3,5-Tri-O-benzyl- β/α -L-xylofuranosyl fluoride (**30/31**) (200 mg, 0.47 mmol) and 1,3-di-O-benzyl glycerol (**13**) (100 μL , 0.4 mmol) were dissolved into a suspension of 4 \AA MS (1.0 g) in Et_2O (5 mL). The suspension was cooled to 0 $^\circ\text{C}$ in an ice bath and SnCl_2 (90 mg, 0.47 mmol) was added in a single portion to initiate the reaction. The reaction mixture was then kept in a refrigerator overnight at 4 $^\circ\text{C}$. The next morning the reaction mixture was filtered and the solvent removed *in vacuo* to give a crude mixture, which was judged to contain a mixture of α/β 1.0:0.8 by ^1H NMR. The crude mixture was purified by FCC to give the two anomers gave the title compound (**37**) (59 mg, 19%) as a colourless oil; R_f 0.48 (hexane/ Et_2O 7:3); $[\alpha]_{\text{D}} -39.6$ (c 1.0, DCM); δ_{H} (400 MHz; CDCl_3) 7.31-7.22 (m, 25H, Ar), 5.35 (d, $J_{1',2'} = 4.3$ Hz, 1H, H-1'), 4.71

(d, $^2J_{\text{PhCHH,PhCHH}} = 11.9$ Hz, 1H, PhCHH), 4.63 (d, $^2J_{\text{PhCHH,PhCHH}} = 11.9$ Hz, 1H, PhCHH), 4.57 (d, $^2J_{\text{PhCHH,PhCHH}} = 12.1$ Hz, 1H, PhCHH), 4.53-4.45 (m, 7H, 3.5 × PhCH₂), 4.43-4.41 (m, 1H, H-4'), 4.31 (dd, $J_{2',3'} = 5.9$ Hz, $J_{3',4'} = 7.0$ Hz, 1H, H-3'), 4.20-4.15 (m, 1H, H-2), 3.97 (dd, $J_{1',2'} = 4.3$ Hz, $J_{2',3'} = 5.9$ Hz, 1H, H-2'), 3.74-3.54 (m, 6H, H-5'a,1,3,5'b); δ_{C} (100 MHz; CDCl₃) 138.4, 138.4, 138.3, 138.3, 137.9, 128.4, 128.4, 128.3, 128.3, 128.0, 127.7, 127.7, 127.6, 127.6, 127.5, 127.5 (Ar), 99.9 (C1'), 83.8 (C2;), 81.6 (C3'), 76.0 (C4'), 75.4 (C2), 73.4, 73.4, 73.3, 72.4, 71.8 (4 × PhCH₂), 71.5 (C1), 70.4 (C3), 69.4 (C5'); HRMS (ESI⁺) m/z calc. for C₄₃H₄₆O₇Na⁺ 697.3141 ([M+Na]⁺) found 697.3129 [M+Na]⁺.

The β anomer (32 mg, 12%) was a colourless oil; R_f 0.54 (hexane/Et₂O 7:3); $[\alpha]_{\text{D}} +5.6$ (c 1.0, DCM); δ_{H} (400 MHz; CDCl₃) 7.32-7.23 (m, 25H, Ar), 5.31 (d, $J_{1',2'} = 1.9$ Hz, 1H, H-1'), 4.58-4.40 (m, 11H, 5 × PhCH₂, H-4'), 4.11-4.06 (m, 3H, H-2',3',2), 3.76 (dd, $J_{4',5'a} = 4.9$ Hz, $^2J_{5'a,5'b} = 10.3$ Hz, 1H, H-5'a), 3.71 (dd, $J_{4',5'b} = 3.7$ Hz, $^2J_{5'a,5'b} = 10.3$ Hz, 1H, H-5'b), 3.71-3.55 (m, 4H, H-1,3); δ_{C} (100 MHz; CDCl₃) 138.5, 138.4, 138.3, 138.0, 137.7, 128.4, 128.3, 128.3, 128.3, 127.8, 127.7, 127.7, 127.6, 127.6, 127.6, 127.5, 127.5, 127.5 (Ar), 107.0 (C1'), 86.8 (C2'), 82.0 (C3'), 79.9 (C4'), 75.7 (C2), 73.4, 73.3, 73.3, 72.0, 71.8 (5 × PhCH₂), 70.7 (C1), 70.4 (C3), 69.8 (C5');

1,3-Dihydroxypropan-2-yl α -L-xylofuranoside (**4**)

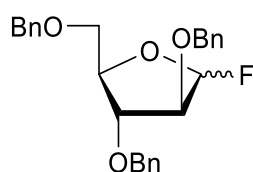


1,3-Bis(benzyloxy)propan-2-yl 2,3,5-tri-*O*-benzyl- α -L-xylofuranoside (**37**) (100 mg, 145 μ mol) was dissolved in a mixture of MeOH/n-PrOH (9:1) (20 mL) and palladium on activated charcoal (10% Pd basis) (50 mg) was added. The system was flushed with N₂ ($\times 3$) followed by H₂ ($\times 3$) and stirred overnight at room temperature. After the system had been flushed with N₂ ($\times 3$) the catalyst was filtered through Celite and the filter was washed with MeOH (20 mL). The organic washes were combined and the solvent was removed under reduced pressure to give the title compound (**4**) (16 mg, 45%) as a colourless oil; R_f 0.28 (DCM/MeOH 85:15); $[\alpha]_{\text{D}} -139$ (c 1.0 MeOH) 5.09 (d, $J_{1',2'} = 4.4$ Hz, 1H, H-1'), 4.16-4.08 (m, 2H, H-3',4'), 3.92 (dd, $J_{1',2'} = 4.4$ Hz, $J_{2',3'} = 4.4$ Hz, 1H, H-2'), 3.65-3.51 (m, 7H, H-2,1,3,5'); δ_{H} (400 MHz; MeOH)

101.3 (C1'), 80.0 (C2), 78.7 (C4'), 78.1 (C2'), 75.7 (C3'), 61.7 (C5'), 61.2 (C1), 61.0 (C3); (HRMS ESI⁺) m/z calc for C₈H₁₆NaO₇⁺ 247.0794 ([M+Na]⁺) found 247.0785 [M+Na]⁺.

The β-anomer (5.6 mg, 29%) was a colourless oil; R_f 0.65 (DCM/MeOH 8:2); [α]_D + 4.6 (c 0.2, MeOH); δ_H(400 MHz; CD₃OD) 5.10 (s, 1H, H-1'), 4.38 (m, 1H, H-4'), 4.12-4.10 (m 2H, H-2',3'), 3.84-3.83 (m, 2H, H-5'a,5'b), 3.77-3.75 (m, 1H, H-2), 3.72-3.59 (m, 4H, H-1,3); δ_C(100 MHz; CD₃OD) 108.0 (C1'), 82.6 (C4'), 81.0 (C2'), 79.4 (C2), 72.3 (C3'), 61.8 (C1), 61.0 (C5',C3); (HRMS ESI⁺) m/z calc for C₈H₁₆NaO₇⁺ 247.0794 ([M+Na]⁺) found 247.0785 [M+Na]⁺.

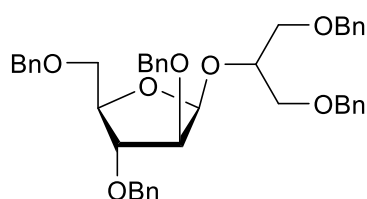
2,3,5-Tri-*O*-benzyl-α/β-D-arabinofuranosyl fluoride (**33/34**)²⁴



2,3,5-Tri-*O*-benzyl-α-D-arabinofuranose (**32**) (1.0 g, 2.4 mmol) was dissolved into dry DCM (10 mL) and the solution cooled in an ice bath. Diethylaminosulfur trifluoride (DAST) (390 μL, 2.9 mmol) was added in a single portion and the reaction mixture was allowed to warm to and was stirred at room temperature for 30 minutes. The reaction mixture was then cooled in an ice bath and MeOH (300 μL) was added to quench any unreacted DAST and the reaction mixture was again allowed to warm to and was stirred at room temperature for 30 minutes. The reaction mixture was then diluted with DCM (20 mL) and washed with saturated aqueous NaHCO₃ solution (2 × 10 mL). The aqueous extract was washed with DCM (3 × 5 mL) and the organic layers were combined, dried over MgSO₄, filtered and dried *in vacuo* to give the title compounds as a 5:3:1 mixture α/β mixture of anomers (**33/34**) (950 mg, 94%). The crude mixture was judged by NMR as clean enough used in the step without further purification; R_f 0.73 (α) 0.66 (β) (hexane/ethyl acetate 8:2); δ_H(400 MHz; CDCl₃) 7.37-7.25 (m, 15H, Ar), 5.78 (d, *J*_{1,F} = 61.5 Hz, 1H, H-1α), 5.62 (dd, *J*_{1,F} = 64.9 Hz, *J*_{1,2} = 3.5 Hz, H-1β), 4.56-4.46 (m, 7H, 3 × PhCH₂ & H-4α), 4.16 (dd, *J*_{2,F} = 9.3 Hz, *J*_{2,3} = 2.0 Hz, 1H, H-2α), 3.97 (dd, *J*_{2,3} = 2.0 Hz, *J*_{3,4} = 5.2 Hz, 1H, H-3α), 3.64-3.57 (m, 2H, H-5α & H-5α'); δ_C(100 MHz; CDCl₃) 137.9, 137.5, 137.0 (3 × Ar), 128.6, 128.5, 128.4, 128.1, 127.9, 127.8, 127.8, 127.8, 127.7,

113.6 (d, $J_{C1,F} = 224.7$ Hz, C1 α), 108.4 (d, $J_{C1,F} = 232.3$ Hz, C1 β), 86.9 (d, $J_{C2,F} = 33.9$ Hz, C2 α), 84.1 (C4 α), 82.5 (C3 α), 73.5, 72.1, 72.1 (3 \times PhCH₂), 69.4 (C5 α); δ_F (376 MHz; CDCl₃) -120.6 (dd, $J_{1,F} = 61.4$ Hz, $J_{2,F} = 9.0$ Hz, α -fluoride), 126.6 (ddd, $J_{1,F} = 64.6$ Hz, $J_{2,F} = 20.6$ Hz, $J_{3,F} = 6.1$ Hz, β -fluoride); HRMS (ESI⁺) m/z calc. for C₂₆H₂₇FO₄Na 445.1786 [M+Na]⁺ found 445.1784 [M+Na]⁺. The ¹H, ¹³C and ¹⁹F NMR diagnostic signals were in agreement with literature values.²⁴

1,3-Bis(benzyloxy)propan-2-yl 2',3',5'-tri-O-benzyl- β -D-arabinofuranoside (**38**)

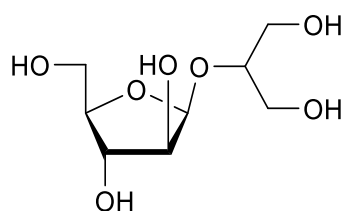


2,3,5-Tri-*O*-benzyl- α/β -D-arabinofuranosyl fluoride (**33/34**) (950 mg, 2.3 mmol) and 1,3-di-*O*-benzyl glycerol (**13**) (540 μ L, 2.2 mmol) were dissolved into a suspension of 4Å MS (1.0 g) in Et₂O (7 mL). The suspension was cooled in an ice bath and SnCl₂ (440 mg, 2.3 mmol) was added in a single portion to initiate the reaction. The reaction mixture was then kept in a refrigerator overnight at 4 °C. The next morning the reaction mixture was filtered and the solvent removed *in vacuo* to give a crude mixture. The anomers were challenging to completely separate by FCC, and as such not all of the crude mixture was purified. Three rounds of chromatography gave the β -anomer (**38**) (560 mg, 37%) also as a colourless oil; R_f 0.46 (hexane/Et₂O 6:4); $[\alpha]_D -38.7$ (c 1.0, CHCl₃); δ_H (400 MHz; CDCl₃) 7.32-7.24 (m, 25H, Ar), 5.32 (d, $J_{1',2'} = 4.4$ Hz, 1H, H-1'), 4.71-4.36 (m, 10H, 5 \times PhCH₂), 4.13-4.06 (m, 3H, H-3',4',2), 4.03 (dd, $J_{1',2'} = 4.4$ Hz, $J_{2',3'} = 7.0$ Hz, 1H, H-2'), 3.71 (dd, $J_{4',5'} = 3.4$ Hz, $^2J_{5a',5b'} = 10.3$ Hz, 1H, H-5a'), 3.64-3.47 (m, 5H, H-5b',1,3); δ_C (100 MHz; CDCl₃) 138.4, 138.3, 138.3, 138.2, 137.9 (5 \times Ar), 128.4, 128.4, 128.4, 128.3, 128.0, 127.8, 127.7, 127.7, 127.7, 127.6, 127.6, 127.6, (Ar), 100.8 (C1'), 83.7 (C2'), 83.1 (C3'), 80.1 (C4'), 75.6 (C2), 73.5, 73.3, 73.1 (3 \times PhCH₂), 72.6 (C1), 72.3, 71.8 (2 \times PhCH₂), 71.3 (C5'), 70.3 (C3); HRMS (ESI⁺) m/z calc. for C₄₃H₄₆O₇ 697.3136 [M+Na]⁺ found 697.3132 [M+Na]⁺.

The 1,2-*trans* α -anomer (47 mg) was as a colourless oil R_f 0.46 (hexane/Et₂O 6:4); $[\alpha]_D + 26.8$ (c 1.0, CHCl₃); δ_H (400 MHz; CDCl₃) 7.35-7.22 (m, 25H, Ar), 5.35 (bs, 1H, H-1'), 4.57-4.41 (m, 10H, 5 \times PhCH₂), 4.23 (dm, $J_{3',4'} = 7.3$ Hz, 1H, H-4'), 4.15-4.09 (m, 1H, H-2), 4.08 (d, $J_{2',3'} = 3.4$ Hz, 1H, H-2'), 3.92 (dd, $J_{2',3'} = 3.4$ Hz, $J_{3',4'} = 7.3$ Hz, 1H, H-3'), 3.70 (dd, $J_{1,2} = 3.8$ Hz, $^2J_{1a,1b} = 10.2$

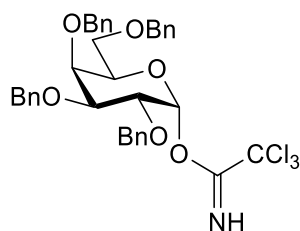
Hz, 1H, H-1a), 3.65-3.54 (m, 5H, H-1b,3,5'); δ_c (100 MHz; CDCl₃) 138.4, 138.3, 138.2, 138.0, 137.7 (5 × Ar), 128.4, 128.3, 128.0, 127.8, 127.7, 127.7, 127.6, 127.6, 127.5 (Ar), 106.1 (C1'), 88.5 (C2'), 83.7 (C3'), 80.3 (C4'), 75.0 (C2), 73.4 73.3, 73.3, 72.1, 71.8 (5 × PhCH₂), 70.8 (C1), 70.5 (C3), 69.6 (C5'); HRMS (ESI⁺) m/z calc. for C₄₃H₄₆O₇ 697.3136 [M+Na]⁺ found 697.3132 [M+Na]⁺.

1,3-Dihydroxypropan-2-yl β-D-arabinofuranoside (5)



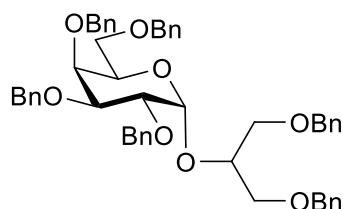
1,3-Bis(benzyloxy)propan-2-yl 2',3',5'-tri-*O*-benzyl- β-D-arabinofuranoside (**38**) (560 mg, 0.8 mmol) was dissolved in a mixture of MeOH/EtOAc (9:1) (50 mL) and palladium on activated charcoal (10% Pd basis) (50 mg) was added. The system was flushed with N₂ (×3) followed by H₂ (×3) and stirred for 48 hours at room temperature. After the system had been flushed with N₂ (×3) the catalyst was filtered through Celite and the filter was washed with MeOH (20 mL). The organic washes were combined and the solvent was removed under reduced pressure to give the title compound (**5**) (80 mg, 45%) as a colourless oil; R_f 0.45 (DCM/MeOH 85:15); [α]_D -78.1 (c 1.0, MeOH); δ_H (400 MHz; MeOH) 5.05 (d, $J_{1',2'} = 4.7$ Hz, 1H, H-1'), 4.18 (dd, $J_{2',3'} = 8.0$ Hz, $J_{3',4'} = 8.0$ Hz, 1H, H-3'), 4.00 (dd, $J_{1',2'} = 4.7$ Hz, $J_{2',3'} = 8.0$ Hz, 1H, H-2'), 3.78-3.73 (m, 3H, H-1,4'), 3.72-3.68 (m, 1H, H-2), 3.66-3.61 (m, 4H, H-5',3); δ_c (100 MHz; MeOH) 101.3 (C1'), 82.5 (C2), 80.8 (C4'), 77.6 (C2'), 73.5 (C3'), 61.7 (C5'), 61.4 (C1,C3); HRMS (ESI⁺) m/z calc. for C₈H₁₆O₇Na⁺ 247.0794 [M+Na]⁺ found 247.0788 [M+Na]⁺.

2,3,4,6-Tetra-*O*-benzyl- α -D-galactopyranosyl trichloroacetimidate (**41**)³⁴



2,3,4,6-Tetra-*O*-benzyl- α -D-galactopyranose (**43**) (200 mg, 0.37 mmol) and CCl_3CN (370 μL , 3.7 mmol) were dissolved into DCM (8 mL) under N_2 and the reaction mixture cooled to 0 $^\circ\text{C}$. DBU (5 μL , 33 μmol) was added and the cooling bath was removed to allow the reaction mixture to stir at room temperature for 2 hours, after which time TLC (hexane/EtOAc 8:2) showed consumption of the starting material. The solvent was evaporated under reduced pressure and the crude reaction mixture was filtered through a silica plug (hexane/EtOAc 8:2) to give the title compound (**41**) (170 mg, 65%) as a yellow oil. δ_{H} (400 MHz; CDCl_3) 8.51 (s, 1H, C=NH), 7.36-7.15 (m, 20H, ArH), 6.52 (d, $J_{1,2} = 3.4$ Hz, 1H, H-1), 4.97 (d, $^2J = 11.3$ Hz, 1H, C⁴OBn), 4.82 (d, $^2J = 11.8$ Hz, 1H, C³OBn), 4.75 (d, $^2J = 11.8$ Hz, 1H, C³OBn), 4.74 (s, 2H, C²OBn), 4.59 (d, $^2J = 11.3$ Hz, 1H, C⁴OBn), 4.46 (d, $^2J = 11.7$ Hz, 1H, C⁶OBn), 4.40 (d, $^2J = 11.7$, 1H, C⁶OBn), 4.24 (dd, $J_{2,3} = 10.0$ Hz, $J_{1,2} = 3.4$ Hz, 1H, H-2), 4.17-4.14 (m, 1H, H-5), 4.06-4.05 (m, 1H, H-4), 4.02 (dd, $J_{2,3} = 10.0$ Hz, $J_{3,4} = 2.8$ Hz, 1H, H-3), 3.64-3.53 (m, 2H, H-6a & H-6b); δ_{C} (100 MHz; CDCl_3) 161.3 (C=NH), 138.6, 138.5, 138.4, 137.7 (4 \times Ph), 129.1 – 127.5 (Ph), 125.3 (CCl_3), 95.2 (C1), 77.8 (C3), 75.6 (C2), 75.0, (OCH₂Ph), 74.7 (C4), 73.5 (OCH₂Ph), 73.0 (OCH₂Ph), 72.9 (OCH₂Ph), 72.2 (C5), 68.3 (C6). ¹H and ¹³C NMR spectra are in good agreement with data extracted from spectra of an anomeric mixture.³⁴

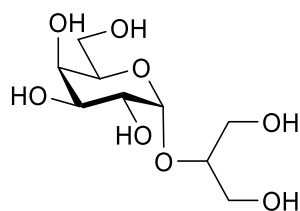
1,3-bis(benzyloxy)propan-2-yl 2',3',4',6'-tetra-*O*-benzyl- α -D-galactopyranoside (**40**)⁹



Tetra-*O*-benzyl- α -D-galactopyranosyl trichloroimidate (**41**) (165 mg, 0.24 mmol) and 1,3-di-*O*-benzyl glycerol (**13**) (140 μL , 0.56 mmol) were dissolved in a mixture of toluene/Et₂O (4:1, 5 mL) and cooled in an ice bath under N_2 . TMSOTf (35 μL , 15 mol%) was added in a single portion and the reaction mixture was allowed to warm to room temperature and stirred

overnight. The solvent mixture was evaporated under reduced pressure and the crude mixture was purified by FCC (hexane/EtOAc 9:1 to 7:3) to give the title compound (**40**) as a colourless oil (70 mg, 37%); R_f 0.51 (hexane/EtOAc 8:2); $[\alpha]_D = +26$ (c 1.0, CHCl_3); δ_H (400 MHz; CDCl_3) 5.23 (d, $J_{1',2'} = 3.7$ Hz, 1H, H-1'), 4.93 (d, $^2J = 11.4$ Hz, 1H, OCH_2Ph), 4.8 (d, $^2J = 11.7$ Hz, 1H, OCH_2Ph), 4.72 (d, $^2J = 11.7$ Hz, 1H, OCH_2Ph), 4.68 (s, 2H, OCH_2Ph), 4.55 (d, $^2J = 11.4$ Hz, 1H, OCH_2Ph), 4.51 (s, 1H, OCH_2Ph), 4.43–4.31 (m, 3H, OCH_2Ph), 4.19–4.16 (m, 1H, H-4'), 4.12–4.10 (m, 1H, H-2), 4.03 (dd, $J_{2',3'} = 9.7$ Hz, $J_{1',2'} = 3.7$ Hz, 1H, H-2'), 3.99–3.96 (m, 1H, H-5'), 3.94 (dd, $J_{2',3'} = 9.7$ Hz, $J_{3',4'} = 2.8$ Hz, 1H, H-3'), 3.64–3.47 (m, 6H, H-6'a,6'b,1,2); δ_C (100 MHz; CDCl_3) 139.0 – 138.2 (6 × Ar-C), 129.1 (Ar-H), 128.4 – 127.4 (16 × Ar-H), 125.32 (Ar-H), 97.0 (C1'), 79.0 (C3'), 77.2 (OCH_2Ph), 76.3 (C2'), 75.2 (C5'), 74.08 (OCH_2Ph), 74.8 (C2), 73.4 (OCH_2Ph), 73.4 (OCH_2Ph), 73.1 (OCH_2Ph), 72.7 (OCH_2Ph), 70.6 (C1), 70.4 (C3), 69.2 (C4'), 69.0 (C6'); HRMS (ESI⁺) m/z calc. for $\text{C}_{51}\text{H}_{54}\text{O}_8\text{Na}$ 817.3716 $[\text{M}+\text{Na}]^+$ found 817.3711 $[\text{M}+\text{Na}]^+$. The ^1H and ^{13}C NMR were in agreement with literature values.⁹

1,3-Dihydroxypropan-2-yl α -D-galactopyranoside (**7**)



1,3-Bis(benzyloxy)propan-2-yl 2',3',4',6'-tetra-O-benzyl- α -D-galactopyranoside (**40**) (70 mg, 90 μmol) was dissolved in MeOH (10 mL) and palladium on activated charcoal (10% Pd basis) (50 mg) was added. The system was flushed with N_2 ($\times 3$) followed by H_2 ($\times 3$) and stirred for 48 hours at room temperature. After the system had been flushed with N_2 ($\times 3$) the catalyst was filtered through Celite and the filter was washed with MeOH (20 mL). The organic washes were combined and the solvent was removed under reduced pressure to give 1,3-dihydroxypropan-2-yl α -D-galactopyranoside (**7**) (16 mg, 72%) as a white powder; $[\alpha]_D = +86^\circ$ (c 1.0, MeOH); δ_H (400 MHz; D_2O) 5.02 (d, $J_{1',2'} = 3.8$ Hz, 1H, H-1'), 3.99–3.96 (m, 1H, H-5'), 3.86 (d, $J_{3',4'} = 2.8$ Hz, 1H, H-4'), 3.78 (dd, $J_{2',3'} = 10.2$ Hz, $J_{3',4'} = 2.8$ Hz, 1H, H-3'), 3.70 (dd, $J_{2',3'} = 10.2$ Hz, $J_{1',2'} = 3.8$ Hz, 1H, H-2'), 3.68–3.67 (m, 2H, H-6'a, 6'b), 3.64–3.60 (m, 5H, H-1,2,3); δ_C (100 MHz; D_2O) 98.0 (C1'), 78.7 (C2), 71.0 (C5'), 69.3 (C3'), 69.2 (C4'), 68.4 (C2'), 61.3 (C1), 61.1 (C3), 60.3 (C6'); HRMS (ESI⁺) m/z calc. for $\text{C}_9\text{H}_{18}\text{O}_8$ 277.0899 $[\text{M}+\text{Na}]^+$ found 277.0898 $[\text{M}+\text{Na}]^+$.

4.6 References:

1. T. Igarashi, M. Satake, and T. Yasumoto, *J. Am. Chem. Soc.*, 1999, **121**, 8499–8511.
2. S. A. Rasmussen, S. Meier, N. G. Andersen, H. E. Blossom, J. Ø. Duus, K. F. Nielsen, P. J. Hansen, and T. O. Larsen, *J. Nat. Prod.*, 2016, **79**, 2250–2256.
3. T. Igarashi, M. Satake, and T. Yasumoto, *J. Am. Chem. Soc.*, 1996, **118**, 479–480.
4. J. Kennedy, J. Wu, K. Drew, I. Carmichael, and A. S. Serianni, *J. Am. Chem. Soc.*, 1997, **119**, 8933–8945.
5. D. K. Hinch and M. Hagemann, *Biochem. J.*, 2004, **383**, 277–283.
6. R. Suhr, O. Scheel, and J. Thiem, *J. Carbohydr. Chem.*, 1998, **17**, 937–968.
7. A. Courtois, *Mar. Drugs*, 2008, **6**, 407–417.
8. B. Thollas and C. Boisset, *Synlett*, 2007, **2007**, 1736–1738.
9. M. Weïwer, T. Sherwood, and R. J. Linhardt, *J. Carbohydr. Chem.*, 2008, **27**, 420–427.
10. M. Horisberger, B. A. Lewis, and F. Smith, *Carbohydr. Res.*, 1972, **23**, 175–182.
11. A. J. Charlson, P. A. J. Gorin, and A. S. Perlin, *Can. J. Chem.*, 1957, **35**, 365–373.
12. W. Koenigs and E. Knorr, *Berichte der Dtsch. Chem. Gesellschaft*, 1901, **34**, 957–981.
13. D. Crich, A. L. J. Beckwith, C. Chen, Q. Yao, I. G. E. Davison, R. W. Longmore, C. Anaya de Parrodi, L. Quintero-Cortes, and J. Sandoval-Ramirez, *J. Am. Chem. Soc.*, 1995, **117**, 8757–8768.
14. Y. D. Wu and K. N. Houk, *J. Am. Chem. Soc.*, 1987, **109**, 908–910.
15. N. Bartlett, L. Gross, F. Péron, D. J. Asby, M. D. Selby, A. Tavassoli, and B. Linclau, *Chem. Eur. J.*, 2014, **20**, 3306–3310.
16. R. Das and B. Mukhopadhyay, *ChemistryOpen*, 2016, **5**, 401–433.
17. C. Marino, O. Varela, and R. M. de Lederkremer, *Carbohydr. Res.*, 1989, **190**, 65–76.
18. Q. Zhang and H. Liu, *J. Am. Chem. Soc.*, 2000, **122**, 9065–9070.
19. V. M. Mendoza, G. A. Kashiwagi, R. M. de Lederkremer, and C. Gallo-Rodriguez, *Carbohydr. Res.*, 2010, **345**, 385–396.
20. C. Gauthier, J. Legault, S. Lavoie, S. Rondeau, S. Tremblay, and A. Pichette, *Tetrahedron*, 2008, **64**, 7386–7399.
21. B. Mukhopadhyay, K. P. R. Kartha, D. A. Russell, and R. A. Field, *J. Org. Chem.*, 2004, **69**, 7758–7760.
22. T. Mukaiyama, Y. Hashimoto, and S. Shoda, *Chem. Lett.*, 1983, 935–938.
23. H. Uchiro and T. Mukaiyama, *Chem. Lett.*, 1996, 271–272.
24. W. Rosenbrook, D. A. Riley, and P. A. Lartey, *Tetrahedron Lett.*, 1985, **26**, 3–4.

25. G. H. Posner and S. R. Haines, *Tetrahedron Lett.*, 1985, **26**, 5–8.
26. A. Cossé-Barbi, D. . Watson, and J. . Dubois, *Tetrahedron Lett.*, 1989, **30**, 163–166.
27. H. A. V Kistemaker, H. S. Overkleef, G. A. Van Der Marel, and D. V. Filippov, *Org. Lett.*, 2015, **17**, 4328–4331.
28. S. S. Nigudkar and A. V Demchenko, *Chem. Sci.*, 2015, **6**, 2687–2704.
29. B. Yu and H. Tao, *Tetrahedron Lett.*, 2001, **42**, 2405–2407.
30. H.-S. Dang, B. P. Roberts, J. Sekhon, and T. M. Smits, *Org. Biomol. Chem.*, 2003, **1**, 1330–1341.
31. I. Konstantinova, K. Antonov, I. Fateev, A. Miroshnikov, V. Stepchenko, A. Baranovsky, and I. Mikhailopulo, *Synthesis (Stuttg.)*, 2011, **2011**, 1555–1560.
32. E. C. Garnier and L. S. Liebeskind, *J. Am. Chem. Soc.*, 2008, **130**, 7449–7458.
33. W. R. Longworth and C. P. Mason, *J. Chem. Soc. A Inorganic, Phys. Theor.*, 1966, 1164–1167.
34. N. Santschi and R. Gilmour, *European J. Org. Chem.*, 2015, **2015**, 6983–6987.

**5 Synthesis of a glycosylated
prymnesin-1 inspired fragment with a
view to developing an antibody based
prymnesin toxin detection device**

5.1 Introduction

5.1.1 Detection of *Prymnesium parvum*

One of the simplest methods of detecting *Prymnesium parvum* is by optical light microscopy.¹ More recently, solid phase cytometry (SPC) methods have been employed using monoclonal antibodies to quantify the levels of some strains of *P. parvum* in natural samples.^{1,2} For example, Moreau *et al.*² raised monoclonal antibodies against five strains of *P. parvum* in mice; these antibodies were then used in an indirect immunofluorescence assay, and the levels of algae quantified by SPC. This method was shown to work with natural *P. parvum* samples, although the antibodies exhibited very narrow specificity for only a few *P. parvum* strains.² Real-time polymerase chain reaction (PCR) detection and quantification has also been developed for several strains of *P. parvum*.³ Galluzzi *et al.*³ have developed a quantitative polymerase chain reaction (qPCR) assay designed on the internal transcribed spacer 2 rDNA region of *P. parvum*. They found this assay to be both sensitive and specific to *P. parvum*, with a limit of detection of 2500 cells per mL. Project collaborators at the University of East Anglia (UEA) have recently developed a qPCR assay specific to the strain of *P. parvum* found in the Norfolk Broads.

It is worth noting, however, that none of these methods can help with quantifying toxin levels in water samples. It has been noticed that in some cases blooms of *P. parvum* do not necessarily lead to fish kills, which would suggest that there is not an active mode of toxin release into water systems.⁴ Work in our group by Wagstaff *et al.*⁵ has reported a new double stranded DNA megavirus, PpDNAV, which infects the local strain of *P. parvum* in the Norfolk Broads. In their paper Wagstaff *et al.*⁵ suggest that viral infection of *Prymnesium* blooms leads to rapid cell lysis of a *P. parvum* population, and as such there is a passive mass toxin release into the water system. It would therefore seem prudent not to rely too heavily on *P. parvum* cell counts alone when assessing the likelihood of a prymnesin toxin induced fish-kill.

5.1.2 Detection of polyketide algal toxins

Antibody based detection and quantification systems have been developed for polyketide algal toxins such as okadaic acid and brevetoxins.^{6,7} For example Elliot *et al.*⁸ developed a competitive immunoassay lateral flow device for the polyketide toxin okadaic acid which is the basis for the schematic shown in Figure 5.1. A sample is loaded onto the sample pad where it is wicked through the reagent pad containing colloidal gold nanoparticles

conjugated with antitoxin antibodies. If the sample contains toxin then this binds with the antitoxin antibodies on the gold nanoparticles (AuNP). The resulting complex is then wicked through a nitrocellulose membrane containing a test zone with protein bound toxin and a control zone with surface bound anti-species antibody. The test zone captures any antitoxin antibody-AuNP conjugate which is not already bound with toxin in the sample. Therefore, the more toxin present in the sample, the lower the intensity of the signal at the test zone. The control zone anti-species antibody will always bind with antitoxin antibodies, regardless of whether or not they have bound with toxin.⁸

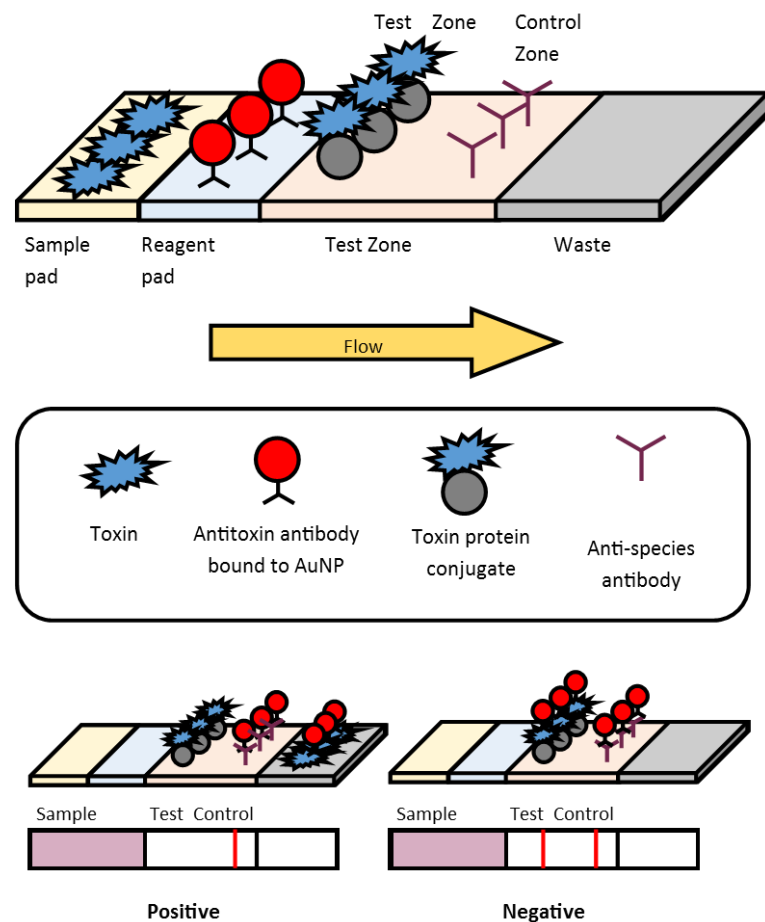


Figure 5.1 - Diagram of a competitive immunoassay lateral flow device, showing the composition of a typical test strip.⁸ The key interactions for a positive and negative result due to the presence or lack thereof of toxin in a sample are also shown.

Because the intensity of the test response is inversely proportional to the amount of toxin present in a sample, Elliot *et al.*⁸ were able to use a commercially available immunofluorescence assay reader to quantify the level of okadaic acid in a sample, with a limit of detection was 25 µg/kg of shellfish.

A lateral flow immunodipstick device has been developed by Zhang *et al.*⁹ for the detection and quantification of the algal cyclic polyether neurotoxin, brevetoxin B, which was shown to work with spiked seafood samples as well as lab based controls. By using hollow gold-nanospheres rather than gold colloids they could obtain a limit of detection for brevetoxin B of between 0.1 – 1.5 ng/mL. The increase in sensitivity may be attributed to the comparatively large surface area of hollow nanoparticles, which allows for a higher loading of antibodies when compared with non-hollow nanoparticles.¹⁰

To date, however, no such system has been developed for prymnesin toxins. This is most probably because of the difficulties involved in obtaining sufficient quantities of suitably purified toxins for animal immunisation; Igarashi *et al* (1996).¹¹ obtained 10 mg of prymnesin-1 and 15 mg of prymnesin-2 from 400 L of *P. parvum* culture, whilst Rasmussen *et al.*¹² obtained just 1.8 mg of prymnesin-B1 and 1.0 mg of prymnesin-2 from 100 L of *P. parvum* culture. As well as the toxin required for antibody production, toxin is also required for a competitive immunoassay device, and as such it is not feasible to access suitable quantities of prymnesin toxins from lab extracts. An alternative strategy would be to try and use a synthetic fragment of a prymnesin toxin (Figure 5.2).

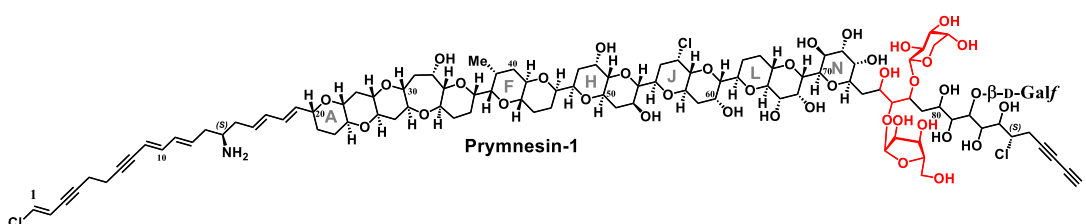


Figure 5.2 – The chemical structure of prymnesin-1, with the synthetic target region (glycosylated with α -L-arabinopyranose and α -D-ribofuranose) highlighted in red.

5.1.3 Exploring antibody based prymnesin detection

The glycosylated region of prymnesin-1 (Figure 5.2) offers an interesting target for producing antibodies. Antibodies to carbohydrates can give ‘exquisite specificity and sensitivity’,¹³ which make them potentially very powerful tools for the detection of prymnesin toxins. However, carbohydrates are themselves poor antigens which only elicit a B-cell response; this results in the production of low affinity IgM antibodies with no long term memory.^{13,14} Furthermore, repeated doses of a carbohydrate antigen may lead to a reduction in antibody production (hypo-responsiveness).¹⁴ By conjugating the carbohydrate antigen with a carrier protein, it is possible to elicit a T-cell response which leads to antibody production and

immune memory.^{14,15} This leads to the production of higher concentrations of antibodies, and an elevated immune response towards booster immunisations. The choice of carrier protein is partly dictated by the species being immunised against the glycoprotein. For human immunisation, diphtheria or tetanus toxoid are often used as the host is often already vaccinated against these antigens, and so a better immune response is seen.¹³ However, this is unlikely the case for animals, and as such the much cheaper alternative, bovine serum albumin (BSA) has proved an effective and convenient carrier protein.¹³ For joining the carbohydrate based prymnesin fragment with a carrier protein there are a plethora of available methods,¹⁶ and some of these are discussed in more detail later in this chapter.

A general overview of the process envisaged is shown in Figure 5.3, whereby a glycosylated fragment inspired by prymnesin-1 is conjugated to a carrier protein decorated with a suitable linker. The blue star on the fragment and the red stars on the protein linkers represent complimentary functional groups for 'click' or cross coupling reactions. Once coupled, this toxin fragment-protein conjugate would then be used to inoculate an animal, the immune system of which produces antibodies against the antigen presented by the carrier protein.¹⁵ These antibodies would be harvested from the animal and if found to be specific for the prymnesin-1 toxin then they would be incorporated into a lateral flow device (Figure 5.1).^{17,18} Such a device would be of use to stakeholders in the project as it would allow a very simple, cost effective way of detecting prymnesin-1 toxins in waterways.

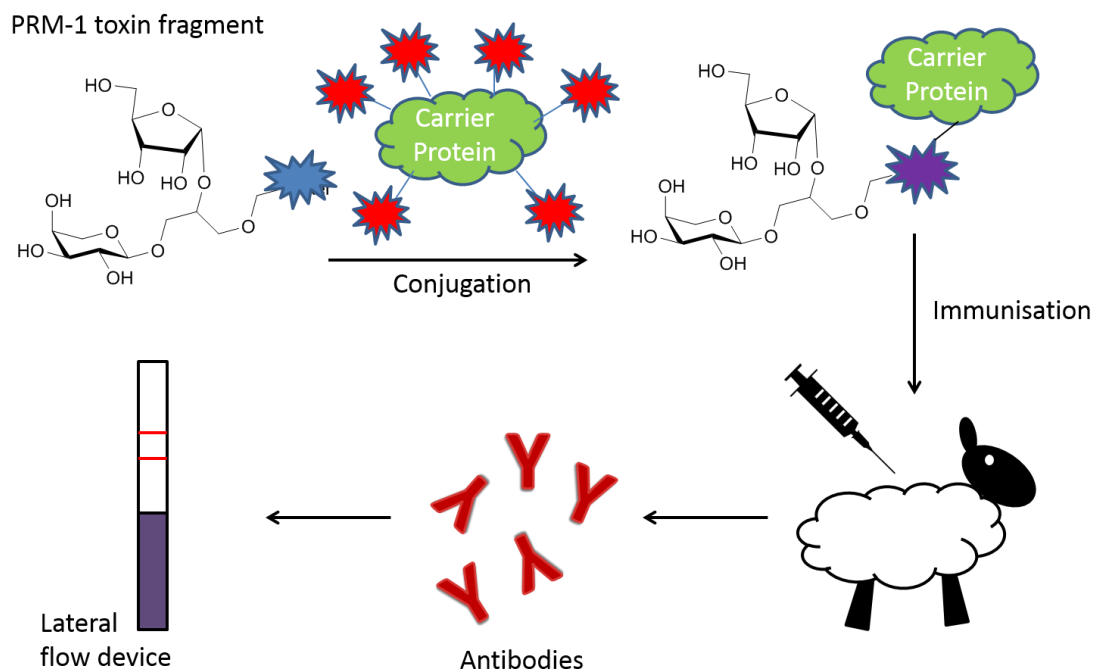


Figure 5.3 – An abstract overview of how a synthetic fragment might be utilised to develop a lateral flow device based toxin detection system. Cross coupling groups on the fragment and linkers on the carrier protein are shown as blue and red stars respectively. Cross coupling gives a fragment-protein conjugate which is then used to immunise a suitable animal with a view to producing antibodies against the antigen.¹³ If the antibodies prove specific and sufficiently sensitive towards PRM-1, these antibodies would be used to produce a lateral flow device for detecting and quantifying PRM-1 in waterways.¹⁸

Building on the experience gained in synthesising the glyceryl glycoside fragments inspired by the various prymnesin toxins, we decided to try and synthesise a slightly larger fragment containing two sugar moieties with a view to using it to raise antibodies for prymnesin toxin detection. There are a few benefits to using a synthetic fragment. First it is possible to ensure the fragment being used is homologous; secondly if the antibodies raised from the fragment do show a response to the whole toxin, it is easier to determine which part of the toxin is being detected. Finally, the stereochemistry of the prymnesin backbones in the glycosylated regions of the toxin are currently undefined. If antibodies raised against one fragment isomer show an immune response when challenged with the whole prymnesin toxin but those from the other fragment isomer do not, it may help to elucidate the stereochemistry at the analogous backbone region of the natural toxin.

5.2 Chemistry

5.2.1 Retrosynthetic analysis of toxin fragment

The retrosynthetic pathway shown in Scheme 5.1 was used to plan the synthetic pathway towards the glycosylated toxin fragment inspired by prymnesin-1. Step i) in the pathway considered the final molecule which would be present before global deprotection (**2**). The 1,2-*cis* α -ribose linkage would require non-participating protecting groups, and so benzyl ether groups were selected as 2,3,5-tri-*O*-benzyl ribose is commercially available. The 1,2-*trans* α -L-arabinose linkage would be obtained efficiently using ester protecting groups which would control the stereochemistry of the glycosidic bond by neighbouring group participation.¹⁹ Because per-*O*-benzoyl β -L-arabinopyranose (**1**) was already available from the previous synthesis described in this project (Chapter 4), benzoyl protecting groups were selected.

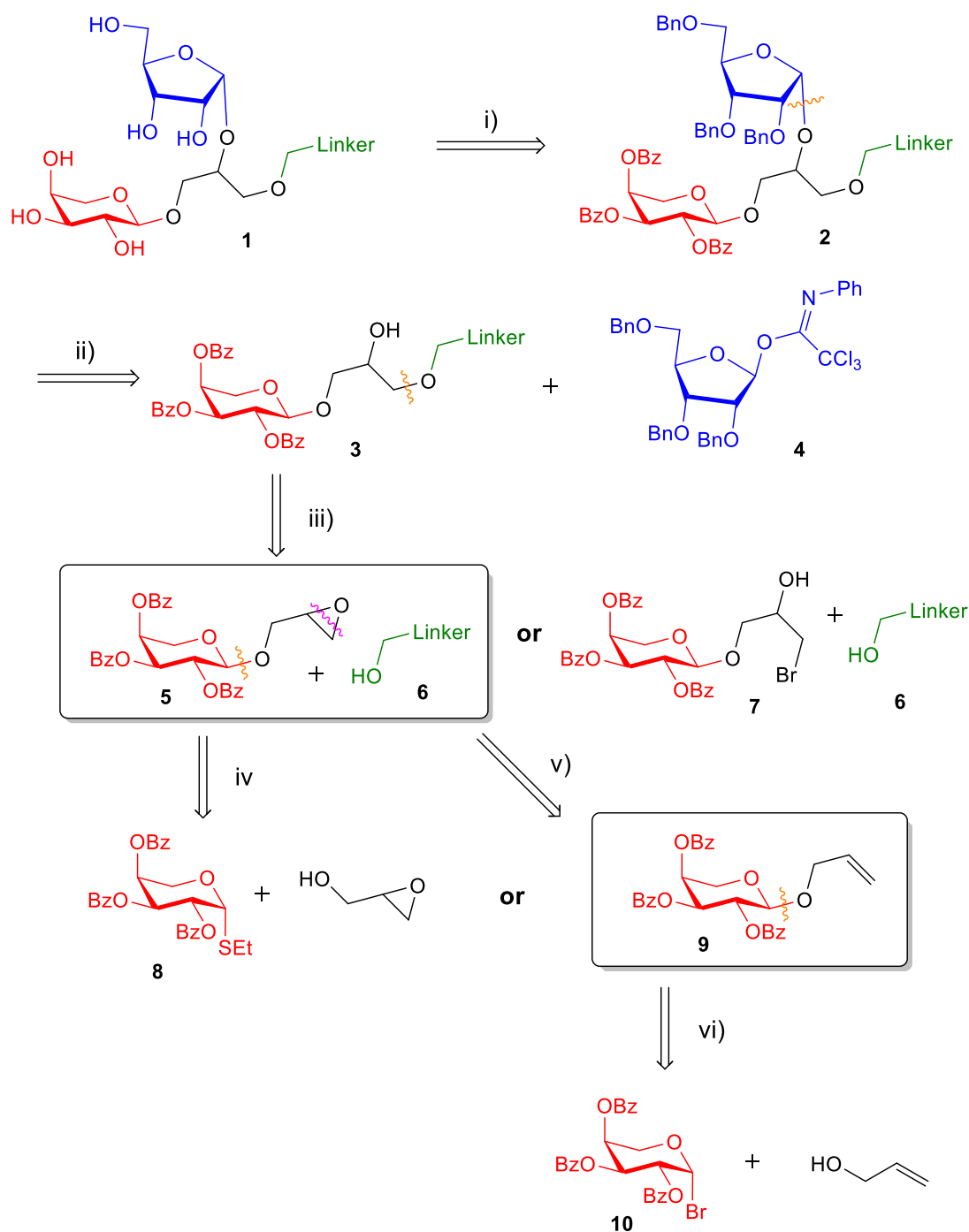
Step ii) in the retrosynthetic pathway breaks the ribose glycosidic linkage. The synthons are an oxygen anion a ribosidic cation, which gives a 2° alcohol (**3**) and an appropriate riboside donor (**4**). For the forward glycosylation step there was some literature precedence to show that 1,2-*cis* glycosylation at this 2° OH group might best be performed using a trifluoroimidate donor and TMSOTf promotor.²⁰⁻²² This led to 2,3,5-tri-*O*-benzyl-1-*O*-[(2,2,2-trifluoro-*N*-phenylethanimidoyl)]- β -D-ribofuranose (**4**) as the ribose donor, the synthesis for which has already been reported in the literature.²²

Step iii) breaks the bond between the fragment and the linker. At this point an open mind was being kept on which linker would be most appropriate for conjugating the fragment onto a carrier protein (see Figure 5.5). The synthons would be a terminal cation on the main fragment and an oxygen anion on the linker. The real reagent for the linker would therefore be an alcohol (**6**). For the main fragment one can imagine the alkyl cation as either an alkyl bromide (**7**), or imagine an intramolecular quenching of the synthon cation by the 2° hydroxyl group to form an epoxide (**5**). Of the two possible fragments, an epoxide seems the most appropriate choice as the alkyl bromide would probably be synthesised from the epoxide anyway.²³ The forward ring opening step has been explored in the literature and attack of the epoxide by an alcohol in the presence of a Lewis acid in a non-polar solvent showed promise of working well.²⁴

Step iv) and v) explore two different ways of installing the epoxide. Step iv) breaks the glycosidic bond to give an appropriate glycosidic donor (**8**) and glycidol as the acceptor. This has the advantage that both enantiomers of glycidol are commercially available as optically pure compounds, leading to an epoxide with known stereochemistry. A similar forward reaction which uses a thiogalactoside to glycosylate glycidol has been reported in the literature.^{25,26} However we had problems replicating this methodology in the lab. By contrast step v) considers the reduction of the epoxide to a corresponding alkene (**9**). The forward reaction for this could correspond to a mCPBA mediated epoxidation of the alkene. The disadvantage to this is that a mixture of *anti* and *syn* epoxide isomers will be formed.^{24,27} Of the two methods it was decided that oxidation of the alkene would be the preferred forward step as both the *syn* and *anti* epoxides were required, and preliminary attempts to glycosylate glycidol had proved unsuccessful.

Step vi) breaks the 1,2-*trans* glycosidic linkage between allyl alcohol and per-*O*-benzoyl α -L-arabinopyranose (**11**). The forward glycosylation step could be performed under Koenigs–Knorr conditions using the corresponding glycosyl bromide (**10**).²⁸ Per-*O*-benzoyl L-arabinopyranose (**11**) had already been synthesised for previous use in this project and allyl alcohol is commercially available.

This retrosynthetic analysis was used to propose a sensible forward synthetic pathway towards a two glycosylated prynnesin-1 fragment (**1**) with a (*R*-) and (*S*-) stereochemistry at the glycerol backbone and a linker for later conjugation onto a carrier protein with a view to antibody production.



Scheme 5.1 – The retrosynthetic analysis used to plan the synthesis of the PRM-1 fragment. i) Ester protecting groups direct 1,2-trans glycosylation by neighbouring group participation, whilst benzyl ether protecting groups are suitable for 1,2-cis glycosylations.¹⁹ ii) Breaking of ribosidic linkage to give the known ribose donor (4) shown in blue.²⁹ iii) Breaking the linker bond gives a terminal carbocation. This could exist as either the alkyl bromide (7) or epoxide (5) shown. iv) The epoxide is cleaved to give the glycosyl donor (8) and glycidol²⁶ or v) the epoxide ring oxygen is cleaved to give an adjacent alkyl anion and cation which could best equate to an alkene (9). vi) Breaking the glycosidic linkage to give a glycosyl bromide (10) and allyl alcohol.

5.2.2 Synthesis of (2-R/S-Oxiranyl)methyl 2',3',5'-tri-O-benzoyl- α -L-arabinopyranoside (5)

L-arabinose was per-*O*-benzoylated using benzoyl chloride and DMAP to give per-*O*-benzoyl β -L-arabinopyranose (**11**) (Scheme 5.2).³⁰ Attempts to use per-*O*-benzoyl β -L-arabinopyranose (**11**) for the $\text{BF}_3 \cdot \text{OEt}_2$ promoted glycosylation of allyl alcohol gave a 3.2:1.0 mixture of α and β anomers as judged by integration of the ^1H NMR H-1' signals (Figure 5.4).

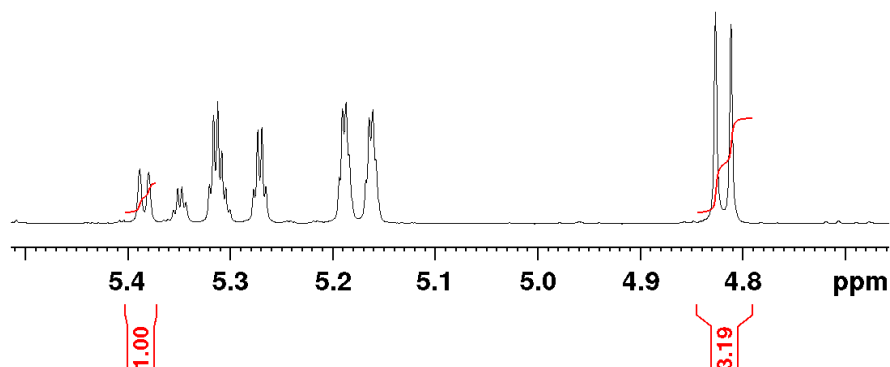
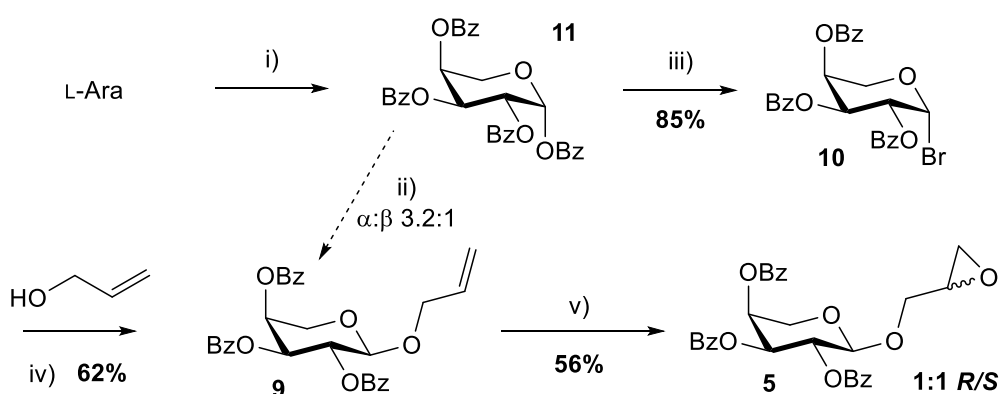


Figure 5.4 – ^1H NMR showing the integration of the H-1' signals for a mixture of prop-2-en-1-yl 2,3,5-tri-*O*-benzoyl- α/β -L-arabinopyranoside.

To ensure only the desired 1,2-*trans* α -anomer was synthesised, the glycosylation was repeated under Koenigs-Knorr conditions (Scheme 5.2).^{19,31}



Scheme 5.2 – The chemical synthesis of (oxiran-2-yl) methyl 2,3,5-tri-*O*-benzoyl- α -L-arabinopyranoside (**5**). i) BzCl , DMAP, Pyr. ii) allyl alcohol, $\text{BF}_3 \cdot \text{OEt}_2$, DCM; iii) 33% v/v HBr/AcOH , DCM. iv) Ag_2CO_3 , DCE, 4ÅMS. v) mCPBA, DCE, reflux.

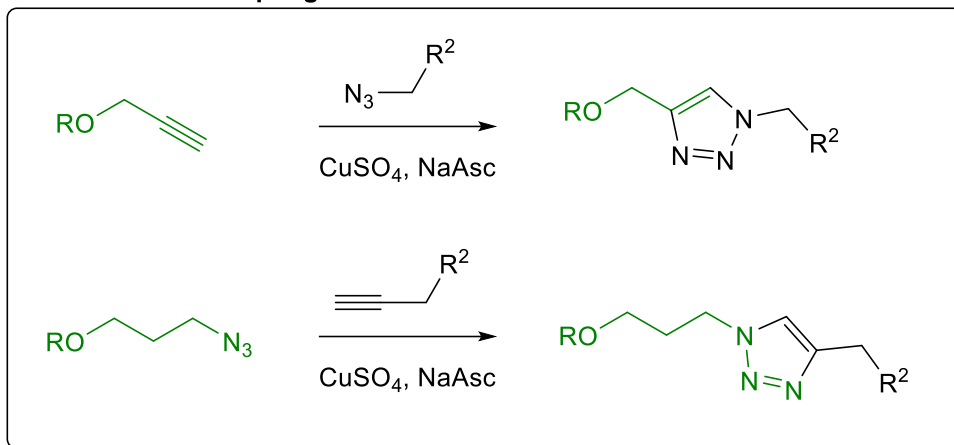
2,3,5-Tri-*O*-benzoyl bromo- β -L-arabinopyranoside (**10**) was produced by treating per-*O*-benzoyl β -L-arabinopyranose (**11**) with 33% v/v HBr in AcOH. The glycosyl bromide donor (**10**) was used to glycosylate allyl alcohol using silver carbonate as the promotor.²⁸ The 1,2-*trans* configuration of prop-2-en-1-yl 2,3,5-tri-*O*-benzoyl- α -L-arabinopyranoside (**9**) was confirmed by ¹H NMR spectrum which showed the H-1' signal at 4.82 ppm as a doublet with a $J_{1,2'}$ coupling value of 6.1 Hz. The next step was the oxidation of the alkene to an epoxide which could subsequently be ring opened to form the glycosyl glycerol; this was achieved using mCPBA.³² The epoxidation gave a 1:1 mixture of (*R*)- and (*S*)- epoxides (**5**) as judged by integration of the H-1' signals of the sugars, but the epoxide diastereoisomers were inseparable by TLC. As the stereochemistry at the glycosylated backbone of prymnesin toxins is not defined in the literature, it was necessary to make both possible isomers of the fragment.^{12,33} Therefore whilst it was unfortunate the two isomers were inseparable, it was not a barrier to further progress as we would need use both isomers in the synthesis anyway. It was still possible to characterise the two isomers of (oxiran-2-yl)methyl 2,3,5-tri-*O*-benzoyl- α -L-arabinopyranoside (**5**) using a combination of HSQCed and COSY 2D NMR to assign the ¹H and ¹³C NMR signals.

5.2.3 Epoxide ring opening to synthesise 3-(3-azidopropoxy)-2-hydroxypropyl 2,3,4-tri-*O*-benzoyl- α -L-arabinopyranoside (**12**)

Next it was necessary to consider ring opening the epoxide to install a functional group which could be used to couple the fragment with a protein bound linker (Figure 5.5). Two coupling reactions were explored, the first was a copper(I)-catalyzed alkyne-azide cycloaddition (CuAAC) to give a 1,2,3-triazole linkage.^{34,35} The second was a carbodiimide crosslinking reaction to give an amide linkage.³⁶

For the CuAAC coupling, an alkyne or azide was required on the prymnesin fragment, and commercially available reagents were considered. It quickly became obvious that having an alkyne on the prymnesin fragment was a problem because the benzyl ether protecting groups on ribose (**4**) which was going to be installed at the 2° glycerol OH would need to be removed by hydrogenation. Although there is some literature precedence for protecting alkyne groups from reduction by hydrogenation, this is by no means perfect and there is still a significant degree of alkyne reduction.³⁷ An alternative strategy involved placing the azide on the prymnesin fragment, but again azides are prone to reduction to amines by hydrogenation.

CuAAC 'Click' coupling



Carbodiimide crosslinking

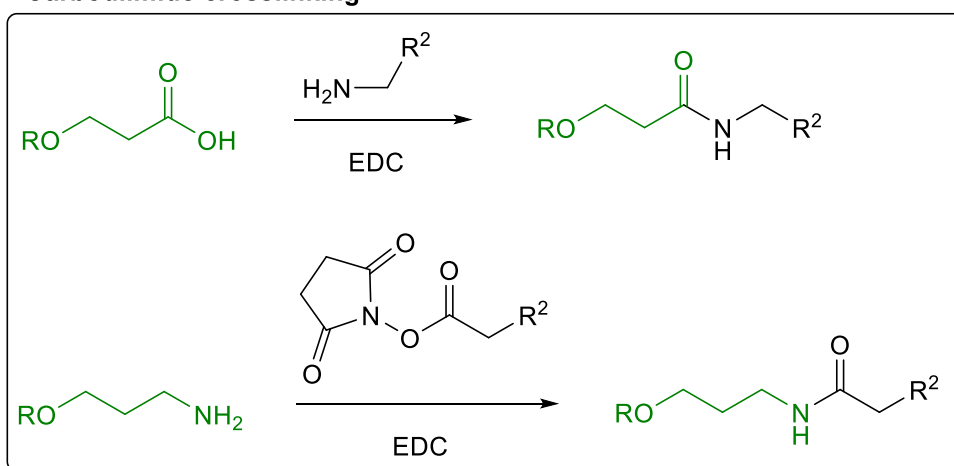
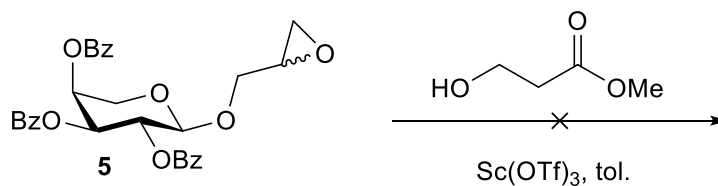


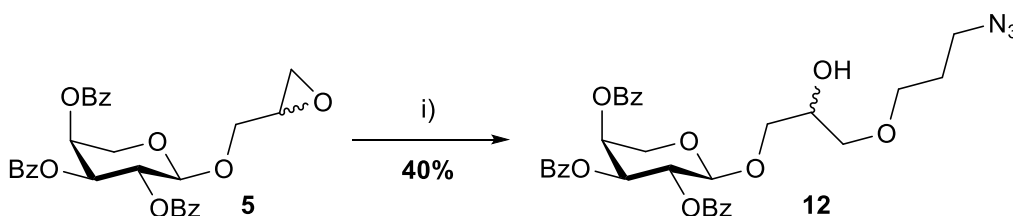
Figure 5.5 – Exploring reactions which could be used to couple the PRM-1 fragments to a protein bound linker. R = PRM-1 fragment, R² = protein bound linker

Carbodiimide crosslinking of the PRM-1 fragment to a protein bound linker would provide a way of utilising functional groups (amines and esters) which are not affected by hydrogenation during global deprotection. The first attempted epoxide ring opening of (2-*R/S*-oxiranyl)methyl 2',3',5'-tri-*O*-benzoyl- α -L-arabinopyranoside (**5**) employed methyl 3-hydroxypropionate and Sc(OTf)₂ as the catalyst.²⁴ This was unsuccessful with 3-hydroxypropionate apparently polymerising to form a single rubber like ball (Scheme 5.3).



Scheme 5.3 - Attempted Lewis-acid catalysed epoxide opening using methyl-3-hydroxypropionate.

It was therefore decided to try and switch the functional groups around and attach the amine group to the toxin fragment. 3-Azido propanol was used as a protected amine linker to ring open the epoxide (Scheme 5.4). The azide acted as a protected amine group to ensure only the alcohol could nucleophilically attack the epoxides (**5**). The azide would be readily reduced to the amine by hydrogenation during the global deprotection steps.



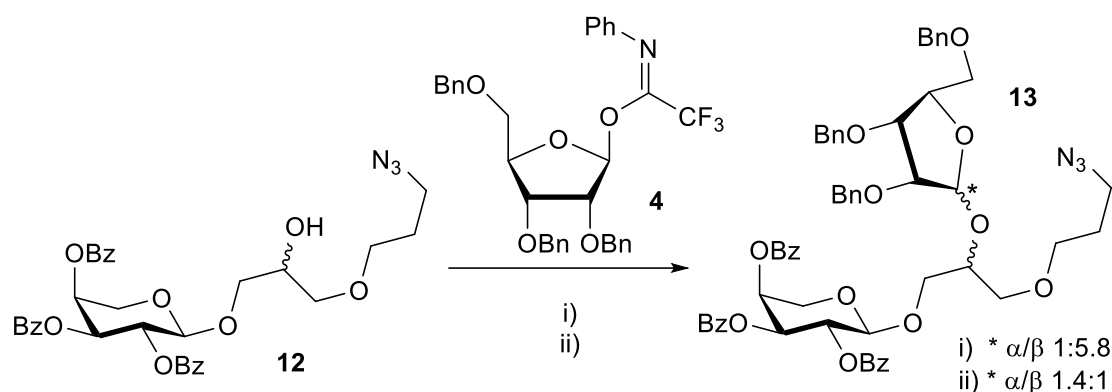
Scheme 5.4 – Epoxide ring opening to give 3-(3-Azidopropoxy)-2-hydroxypropyl 2,3,4-tri-*O*-benzoyl- α -L-arabinopyranoside. i) 3-azidopropanol, Sc(OTf)₃, toluene.

The ring opening (**5**) reaction using 3-azidopropanol and Sc(OTf)₂ was successful, forming 3-(3-azidopropoxy)-2-hydroxypropyl 2,3,4-tri-*O*-benzoyl- α -L-arabinopyranoside (**12**) which was judged to be a 1:1 mixture of (*R*)- and (*S*)- isomers with respect to the 2° glycerol hydroxide group by integration of the H-1' and H-1'* ¹H NMR signals at 4.92 and 4.82 ppm respectively. The isomers were inseparable but it was possible to fully assign the ¹H and ¹³C NMR signals in the mixture using a combination of HSQCed and COSY 2D NMR.

5.2.4 Synthesis of 3-(3-aminopropoxy)-2-(α -D-ribofuranosyloxy)propyl)- α -L-arabinopyranoside (**13**)

With the epoxides successfully ring opened, the new 2° alcohols (**12**) were ready to be used as acceptors in the final glycosylation step which would install an α -ribose 1,2-*cis* linkage (Scheme 5.5). First a suitable ribose donor needed to be synthesised. As a 1,2-*cis* linkage was required, it was necessary to use a ribose donor with non-participating protecting groups. Commercially available 2,3,5-tri-*O*-benzyl α / β -D-ribose was treated with 2,2,2-trifluoro-*N*-

phenylacetimidoyl chloride and caesium carbonate to make 2,3,5-tri-*O*-benzyl-1-*O*-[(2,2,2-trifluoro-*N*-phenylethanimidoyl)]- β -*D*-ribofuranose (**4**).²² This donor has been used several times to good effect by Filippov *et al.*^{20–22} for stereoselective ribosylations using TMSOTf as a promotor and either DCM or DCE as a solvent.



Scheme 5.5 – Continued synthesis: the epoxide ring opening and 1,2-*cis* glycosylation step to give 3-(3-azidopropoxy)-2-[(2',3',5'-tri-*O*-benzyl- α -*D*-ribofuranosyl)oxy]propyl-2'',3'',4''-tri-*O*-benzoyl- α/β -*L*-arabinopyranoside. i) TMSOTf, DCE, 4ÅMS, -30 °C. ii) TMSOTf, DCM, 4ÅMS, -78 °C.

The initial glycosylation of 3-(3-azidopropoxy)-2-hydroxypropyl 2,3,4-tri-*O*-benzoyl- α -*L*-arabinopyranoside (**12**) with 2,3,5-tri-*O*-benzyl-1-*O*-[(2,2,2-trifluoro-*N*-phenylethanimidoyl)]- β -*D*-ribofuranose (**4**) was attempted in DCE at -30 °C. HSQCed and ¹H NMR of the crude reaction mixture allowed for rapid identification of the ribose anomeric signals (as described in Chapter 4, Figure 4.9). A 1,2-*cis* α -ribose linkages give H-1'' signals as doublets and C-1'' shifts of ~100 ppm; by contrast 1,2-*trans* β -ribose linkages showed H-1'' signals as singlets and C-1'' shifts of ~105 ppm.³⁸ Unfortunately it was quickly obvious that the glycosylation at -30 °C had produced predominately the thermodynamic 1,2-*trans* β -riboside, with an α/β ratio of 1.0:5.8 as judged by integration of the H-1'' NMR signals of the crude glycosylation mixture (**13**) (Figure 5.6).

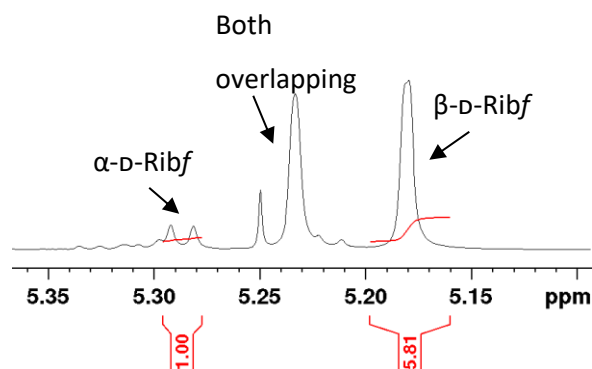


Figure 5.6 – ^1H NMR of the crude glycosylation mixture showing the H-1' signals for the 1,2-*cis* and 1,2-*trans* glycosidic linkages. Glycosylation at $-30\text{ }^\circ\text{C}$ gave predominately the undesired 1,2-*trans* β -D-ribose.

The glycosylation was attempted again in DCM which allowed the reaction mixture to be cooled to $-78\text{ }^\circ\text{C}$ in a dry ice-acetone bath without freezing. This time ^1H NMR of the crude reaction mixture (**13**) showed an excess of the desired kinetic 1,2-*cis* α riboside, with an α/β ratio of 1.4:1 as judged by integration of the H-1'' NMR signals. Because an inseparable 1:1 mixture of acceptors had been used, the glycosylation had resulted in 4 products (2 \times α -ribosides and 2 \times β -ribosides). Because antibody response relies on fit of the antigen, the differing shapes of the two isomers has the potential to lead to very different immune responses.¹³ Fortunately the two α -ribosides were separable from both the crude reaction mixture and also from one another by semi-preparative TLC, and both were purified from the reaction mixture to give the (2*R*-) and (2*S*-) isomers of 3-(3-azidopropoxy)-2-[(2,3,5-tri-*O*-benzyl- α -D-ribofuranosyl)oxy]propyl-2,3,4-tri-*O*-benzoyl- α -L-arabinopyranoside, (**2R-14**) and (**2S-14**) respectively. Once separated the stereochemistry of the 1,2-*cis* α -ribose linkages were confirmed by ^1H NMR with the H-1'' signals appearing as doublets with $J_{1'',2''}$ coupling values of 4.2-4.4 Hz and C-1'' shifts of 101.4-101.5 ppm. The 1,2-*trans* α -L-arabinopyranose linkages were confirmed by the H-1' signals appearing as doublets with $J_{1',2'}$ coupling values of 6.0-7.0 Hz (Figure 5.7).

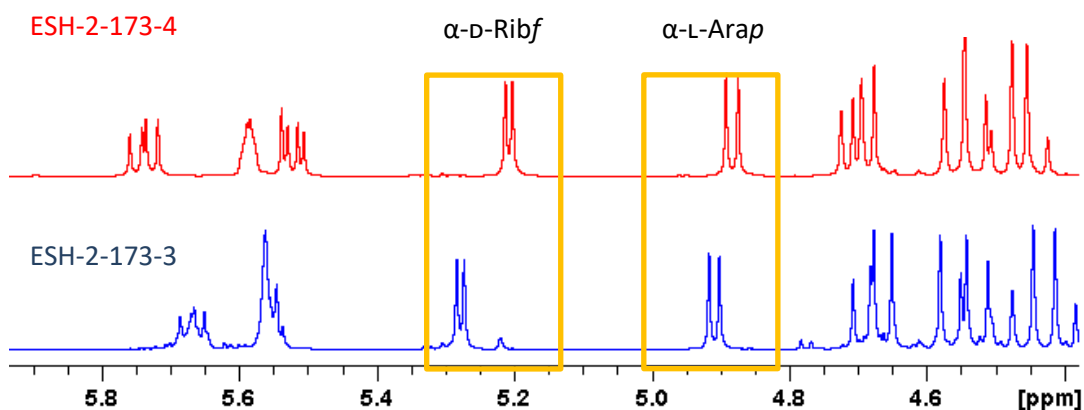


Figure 5.7 – Zoomed ^1H NMR spectra of the separated (2*R*-) and (2*S*-) isomers of 3-(3-Azidopropoxy)-2-[(2,3,5-tri-*O*-benzyl- α -*D*-ribofuranosyl)oxy]propyl-2,3,4-tri-*O*-benzoyl- α -*L* arabinopyranoside (**14**). When these spectra were recorded, I did not know which isomer was which. Therefore the original compound names from the time (ESH-2-173-3 and ESH-2-173-4) are shown in red and blue which will help to clarify the next section (5.2.5).

5.2.5 Distinguishing between the (*R*)- and (*S*)- isomers of (**14**)

Although the (*R*-) and (*S*-) isomers of 3-(3-azidopropoxy)-2-[(2',3',5'-tri-*O*-benzyl- α -*D*-ribofuranosyl)oxy]propyl-2'',3'',4''-tri-*O*-benzoyl- α -*L*-arabinopyranoside (**14**) had been separated, the next challenge was identifying which was which. The lowest energy conformation for both isomers was calculated using MarvinSketch 15.1.19.0 Calculator Plugins (Figure 5.8). There was a noticeable difference in the lowest energy conformations, with the (**2S-14**) isomer having a benzyl protecting group from ribose lying over the 3-azido propanol linker. By contrast the (**2R-14**) isomer showed the aromatic sugar protecting groups all grouped together, with nothing in close proximity to the 3-azido propanol linker.

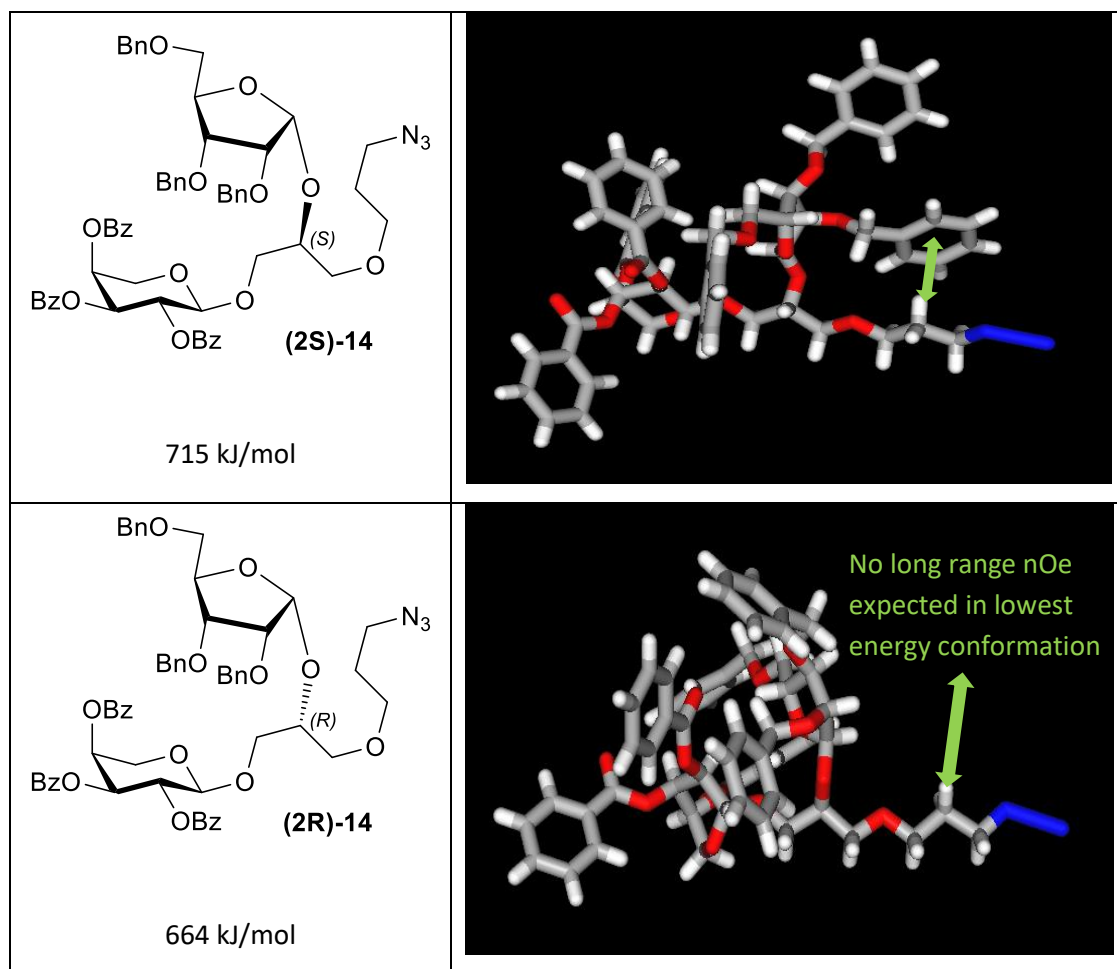


Figure 5.8 - lowest energy calculations and 3D model representations for the (2*R*-) and (2*S*-) isomers of **13**. There is a clear difference in the conformations, with the (2*S*-) isomer having aromatic protons in close proximity with a the CH₂ group on the azido-linker.

As a result of these lowest energy conformation models it was proposed that it should be possible to see long range nOe interactions between the 3-azido propanol linker and a benzyl protecting group on ribose for one of the compounds (the *S*- isomer) but not for the other (the *R*- isomer). NOESY 2D NMR spectra were recorded for both compounds, with 'ESH-2-173-3' showing clear long range coupling between 3-azido propanol and the benzyl protecting groups, whilst 'ESH-2-173-4' shows *no* long-range coupling between 3-azido propanol and the benzyl protecting groups (Figure 5.9). On this basis compound 'ESH-2-173-3' was assigned as the (*S*)- isomer (**2S-14**) and compound 'ESH-2-173-4' was assigned as the (*R*)- isomer (**2R-14**).

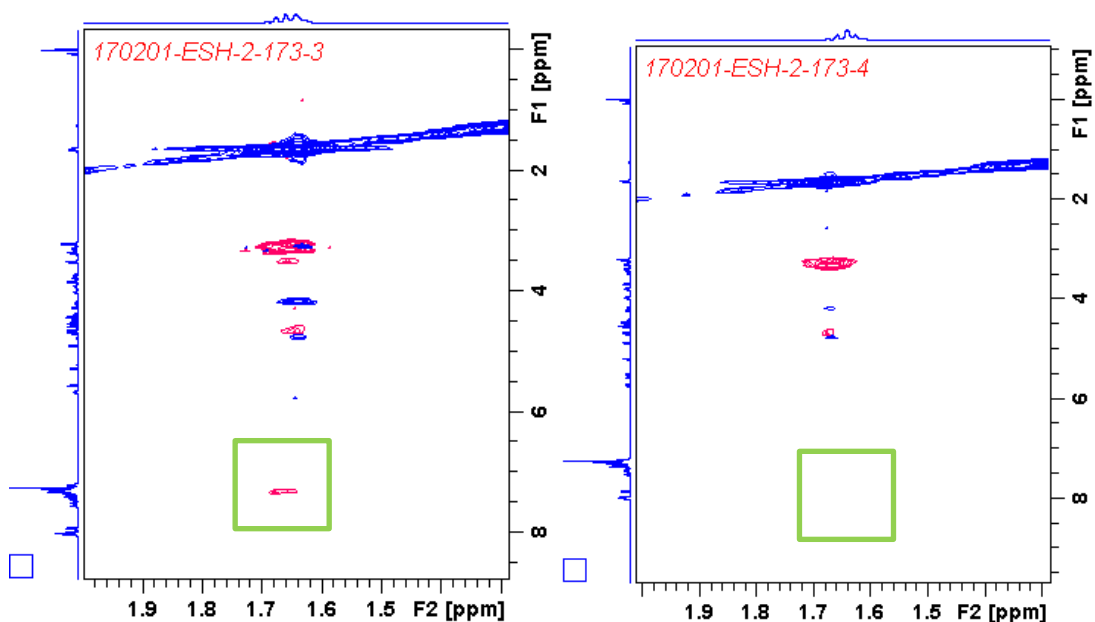
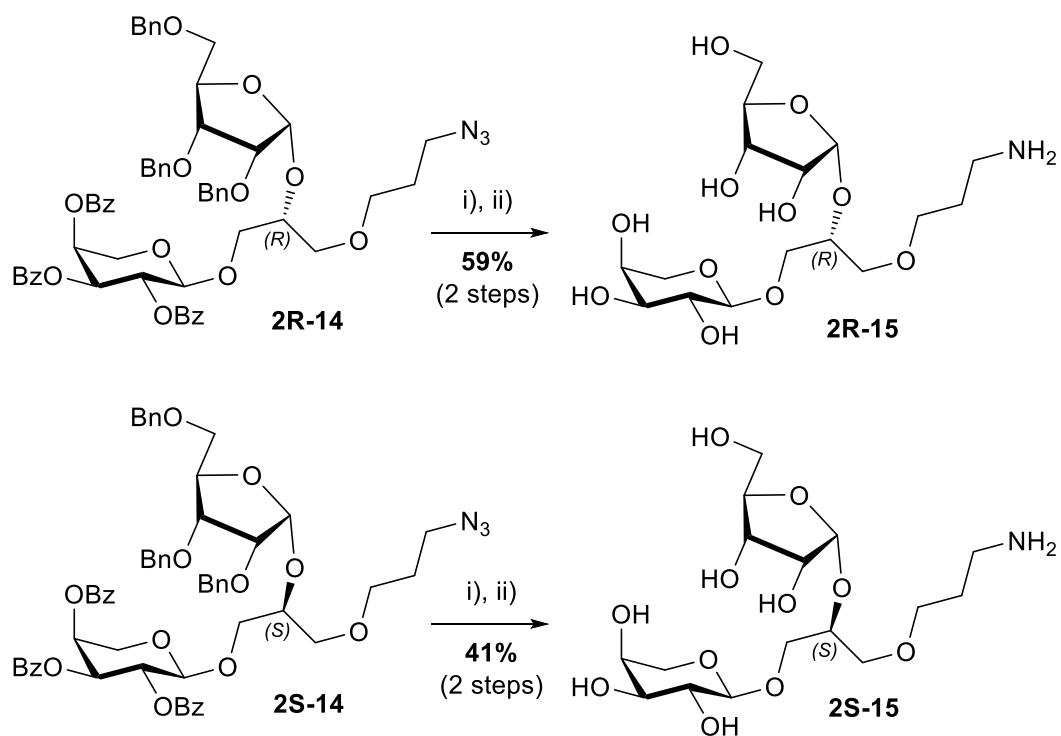


Figure 5.9 - NOESY 2D NMR for compound ESH-2-173-3 shows nOe long range coupling between the benzyl groups and 3-azido propanol linker, and as such was assigned as the (2*S*)- isomer (**2*S*-14**); NOESY 2D NMR for compound ESH-2-173-4 does *not* show any nOe long range coupling between the benzyl groups and 3-azido propanol linker, and as such which was assigned as the (2*R*)- isomer (**2*R*-14**).

Global deprotection was performed by first simultaneously removing the benzyl ether groups from ribose and reducing the azide to an amine by hydrogenation over a Pd/C catalyst (Scheme 5.6). The benzyl protecting groups on L-arabinose were removed by transesterification using a mixture of MeOH/H₂O/Et₃N (5:2:1). This method of removing ester protecting groups was chosen over a sodium methoxide solution because the base, Et₃N, is volatile. By contrast sodium methoxide which is commonly used for carbohydrate de-esterification is removed using a proton resin, which would have also bound with the free amine group on the final products. The inclusion of water in the debenzoylation did lead to some hydrolysis as well which meant that there was some benzoic acid contamination. This was readily removed by passing the final compounds through Dowex® 1X2-400 resin (OH⁻ form) in water.



Scheme 5.6 - global deprotection strategy for the final fragments. i) H₂, 10% Pd/C, EtOAc/MeOH 1:1. ii) MeOH/H₂O/Et₃N (5:2:1)

At the end of the deprotection steps we were left with (2*R*)- and (2*S*)- isomers of 3-(3-aminopropoxy)-2-(α -D-ribofuranosyloxy)propyl α -L-arabinopyranoside, (**2R-15**) and (**2S-15**) respectively, as separate and homologous compounds in 59% and 41% yields (2 steps). The yields might be attributed to some adsorption onto the Pd/C catalyst and also the anion exchange purification step.

5.3 Summary

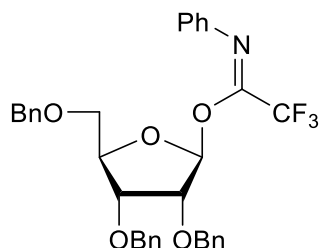
Due to the reported difficulties in producing larger quantities of purified prymnesin toxins, a two small fragment inspired by PRM-1, the (2*R*-) and (2*S*-) isomers of 3-(3-aminopropoxy)-2-(α -D-ribofuranosyloxy)propyl α -L-arabinopyranoside, (**2R-15**) and (**2S-15**) respectively, were chemically synthesised. Because there is no literature guidance for the stereochemistry of the backbone of this region of prymnesin toxins, both the (**2R-15**) and (**2S-15**)- isomers were synthesised. A retrosynthetic analysis of the target compounds was performed which considered the use of participating and non-participating protecting groups on the carbohydrate donors (**2**). The introduction of the glycerol backbone was also considered,

and retrosynthetic analysis showed that the ring opening of an epoxide (**5**) derived from the epoxidation of an alkene (**9**) was found to be the most useful way forward. A selection of functional groups suitable for cross coupling reactions for protein conjugation were also considered (Scheme 5.1), and their installation onto the glycerol backbone, as well as the compatibility with the global deprotection steps were also discussed. For the forward synthesis, 2,3,4-tri-*O*-benzoyl- β -L-arabinopyranosyl bromide (**10**) was used for the Ag_2CO_3 promoted glycosylation of allyl alcohol, which gave exclusively the 1,2-*trans* α -anomer. The alkene (**9**) was then oxidised to an epoxide (**5**) with mCPBA. The epoxide was ring opened with 3-azido propanol in toluene using $\text{Sc}(\text{OTf})_3$ as a Lewis acid catalyst to give 3-(3-azidopropoxy)-2-hydroxypropyl 2,3,4-tri-*O*-benzoyl- α -L-arabinopyranoside (**12**) as an inseparable 1:1 mixture of (2*R*)- and (2*S*)- isomers. This mixture was then glycosylated with 2',3',5'-tri-*O*-benzyl- β -D-ribofuranosyl (*N*-phenyl)-2,2,2-trifluoroacetimidate (**4**) in DCM at -78 °C using TMSOTf as a promotor. Glycosylation gave a mixture of α/β - ribosides in a ratio of 1.4:1 (**13**). The α -ribosides were separable both from the β -ribosides and also from each other to yield both the (2*R*)- and (2*S*)- isomers of 3-(3-azidopropoxy)-2-[(2',3',5'-tri-*O*-benzyl- α -D-ribofuranosyl)oxy]propyl-2'',3'',4''-tri-*O*-benzoyl- α -L-arabinopyranoside ((**2R-14**) and (**2S-14**) respectively) as separate and homologous compounds. The assignment of the stereochemistry at the 2° position of the glycerol backbone was achieved by comparing nOe NMR spectra with computational models of the lowest energy conformations of both isomers. It was noted that for (**2S-14**) one of the benzyl protecting groups on ribose was in close proximity to the azido propanol linker. nOe NMR of the two compounds showed a long-range interaction between the aromatic protecting group and the azido propanol linker for only one of the two isomers, and this was assigned as the (2*S*)- isomer (**2S-14**). Global deprotection was achieved by hydrogenation over Pd/C followed by transesterification to give (2*R*)- and (2*S*)- 3-(3-aminopropoxy)-2-(α -D-ribofuranosyloxy)propyl α -L-arabinopyranoside ((**2R-15**) and (**2S-15**) respectively). Due to time constraints, and also a very late discovery in our lab that prymnesin-B1 (which is glycosylated with β -D-galactopyranose)¹² would seem to be the toxin produced by the *P. parvum* strain in the Norfolk Broads, the fragment was not used for further conjugation or immunisation. However now that the fragment is in hand, future attempts could be made to use it as an antigen for antiPRM-1 production.

5.4 Experimental

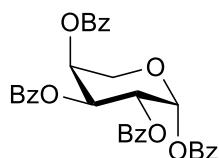
5.4.1 Chemistry

2',3',5'-Tri-*O*-benzyl-β-D-ribofuranosyl (*N*-phenyl)-2,2,2-trifluoroacetimidate (**4**)²²



2,3,5-Tri-*O*-benzyl-β-D-ribofuranose (840 mg, 2.0 mmol), 2,2,2-trifluoro-*N*-phenylacetimidoyl chloride (600 μL, 4.0 mmol), caesium carbonate (720 mg, 2.2 mmol) and water (100 μL) were dissolved into acetone and stirred for 3 hours at room temperature. The reaction mixture was then filtered through Celite and the solvent was removed *in vacuo* to give a crude syrup. The crude mixture was purified by FCC to give the title compound (**4**) (800 mg, 59%) as an off white powder; R_f 0.61 (hexane/EtOAc 8:2); δ_H (400 MHz; CDCl₃) 7.54-7.52 (m, 3H, Ar), 7.32-7.08 (m, 17H, Ar), 6.79 (d, $J = 7.8$, 1H), 6.32 (bs, 1H, H-1), 4.66-4.43 (m, 7H, 3 × CH₂Ph & H-4), 4.17-4.06 (m, 1H, H-3), 3.70 (dd, $J_{4,5} = 2.8$ Hz, $^2J_{5a,5b} = 10.9$ Hz, 1H, H-5), 3.59 (dd, $J_{4,5'} = 5.2$ Hz, $^2J_{5a,5b} = 10.9$ Hz, 1H, H-5'); δ_C (100 MHz; CDCl₃) 143.8 (C=N), 138.1, 137.5, 137.4, 135.4, 129.5, 128.8, 128.5, 128.5, 128.4, 128.2, 128.1, 128.0, 128.0, 127.7, 126.3, 124.4 (Ar), 119.7 (CF₃), 102.5 (C1), 82.3 (C4), 78.7 (C2), 77.4 (C3), 73.4, 72.8, 72.4 (3 × CH₂Ph), 70.2 (C5); δ_F (376 MHz; CDCl₃) -75.6 (CF₃); LRMS (ESI⁺) m/z calc. for C₃₄H₃₂F₃NO₅Na⁺ 614.2 [M+Na]⁺ found 613.6 [M+Na]⁺. The NMR data were in accordance with the literature.²²

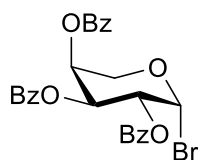
Per-*O*-benzoyl-β-L-arabinopyranose (**11**)³⁰



A solution of L-arabinose (1.0 g, 6.7 mmol) and DMAP (1 mol %) in dry pyridine (15 mL) was cooled in an ice bath and benzoyl chloride (5.0 mL, 43 mmol) was added dropwise over 30 minutes. The reaction mixture allowed to warm and stirred overnight at room temperature. The solvent was removed *in vacuo* and the crude mixture was dissolved in EtOAc (20 mL) and washed with 1M HCl solution (3 × 5 mL) to remove any residual pyridine. The organic layer

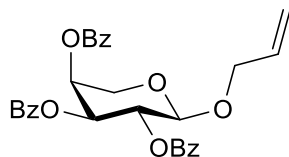
was dried over MgSO₄ and the solvent was removed under reduced pressure before the crude mixture was purified by FCC to give the title compound (**11**) (3.40 g, 90%) as a white foam, R_f 0.4 (hexane/EtOAc 3:1); [α]_D +301 (c 1.0, CHCl₃) (lit.³⁰ +291.2 (c 0.1, CHCl₃)); δ_H(400 MHz; CDCl₃) 8.14-8.12 (m, 4H, Ar), 7.90-7.87 (m, 4H, Ar), 7.65-7.61 (m, 2H, Ar), 7.55-7.45 (m, 6H, Ar), 7.32-7.28 (m, 4H, Ar), 6.87 (bs, 1H, H-1), 6.07-6.06 (2H, m, H-2,3), 5.91-5.89 (m, 1H, H-4), 4.42 (dd, J_{4,5a} = 1.0 Hz, ²J_{5a,5b} = 13.5 Hz, 1H, H-5a), 4.18 (dd, J_{4,5b} = 2.1 Hz, ²J_{5a,5b} = 13.5 Hz); δ_C(100 MHz; CDCl₃) 165.8, 165.7, 165.6, 164.7 (4 × C=O), 133.8, 133.6, 133.5, 133.4, 129.9, 129.8, 129.4, 129.1, 128.9, 128.8, 128.8, 128.6, 128.4, 128.4 (Ar), 91.1 (C1), 69.5 (C4), 68.2 (C3), 67.8 (C2), 63.0 (C5). ¹H and ¹³C NMR values were in agreement with literature values³⁰

2,3,4-Tri-*O*-benzoyl-β-L-arabinopyranosyl bromide (**10**)³⁹



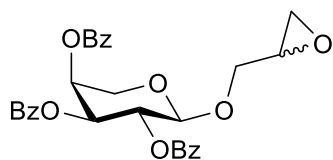
Per-*O*-benzoyl-β-L-arabinopyranose (**11**) (2.4 g, 4.2 mmol) was dissolved into dry DCM (10 mL) under N₂. A solution of 33% HBr in AcOH (2.5 mL) was added in a single portion and the reaction mixture stirred for 3 hours at room temperature after which time TLC (hex/EtOAc 3:1) showed consumption of the start material. The solvent was removed under reduced mixture pressure and the reaction re-dissolved into EtOAc (10 mL) before being washed with ice cold saturated NaHCO₃ (3 × 3 mL). The organic layer was dried over MgSO₄ and the solvent removed under reduced pressure to give the title compound (**10**) (2.1 g, 95%) as an oil which was immediately used in the next step, R_f 0.42 (hexane/EtOAc 3:1); δ_H(400 MHz; CDCl₃) 8.11-8.08 (m, 1H, Ar), 8.03-8.01 (m, 1H, Ar), 7.87-7.85 (m, 1H, Ar), 7.63-7.30 (m, 9H, Ar), 6.94 (d, J_{1,2} = 3.9 Hz, 1H, H-1), 6.00 (dd, J_{2,3} = 10.5 Hz, J_{3,4} = 3.9 Hz, 1H, H-3), 5.84-5.83 (m, 1H, H-4), 5.71 (dd, J_{1,2} = 3.9 Hz, J_{2,3} = 10.5 Hz, 1H, H-2), 4.47 (dm, ²J_{5a,5b} = 12.9 Hz, 1H, H-5a), 4.23 (dd, J_{4,5b} = 1.9 Hz, ²J_{5a,5b} = 12.9 Hz, 1H, H-5b); δ_C(100 MHz; CDCl₃) 165.6, 165.6, 165.4 (3 × C=O), 133.8, 133.7, 133.4, 130.0, 129.9, 129.8, 128.7, 128.6, 128.4 (12 × Ar) 89.8 (C1), 68.9 (C4), 68.7 (C2), 65.0 (C3), 60.4 (C5). The ¹H NMR were in agreement with literature values.³⁹

Prop-2-en-1-yl 2,3,5-tri-*O*-benzoyl-α-L-arabinopyranoside (**9**)



2,3,4-Tri-*O*-benzoyl- β -L-arabinopyranosyl bromide (**10**) (1.8 g, 3.5 mmol) and allyl alcohol (290 μ L, 4.2 mmol) were dissolved in DCE (30 mL). 4Å MS (2.0 g) were added and the solution was stirred at room temperature for 30 minutes to remove any moisture. Silver carbonate (1.2 g, 4.2 mmol) was added and the reaction mixture was stirred in the dark at room temperature overnight. The reaction mixture was then filtered through Celite and the volatile components were evaporated *in vacuo* to give a crude syrup which was purified by FCC to give the title compound (**9**) (1.1 g, 62%) as a colourless oil. R_f 0.64 (hexane/EtOAc 7:3); $[\alpha]_D^{+106^\circ}$ ($c = 1.0$, CHCl_3); δ_H (400 MHz; CDCl_3) 8.05–8.01 (m, 4H, Ar), 7.94 (dd, $^4J_{B,B'} = 1.4$ Hz, $J_{B,C} = 8.5$ Hz, 2H, Ar), 7.59–7.31 (m, 9H, Ar), 5.86 (m, 1H, H-2), 5.74 (dd, $J_{1',2'} = 6.1$ Hz, $J_{2',3'} = 8.7$ Hz, 1H, H-2'), 5.71–5.68 (m, 1H, H-4'), 5.62 (dd, $J_{2',3'} = 8.7$ Hz, $J_{3',4'} = 3.4$ Hz, 1H, H-3'), 5.29 (dq, $J_{2,3a} = 17.3$ Hz, $^2J_{3a,3b} = 1.7$ Hz, 1H, H-3a), 5.17 (dq, $J_{2,3b} = 10.5$ Hz, $^2J_{3a,3b} = 1.7$ Hz, 1H, H-3b), 4.82 (d, $J_{1',2'} = 6.1$ Hz, 1H, H-1'), 4.38 (ddt, $J_{1a,1b} = 13.1$ Hz, $J_{1a,2} = 5.0$ Hz, $^4J_{1a,3} = 1.6$ Hz, 1H, H-1a), 4.33 (dd, $J_{4,5a'} = 4.4$ Hz, $^2J_{5a',5b'} = 12.7$ Hz, 1H, H-5a'), 4.16 (ddt, $J_{1a,1b} = 13.1$ Hz, $J_{1b,2} = 6.2$ Hz, $^4J_{1b,3} = 1.3$ Hz, 1H, H-1b), 3.90 (dd, $J_{4,5b'} = 2.3$ Hz, $^2J_{5a',5b'} = 12.7$ Hz, 1H, H-5b'); δ_C (100 MHz; CDCl_3) 165.7, 165.6, 165.3 (3 \times C=O), 133.5 (C2), 133.4, 133.3, 133.3, 129.9, 129.9, 129.8, 129.8, 129.4, 129.4, 129.1, 128.5, 128.5, 128.4, 117.8 (C3), 99.4 (C1'), 70.5 (C3'), 70.0 (C2'), 69.7 (C1), 68.3 (C4'), 62.3 (C5'); HRMS (ESI⁺) m/z calc. for $\text{C}_{29}\text{H}_{26}\text{O}_8\text{Na}^+$ 525.1525 $[\text{M}+\text{Na}]^+$ found 525.1522 $[\text{M}+\text{Na}]^+$.

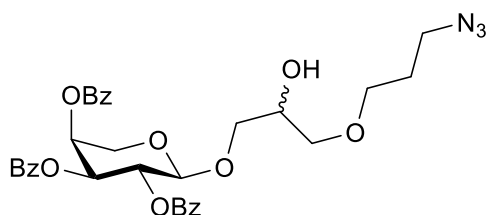
(2-*R/S*-Oxiranyl)methyl 2',3',5'-tri-*O*-benzoyl- α -L-arabinopyranoside (**5**)



Prop-2-en-1-yl 2,3,5-tri-*O*-benzoyl- α -L-arabinopyranoside (**9**) (1.1 g, 2.2 mmol) and mCPBA (450 mg, 2.6 mmol) were dissolved into DCE (20 mL) and heated to 80 °C overnight. The solvent was removed *in vacuo*, the crude product was re-dissolved into EtOAc (10 mL) and washed with sat. sodium bicarbonate solution (3 \times 3 mL). The organic layer was then separated and dried over MgSO_4 , filtered and the solvent evaporated *in vacuo* to give the

title compounds (**5**) (640 mg, 45%) as a white powder (1:1 mixture of diastereoisomers, as judged by the integration of the H-1' signals at 4.92 and 4.82 ppm). R_f 0.5 (hexane/EtOAc 7:3); δ_H (400 MHz; $CDCl_3$) 8.08-7.94 (m, 12H, Ar), 7.60-7.32 (m, 18H, Ar), 5.73 (dd, $J_{1',2'} = 6.0$ Hz, $J_{2',3'} = 8.4$ Hz, 2H, H-2',2'*), 5.70-5.69 (m, 2H, H-4',4'*), 5.62 (dd, $J_{2',3'} = 8.4$ Hz, $J_{3',4'} = 3.4$ Hz, 2H, H-3',3'*), 4.92 (d, $J_{1'a,2'} = 6.0$ Hz, 1H, H-1'), 4.82 (d, $J_{1'b,2'} = 6.0$ Hz, 1H, H-1'*), 4.34 (m, 2H, H-5a',5a'*), 4.09 (dd, $J_{1a,1b} = 12.0$ Hz, $J_{1a,2} = 3.0$ Hz, 1H, H-1a), 3.91 (dd, $^2J_{5a',5b'} = 12.1$ Hz, $J_{4,5''} = 3.0$ Hz, 2H, H-5b',5b'*), 3.85 (dd, $J_{1a^*,1b^*} = 12.0$ Hz, $J_{1a^*,2^*} = 5.1$ Hz, 2H, H-1a*, H-1b*), 3.19-3.12 (m, 2H, H-2, 2*), 2.76-2.73 (m, 2H, H-3a,3a*), 2.62 (dd, $^2J_{3b^*,3a^*} = 5.1$ Hz, $J_{3b^*,2^*} = 2.6$ Hz, 1H, H-3b*), 2.58 (dd, $^2J_{3b^*,3a^*} = 5.1$ Hz, $J_{3b^*,2^*} = 2.6$ Hz, 1H, H-3a*); δ_C (100 MHz; $CDCl_3$) 165.7, 165.6, 165.3, (3 \times C=O), 133.4, 133.4, 133.3, 130.2, 129.9, 129.8, 129.4, 129.3, 129.1, 128.5, 128.4, 128.3, 100.5 (C1'), 100.2 (C1'*), 70.4 (C3'), 70.2 (C3'*), 69.9, (C2'), 69.9 (C2'*), 69.9 (C1), 68.9 (C1*), 68.2 (C4), 68.1 (C4*), 50.7 (C2), 50.4 (C2*), 44.3 (C3), 44.1 (C3*); HRMS (ESI⁺) m/z calc. for $C_{29}H_{26}O_9Na^+$ 541.1469 [M+Na]⁺ found 541.1467 [M+Na]⁺.

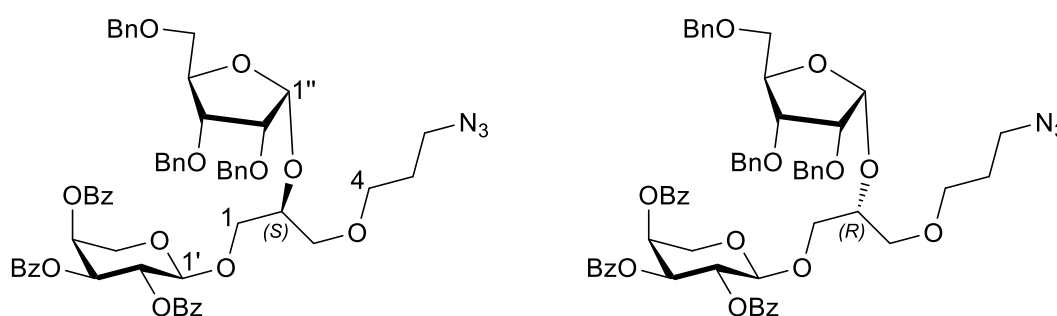
3-(3-Azidopropoxy)-2-hydroxypropyl 2,3,4-tri-O-benzoyl- α -L-arabinopyranoside (**12**)



(2-*R/S*-Oxiranyl)methyl 2',3',5'-tri-*O*-benzoyl- α -L-arabinopyranoside (**5**) (1.0 g, 1.9 mmol), 3-azido propanol (230 μ L, 2.5 mmol) and $Sc(OTf)_3$ (140 mg, 15 mol%) were dissolved into toluene (100 mL) and stirred vigorously at room temperature overnight. The reaction mixture was then washed with sat. sodium bicarbonate solution (3 \times 30 mL) and the organic layer dried over $MgSO_4$, filtered and the solvent evaporated *in vacuo*. The crude product was then purified by FCC to give the title compounds (**12**) (480 mg, 40%) as a colourless oil (1:1 mixture of diastereoisomers as judged by the integration of the 1H signals at 4.81 and 4.79 ppm). R_f 0.27 (hexane/EtOAc 7:3); δ_H (400 MHz; $CDCl_3$) 8.08-8.00 (m, 8H, Ar), 7.93-7.90 (m, 4H, Ar), 7.61-7.30 (m, 18H, Ar), 5.74 (dd, $J_{1',2'} = 6.5$ Hz, $J_{2',3'} = 8.9$ Hz, 2H, H-2', H-2'*), 5.71-5.67 (m, 2H, H-4', H-4'*), 5.61 (dd, $J_{2',3'} = 8.9$ Hz, $J_{3',4'} = 3.5$ Hz, 2H, H-3',3'*), 4.81 (d, $J_{1',2'} = 6.5$ Hz, 1H, H-1'), 4.79 (d, $J_{1'',2''} = 6.5$ Hz, 1H, H-1'*), 4.34 (dd, $J_{5,5'} = 12.9$ Hz, $J_{4,5} = 3.7$ Hz, 2H, H-5',5'*), 3.98-3.86 (m, 6H, H-5'',5''*,2,2*,3a,3a*), 3.75 (dd, $^2J_{3a,3b} = 10.2$ Hz, $J_{2,3a} = 4.4$ Hz, 1H, H-3b), 3.67 (dd, $^2J_{3a^*,3b^*} = 9.8$ Hz, $J_{2,3a^*} = 3.5$ Hz, 1H, H-3b*), 3.45-3.28 (m, 10H, H-

4,1a,1a*,1b,1b*,6,6*), 2.35 (s, 1H, OH), 2.17 (s, 1H, OH*), 1.78-1.73 (m, 2H, H-5,5*); δ_c (100 MHz; CDCl₃) 165.7, 165.6, 165.3 (3 × C=O), 133.5, 133.4, 129.9, 129.9, 129.8, 129.4, 129.3, 129.2, 129.0, 128.5, 128.5, 128.4, 128.2, 101.5 (C1), 101.4 (C1*), 71.6 (C4), 71.6 (C4*), 71.3 (C3), 71.1 (C3*), 70.6 (C3'3'*), 69.3 (C2), 69.3 (C2*), 68.4 (C4',4'*), 68.0 (C1,1*), 63.0 (C5',5'*), 48.4 (C6,6*), 29.0 (C5), 28.9 (C5*); HRMS (ESI⁺) m/z calc. for C₃₂H₃₃N₃O₁₀Na⁺ 642.2058 [M+Na]⁺ found 642.2051 [M+Na]⁺.

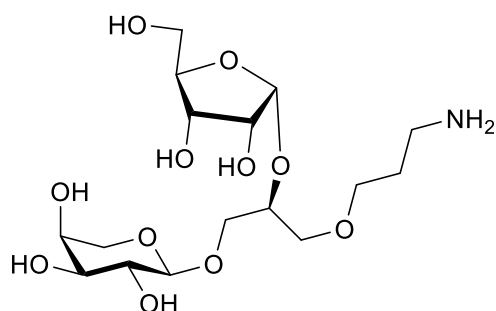
3-(3-Azidopropoxy)-2-[(2',3',5'-tri-O-benzyl- α -D-ribofuranosyl)oxy]propyl-2'',3'',4''-tri-O-benzoyl- α -L-arabinopyranoside (14)



3-(3-Azidopropoxy)-2-hydroxypropyl 2,3,4-tri-O-benzoyl- α -L-arabinopyranoside (**12**) (200 mg, 0.3 mmol) and 2',3',5'-tri-O-benzyl- β -D-ribofuranosyl (*N*-phenyl)-2,2,2-trifluoroacetimidate (**4**) (270 mg, 0.45 mmol) were co-evaporated with dichloroethane (3 × 10 mL) before being dissolved into dry dichloromethane (10 mL). Freshly prepared 4Å MS (1.0 g) were added and the suspension was stirred under a nitrogen atmosphere for 30 minutes. The reaction mixture was then cooled to -78 °C and TMSOTf (11 μ L, 60 μ mmol) was added by syringe. After 2 hours of stirring at -78 °C, the reaction was quenched with NEt₃ (20 μ L) and the solvents were removed *in vacuo*. Excess acceptor was removed by FCC and the diastereomeric products were then separated by preparative TLC (hexane/EtOAc 6:4) to give (**2S-14**) (30 mg, 10%) as a colourless oil. R_f 0.53 (hexane/EtOAc 6:4); $[\alpha]_D^{+120}$ (c 1.0, CHCl₃); δ_H (400 MHz; CDCl₃) 8.04-8.00 (m, 4H, Bz), 7.93 (dd, $J = 8.2$ Hz, $J = 1.1$ Hz, 2H, Bz), 7.57-7.19 (m, 24H, Ar), 5.67 (dd, $J_{1',2'} = 6.0$ Hz, $J_{2',3'} = 7.9$ Hz, 1H, H-2'), 5.56 (m, 2H, H-4',3'), 5.23 (d, $J_{1'',2''} = 4.4$ Hz, 1H, H-1''), 4.91 (d, $J_{1',2'} = 6.0$ Hz, 1H, H-1'), 4.69 (d, $^2J_{CHHPH, CHHPH} = 10.0$ Hz, 1H, CHHPH), 4.66 (d, $^2J_{CHHPH, CHHPH} = 10.0$ Hz, 1H, CHHPH), 4.56 (d, $^2J_{CHHPH, CHHPH} = 15.2$ Hz, 1H, CHHPH), 4.53 (d, $^2J_{CHHPH, CHHPH} = 15.2$ Hz, 1H, CHHPH), 4.46 (d, $^2J_{CHHPH, CHHPH} = 12.2$ Hz, 1H, CHHPH), 4.40 (d, $^2J_{CHHPH, CHHPH} = 12.2$ Hz, 1H, CHHPH), 4.27 (dd, $J_{3'',4''} = 7.4$ Hz, $J_{4'',5''} = 3.7$ Hz, 1H, H-4''), 4.20 (dd, $J_{4',5a'} = 3.8$ Hz, $^2J_{5a',5b'} = 12.8$ Hz, 1H, H-5a'), 4.03-4.00 (m, 1H, H-2), 3.92 (dd,

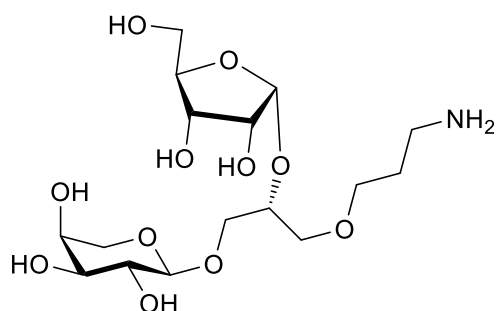
$J_{2,3a} = 6.3$, $J_{3a,3b} = 10.9$, 1H, H-3a), 3.86-3.81 (m, 2H, H-3'',3b), 3.77 (dd, $J_{1'',2''} = 4.4$ Hz, $J_{2'',3''} = 6.5$ Hz, 1H, H-2''), 3.72 (dd, $J_{4',5b'} = 1.8$ Hz, ${}^2J_{5a',5b'} = 12.8$ Hz, 1H, H-5b'), 3.51 (d, $J_{1,2} = 5.4$ Hz, 2H, H-1), 3.36 (dd, $J_{4'',5''} = 3.7$ Hz, ${}^2J_{5a'',5b''} = 3.7$ Hz, 2H, H-5a'',5b''), 3.34-3.26 (m, 2H, H-4), 3.27 (t, $J_{5,6} = 6.8$ Hz, 2H, H-6), 1.69-1.62 (m, 2H, H-5); δ_c (100 MHz; CDCl₃) 165.7, 165.6, 165.3 (3 × C=O), 138.4, 138.1, 138.0, 133.3, 133.3, 129.9, 129.9, 129.5, 129.2, 128.5, 128.4, 128.4, 128.4, 128.4, 128.3, 128.1, 127.8, 127.7, 127.7, 127.6, 127.6, 127.6, 101.4 (C1''), 100.5 (C1'), 81.8 (C4''), 75.7 (C2), 75.6 (C3''), 74.4 (CH₂Ph), 72.4 (CH₂Ph), 72.2 (CH₂Ph), 71.5 (C1), 70.5 (C3'), 70.1 (C2'), 70.0 (C5''), 67.0 (C3), 68.5 (C4'), 67.9 (C4), 62.2 (C5'), 48.4 (C6), 29.1 (C5); HRMS (ESI⁺) m/z calc. for C₅₈H₅₉N₃O₁₄Na⁺ 1044.3889 [M+Na]⁺ found 1044.3890 [M+Na]⁺ and **(2R-14)** (45 mg, 15%) as a colourless oil. R_f 0.45 (hexane/EtOAc 6:4); $[\alpha]_D + 95.9$ (c 1.0, CHCl₃); δ_H (400 MHz; CDCl₃) 8.01-8.00 (m, 4H, Bz), 7.87 (dd, $J = 8.2$ Hz, $J = 1.0$ Hz, 2H, Bz), 7.56-7.22 (m, 24H, Ar), 5.74 (dd, $J_{1',2'} = 7.0$ Hz, $J_{2',3'} = 9.4$ Hz, 1H, H-2'), 5.60-5.58 (m, 1H, H-4'), 5.52 (dd, $J_{2',3'} = 9.4$ Hz, $J_{3',4'} = 3.6$ Hz, 1H, H-3'), 5.21 (d, $J_{1'',2''} = 4.2$ Hz, 1H, H-1''), 4.88 (d, $J_{1',2'} = 7.0$ Hz, 1H, H-1'), 4.71 (d, ${}^2J_{CHHPh, CHHPh} = 12.1$ Hz, 1H, CHHPh), 4.69 (d, ${}^2J_{CHHPh, CHHPh} = 12.1$ Hz, 1H, CHHPh), 4.56 (d, ${}^2J_{CHHPh, CHHPh} = 11.7$ Hz, 1H, CHHPh), 4.53 (d, ${}^2J_{CHHPh, CHHPh} = 11.7$ Hz, 1H, CHHPh), 4.50 (d, ${}^2J_{CHHPh, CHHPh} = 11.9$ Hz, 1H, CHHPh), 4.44 (d, ${}^2J_{CHHPh, CHHPh} = 11.9$ Hz, 1H, CHHPh), 4.24 (dd, $J_{3'',4''} = 8.3$ Hz, $J_{4'',5''} = 4.0$ Hz, 1H, H-4''), 4.18 (dd, $J_{4',5a'} = 3.3$ Hz, ${}^2J_{5a',5b'} = 13.1$ Hz, 1H, H-5a'), 4.02-3.95 (m, 2H, H-3a,2), 3.85-3.79 (m, 2H, H-3b,3''), 3.72-3.69 (m, 2H, H-5b',2''), 3.50 (dd, $J_{4'',5''} = 5.0$ Hz, ${}^2J_{5a'',5b''} = 10.3$ Hz, 1H, H-5a''), 3.45-3.39 (m, 2H, H-5b'',1), 3.34-3.27 (m, 2H, H-4), 3.22 (t, $J_{5,6} = 7.0$ Hz, 2H, H-6), 1.67-1.61 (m, 2H, H-5); δ_c (100 MHz; CDCl₃) 165.7, 165.6, 165.3 (3 × C=O), 133.3, 133.3, 129.9, 129.8, 129.4, 129.4, 129.1, 128.5, 128.4, 128.4, 128.3, 128.1, 128.0, 127.7, 127.7, 127.6, 101.5 (C1''), 101.1 (C1'), 81.6 (C4''), 77.7 (C2''), 75.7 (C2), 75.5 (C3''), 73.5 (CH₂Ph), 72.3 (CH₂Ph), 72.3 (CH₂Ph), 71.0 (C3'), 70.6 (C5''), 70.2 (C2'), 70.0 (C1), 69.2 (C3), 68.9 (C4'), 67.9 (C4), 63.3 (C5'), 48.4 (C6), 29.0 (C5); HRMS (ESI⁺) m/z calc. for C₅₈H₅₉N₃O₁₄Na⁺ 1044.3889 [M+Na]⁺ found 1044.3885 [M+Na]⁺.

(2S)-3-(3-aminopropoxy)-2-(α -D-ribofuranosyloxy)propyl α -L-arabinopyranoside (2S-15)



(2S)-3-(3-Azidopropoxy)-2-[(2',3',5'-tri-*O*-benzyl- α -D-ribofuranosyl)oxy]propyl-2'',3'',4''-tri-*O*-benzoyl- α -L-arabinopyranoside (**2S-14**) (30 mg, 29 μ mol) was dissolved in a mixture of MeOH (10 mL) and EtOAc (5 mL) and hydrogenated palladium on activated charcoal (10% Pd basis) (5 mg) under a hydrogen pressure of \sim 15 PSI at 50 $^{\circ}$ C for 24 hours. The resulting mixture was filtered through Celite and the filter was washed with additional MeOH (25 mL). The solvent was removed *in vacuo* and the resulting crude mixture was dissolved in a mixture of MeOH/H₂O/NEt₃ (5:2:1 mL) and stirred at room temperature overnight. The solvent mixture was evaporated *in vacuo* and the crude mixture was passed through a short column of Dowex[®] 1X2-400 resin (OH⁻ form) in water. The water was removed by lyophilisation to give (**2S-15**) (7.4 mg, 41 %) as a white powder. $[\alpha]_D^{+35.5}$ (c 1.0, H₂O); δ_H (400 MHz; D₂O) 5.24 (t, $J_{1'',2''} = 3.9$ Hz, 1H, H-1''), 4.29 (d, $J_{1',2'} = 7.6$ Hz, 1H, H-1'), 4.11 (dd, $J_{3'',4''} = 7.6$ Hz, $J_{4'',5''} = 3.7$ Hz, 1H, H-4''), 4.05-3.92 (m, 4H, H-4',2'',3'',3a), 3.87-3.82 (m, 2H, H-5',2), 3.74 (dd, $J_{2,3a} = 4.9$ Hz, $J_{3a,3b} = 10.5$ Hz, 1H, H-3b), 3.70-3.47 (m, 8H, H-1,5a'',5''b,3',5b',4,2'), 2.83 (t, $J_{5,6} = 7.2$ Hz, 1H, H-6), 1.80-1.73 (m, 1H, H-5); δ_C (100 MHz; CDCl₃) 103.5 (C1'), 102.0 (C1''), 84.7 (C4''), 75.7 (C4'), 72.3 (C3'), 71.4 (C2''), 70.7 (C2'), 69.7 (C1), 69.6 (C3''), 69.6 (C3), 69.1 (C4), 68.2 (C2), 66.3 (C5'), 61.4 (C5''), 37.7 (C6), 29.0 (C5); HRMS (ESI⁺) *m/z* calc. for C₁₆H₃₁NO₁₁Na⁺ 414.1970 [M+Na]⁺ found 414.1969 [M+Na]⁺

(2R)-3-(3-aminopropoxy)-2-(α -D-ribofuranosyloxy)propyl α -L-arabinopyranoside (2R-15)



(2R)-3-(3-Azidopropoxy)-2-[(2',3',5'-tri-*O*-benzyl- α -D-ribofuranosyl)oxy]propyl-2'',3'',4''-tri-*O*-benzoyl- α -L-arabinopyranoside (**2R-15**) (45 mg, 44 μ mol) was dissolved in a mixture of MeOH (10 mL) and EtOAc (5 mL) and hydrogenated with palladium on activated charcoal (10% Pd basis) (5 mg) under a hydrogen pressure of \sim 15 PSI at 50 $^{\circ}$ C for 24 hours. The resulting mixture was filtered through Celite and the filter was washed with additional MeOH (25 mL). The solvent was removed *in vacuo* and the resulting crude mixture was dissolved in a mixture of MeOH/H₂O/NEt₃ (5:2:1 mL) and stirred at room temperature overnight. The solvent mixture was evaporated *in vacuo* and the crude mixture was passed through a short column of Dowex 1X2-400 resin (OH⁻ form) in water. The water was removed by lyophilisation to give (**2R-15**) (10.7 mg, 59%) as a white powder. $[\alpha]_D +40.4$ ($c = 1.0$, H₂O); δ_H (400 MHz; D₂O) 5.24 (d, $J_{1'',2''} = 4.4$ Hz, 1H, H-1''), 4.29 (d, $J_{1',2'} = 7.7$ Hz, 1H, H-1'); 4.07 (dd, $J_{3'',4''} = 6.6$ Hz, $J_{4'',5a''} = 3.7$ Hz, 1H, H-4''), 4.04-4.00 (m, 2H, H-4',2''), 3.95 (dd, $J_{2'',3''} = 3.5$ Hz, $J_{3'',4''} = 6.6$ Hz, 1H, H-3''), 3.90-3.83 (m, 4H, H-3a, 2, 5a'), 3.75 (dd, $J_{2,3b} = 4.4$ Hz, $J_{3a,3b} = 11.4$ Hz, 1H, H-3b), 3.68 (dd, $J_{4'',5a''} = 3.7$ Hz, $J_{5a'',5b''} = 12.4$ Hz), 1H, H-5a''), 3.63-3.46 (m, 8H, H-1,5b'',3',5',4,2'), 2.60 (t, $J_{5,6} = 6.9$ Hz, 1H, H-6), 1.70-1.61 (m, 1H, H-5); δ_C (100 MHz; CDCl₃) 103.4 (C1'), 101.9 (C1''), 84.7 (C4'') 75.7 (C4'), 72.3 (C3'), 71.3 (C2''), 70.7 (C2'), 70.2 (C1), 69.6 (C3''), 69.3 (C4), 69.1 (C3), 68.2 (C2), 66.2 (C5'), 61.5 (C5''), 37.7 (C6), 31.4 (C5); HRMS (ESI⁺) m/z calc. for C₁₆H₃₁NO₁₁Na⁺ 414.1970 [M+Na]⁺ found 414.1968 [M+Na]⁺.

5.5 References

1. S. R. Manning and J. W. La Claire, *Mar. Drugs*, 2010, **8**, 678–704.
2. N. J. West, R. Bacchieri, G. Hansen, C. Tomas, P. Lebaron, and H. Moreau, *Appl. Environ. Microbiol.*, 2006, **72**, 860–868.
3. L. Galluzzi, E. Bertozzini, A. Penna, F. Perini, A. Pigalarga, E. Graneli, and M. Magnani, *Let. Appl. Microbiol.*, 2008, **46**, 261–266.
4. P. A. Holdway, R. A. Watson, and B. Moss, *Freshw. Biol.*, 1978, **8**, 295–311.
5. B. Wagstaff, I. Vladu, J. Barclay, D. Schroeder, G. Malin, and R. Field, *Viruses*, 2017, **9**, 40.
6. L. Levine and Y. Shimizu, *Toxicol.*, 1992, **30**, 411–418.
7. J. Naar, A. Bourdelais, C. Tomas, J. Kubanek, P. L. Whitney, L. Flewelling, J. L. Karen Steidinger, and D. G. Baden, *Environ. Health Perspect.*, 2002, **110**, 179–185.
8. W. Jawaid, J. P. Meneely, K. Campbell, K. Melville, S. J. Holmes, J. Rice, and C. T. Elliott, *J. Agric. Food Chem.*, 2015, **63**, 8574–8583.
9. K. Zhang, J. Wu, Y. Li, Y. Wu, T. Huang, and D. Tang, *Microchim. Acta*, 2014, **181**, 1447–1454.
10. D. Wu, R. Li, H. Wang, S. Liu, H. Wang, Q. Wei, and B. Du, *Analyst*, 2012, **137**, 608–613.
11. T. Igarashi, M. Satake, and T. Yasumoto, *J. Am. Chem. Soc.*, 1996, **118**, 479–480.
12. S. A. Rasmussen, S. Meier, N. G. Andersen, H. E. Blossom, J. Ø. Duus, K. F. Nielsen, P. J. Hansen, and T. O. Larsen, *J. Nat. Prod.*, 2016, **79**, 2250–2256.
13. J. Heimburg-Molinari and K. Rittenhouse-Olson, in *Glycomics*, Humana Press, Totowa, NJ, 2009, vol. 534, pp. 341–357.
14. M. Bröker, F. Berti, J. Schneider, and I. Vojtek, *Vaccine*, 2017, **35**, 3286–3294.
15. M. E. Pichichero, *Hum. Vaccin. Immunother.*, 2013, **9**, 2505–2523.
16. C. P. Stowell and Y. C. Lee, in *Advances in Carbohydrate Chemistry and Biochemistry*, ed. Intergovernmental Panel on Climate Change, Cambridge University Press, Cambridge, 1980, vol. 37, pp. 225–281.
17. M. Leenaars and C. F. M. Hendriksen, *ILAR J.*, 2005, **46**, 269–279.
18. M. Sajid, A. N. Kawde, and M. Daud, *J. Saudi Chem. Soc.*, 2015, **19**, 689–705.
19. R. Das and B. Mukhopadhyay, *ChemistryOpen*, 2016, **5**, 401–433.
20. H. A. V Kistemaker, H. S. Overkleeft, G. A. Van Der Marel, and D. V. Filippov, *Org. Lett.*, 2015, **17**, 4328–4331.
21. H. A. V Kistemaker, G. J. V. D. H. van Noort, H. S. Overkleeft, G. A. van der Marel, and D. V. Filippov, *Org. Lett.*, 2013, **15**, 2306–2309.

22. G. J. Van Der Heden Van Noort, H. S. Overkleeft, G. a. Van Der Marel, and D. V. Filippov, *Org. Lett.*, 2011, **13**, 2920–2923.
23. J. Chen, C. S. Jiang, W. Q. Ma, L. X. Gao, J. X. Gong, J. Y. Li, J. Li, and Y. W. Guo, *Bioorganic Med. Chem. Lett.*, 2013, **23**, 5061–5065.
24. G. Bellucci, G. Catelani, C. Chiappe, F. D’Andrea, and G. Grigò, *Tetrahedron: Asymmetry*, 1997, **8**, 765–773.
25. Y. Nishida, Y. Shingu, Y. Mengfei, K. Fukuda, H. Dohi, S. Matsuda, and K. Matsuda, *Beilstein J. Org. Chem.*, 2012, **8**, 629–639.
26. J. Lindberg, S. C. . Svensson, P. Pålsson, and P. Konradsson, *Tetrahedron*, 2002, **58**, 5109–5117.
27. K. Omura and D. Swern, *Tetrahedron*, 1978, **34**, 1651–1660.
28. W. Koenigs and E. Knorr, *Berichte der Dtsch. Chem. Gesellschaft*, 1901, **34**, 957–981.
29. B. Yu and H. Tao, *Tetrahedron Lett.*, 2001, **42**, 2405–2407.
30. C. Gauthier, J. Legault, S. Lavoie, S. Rondeau, S. Tremblay, and A. Pichette, *Tetrahedron*, 2008, **64**, 7386–7399.
31. S. Bernstein and R. B. Conrow, *J. Org. Chem.*, 1971, **36**, 863–870.
32. R. Suhr, O. Scheel, and J. Thiem, *J. Carbohydr. Chem.*, 1998, **17**, 937–968.
33. T. Igarashi, M. Satake, and T. Yasumoto, *J. Am. Chem. Soc.*, 1999, **121**, 8499–8511.
34. V. V. Rostovtsev, L. G. Green, V. V. Fokin, and K. B. Sharpless, *Angew. Chem - Int. Ed.*, 2002, **41**, 2596–2599.
35. C. W. Tornøe, C. Christensen, and M. Meldal, *J. Org. Chem.*, 2002, **67**, 3057–3064.
36. J. Conde, J. T. Dias, V. Grazú, M. Moros, P. V. Baptista, and J. M. de la Fuente, *Front. Chem.*, 2014, **2**, 1–27.
37. C. J. Palmer and J. E. Casida, *Tetrahedron Lett.*, 1990, **31**, 2857–2860.
38. T. Mukaiyama, Y. Hashimoto, and S. Shoda, *Chem. Lett.*, 1983, 935–938.
39. H.-S. Dang, B. P. Roberts, J. Sekhon, and T. M. Smits, *Org. Biomol. Chem.*, 2003, **1**, 1330–1341.

6 Appendices

Table 6.1 – Database of relative retention times and MRM transitions of selected sugar nucleotides.¹ Sugar nucleotides synthesised by me (Chapter 2) are shown in bold.

Sugar Nucleotide	Relative Retention time	MRM transitions	Fragment
UDP-Glc	1.00	565 → 323	[NMP-H] ⁻
		565 → 79	[H ₃ PO ₄ -H ₃ O] ⁻
UDP-Galp	0.92	565 → 323	[NMP-H] ⁻
		565 → 159	[H ₄ P ₂ O ₇ -H ₃ O] ⁻
UDP-α-D-galactofuranose (UDP-Galf)	1.10	565 → 323	[NMP-H]⁻
		565 → 159	[H₄P₂O₇-H₃O]⁻
UDP-GlcNAc	0.98	606 → 385	[NDP-H-H ₂ O] ⁻
		606 → 159	[H ₄ P ₂ O ₇ -H ₃ O] ⁻
UDP-GlcNAcA	0.89	620 → 403	[NDP-H] ⁻
		620 → 159	[H ₄ P ₂ O ₇ -H ₃ O] ⁻
UDP-2-amino-2-deoxy-α-D-glucose (UDP-GlcN)	0.90	564 → 385	[NDP-H-H ₂ O] ⁻
		564 → 273	?
UDP-2-amino-2-deoxy-α-D-galactose (UDP-GalN)	0.86	564 → 385	[NDP-H-H ₂ O] ⁻
		564 → 273	?
UDP-2,3-diacetamido-2,3-dideoxy-α-D-glucuronic acid (UDP-GlcdiNAcA)	0.95	661 → 403	[NDP-H] ⁻
		661 → 159	[H ₄ P ₂ O ₇ -H ₃ O] ⁻
UDP-GlcA	0.74	579 → 403	[NDP-H] ⁻
		579 → 323	[NMP-H] ⁻
UDP-2-deoxy-2-fluoro-α-D-galactose (UDP-2F-Gal)	0.94	567 → 385	[NDP-H-H ₂ O] ⁻
		567 → 159	[H ₄ P ₂ O ₇ -H ₃ O] ⁻

UDP-β-L-rhamnose	0.84	549 → 323	[NMP-H] ⁻
(UDP-L-Rha)		549 → 159	[H ₄ P ₂ O ₇ -H ₃ O] ⁻
UDP-L-Araf	1.05	535 → 323	[NMP-H] ⁻
		535 → 159	[H ₄ P ₂ O ₇ -H ₃ O] ⁻
UDP-L-Arap	0.81	535 → 323	[NMP-H] ⁻
		535 → 159	[H ₄ P ₂ O ₇ -H ₃ O] ⁻
UDP-Xylp	0.99	535 → 323	[NMP-H] ⁻
		535 → 159	[H ₄ P ₂ O ₇ -H ₃ O] ⁻
UDP-α-D-mannose	0.81	565 → 403	[NDP-H]⁻
		565 → 159	[H₄P₂O₇-H₃O]⁻
dTDP-α-D-glucose	1.39	563 → 321	[NMP-H] ⁻
(dTDP-Glc)		563 → 241	[Glc-1-P-H-H ₂ O] ⁻
dTDP-β-L-rhamnose	1.35	547 → 321	[NMP-H] ⁻
(dTDP-L-Rha)		547 → 225	c[Rha-1-P-H-H ₂ O] ⁻
GDP-Glc	1.56	604 → 362	[NMP-H] ⁻
		604 → 241	c[Glc-1-P-H-H ₂ O] ⁻
GDP-β-L-galactose	1.51	604 → 442	[NDP-H] ⁻
(GDP-L-Gal)		604 → 423	[NDP-H-H ₂ O] ⁻
GDP-Man	1.43	604 → 442	[NDP-H] ⁻
		604 → 424	[NDP-H-H ₂ O] ⁻
GDP-L-Fuc	1.60	588 → 442	[NDP-H] ⁻
		588 → 344	[NMP-H-H ₂ O] ⁻
GDP-α-D-arabinopyranose (GDP-Arap)	1.53	574 → 442	[NDP-H]⁻
		574 → 362	[NMP-H]⁻

GDP- β -L-xylopyranose (GDP-L-Xylp)	1.52	574 \rightarrow 442	[NDP-H] ⁻
		574 \rightarrow 424	[NDP-H-H ₂ O] ⁻
ADP-Glc	1.65	588 \rightarrow 346	[NMP-H] ⁻
		588 \rightarrow 241	[Glc-1-P-H-H ₂ O] ⁻
5''-(adenosine 5'-pyrophosphoryl)-D-ribose (ADP-Rib)	1.64	558 \rightarrow 346	[NMP-H] ⁻
		558 \rightarrow 159	[H ₄ P ₂ O ₇ -H ₃ O] ⁻

Table 6.1 - adapted from M. Rejzek, L. Hill, E. S. Hems, S. Kuhaudomlarp, B. A. Wagstaff, R. A. Field, *Methods in Enzymology*, Elsevier, 2017 (Article in Press).
<https://doi.org/10.1016/bs.mie.2017.06.005>

Table 6.2 - values for 2° position on the glyceryl glycosides, compared with literature value for analogous glycosylated part of prymnesin backbone

	PRM-1 α -D-Ribf		PRM-1 α -L-Arap		PRM-1 β -D-Galf		PRM-2 α -L-Xylf		PRM-2† β -D-Araf		PRM-B1 α -D-Galp	
	¹ H	¹³ C	¹ H	¹³ C	¹ H	¹³ C	¹ H	¹³ C	¹ H	¹³ C	¹ H	¹³ C
Lit.	3.84 ^a	87.8 ^a	4.53 ^a	78.3 ^a	4.48 ^a	78.6 ^a	3.76 ^a	88.0 ^a	3.76 ^{a*}	88.0 ^{a*}	3.59 ^b	90.3 ^b
Synth.	3.68 ^c	79.0 ^c	3.75 ^c	81.1 ^c	3.63 ^c	78.8 ^c	3.64 ^c	80.0 ^c	3.70 ^c	82.5 ^c	3.62 ^d	78.7 ^d

† Rasmussen et al.² have drawn PRM-2 as glycosylated with β -D-Araf but there is no data or discussion to support this in the paper; * The α -L-Xylf published values are used as a substitute. ^a Values for *N*-acetylated PRM-1/2 using CD₃OD/C₅D₅N 1:1 as solvent; ^b Values for PRM-B1 using CD₃OD as solvent; ^c CD₃OD as solvent; ^d D₂O as solvent.

Translated tri-functional protein sequence from *Prymnesium parvum* (Texoma 1) was acquired from the publicly available MMETSP database.² We believe this protein may be responsible from the biogenesis of GDP- β -L-Xylf.

Ara-4-epimerase, Galp mutase, unknown (lack of homology with NCBI dataset)

>*Prymnesium parvum*

MGVPPFVRRKLTQVTNVLVTGGGGFIGSHFALSIDKKGFNITLVDDLRSIETVLRQLALAAQHGQEL
HFEQLDVNEGFKMAALLKRNVDLVXHFSGNAYVGESMSMPQEYYQNITASTVSLVRAMHSAGVHKL
IFSSCATFGAPKQFPITEASPQRPTNPYQQAQLQAEQAIVAFRAQERAGAPFSAALLRYFNIGADPD
GRLGPHLRHEANAKFPRIVDAAYDVALGVREKMTVMGSSFPKDGSAQRDYIHVSDLVHAHLKLMYAL
RDNDLLFYNVGNGQPYTVLEIVEQVRQVTGKPIPIITLSKERPGDPPILYTDPAKIQYEIGWRPRYPDIHSM
ILHGWNWRVKHYGRPPAPSIDPLAHNGACFNSTTDEAPPLGNNPRIVVIGAGPTGLCAAYRTELGYTN
WELVEATAKPSGLACTIQDEXKFQWDIGVHCLFSHFEEFDALLDNMLPPKDWLYHQRYSPARMRGTW
VGYPVQSNLWRLPEAEVSGIADLAQKEVTPQKSGAQIRNFKDWLEAGFGKALDTDFMAPYNAKVWA
HPAEEMNYIWWGERVATIQFKNILSNVINKRDAPAWGPNAQFRYPMNGTGHIWVKVFDALPKERKRL
GARXEKVHTKPGAKAVVLQDGTTRIPFDGLLSTMPLPHLLRMTDPDHELAELAEGNNGAADHSKFKHQT
ANIIGVGIDGTAMPAALNGVHWVYFPEKEYIFYRVTVLSNFSPLMVAKPFKQWSLLIEVSESRRHEVLA
LKGDRALRARVIEGLHMSGMLPRNATIVSVWDTRLEYGYPVYVERN MHVHAADKALRQLGVWSR
GRFGSWKEYE VGNQDHSCMLGYDAVDSMLFGGNDQGREATFNLPNKVNNMVRPYDRMFDRDELAR
QAGRQHTFGAPYRRLKQLPQWDWVTYHCRGTDEWLDKIREVMIAQPEDTKWLIHGVEVCGFAKVKR
PMHEMLREGLNHHDRIPHPMADSAPTPFPVSGWVRHIIAHYKRLPDILFFAPSDVPASSRLEFSSSGRGS
IAAMKESADFGMWGTRIVDMPAAMHTTFCVWVPLTARA EKRLKRSCPERVVTMAEPVILVSKSRIL
NTPLETWKKVLSLLEDATAGKGNDELFSFGWHLLFGQGTVLPFRFMHEHWTAARPRAAARGSGNLSEA
ASSKRRGLRAWSSGSKHNSCHESAASNARTWFLFDARMATSGGRVAAMMPTCGLD

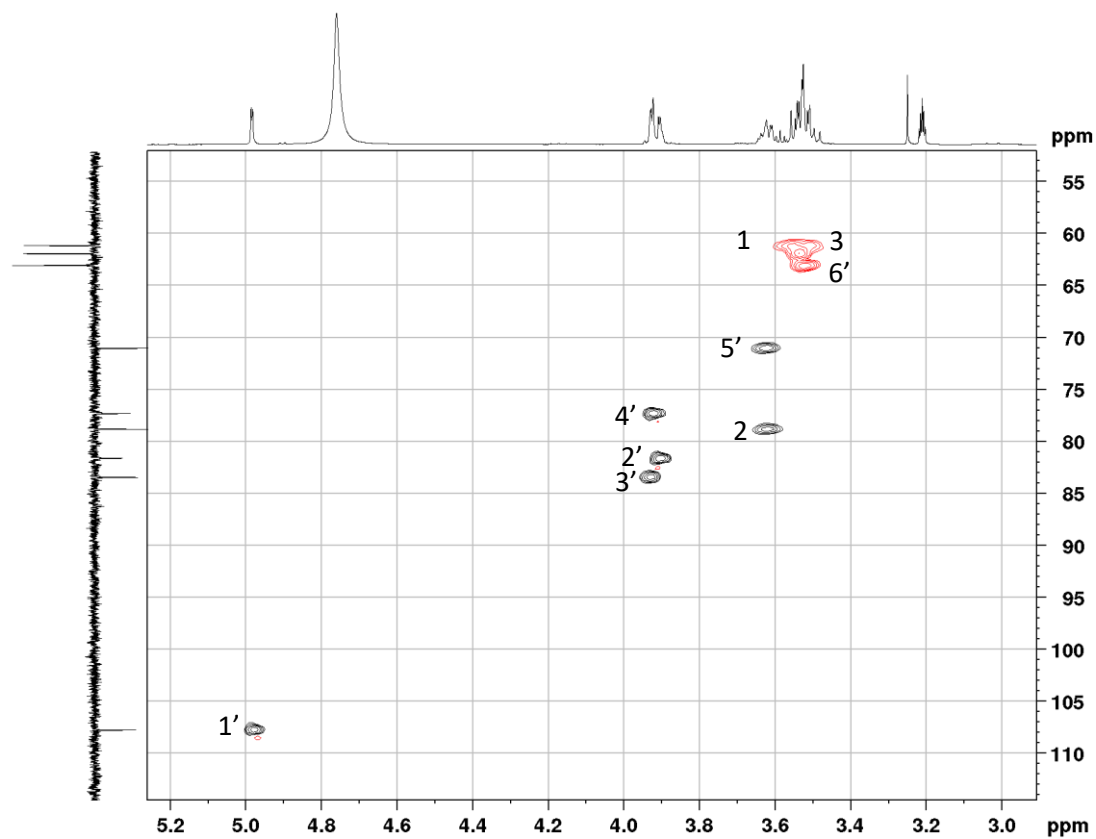


Figure 6.1 - HSQCed 2D NMR spectrum for 1,3-dihydroxypropan-2-yl- β -D-galactofuranoside

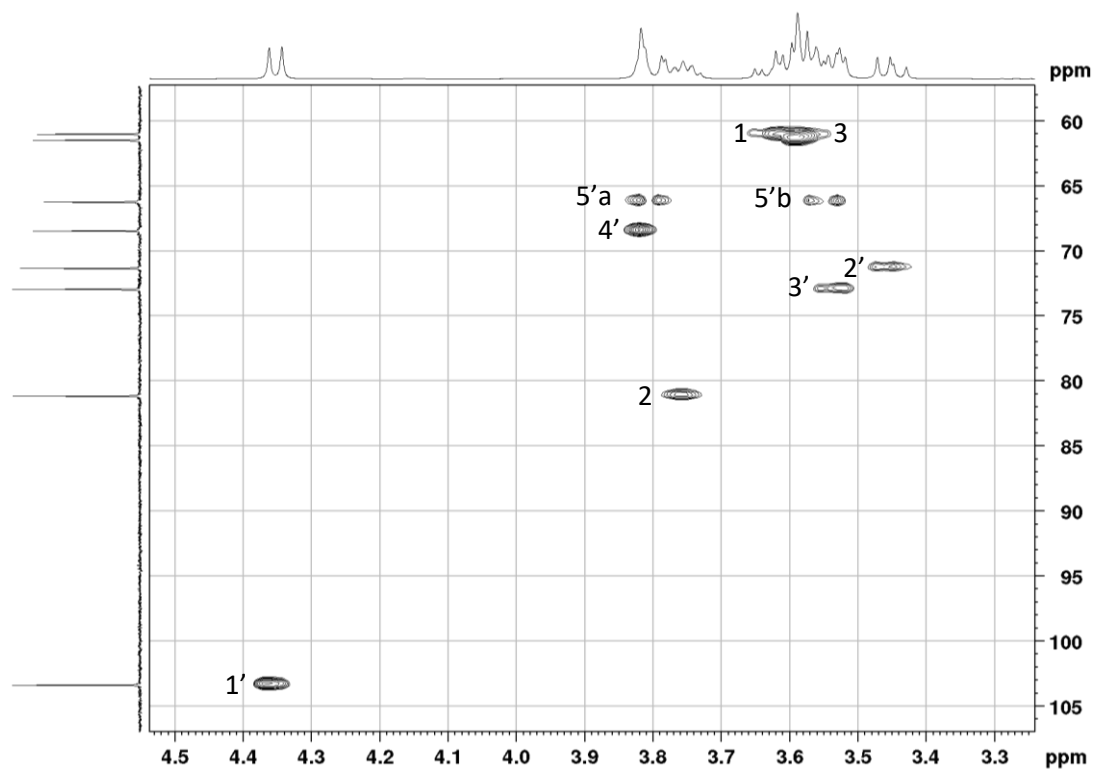


Figure 6.2 – Assigned HSQC NMR spectrum of 1,3-dihydroxypropan-2-yl α -L-arabinopyranoside.

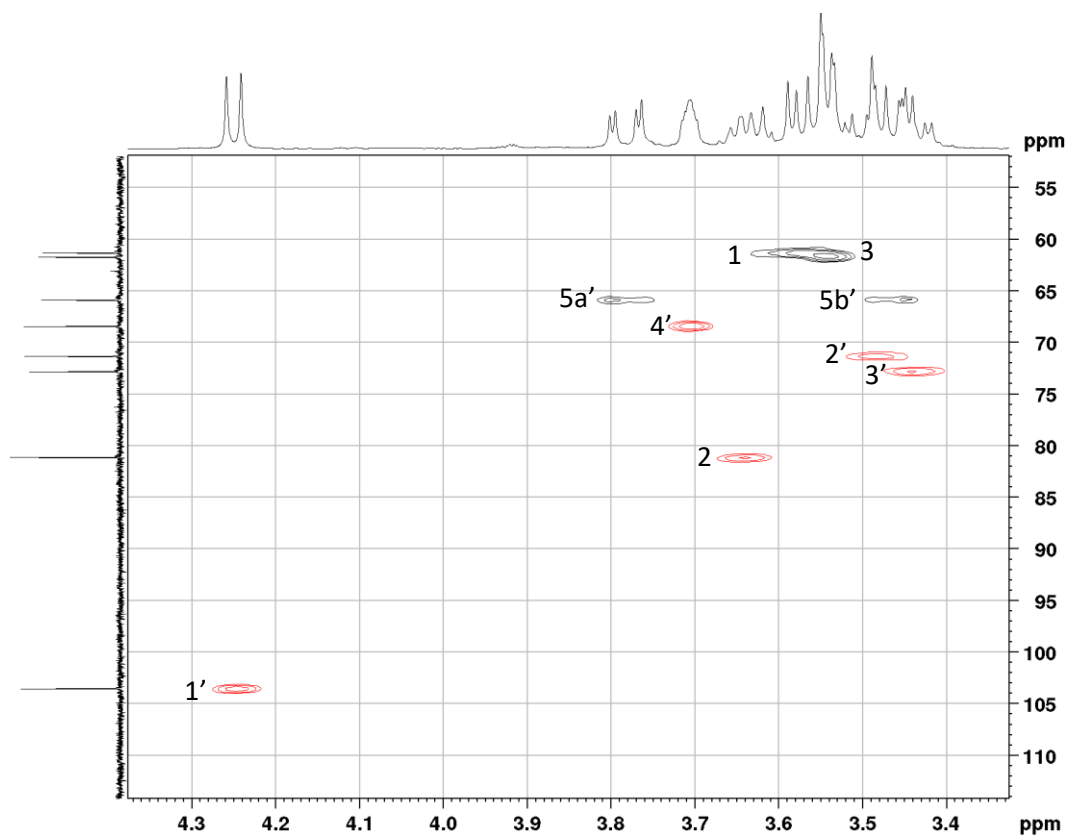


Figure 6.3 - HSQCed NMR spectrum for 1,3-dihydroxypropan-2-yl β -D-arabinopyranoside.

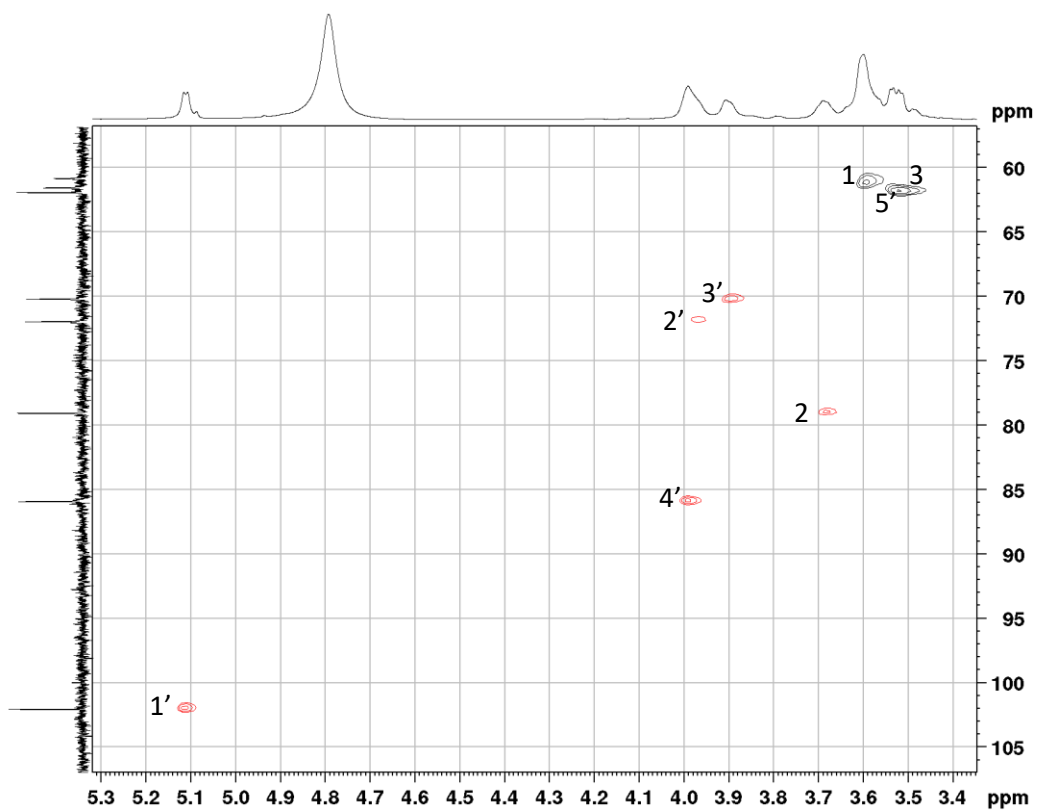


Figure 6.4 - HSQCed NMR spectrum of 1,3-dihydroxypropan-2-yl α -D-ribofuranoside

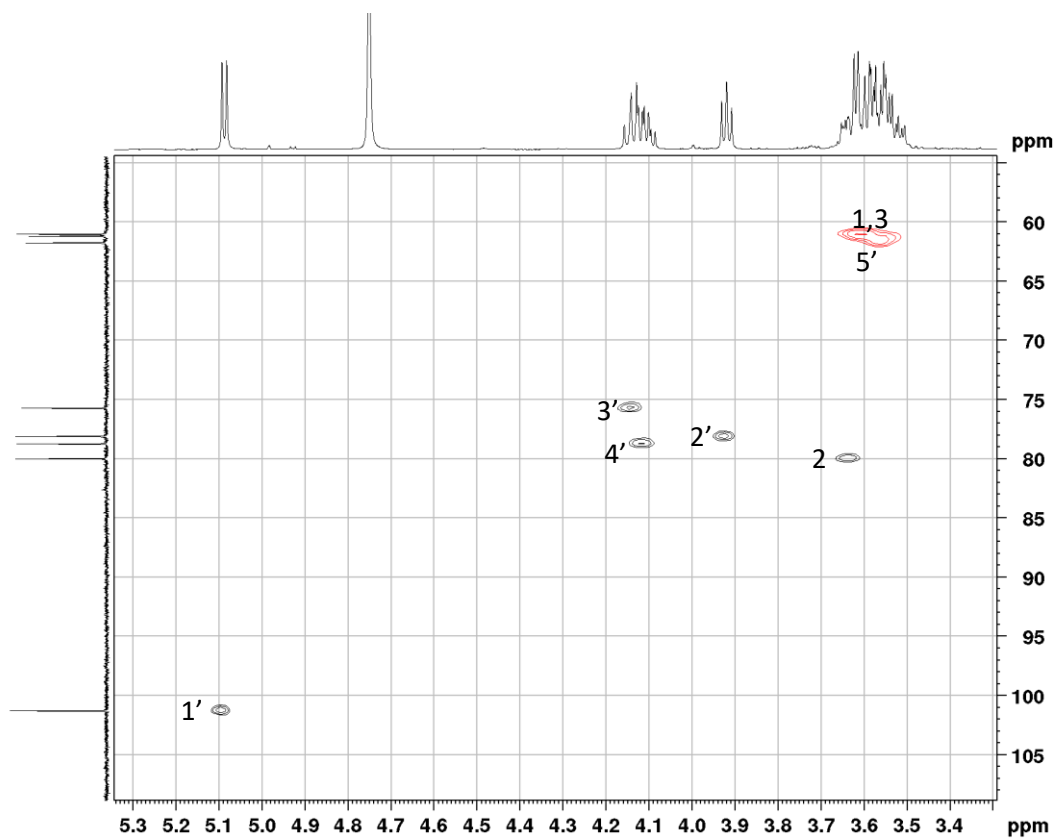


Figure 6.5 - HSQCed NMR spectrum of 1,3-dihydroxypropan-2-yl α -L-xylofuranoside

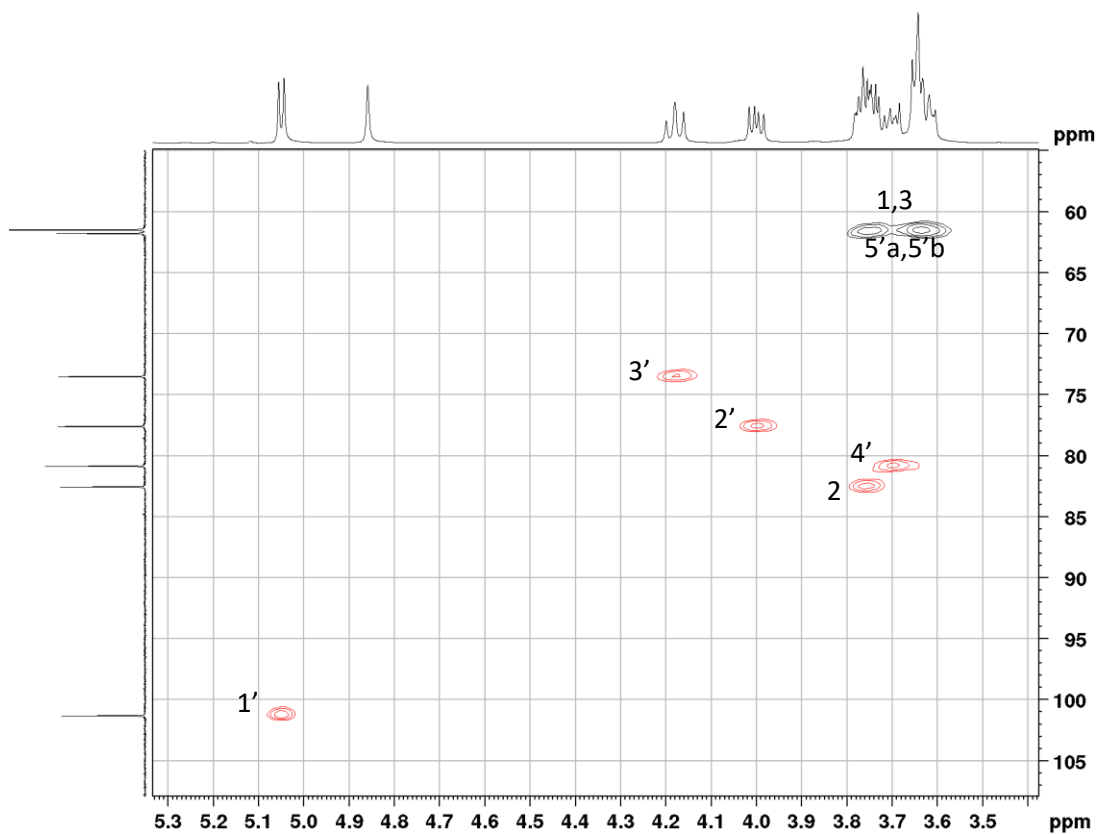


Figure 6.6 - HSQCed NMR spectrum of 1,3-dihydroxypropan-2-yl β -D-arabinofuranoside

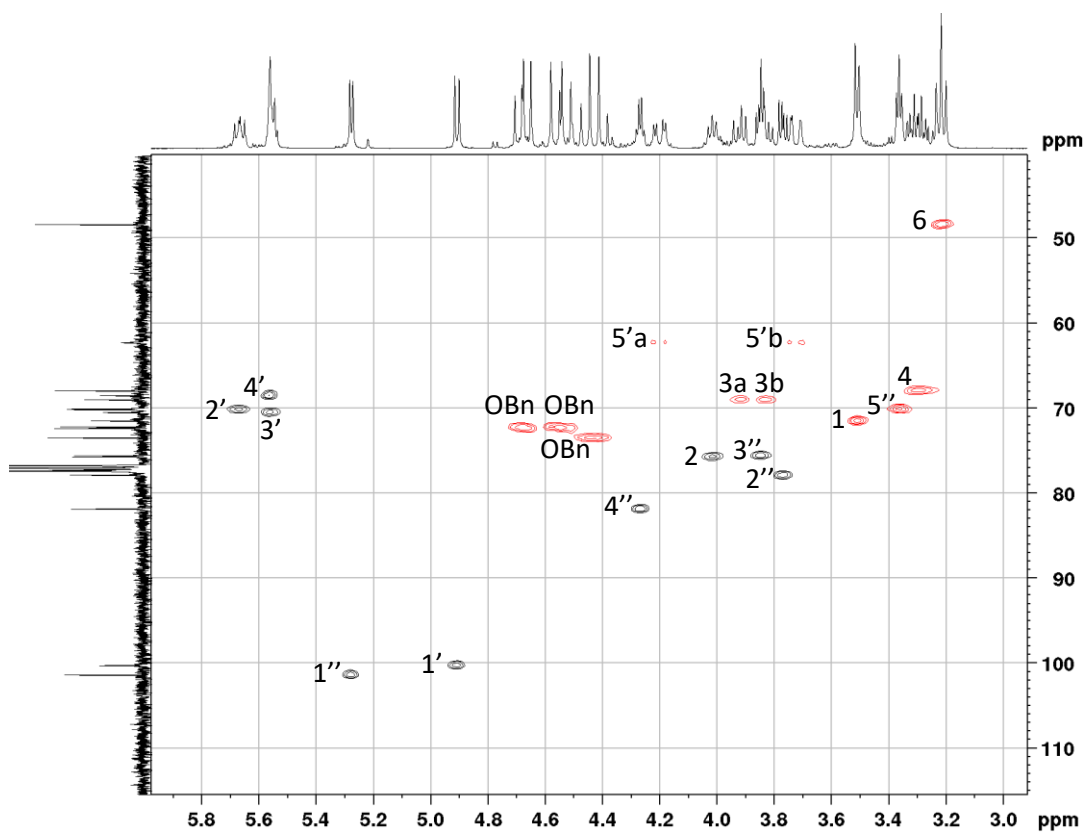


Figure 6.7 – Zoomed HSQCed spectrum of 3-(3-Azidopropoxy)-2R-[(2',3',5'-tri-O-benzyl- α -D-ribofuranosyl)oxy]propyl-2'',3'',4''-tri-O-benzoyl- α -L-arabinopyranoside

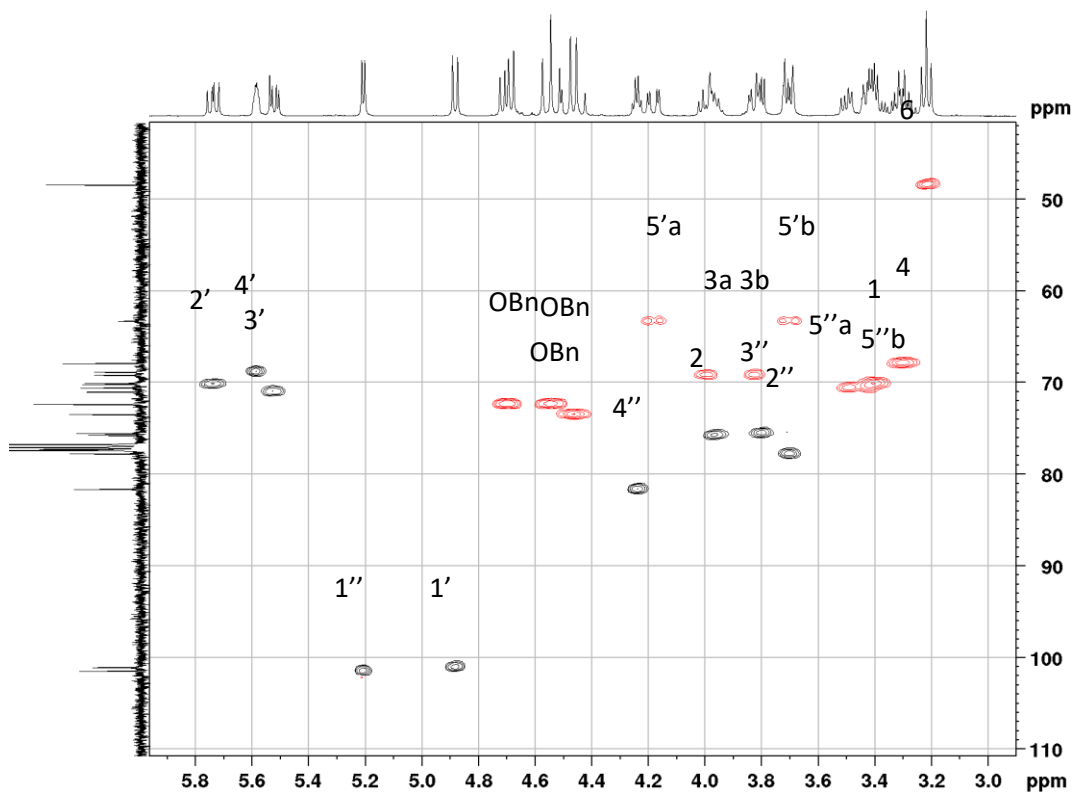


Figure 6.8 – Zoomed HSQCed spectrum of 3-(3-Azidopropoxy)-2S-[(2',3',5'-tri-O-benzyl- α -D-ribofuranosyl)oxy]propyl-2'',3'',4''-tri-O-benzoyl- α -L-arabinopyranoside

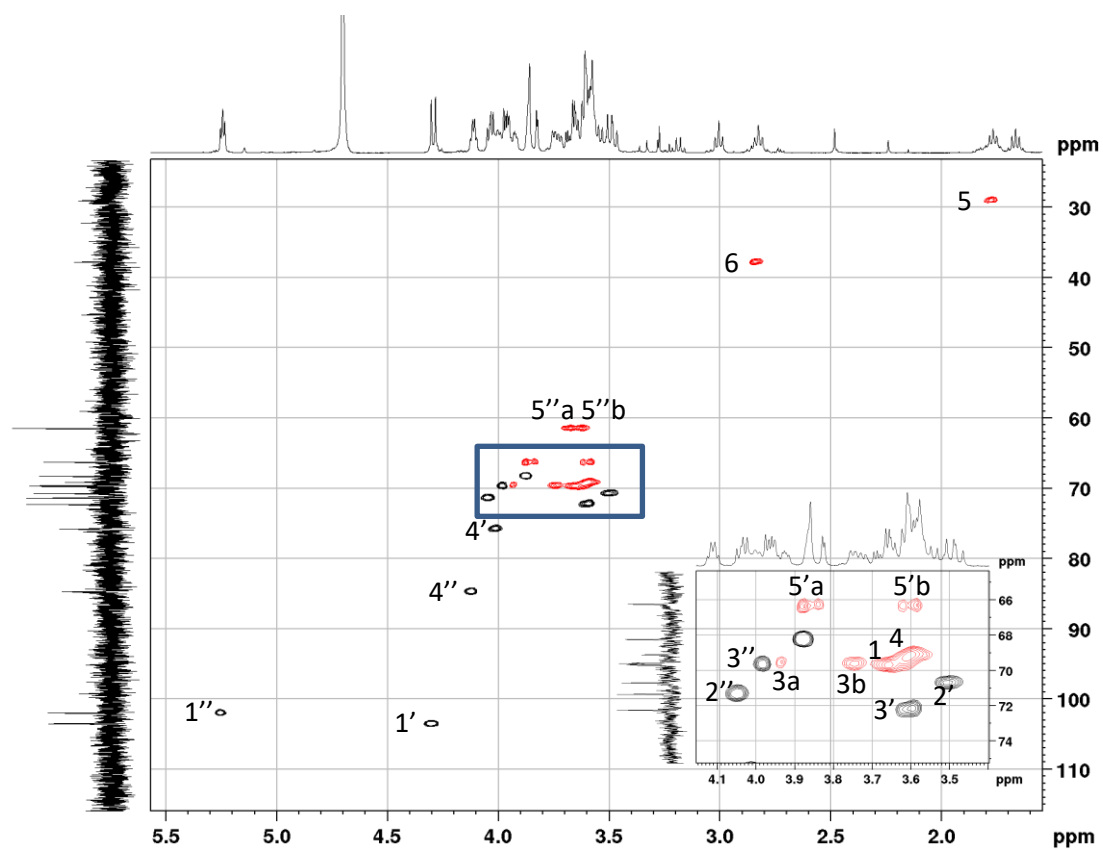


Figure 6.9 - Zoomed HSQCed spectrum of 3-(3-aminopropoxy)-2S-(α -D-ribofuranosyloxy)propyl α -L-arabinopyranoside

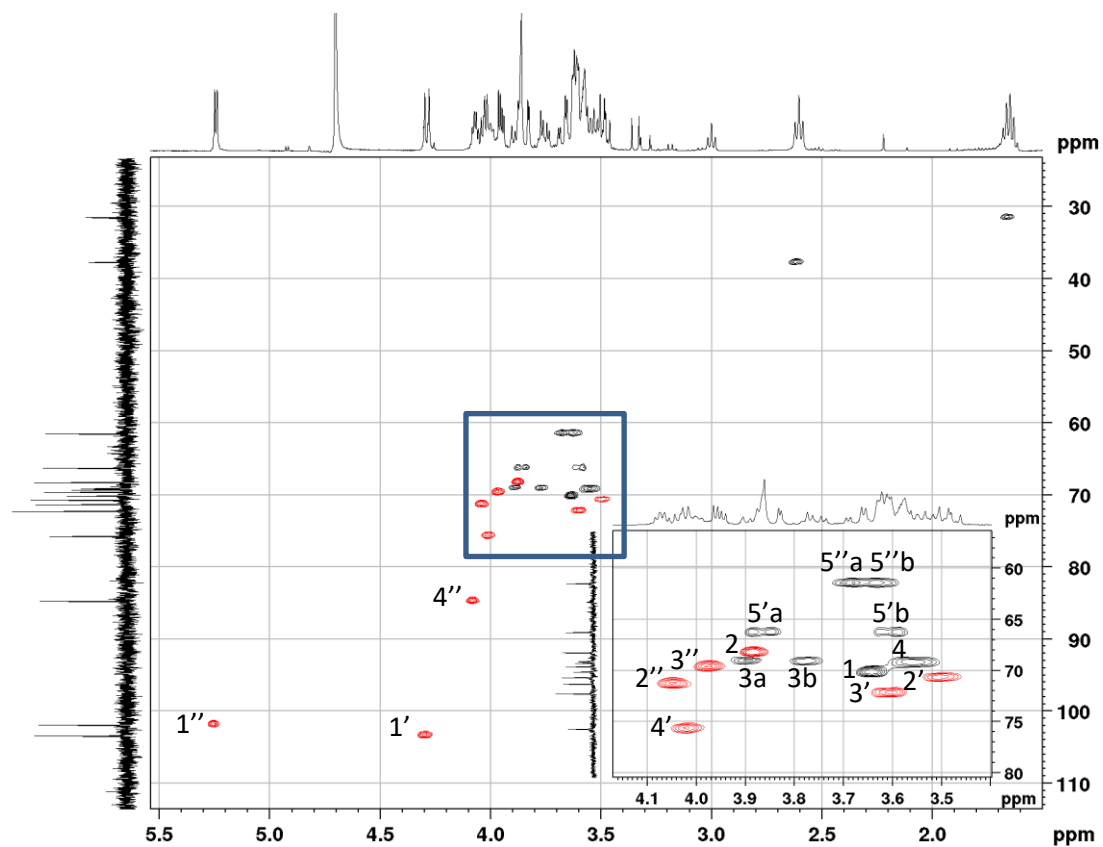


Figure 6.10 – Zoomed HSQCed spectrum of 3-(3-aminopropoxy)-2R-(α -D-ribofuranosyloxy)propyl α -L-arabinopyranoside

6.1 References

1. M. Rejzek, L. Hill, E. S. Hems, S. Kuhaudomlarp, B. A. Wagstaff, and R. A. Field, in *Methods in enzymology*, Elsevier Inc., 1st edn., 2017, pp. 1–30.
2. P. J. Keeling, F. Burki, H. M. Wilcox, B. Allam, E. E. Allen, L. A. Amaral-Zettler, E. V. Armbrust, J. M. Archibald, A. K. Bharti, C. J. Bell, B. Beszteri, K. D. Bidle, C. T. Cameron, L. Campbell, D. A. Caron, R. A. Cattolico, J. L. Collier, K. Coyne, S. K. Davy, P. Deschamps, S. T. Dyhrman, B. Edvardsen, R. D. Gates, C. J. Gobler, S. J. Greenwood, S. M. Guida, J. L. Jacobi, K. S. Jakobsen, E. R. James, B. Jenkins, U. John, M. D. Johnson, A. R. Juhl, A. Kamp, L. A. Katz, R. Kiene, A. Kudryavtsev, B. S. Leander, S. Lin, C. Lovejoy, D. Lynn, A. Marchetti, G. McManus, A. M. Nedelcu, S. Menden-Deuer, C. Miceli, T. Mock, M. Montresor, M. A. Moran, S. Murray, G. Nadathur, S. Nagai, P. B. Ngam, B. Palenik, J. Pawlowski, G. Petroni, G. Piganeau, M. C. Posewitz, K. Rengefors, G. Romano, M. E. Rumpho, T. Ryneerson, K. B. Schilling, D. C. Schroeder, A. G. B. Simpson, C. H. Slamovits, D. R. Smith, G. J. Smith, S. R. Smith, H. M. Sosik, P. Stief, E. Theriot, S. N. Twary, P. E. Umale, D. Vaultot, B. Wawrik, G. L. Wheeler, W. H. Wilson, Y. Xu, A. Zingone, and A. Z. Worden, *PLoS Biol.*, 2014, **12**, e1001889.